OPTIMUM DESIGN OF SWAY FRAMES

BY

MUHAMMAD ANWARUL ISLAM
B Sc Engg, B Arch, M Sc Engg

A thesis submitted to the University of Warwick
for the degree of Doctor of Philosophy.

Research carried out in the Department of Engineering,
University of Warwick.

September, 1978.

To my family — Nazmun, Naela and Naushad .

SUMMARY

The work presented in this thesis consists mainly of three design methods for sway frames based on the minimum-weight concept. For multistorey frames the aim has been to produce quick, simple and inexpensive design methods that can be used without recourse to a large computer.

The proposed direct design procedure for multistorey sway frames to limiting deflections at working load is suitable for hand calculation and the discrete properties of standard rolled sections can be taken into consideration. Design charts have been presented to reduce the amount of calculation.

For the design of multistorey frames to strength, stability and deflection requirements, an approximate elastic-plastic analysis procedure has been developed using substitute frames. Design by this method is based on the frame behaviour upto collapse while satisfying the permissible deflections at working load as specified by the codes. For small frames, hand calculations can be used, whereas simple programmes suitable for desk-top computers enable rapid design of large frames.

A computer analysis procedure for members with varying cross-sections has been developed using the matrix displacement method. This has been used to evolve an optimum design method for single-bay pitched-roof tapered portal frames to strength and deflection requirements. A linear programming technique has been used to solve the non-linear functions of the optimisation problem by following a multi-linear path.

CONTENTS

ACKNOWLEDGEMENTS

The research work reported in this thesis has been made possible by the continual help, guidance and encouragement of Dr.D.Anderson, to whom the author is immensely grateful.

The author wishes to express his thanks to Professor R.P.Johnson for arranging the financial grant which helped in continuing the research work.

Thanks are also due to Butler Buildings (U.K.) Ltd for making available the design report for a tapered portal frame.

Finally, the cooperation of the personnel of the Computer Unit, University of Warwick, and the efforts of Mrs.A.M.Shaw in typing the thesis are thankfully acknowledged.

NOTATIONS

a	Weight/inertia ratio of a rolled section
$\underline{A}$	Displacement transformation matrix
A_f	Cross-sectional area of flange
b	Multiplication factor for cost function
c	Cost of a member (chapter II)
$c, c_1, c_2, \ldots$	Stability functions
C	Total cost of a frame
d	Depth of a member
d_e	Equivalent depth of an I-section
D_o, D_1, D_x	Expressions for depth of a tapered member
E	Modulus of elasticity
$f(\ )$	Expression for a function
f_a	Axial stress
f_b	Bending stress
f_{bc}	Compressive bending stress
f_c	Compressive axial stress
f_1, f_1	Stress index
f_t	Thickness of flange of I-section
f_w	Width of flange of I-section
F	Total horizontal shear in a storey
F_a	Allowable axial stress
F_b	Allowable bending stress
FEM	Fixed end moment in a member
$g(\ )$	Expression for a function
h	general term for height/storey height
H	Equivalent stiffness ratio (chapter I), applied horizontal shear at each intermediate level of a regular frame (chapter II)

I , I'	General terms for the moment of inertia of a member
k	General term for the nominal stiffness (I/L) of a member
$\underline{k}$	Member stiffness matrix
K	General term for the stiffness of a substitute frame
$\underline{K}$	Overall stiffness matrix
l	General expression for the length of a member/width of a bay
ln	$\log_e$
L	Length of a member/width of a bay, total width of a frame (chapter III)
$\underline{L}$	Applied load vector
m	Number of bays (chapters II and III), number of variables in optimisation problem (chapter VII)
M	General term for bending moment
M_p	General term for plastic moment of a member
Mp'	Reduced plastic moment
n	Indicator of the location of storey in a multistorey frame (chapters II and III), number of constraints in optimisation problem (chapter VII), stability function
n_1	Number of subdivisions in a stanchion
n_2	Number of subdivision in a rafter
o	No-shear stability function
p_c	Permissible compressive axial stress
p_{bc}	Permissible compressive bending stress
P	H/m (chapter II)

P_1 , P_2, P_3	Total horizontal shear in a storey of a multistorey frame
$\underline{P}$	Vector of member forces
q	General term for cost factor
r	Bay width/height ratio in a regular frame
s, s_1 , s_2	Stability function
s"	Merchant function
S	Shear in a member (chapter VI), total horizontal shear in a column
t	Total number of storeys in a multistorey frame
u	Axial deformation of a member
v_i	Variables in optimisation problem
V_A, V_B, V_C	Vertical reaction in a member
w	Weight per unit length of a rolled section
w_t	Thickness of web of I-section
W	Total distributed load in a beam
x_A , x_B	Horizontal displacements of joints A and B of member AB
$\underline{x}$	Joint displacement matrix in overall co-ordinates of a frame
Y_A , Y_B	Vertical displacements of joints A and B of member AB
Z	Cost function/Objective function
α	Slip coefficient (chapter I), inclination of a member
δ_b , δ_t	Actual horizontal deflections of a storey
Δ	General term for horizontal sway deflection of a storey
Δ_b , Δ_t	Permissible horizontal deflections of a storey
Δv	Increment in the dimension/variable in optimisation problem

θ	General term for joint rotation
θ_H	Hinge rotation
	General term for sway angle
ρ	Ratio of axial load to Euler load
λ	General term for load factor
λ_1	Permissible load factor for vertical load only
λ_2	Permissible load factor for combined vertical and horizontal loads
λ_c	Elastic critical load factor
λ_f	Collapse load factor/elastic-plastic failure load factor
λ_p	Rigid-plastic load factor
λ_{cr}	Required elastic critical load factor
λ_{fr}	Desired failure load factor

The terms c, C , k, K , U , V, W, X, Y and Z with or without subscripts have been used to express constants.

CHAPTER I

INTRODUCTION

1.1 EARLY DESIGN METHOD FOR MULTISTOREY FRAMES

The traditional approach to the design of braced multistorey frames is to use the 'simple design' method [1, 2], in which the beam-column connections are considered to be pinned. This renders the beams simply-supported. The columns are designed for axial load, as well as for the end moments caused by the beam reactions acting at an assumed eccentricity with respect to the column axis. Wind forces acting at the building facade are transmitted to stiff bracing elements by the floors acting as deep beams. In this way the presence in the frame of bending moments and other member forces due to wind load is avoided. The design is based on linear elastic behaviour of the structural material. Cross-sections of the members are chosen in such a way that nowhere in the frame do the internal stresses exceed certain permissible values.

In an unbraced structure each frame has to be designed to resist bending due to its share of wind load. Three of the several approximate methods for the calculation of moments due to wind load in the members of a multistorey frame are explained in reference [3]. These are (i) the continuous Portal method, (ii) the Cantilever method and (iii) the Portal method. The basic assumptions in all the three methods are :

(i) Wind loads are applied at floor levels.

(ii) The total horizontal shear at any level is resisted by the columns immediately below that level.

(iii) There is a point of contraflexure in each column at mid-height between floor levels.

The most commonly used of the three methods, i.e., the Portal method, makes two further assumptions. These are :

(iv) There is a point of contraflexure at mid-span of each beam.

(v) Each bay acts as a simple portal and the total horizontal load is divided between the bays in proportion to their spans. With equal bays this results in no vertical load in the internal columns.

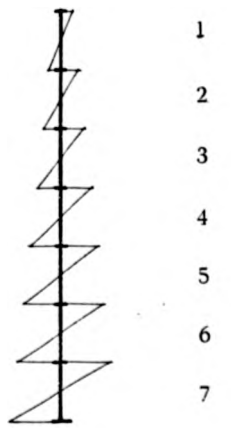

Figure 1.1

Figure (1.1) shows the typical bending moment diagram due to wind forces in the column of a seven-storey frame given by the above method.

The common approach to the design of sway frames has usually been to combine the 'simple design' method for vertical loading with one of these approximate methods for the calculation of moments due to wind. Superimposition of the two is assumed to give the resulting

bending moments and other member forces for the combined effects of vertical and wind loads. However, it should be noted that one makes contradictory assumptions about the behaviour of joints which are taken to be pinned under vertical loading and rigid under wind load. Baker and Holder [4] showed that practical joints made of rivets or high tensile black bolts are nowhere near pinned under the effect of vertical loading. The rigidity of the joints produces restraining moments at the ends of a beam reducing the maximum design moments by 17% to 25% at the same time causing large end moments in the columns. Baker and Williams [4] have introduced the term 'slip coefficient' (α) for a joint to relate the moment transmitted by it and its rotation. A measure of beam-to-column stiffness, termed the 'equivalent stiffness ratio', H, is then given by

$$H = \frac{k_{beam}/k_{column}}{1 - 3\alpha} \qquad (1.1)$$

where k is the rotational stiffness I/L, I being the moment of inertia of the member and L its length.

They have also shown that all the columns in a frame do not necessarily bend in double-curvature under wind loading, particularly in frames with weak beams.

Figure (1.2) shows the possible pattern of bending moment diagram due to wind load in columns of a seven-storey frame with low stiffness ratio. This clearly shows the effect of flexibility of connections and the possibility of single-curvature bending without any point of contraflexure. The 'Steel Structures Research Committee' [4], which was responsible for the above investigations, published its observations regarding the effect of joint rigidity on the internal forces of frame members due to vertical and horizontal loading but

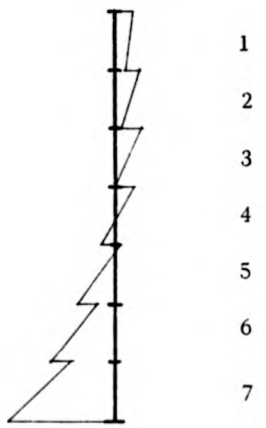

Figure 1.2

the 'Draft Rules for Design ', now used as 'Semi-Rigid Design' [1], are given for braced frameworks only.

With the introduction of friction-grip bolts and welded connections the joints can now be designed to have the same load carrying capacity as the members themselves. It is usually assumed that these rigid joints rotate as a whole without any angle-change between the members.

Rigidity of joints, however, makes a frame statically indeterminate. The accurate assessment of member forces in such a frame is a lengthy and complicated procedure as it involves the solution of a number of simultaneous equations. Moreover, it has long been realised that a highly indeterminate multistorey frame has a greater load-carrying capacity than permitted by the elastic design method of providing

the strength of an individual member according to the requirement to satisfy the allowable stresses. These have led to the application of rigid-plastic theory in structures which enables the design of a frame to be based on its overall ultimate strength.

1.2 PLASTIC DESIGN

The rigid-plastic design method is based on the gradual formation of fully-yielded cross-sections at isolated points in the members of the frame. Such cross-sections, called plastic hinges, rotate at constant moment as the loading increases, till the frame collapses due to the formation of sufficient number of plastic hinges to cause a mechanism. An acceptable design solution by this method should satisfy the conditions that (i) such a mechanism does not occur before a specified load level, expressed as a factor of the working load, has been reached, (ii) the bending moment distribution is in equilibrium with the applied loads and (iii) the bending moments do nowhere exceed the corresponding plastic moments of resistance. The solution is obtained by studying the above conditions with alternative arrangements of hinges required to cause a mechanism at the desired factored load.

Whereas, for quick and economical design of multistorey frames the elastic design method has to depend on certain simplifying, but not always correct [4], assumptions to make the structure statically determinate, in the plastic method no such assumptions are required. In the latter method, the hinges formed at discrete locations in the frame make it statically determinate provided collapse does not occur due to some local mechanism in only a part of the frame. Design by this method allows the designer to fix the load factor for collapse and thus has a definite factor of safety over the working load. This is in contrast to elastic permissible stress design in

which the factor of safety against collapse varies from structure to structure and is generally unknown.

1.3 STABILITY OF FRAMES

The load deflection relationship of a frame assuming linear elastic behaviour of material is usually represented by the straight line OL of figure (1.3). However, the effect of secondary moments due to the

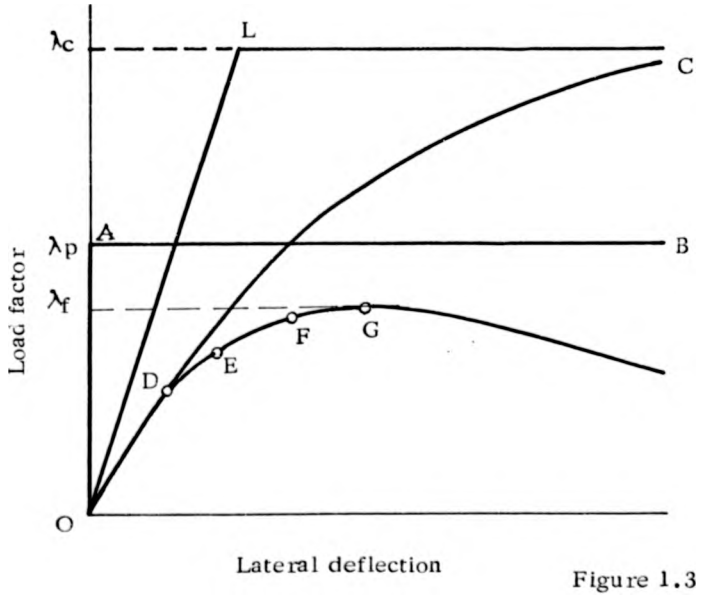

Figure 1.3

axial forces acting on in-plane deflections (the P-Δ effect) causes the overall stiffness of the frame to deteriorate as the applied load increases and the load-deflection relationship takes a non-linear form. If the frame is assumed to remain elastic upto the point of collapse, its load-deflection relationship will follow the curve ODC and not the straight

line OL. The load factor λ_c is the 'elastic failure' load which is very close in value to the 'elastic critical' load at which bifurcation of equilibrium would occur under vertical joint loads only.

One of the assumptions on which the rigid-plastic design method is based is that the deflections in the frame are negligible until the collapse state has been reached. In figure (1.3) the rigid-plastic load-deflection behaviour is represented by the lines OA and AB, λ_p being the rigid-plastic failure load. At λ_p the overall stiffness of the frame vanishes and there is infinite deflection causing collapse of the frame. Such assumption of negligible deflections in the precollapse state is generally applicable in frames braced against sidesway and in some cases of low-rise sway frames where the effect of wind load is very little. In general the horizontal deflections in sway frames are much too significant to be neglected and they cause rapid deterioration of the overall stiffness of a frame.

Wood [5] uses the term 'deteriorated critical load' to express the modified critical load of the remaining parts of a frame after the formation of a new plastic hinge. He has shown that in a four-storey one-bay frame, the deteriorated critical load is less than half of the original critical load after the formation of only two hinges. It is therefore possible for a frame to lose all its stiffness before the occurrence of full mechanism, thus resulting in its collapse at a load factor less than λ_p, the plastic failure load. Hence, the rigid-plastic design method has been found generally unsuitable for sway frames.

Assuming that all the members of a frame remain fully elastic except at discrete points at which plastic hinges form, the curve ODEFG represents the load-deflection behaviour of a frame, points

D, E, F and G indicating the formation of hinges. This is the elastic-plastic behaviour [6, 7, 8] of a frame which takes into consideration the deterioration of frame stiffness due to the effect of axial forces in the members and the formation of plastic hinges at discrete locations. The elastic-plastic failure load is given by λ_f. The elastic-plastic curve ODEFG is a very realistic representation of the actual frame behaviour as the overall instability of the frame due to gradual deterioration of its stiffness is duly considered.

An empirical expression for the actual failure load of a frame in relation to its elastic critical load and the plastic failure load has been proposed by Merchant. It is based on Rankine's original proposal [9] concerning the failure load of an isolated pin-ended strut and is given as

$$1/\lambda_f = 1/\lambda_c + 1/\lambda_p \qquad (1.2)$$

This is known as the Merchant-Rankine formula [10].

Some approximate methods are available for the calculation of λ_c [11, 12, 13, 14] and also for rapid calculation of λ_p [15 , 16] for use with the Merchant-Rankine formula in determining the failure load of a frame. Equation (1.2), however, is essentially an analysis formula and is not a tool for the direct design of a frame.

The necessity for a direct ultimate-load design method for multi-storey sway frames by using hand calculation led to Heyman proposing a method [17]where a pattern of plastic hinges is assumed involving collapse in both beams and columns. Full plastic moments of the beams and columns are calculated with the factored load.

While the beam sections are chosen to satisfy the calculated plastic moments, columns are designed to remain elastic under the combined action of these moments and axial forces. As a safeguard against instability it is suggested that at working load (i) plastic hinges will not be allowed to form and (ii) the deflections will remain within acceptable values. An approximate method of calculating the deflections has been suggested and a process of moment distribution is used to check the yield criterion at working load.

Holmes and Gandhi [18] proposed a method of rigid-plastic design in which modification factors are used in the expressions for the required plastic moment of a member to safeguard against instability. The modification factors which depend on the 'stability functions' m, n and o and the Euler ratio ρ of the members, allow for the reduction of column stiffnesses due to compressive axial forces, the reduction of beam stiffnesses due to the formation of plastic hinges, additional moment in columns due to sway deflections and the effect of the point of contraflexure not occurring at the mid-height of the columns. Initial sections for the members are calculated by assuming the values of these modification factors as unity. Actual modification factors are then calculated on the basis of the section properties, a new design solution is obtained and the process is repeated until two successive solutions are identical. An approximate method is used to calculate the sway deflection of the frame by computer.

Holmes and Sinclair-Jones [19] have used the same principle and developed more accurate methods for dealing with boundary regions of the frame, i.e. the topmost storey, the bottom storey and the external columns, and also for predicting the modification factor.

A team of researchers at the Lehigh University developed a design method [20] in which the initial values of sway deflections at the factored combined load are assumed. These enable the formulation of equilibrium equations for each storey based on the properties of the initial set of sections obtained for vertical load only. The deformed shape due to wind load and the bending moments are estimated and the beam members are designed to collapse at a specific load factor . A moment redistribution procedure is used to estimate the bending moments and sections for the columns are selected. The sway-deflections are then estimated by a slope-deflection method and the frame redesigned, if necessary. As a check against instability, the beams and columns of the designed frame are split into subassemblages and the maximum shear resistance of each storey is obtained from charts prepared to give the variation of such subassemblage's sway deflection with increasing wind shear. The shear resistance capacity of each storey is compared with the applied shear force at the ultimate load.

All the methods discussed above were attempts towards finding an ultimate-load design method for plane multi-storey sway frames considering the instability effects ignored by rigid-plastic design. Basically, these attempts were intended to provide the designer with a simple hand/desk method, quick, inexpensive and easy to use without involving difficult calculations.

None of the methods, however, can be considered to be accurate as all of these depend on several initial assumptions which may not always prove to be right. The first method [17] does not consider the effects of instability in the design process and suggests control of deflections and maintenance of elastic properties at working load as a measure against instability. In the second [18] and the third [19] method, where modification factors are used for calculating the

required member sizes to avoid instability, there is no certainty about the safety or the economy of the design solution. Moreover, in all these three methods a hinge pattern has to be assumed to make the structure statically determinate which has been shown to be unrealistic and far from the actual behaviour of the frame at failure [5,6] . The fourth method [20] is based on an assumption of the frame behaviour under load which influences the accuracy and therefore the degree of safety and economy of the design.

The hinge formation pattern, joint displacements and hinge rotations at various stages of loading are the essential data required by a designer to assess the strength and stiffness of a frame. A method which provides this information may lead to a rational design process resulting in safety and economy in the final design solution.

1.4 COMPUTER METHODS : ELASTIC-PLASTIC DESIGN

With the advent of digital computers highly indeterminate rigid-jointed multi-storey frames could be designed on the basis of elastic theory by using the matrix methods of structural analysis. Livesley [21] developed methods to analyse elastic frames with or without considering the instability effects due to axial forces in the members. Both he and Jennings and Majid [22] used the matrix displacement method in which the unknown joint displacements are obtained by solving the matrix equation

required member sizes to avoid instability, there is no certainty about the safety or the economy of the design solution. Moreover, in all these three methods a hinge pattern has to be assumed to make the structure statically determinate which has been shown to be unrealistic and far from the actual behaviour of the frame at failure [5, 6] . The fourth method [20] is based on an assumption of the frame behaviour under load which influences the accuracy and therefore the degree of safety and economy of the design.

The hinge formation pattern, joint displacements and hinge rotations at various stages of loading are the essential data required by a designer to assess the strength and stiffness of a frame. A method which provides this information may lead to a rational design process resulting in safety and economy in the final design solution.

1.4 COMPUTER METHODS : ELASTIC-PLASTIC DESIGN

With the advent of digital computers highly indeterminate rigid-jointed multi-storey frames could be designed on the basis of elastic theory by using the matrix methods of structural analysis. Livesley [21] developed methods to analyse elastic frames with or without considering the instability effects due to axial forces in the members. Both he and Jennings and Majid [22] used the matrix displacement method in which the unknown joint displacements are obtained by solving the matrix equation

$$\underline{X} = \underline{K}^{-1} \underline{L} \qquad (1.3)$$

where $\underline{X}$ is the joint-displacement matrix, $\underline{K}$ is the overall stiffness matrix given by the slope-deflection equations, and $\underline{L}$ is the external load matrix. Member forces are then calculated using these joint displacements. In the non-linear analysis the effects of the reduction of member stiffnesses due to axial load in the members are obtained by using the stability functions introduced by Livesley [21]. Iterative calculation is necessary as the axial forces in the members, required to calculate the stability functions, are unknown initially.

However, application of these methods was restricted to small frames because of the large space required for storage of information in the computer. Jennings [23] developed a compact method for the storage and solution of the stiffness equations. In his method the elements in each row of the stiffness matrix in between the first non-zero element and that on the leading diagonal are stored in a vector form in the 'main sequence' and are identified by a second vector of 'address sequence.' The latter vector indicates the positions, in the main sequence, of the leading diagonal elements of each row of the symmetrical stiffness matrix.

All these techniques have been used by Majid and Anderson [7] to develop an efficient method for linear and non-linear elastic analysis of large multi-storey frames.

As stated earlier, for sway frames, a realistic evaluation of the failure load considering the reduction of stiffness due to both compressive axial force and the formation of plastic hinges can be obtained by the elastic-plastic analysis. In this method the non-linear load-deflection behaviour of the frame, represented by the curve

ODEFG of figure (1.3) is traced upto collapse and thereby the location of every hinge and the load factors at which these are formed are exactly identified. Majid and Anderson [7] have extended their program of non-linear elastic analysis to develop a program for such non-linear elastic-plastic analysis.

In analysis by the elastic-plastic method a plastic hinge is considered to behave like a real hinge with a constant moment which is the plastic hinge moment Mp of the member while the rest of the member is assumed to behave elastically. The point of action of a concentrated load is considered as a joint and the length of member between the two joints is considered as a member itself. Analysis of the frame is carried out after the formation of each hinge to find out the location of the next hinge and the load factor at which it will form. This is done by extrapolating the bending moment at the end of each member towards its plastic hinge moment, Mp. As the value of Mp will be reduced at the extrapolated load factor due to the increase of axial force, extrapolation of the axial force and the corresponding reduced plastic moment, Mp', are also required. By a process of iteration, the lowest load factor at which the bending moment at the end of a member reaches its reduced plastic moment is found and a hinge is inserted at the corresponding end of the member. The overall stiffness matrix, $\underline{K}$ is modified to include elements for the additional hinge rotation. The reduced plastic moment of the member is introduced in the respective row of the external load vector, $\underline{L}$. The process continues till the determinant of the overall stiffness matrix of the frame becomes negative, indicating the collapse of the frame. The possibility of a hinge stopping rotating when other hinges have formed in the

frame has been taken into account by identifying such hinges and considering them as inactive [8]. Davies [24] has extended the above method by taking into consideration the effect of reversal in the direction of hinge rotation. Vijakkhana et al [25] have proposed a method of elastic-plastic analysis of unbraced frames which includes the effects of strain reversal due to unloading of plastic hinges.

Majid and Anderson [26] have also proposed a design method based on elastic-plastic analysis to satisfy the strength and stability requirements of a frame. A set of lower-bound sections for the members based on minimum strength requirements, is selected and the frame analysed. Members are redesigned and the process repeated until the following design criteria are satisfied.

(i) Under the combined effects of vertical and wind loading the frame should not collapse below the permissible load factor λ_2.

(ii) Under vertical load only the frame should not collapse below the permissible load factor λ_1.

(iii) No plastic hinge should develop in a beam below the load factor of unity and the frame should be entirely elastic under the working load.

(iv) No plastic hinge should develop in a column below the permissible load factor λ_2 under combined loading or λ_1 under vertical loading.

Although the elastic-plastic analysis method can be used to study the realistic behaviour of multistorey frames such an analysis

involves a complex process of iterative calculations and requires the services of a large computer. Even for small frames the analysis procedure is beyond the capacity of the usual desk-top computers available in the design offices.

The elastic-plastic design method is based on very realistic design criteria. However, the provision for the hinges not to form in columns at λ_2 and in the beams at $\lambda=1$ does not ensure against excessive deflections in the frame causing impairment of its serviceability. As a result, a large number of iterations may be required for frames subject to high wind load to satisfy the code requirements on maximum permissible deflections even after a satisfactory solution for strength and stability requirements has been found. The design method, however, is essentially a procedure requiring extensive storage space and process time in a large computer and remains as an academic research product to which a designer of the building industry cannot afford to have any access.

1.5 DESIGN BY MERCHANT-RANKINE APPROACH

The Merchant-Rankine approach is the only simple method currently available to a designer for use in the ultimate-load design of multi-storey sway frames to strength and stability requirements. Equation (1.2) has been found to be fairly conservative unless the wind load is appreciably high. Wood [11] proposed the following modification which makes some allowances for the combined effect of strain-hardening and composite action with cladding.

$$1/\lambda_f = 1/\lambda_c + 0.9/\lambda_p \qquad (1.4)$$

involves a complex process of iterative calculations and requires the services of a large computer. Even for small frames the analysis procedure is beyond the capacity of the usual desk-top computers available in the design offices.

The elastic-plastic design method is based on very realistic design criteria. However, the provision for the hinges not to form in columns at λ_2 and in the beams at $\lambda=1$ does not ensure against excessive deflections in the frame causing impairment of its serviceability. As a result, a large number of iterations may be required for frames subject to high wind load to satisfy the code requirements on maximum permissible deflections even after a satisfactory solution for strength and stability requirements has been found. The design method, however, is essentially a procedure requiring extensive storage space and process time in a large computer and remains as an academic research product to which a designer of the building industry cannot afford to have any access.

1.5 DESIGN BY MERCHANT-RANKINE APPROACH

The Merchant-Rankine approach is the only simple method currently available to a designer for use in the ultimate-load design of multi-storey sway frames to strength and stability requirements. Equation (1.2) has been found to be fairly conservative unless the wind load is appreciably high. Wood [11] proposed the following modification which makes some allowances for the combined effect of strain-hardening and composite action with cladding.

$$1/\lambda_f = 1/\lambda_c + 0.9/\lambda_p \qquad (1.4)$$

Both the E.C.C.S. [27] and the B/20 Draft Specification [28] permit the use of equation (1.4) for calculation of the failure load of multi-storey frames. The use is, however, subject to conditions. (i) For frames having $\lambda_c/\lambda_p \geq 10$ λ_f is limited to λ_p . (ii) For frames having $\lambda_c/\lambda_p < 4$ equation (1.4) is not valid and a full non-linear elastic-plastic analysis is necessary.

The first condition is in general applicable to 'braced' frames for which a design method by hand calculation is available [29]. For the frames falling under the second category equation (1.4) will give higher values of λ_f than those given by accurate elastic-plastic analysis.

As stated in Sec. (1.3) design of frames using equation (1.4) is an iterative process involving calculation of λ_c and λ_p for trial design followed by modification of the member sizes to keep λ_f within the permissible limit. Of the four methods mentioned in Sec. (1.3) for calculating λ_c [11, 12, 13, 14] the one by Wood [11] uses a substitute frame based on the work of Grinter.

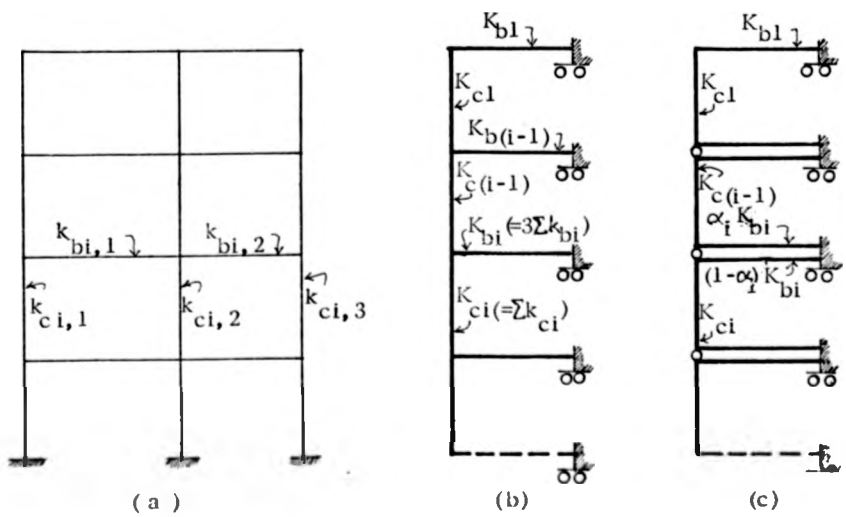

(a) (b) (c)

Figure 1.4

Both the E.C.C.S. [27] and the B/20 Draft Specification [28] permit the use of equation (1.4) for calculation of the failure load of multi-storey frames. The use is, however, subject to conditions. (i) For frames having $\lambda_c/\lambda_p \geq 10$ λ_f is limited to λ_p . (ii) For frames having $\lambda_c/\lambda_p < 4$ equation (1.4) is not valid and a full non-linear elastic-plastic analysis is necessary.

The first condition is in general applicable to 'braced' frames for which a design method by hand calculation is available [29]. For the frames falling under the second category equation (1.4) will give higher values of λ_f than those given by accurate elastic-plastic analysis.

As stated in Sec. (1.3) design of frames using equation (1.4) is an iterative process involving calculation of λ_c and λ_p for trial design followed by modification of the member sizes to keep λ_f within the permissible limit. Of the four methods mentioned in Sec. (1.3) for calculating λ_c [11, 12, 13, 14] the one by Wood [11] uses a substitute frame based on the work of Grinter.

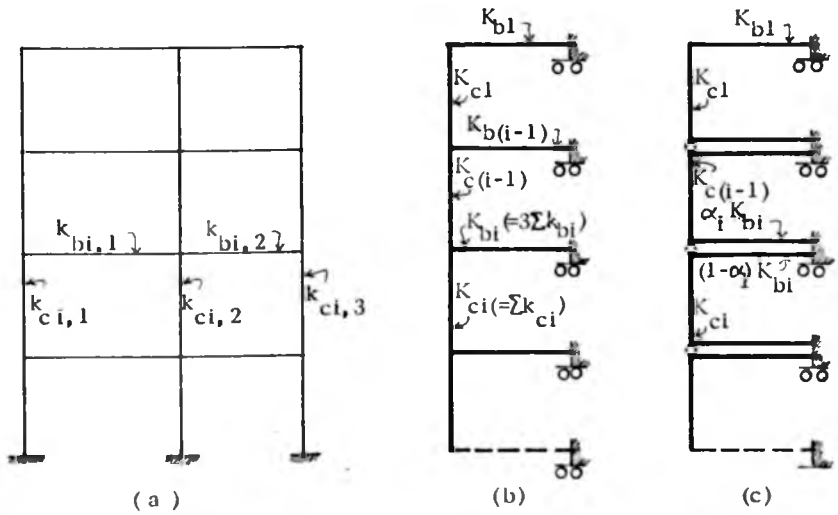

Figure 1.4

Figure (1.4b) shows the substitute frame used by Wood for the original frame shown in (1.4a). Neglecting the reduction of stiffness due to the effects of axial forces the stiffness, K_b of a beam in the substitute frame at any level is given by $3\Sigma k_b$ where k_b is the nominal stiffness I/L of a beam at that level in the real frame, I being the moment of inertia and L the span of a beam. The stiffness of the column of a Grinter frame at any storey is given by Σk_c where k_c is the nominal stiffness of a column of the real frame in that storey. A process of 'stiffness distribution' is used in the substitute frame to find the total rotational stiffness of a joint at different load factors. By plotting these values the critical load for a joint, at which the total rotational stiffness is zero, is obtained. The lowest of these critical values given by the different joints is the elastic critical load, λ_c , for the whole frame. A quick method for predicting the most vulnerable joint by using design curves (figure 9 of reference [11]) can be used to reduce the analysis to the investigation of one joint only. The effect of compressive axial forces in the columns as well as that of plasticity in beams may be taken into consideration in this method. Hence it can also be used to find the 'deteriorated' elastic critical load of a frame after the formation of plastic hinges in the beams. The method has been extended to calculate the sway deflections of a frame in the elastic range. Further explanation of the principle of substitute Grinter frame and stiffness distribution to calculate deflections is presented in Chapter IV (Sec. 4.3) of this thesis .

In a recently published paper Williams [14] has presented a simplified procedure of designing a frame by using the modified Merchant-Rankine formula. As the desired failure load, λ_{fr} , is known, equation (1.4)

gives the required elastic critical load, λ_{cr}, of a frame as

$$\lambda_{cr} = \frac{\lambda_p \lambda_{fr}}{\lambda_p - 0.9\lambda_{fr}} \tag{1.5}$$

Equation (1.4) is valid for $4 \leqslant \lambda_c / \lambda_p \leqslant 10$ and $\lambda_f = \lambda_p$ for $\lambda_c / \lambda_p > 10$. So the designed frame must satisfy the following conditions,

$$\lambda_c \geqslant 4\lambda_p \tag{1.6}$$

$$\lambda_{fr} \leqslant \lambda_p \leqslant 1.15\lambda_{fr} \tag{1.7}$$

Starting with a trial design whose λ_p has been calculated and found satisfying the condition given by equation (1.7), calculations are made to check whether its elastic critical load is greater than λ_{cr} (equation 1.5) and $4\lambda_p$.

A simple method for calculating a lower-bound on λ_c for a frame has been obtained by modifying the substitute frame to that shown in figure (1.4c). Each beam is split longitudinally with the stiffness K_{bi} divided into the portions $\alpha_i K_{bi}$ and $(1 - \alpha_i) K_{bi}$. The two portions of the beams are fixed together at the right-hand ends and, like the Grinter frame, connected to a roller. On the left-hand ends they are rigidly connected to the respective columns whereas the columns are pinned together at the beam levels. Each "cell" of this modified substitute frame buckles independently and hence a lower-bound on λ_c

for the frame is equal to the lowest λ_c of any of the cells which are calculated by using figure (9) of reference [11]. Initially, values of α_i are selected intuitively and if the lower-bound λ_c given by the calculations satisfied equation (1.5 and 1.6) then it is not necessary to calculate the actual λ_c. If the above conditions are violated the designer may be able to avoid altering the design itself by simply modifying the values of α_i to obtain a closer lower-bound on the elastic critical load of the frame. It has been shown that if the actual elastic critical load of the frame is equal to or more than the required value then refining the choice of α_i will enable the designer to reach that value.

Though the method has simplified the Merchant-Rankine approach for the design of multistorey sway frames, it may still involve a large amount of iterative calculations to obtain a safe design. However, the most difficult aspect of the Merchant-Rankine approach is now the calculation of rigid-plastic failure load. Finding the right mechanism for a large multistorey frame is a complex operation.

A solution obtained by using the Merchant-Rankine formula may not satisfy the specified limitations on the horizontal deflections and further modification may be required. Moreover, the final design solution may not be the most economic one.

1.6 OPTIMUM DESIGN

Application of rigorous optimisation techniques to the rigid-jointed framed structure creates complex mathematical problems. When rigid-plastic theory is used, which makes the structure statically determinate, the minimum-weight design of small frames may become

comparatively simple if a linear relationship between the plastic moment capacity and weight per unit length of standard rolled sections is assumed to exist. But for multistorey buildings with a large number of members and various possible collapse mechanisms the optimisation problem can only be solved by using a computer. The principle of such minimum-weight rigid-plastic design of frames by linear programming technique, e.g.,the simplex method, is given in some of the recently published text books [8, 30].

An attempt has also been made to find a method for minimum-weight design considering the discrete nature of the available standard sections [31]. But all these methods, being based on rigid-plastic theory, neglect frame instability effects and are therefore not generally applicable to multistorey sway frames.

In the elastic design method, the optimum design of a frame is a non-linear problem even if the instability effects of axial forces in the members are ignored. Unlike the procedure of optimum plastic design,optimum elastic design is an iterative process which can conveniently start with a lower-bound solution. Changes in the sectional properties of a member, required to reach the feasible solution, cause redistribution of internal forces in the members and changes in the joint displacements of the frame. Constraints of optimisation are usually the stresses and deflections which depend on the internal forces and displacements. The relationships between the variations of these stresses and deflections and changes in the weight of a member causing such variations are not linear , even if a linear relationship is assumed to exist between the inertias of the standard sections and their respective weights per unit length.

Hence the linear programming techniques cannot be used to solve such problems. Several methods of non-linear programming are available to solve such problems but these are complex and involve large amounts of computer time and storage. Linear programming methods may, however, be used in the solution of non-linear problems by using iterative procedure. Each iteration consists of a small linearised step of the problem. Different methods of solving a non-linear problem by such linearisation and iteration, e.g. the cutting plane method, piecewise linearisation method etc., have been discussed in detail in reference [32]. It has also been shown that these methods have limitations in their applicability in structural design problems. For example, none of these methods can deal with a problem where either the constraints or the objective function include terms expressed as the product of two variables. Moreover, solution of non-linear problems by these methods may not lead to the global optimum if the objective function and the feasible region, as defined by the constraints, are not convex and the given solution may only be an approximation of one of the local optima.

In multi-storey steel frames it is usual practice to use available rolled sections unless, in special cases, built-up sections are found economical. Application of rigorous optimisation techniques in such frames may prove to be a futile exercise as, due to the absence of a continuous range of rolled sections, the selection of member sizes are limited to a handful of sections. Very often a heavier section has to be used though not required by the design solution. So a simple and inexpensive method giving approximate minimum-weight design solution is likely to be more useful for design of multistorey sway frames.

1.7 PORTAL FRAMES

Unlike multistorey frames, the design of portal frames with built-up sections fabricated to desired sizes may, in many cases, be found to be economical. Flat or pitched roof portal frames with tapered members have long been in use for industrial and other types of buildings to achieve economy. Application of rigorous optimisation techniques in the design of such frames is likely to prove worthwhile as the exact dimension of the members given by the optimum solution can be used in the actual structure. It is, however, unlikely that the absolute 'minimum-weight' design solution will necessarily be the most economic one unless the constraints of fabrication and erection are also taken into consideration.

Linear elastic design methods for portal frames with uniform members are available in reference [3] where expressions for the bending moments of the members are given in terms of the dimensions of the frame, ratio of inertias of the rafter and stanchion and the external loading. Plastic design method of such frames for strength requirements to B.S.449 are also available [33] and the lateral-torsional instability of the stanchions can be prevented by using the design charts developed by Horne [34].

An elastic design method for tapered members with variable web depth, other cross-sectional dimensions remaining uniform, has been proposed by Lee et al [35]. The method is based on the AISC interaction formula for prismatic members, as given below, which is extended to tapering members.

$$\left(\frac{f_a}{F_a}\right)_O + \left(\frac{f_b}{F_b}\right)_L \leq 1 \qquad (1.8)$$

where F_a and F_b are the allowable axial and bending stresses obtained from lateral and torsional buckling considerations, suffices O and L refer to the smaller and larger end of a column respectively in the case of a tapering member.

Modifying length factors are introduced into the values of F_a and F_b. These factors are obtained by solving the basic differential equations of flexure and torsion using variable stiffness properties and are finally expressed in terms of the tapering angle. In analysing the effects of axial and bending stresses the member is assumed to be prismatic.

A recent method proposed by Just [36] uses finite element technique to analyse frames with tapered members by developing a displacement function for members with trapezoidal webs.

None of the above methods, however, are capable of directly generating optimum design for portal frames having members of variable cross-sections.

1.8 DESIGN TO DEFLECTION LIMITATIONS

It has been stated in Sec. (1.3) that one of the main reasons for instability in unbraced multistorey frames is the sway deflection caused by wind forces. Besides causing reduction of frame stiffness, excessive deflections may impair the efficiency of the building and of its contents and/or lead to damage to finishes. As a safeguard against these, the codes [1, 28] usually specify the acceptable limits of horizontal and vertical deflection in buildings.

It has been shown [5, 6] that the design of multistorey steel sway frames subject to high but realistic wind forces may be governed by limiting horizontal deflections at working load. Similar constraints may also be true for one-storey buildings like the pinned-base portal frames. On many occasions, the portal frames are designed as pinned-base frames due to uncertainty of the behaviour of foundations. Control of horizontal spread is also necessary for portal frames with overhead travelling cranes, even with fixed supports.

A number of methods for the design of frames to deflection limitations have been proposed. Stevens [37, 38] suggested that the real basis for design should be the prevention of unacceptable deformations under working load and proposed two methods, neither of which was based on accurate analysis of the frame's behaviour as a whole. Majid and Elliot [39] produced design charts for the optimum design of single-bay fixed base portal frames to deflection constraints by using computer analysis.

More recently Moy [40, 41] proposed a method for sway frames in which an initial design with adequate strength but inadequate stiffness is corrected to satisfy permissible limits on horizontal deflections. The frame is divided into subassemblages on the basis of the assumptions of the Portal method [3] and expressions for the storey stiffnesses are obtained in terms of the member inertias of the storey and permissible sway deflection at working load.

Anderson and Salter [42] proposed a computer method for the optimum design of sway frames to limiting deflections using the matrix displacement method of analysis and simplex method of linear programming. Horne and Morris [43] developed a method similar to that of Majid and Anderson's elastic-plastic design program [26] which incorporates both deflection and the ultimate-load design criteria. The method is, however, approximate as the elastic-plastic analysis has been avoided by using magnification factors on a linear elastic analysis.

The proposal of reference [39] is restricted to portal frames only and uses standard rolled sections. Both this method and the one in reference [43] uses non-linear programming technique. The method of reference [40] is based on hand calculation but it requires a preliminary design and repeated calculations to arrive at a feasible solution. The method proposed in reference [42] is a direct design method assuming a tri-linear relationship for the weight-inertia ratio of the standard rolled sections. However, the design procedure requires the services of a computer and the final solution may not satisfy the strength requirements.

1.9 SUMMARY OF THE BACKGROUND AND SCOPE OF PRESENT WORK

In multistorey buildings the wind load is usually resisted either by a stiff core or by specially designed bracing frames, thus rendering the beams and columns free from bending effects due to horizontal forces. Such construction may, in some cases, be found undesirable in order to satisfy other functional requirements of the building. In such cases the transverse framing is designed as a plane sway frame and the horizontal forces are resisted by bending in the members of the frame.

The design of multistorey sway frames with realistic wind loading may usually be governed by the limitations specified by the codes on the permissible horizontal deflection of each storey for non-impairment of serviceability of the buildings. The permissible deflections are specified in terms of the storey-heights at working load [1,28] and it has also been recommended that at this load factor the frame should remain elastic in consideration of both strength and serviceability of the structure [26, 40].

The work presented in this thesis began with an attempt to find a direct design method to limiting horizontal deflections at working load. Chapters II and III present simple methods for the optimum design of plane rigid-jointed multistorey rectangular steel sway frames to limiting values of horizontal deflection. The design expressions, based on linear weight-inertia relationship of standard steel sections, are suitable for hand calculation. The optimum design solution may not always lead to overall economy of the building. For example, the use of some economic sections with comparatively deep cross-section may prove to be expensive in

terms of increased height of the building resulting in extra cost for columns, cladding etc. However, the design equations can be used to calculate alternative feasible designs and the final choice made after comparative cost analysis. Expressions have also been developed with the exact weight-inertia relationship of the discrete sections and design charts have been presented which enable the member inertias of the intermediate floors to be obtained directly.

For the design of unbraced multistorey frames to satisfy strength and stability requirements, several hand/desk methods have been proposed so far, none of which ensures a safe and economic solution. The only acceptable method is the indirect design by modified Merchant-Rankine formula (equation 1.4). This is a repetitive analysis procedure and involves the calculation of λ_p which can be very difficult for large frames. Moreover, it does not cover the full range of sway frames and obtaining the most economic section by this method may require a large number of repetitions. The analysis method generally applicable to all sway frames is the non-linear elastic-plastic method by computer which gives the actual behaviour of a frame upto collapse. Design of a frame by the elastic-plastic method, however, requires the services of a large-capacity computer and is an expensive operation.

In chapter IV of the thesis an approximate elastic-plastic analysis procedure has been proposed which is suitable for hand calculation in case of low-rise frames and for use on a desk-top computer for larger frames. The method uses Grinter-type substitute frame to calculate sway deflections in the elastic-plastic range. Limited frames, similar to the 'limited substitute frames' of JCR 2 method [29] for braced frames, are used to calculate the joint and hinge rotations. By repeated analyses at a number of load

factors the sequence of hinge formation and an approximate failure load may also be obtained. In chapter V this analysis procedure has been used to develop a design method for sway frames satisfying strength, stability and deflection limitations. The method enables the design of a frame which will collapse or be very close to collapse at a desired load factor and satisfy the permissible sway deflections at the working load. The design procedure, which starts with an infeasible lower-bound solution, produces a practical minimum-weight design with standard rolled sections.

Considering the fact that for many portal frame type of structures fabricated tapered members are found to be economic and are in considerable use for pitched-roof portals, a method of analysis of frames with tapered members has been derived and presented in Chapter VI. This method has been used in Chapter VII to develop an optimum design procedure of single-bay pitched-roof portal frames. Due to the necessity of control of deflections in such frames, the design criteria includes both strength and deflection constraints at working load. The matrix displacement method and linear programming techniques have been used in this computer approach for optimum design.

CHAPTER II

MULTISTOREY REGULAR FRAMES : OPTIMUM DESIGN TO DEFLECTION LIMITATIONS.

2.1 INTRODUCTION

In current practice, adequate stiffness in multistorey sway frames is usually obtained by analysis of trial designs using a computer program or an approximate hand method. The effect of cladding, floors etc. can be included in the analysis[44] if an assessment of the stiffness of these components and their connections can be made. Otherwise, the problem may be simplified by choosing a suitably high value of permissible deflection for the bare frame to allow for the stiffening effect.

The existing BS 449[1] does not recommend any specific value as the limit of horizontal deflection for multistorey frames , although for single-storey buildings a limit of $^{1}/_{325}$ of the height of stanchion has been specified. The clause on deflection limits proposed in the B/20 Draft Specification[28] which will replace BS 449 recommends the following :

" The deflection of a building or of any part of a building shall be limited so as not to impair the strength or efficiency of the building or of its contents, nor be unsightly or cause damage to the finish or inconvenience to the occupants.

Deflections of members ... shall not exceed ... the limits unless it can be shown that greater deflections would not impair the strength or efficiency of the structure or lead to damage to finishes. "

The limits are

" Tops of columns in single-storey buildings ... ... Height /300

In each storey of a building with more than one storey ... Height of storey under consideration/300 "

It has been stated in Chapter I that the need for adequate horizontal stiffness usually governs the design of most multistorey sway frames subjected to reasonably high wind forces. Considering the extent of limitations on horizontal deflections proposed in the B/20 Draft Specification, it is believed that the rational approach for the design of such frames will be to consider sway deflections before satisfying the strength requirements.

2.2 OUTLINE OF THE PRINCIPLES OF DESIGN

The design method proposed in this chapter generates the optimum values of the required moments of inertia for the different members of a multistorey sway frame so as to satisfy horizontal deflection limitations at working load.

The simplicity of the method derives from two assumptions. Firstly, the vertical loads are assumed to have a negligible effect on horizontal deflections. Secondly, a point of contraflexure is taken to exist under horizontal loading at the mid-height of each column (except in the bottom storey) and at the midspan of each beam. These assumptions have been made in many design methods already proposed [40] and accurate analyses show them to be reasonable. Thus, the frame is made statically determinate above the bottom storey and each storey can be considered in isolation. Expressions relating the

sway deflection over a storey height to the inertias of the corresponding columns and surrounding beams can then be derived. When these expressions are linked to a cost function, economical solutions can be obtained by a process of optimisation.

The relationship between the mass per unit length of standard rolled sections and their respective moments of inertia is far from linear. The mass-inertia ratio of Universal Beams varies from 1.0647×10^{-4} to $.0541 \times 10^{-4}$ (in kg/cm^5) and that for Universal Columns varies from $1{\cdot}8211 \times 10^{-4}$ to $0{\cdot}2304 \times 10^{-4}$. A curve showing this relationship for a set of 'economical sections' representing the rolled Universal Beams which have the maximum mass-inertia ratio (table 2·1) is shown in figure (2.1). Table (2.2) shows a similar set of economical Universal Column sections. Besides the non-linearity of the weight-inertia ratio of the standard sections, the total cost of a frame is not a linear function of the weight of the frame members. The weight of connections necessary for a particular frame may vary in a different manner for different design solutions. Although it is common practice to estimate the total weight of a frame by increasing the weight of a plain member by a certain percentage to include the weight of connections, the increase applied to beams may be different to that of columns. Finally the rates for supply, delivery and erection may vary from member to member.

Considering the contribution of a single member to the total cost, if the last two items are combined and allowed for by a multiplication factor, b, the cost, c , of a member of length, L, is given by

$$c = b\ (wL) \qquad (2.1)$$

where w is the weight per unit length of the standard section selected for the member.

sway deflection over a storey height to the inertias of the corresponding columns and surrounding beams can then be derived. When these expressions are linked to a cost function, economical solutions can be obtained by a process of optimisation.

The relationship between the mass per unit length of standard rolled sections and their respective moments of inertia is far from linear. The mass-inertia ratio of Universal Beams varies from 1.0647×10^{-4} to $.0541 \times 10^{-4}$ (in kg/cm^5) and that for Universal Columns varies from $1{\cdot}8211 \times 10^{-4}$ to $0{\cdot}2304 \times 10^{-4}$. A curve showing this relationship for a set of 'economical sections' representing the rolled Universal Beams which have the maximum mass-inertia ratio (table 2·1) is shown in figure (2.1). Table (2.2) shows a similar set of economical Universal Column sections. Besides the non-linearity of the weight-inertia ratio of the standard sections, the total cost of a frame is not a linear function of the weight of the frame members. The weight of connections necessary for a particular frame may vary in a different manner for different design solutions. Although it is common practice to estimate the total weight of a frame by increasing the weight of a plain member by a certain percentage to include the weight of connections, the increase applied to beams may be different to that of columns. Finally the rates for supply, delivery and erection may vary from member to member.

Considering the contribution of a single member to the total cost, if the last two items are combined and allowed for by a multiplication factor, b, the cost, c , of a member of length, L, is given by

$$c = b\ (wL) \qquad (2.1)$$

where w is the weight per unit length of the standard section selected for the member.

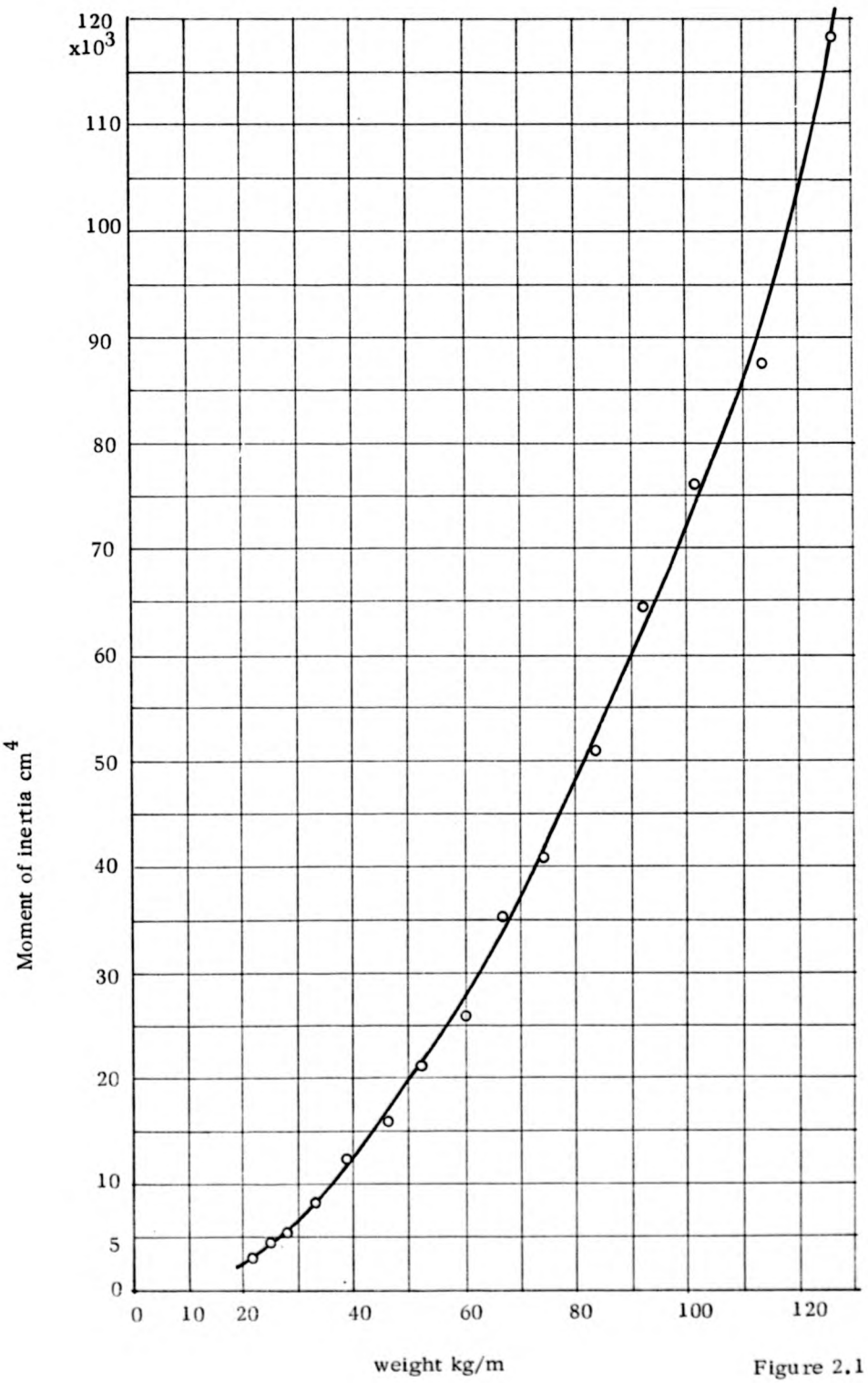
120
x10^3
110
100
90
80
70
60
50
40
30
20
10
5
0
Moment of inertia cm^4
0
10
20
40
60
80
100
120
weight kg/m

Figure 2.1

UB sections	Inertia cm^4	q $\times 10^{-4}$ kg/cm^5
254 x 102 x 22	2863	0.77
305 x 102 x 25	4381	0.57
305 x 102 x 28	5415	0.52
356 x 127 x 33	8167	0.40
406 x 140 x 39	12408	0.31
406 x 140 x 46	15603	0.29
457 x 152 x 52	21345	0.24
457 x 152 x 60	25464	0.24
533 x 165 x 66	35083	0.19
533 x 165 x 73	40414	0.18
610 x 178 x 82	55779	0.15
610 x 178 x 91	63970	0.14
610 x 229 x 101	75549	0.13
610 x 229 x 113	87260	0.13
686 x 254 x 125	117700	0.11

Table 2.1

UB sections	Inertia cm^4	q $\times 10^{-4}$ kg/cm^5
254 x 102 x 22	2863	0.77
305 x 102 x 25	4381	0.57
305 x 102 x 28	5415	0.52
356 x 127 x 33	8167	0.40
406 x 140 x 39	12408	0.31
406 x 140 x 46	15603	0.29
457 x 152 x 52	21345	0.24
457 x 152 x 60	25464	0.24
533 x 165 x 66	35083	0.19
533 x 165 x 73	40414	0.18
610 x 178 x 82	55779	0.15
610 x 178 x 91	63970	0.14
610 x 229 x 101	75549	0.13
610 x 229 x 113	87260	0.13
686 x 254 x 125	117700	0.11

Table 2.1

UB sections	Inertia cm^4	q $\times 10^{-4} kg/cm^5$
152 x 152 x 23	1263	1·82
152 x 152 x 30	1742	1·72
152 x 152 x 37	2218	1·67
203 x 203 x 46	4564	1·01
203 x 203 x 52	5263	0·99
203 x 203 x 60	6088	0·99
203 x 203 x 71	7647	0.93
254 x 254 x 73	11360	0.64
254 x 254 x 89	14307	0.62
305 x 305 x 97	22202	0.44
305 x 305 x 118	27601	0.43
356 x 368 x 129	40246	0.32
356 x 368 x 153	48525	0.32
356 x 368 x 177	57153	0.31
356 x 368 x 202	66307	0.30

Table 2.2.

If the weight-inertia relationship of the section is given by $w = a I$, I being the moment of inertia of the section, equation (2.1) can be written as

$$c = ab\,(IL)$$
$$= qIL \qquad (2.2)$$

where q (= ab) is the cost factor.

The cost function z for a storey of a multistorey frame may then be expressed in terms of the inertias and the respective lengths of the members in the storey as

$$Z = \sum_{i=1}^{t} q_i I_i L_i \qquad (2.3)$$

where $i = 1, 2 \ldots\ldots, t$ and

t is the total number of members in the storey.

2.3 EXPRESSIONS FOR INTERMEDIATE STOREYS

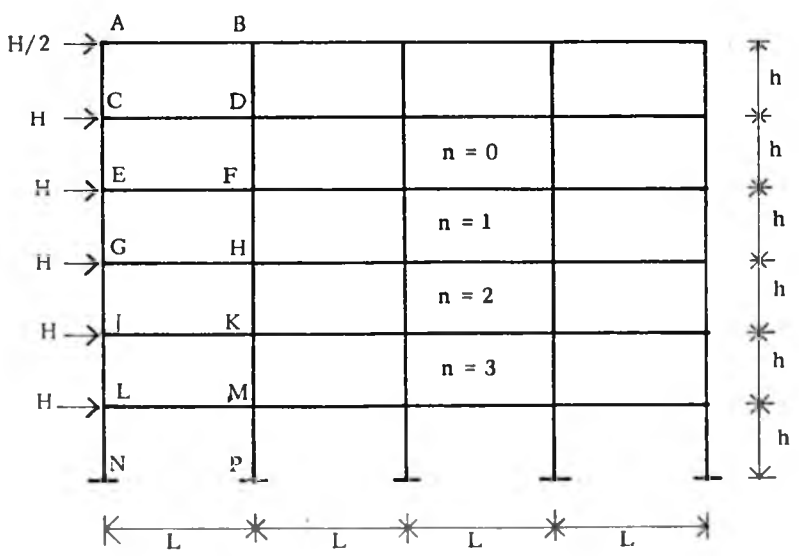

Figure 2.2

Figure (2.2) shows a 'regular' frame where all the storeys are of equal height, the bays are of equal width and the horizontal loads acting at the floor levels are of equal magnitude. Following the usual assumption of the portal method as discussed in Chapter I (Sec. 1.1), the shear in an internal column is $P(n + 1{\cdot}5)$, where $P = H/m$, H being the applied horizontal load at each intermediate level and m the number of bays. n is the indicator of the location of the storey as shown in figure (2.1). The value of n is zero for the uppermost of the intermediate storeys (i.e. the storey immediately below the topmost storey). and increases downwards. Shear in the external columns is half of that in the internal columns. It can also be shown that the axial load in an internal column is zero. Axial deformations in the external columns and in the beams are neglected, and the sway deflection, Δ, over a storey height is therefore constant for a particular storey.

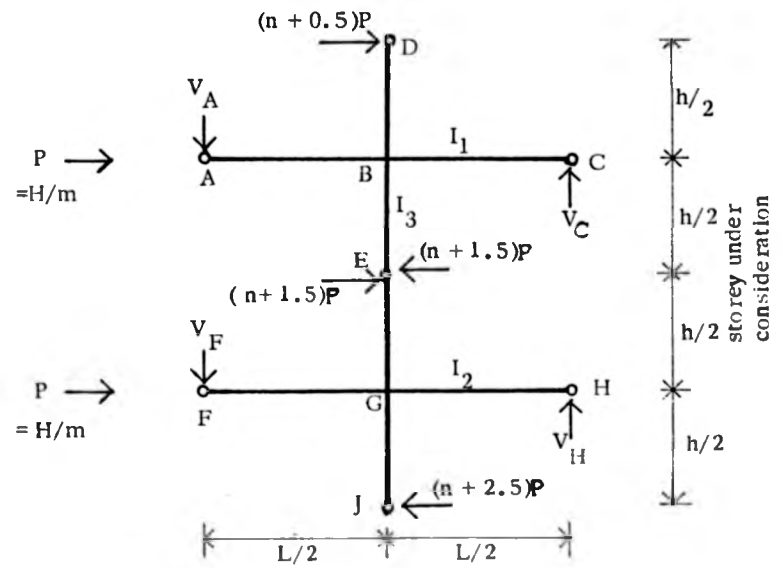

Figure 2.3

A typical internal subassemblage is shown in figure (2.3) where I_1 and I_2 denote the inertias of the upper and lower beam respectively for the storey under consideration and I_3 is the inertia of an internal column.

For the beam AB the slope-deflection equations give

$$M_{AB} = \frac{EI_1}{L} (4\theta_A + 2\theta_B) \quad \ldots \quad (2.4)$$

$$M_{BA} = \frac{EI_1}{L} (2\theta_A + 4\theta_B) \quad \ldots \quad (2.5)$$

where M_{AB} and M_{BA} are the clockwise bending moments acting on AB, at A and B respectively; θ_A and θ_B are the corresponding rotations; E is the Young's modulus of elasticity.

As it is assumed that M_{AB} is zero, equations (2.4) and (2.5) give

$$M_{BA} = \frac{6EI_1}{L} \theta_B \quad (2.6)$$

Taking moments about C for the region ABCDE.

$$V_A \frac{L}{2} = (n + 1) \frac{Ph}{2} \quad (2.7)$$

As the left hand sides of (2.6) and (2.7) are equal,

$$\theta_B = \frac{(n+1)PhL}{12EI_1} \quad (2.8)$$

Similarly, considering the region FGHEJ

$$\theta_G = \frac{(n+2)\,PhL}{12\,EI_2} \qquad (2.9)$$

where θ_G is the clockwise rotation of joint G

Applying slope-deflection equations to column BG,

$$M_{BG} = \frac{EI_3}{h}\left(4\theta_B + 2\theta_G - \frac{6\Delta}{h}\right) \qquad (2.10)$$

$$M_{GB} = \frac{EI_3}{h}\left(2\theta_B + 4\theta_G - \frac{6\Delta}{h}\right) \qquad (2.11)$$

where M_{BG} and M_{GB} are the clockwise bending moments acting on BG, at B and G respectively; Δ is the horizontal sway of BG, taken as positive when it tends to rotate the member clockwise.

As a point of contraflexure has been assumed at the mid-height of BG, $M_{BG} = M_{GB}$ and from equations (2.10) and (2.11)

$$\theta_B = \theta_G \qquad (2.12)$$

Hence, from (2.8) and (2.9)

$$I_1 = \frac{n+1}{n+2} I_2 \qquad (2.13)$$

Taking moment about G for GE

$$M_{GB} = - \frac{Ph}{2} (n + 1.5) \qquad (2.14)$$

Equating (2.11) and (2.14) and substituting for θ_B, θ_G and I_1, by equations (2.8), (2.9) and (2.13), the following expression for I_2 is obtained

$$I_2 = \frac{Prh^3 (n + 2) I_3}{12E\Delta I_3 - Ph^3 (n + 1.5)} \qquad (2.15)$$

where $r = L / h$

From (2.13) and (2.15) I_1 can be expressed in terms of I_3 as

$$I_1 = \frac{Prh^3 (n + 1) I_3}{12E\Delta I_3 - Ph^3 (n + 1{\cdot}5)} \qquad (2.16)$$

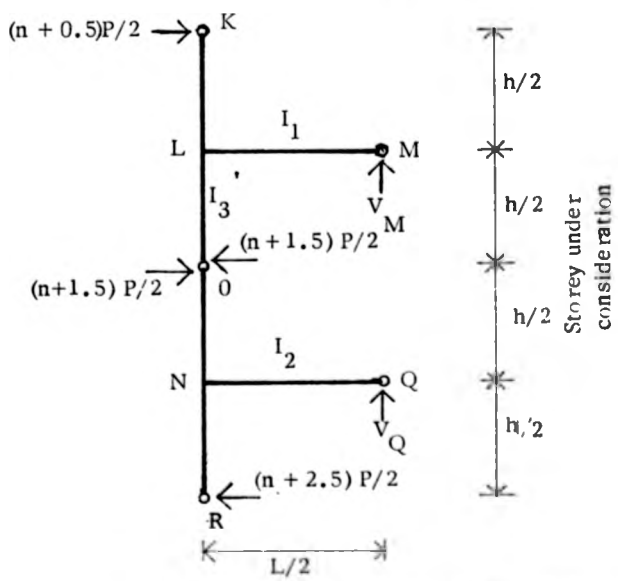

Figure 2.4

Figure (2.4) shows the external subassemblage of an intermediate storey where I_3' is the inertia of the external column. Proceeding as above

$$\theta_L = \frac{(n+1)PhL}{12EI_1} \qquad (2.17)$$

$$\theta_N = \frac{(n+2)PhL}{12EI_2} \qquad (2.18)$$

Again, for $M_{LN} = M_{NL}$, $\theta_L = \theta_N$ and from (2.17) and (2.18) the expression for I_1 is given once more by equation (2.13). Applying slope deflection equations to the column LN and substituting for θ_L, θ_N and I_1, the expression for I_2 is given by

$$I_2 = \frac{2Prh^3(n+2)I_3'}{24E\Delta I_3' - Ph^3(n+1.5)} \qquad (2.19)$$

Equating equations (2.15) and (2.19)

$$I_3' = I_3/2 \qquad (2.20)$$

Equations (2.16), (2.19) and (2.20) express the moment of inertia of all the members of an intermediate storey in terms of I_3, the inertia of the interior columns. The terms P, r, h and n are constants for the storey and in a design problem Δ is the permissible deflection over the storey height, a known quantity.

The cost of a complete frame may be represented by

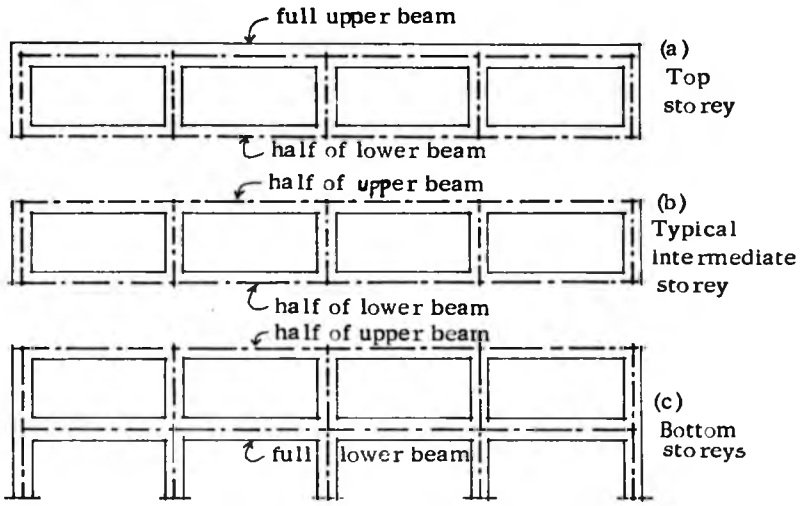

Figure 2.5

t'he summation of the cost of individual storeys by proper allocation of members to the cost function of the different storeys .Figure (2.5) shows the proposed arrangement. A typical intermediate storey will consist of half the total length of its upper and lower beams and the total length of all the columns in the storey (figure 2.5b). The topmost storey will consist of the total length of the upper beams, half the total length of the lower beams and the total length of columns (figure 2.5a). The bottom two storeys will consist of half the total length of the upper beams and the total length of the lower beams of the upper storey and the total length of columns in the two storeys (figure 2.5c) .

So, for a typical intermediate storey equation (2.3) may be expanded to express the cost function as

$$Z = \frac{mrh}{2}(q_1 I_1 + q_2 I_2) + (m-1)hq_3 I_3 + 2hq_4 I_3' \qquad (2.21)$$

where q_1 , q_2 , q_3 and q_4 are the cost factors related to I_1 , I_2 , I_3 and I_3' respectively.

Using equations (2.16), (2.19) and (2.20) values of I_1, I_2 and I_3' may now be substituted in equation (2.21) and Z obtained in terms of I_3 alone.

For minimum cost

$$\frac{dZ}{dI_3} = 0 \qquad (2.22)$$

Treating the cost factors as constants the expression for optimum value of I_3 is given as,

$$I_3 = \frac{Ph^3}{24 E \Delta}\left[2(n+1{\cdot}5) + r\sqrt{\frac{2m(n+1{\cdot}5)}{(m-1)q_3+q_4}\left\{q_1(n+1\ \ )+q_3(n+2)\right\}}\right] \qquad (2.23)$$

All the terms on the right hand side of equation (2.23) are known, except the cost factors q_1, q_2, q_3 and q_4. For the purpose of design, initial values of these cost factors may be taken as unity and the required value of I_3 calculated. Once I_3 is determined I_1, I_2 and I_3' follow from equations (2.16), (2.19) and (2.20) and the appropriate sections for the initial design are selected. If the factor 'b' of equation (2.1) is assumed to be constant for all the members of a frame, the cost factor 'q' can be expressed only by the factor 'a' of equation (2.2) which is the weight-inertia ratio of a section. When the initial sections for I_1, I_2, I_3 and I_3' have been selected, corresponding values of q_1, q_2, q_3 and q_4 can be obtained from the standard table of section properties. Equation (2.23)

is then used with these values of cost factors to calculate a new value of I_3 and correspondingly the new values of I_2, I_1 and I_3'. Iteration may be necessary to obtain a convergence when the set of sections given by two successive calculations is the same.

2.4 EXPRESSIONS FOR THE TOP STOREY

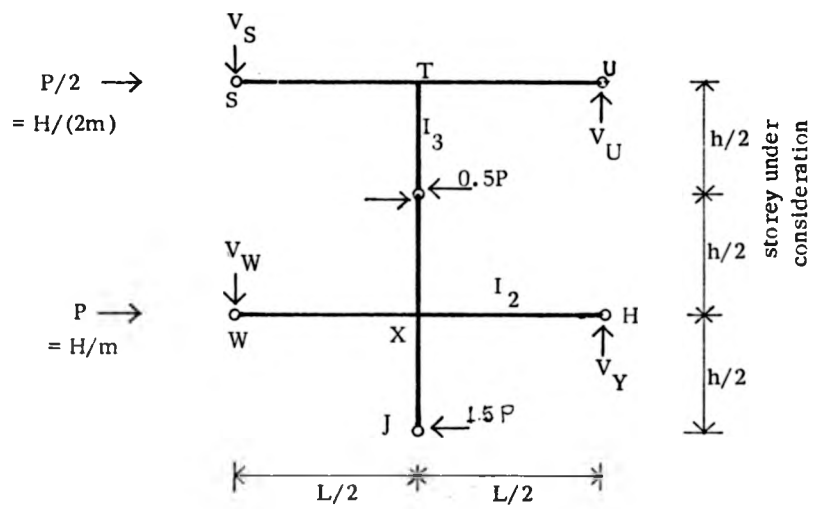

Figure 2.6

Figure (2.6) shows the subassemblage on which the design is based. Proceeding in a manner similar to that of the intermediate storey,

$$\theta_T = \frac{PhL}{48EI_1}$$

$$\theta_X = \frac{PhL}{12EI_2}$$

For $M_{TX} = M_{XT}$, $\theta_T = \theta_X$ which gives

$$I_1 = I_2/4 \qquad (2.24)$$

Again, from the slope deflection equations of column TX and substituting for the values of θ_T , θ_X and I_1 ,

$$I_2 = \frac{2P rh^3 I_3}{24E\Delta I_3 - Ph^3} \qquad (2.25)$$

From (2.24) and (2.25) ,

$$I_1 = \frac{Prh^3 I_3}{48E\Delta I_3 - 2Ph^3} \qquad (2.26)$$

Considering the external subassemblage ,

$$I_3' = I_3/2 \qquad (2.27)$$

As per discussion in Sec.2.3 (figure 2.5a) the cost of the top storey will be represented by

$$Z = mrhq_1 I_1 + \frac{mrh}{2} q_2 I_2 + (m-1) hq_3 I_3 + 2hq_4 I_3' \qquad (2.28)$$

Substituting for I_1 , I_2 , I_3' in (2.28) and minimizing Z the following expression is obtained

$$I_3 = \frac{Ph^3}{24E\Delta} \left[1 + r\sqrt{\frac{m(q_1 + 2q_2)}{2(m-1)q_3 + 2q_4}} \right] \qquad (2.29)$$

2.5 EXPRESSIONS FOR THE BOTTOM TWO STOREYS OF PINNED BASE FRAME

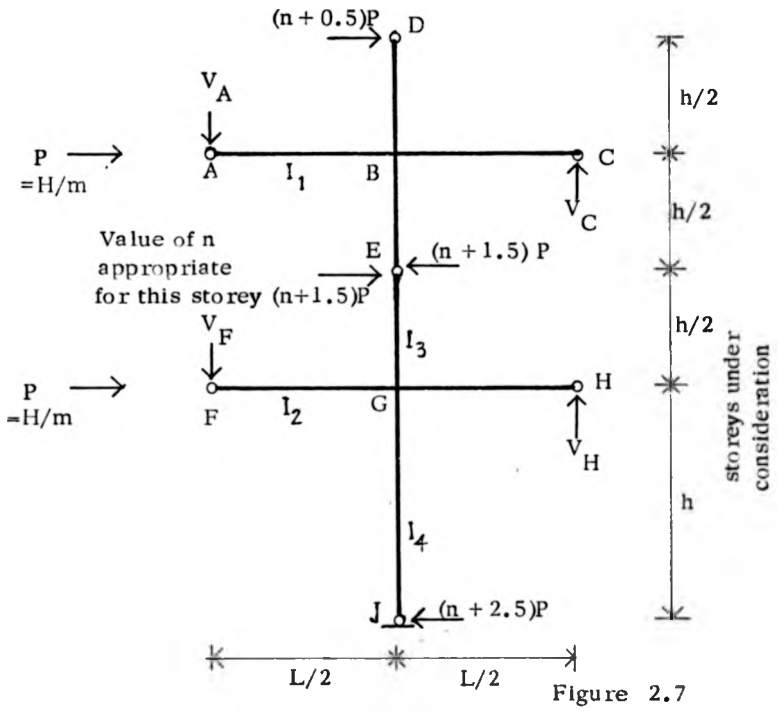

Figure 2.7

Figure (2.7) shows the subassemblage for the bottom two storeys of a pinned base frame. Proceeding as in Sec.(2.3), θ_B is found to be the same as given by equation (2.8), in which n takes the appropriate value for the storey next to the bottom, while θ_G is given as

$$\theta_G = \frac{(3n + 6{\cdot}5)\, Ph\, L}{24EI_2} \qquad (2.30)$$

From the expressions of θ_B and θ_G

$$I_1 = \frac{2(n+1)}{(3n+6.5)} I_2 \qquad (2.31)$$

Allowing the same horizontal deflection, Δ, in both the storeys θ_J is given by

$$\theta_J = \tfrac{1}{2} \left(\frac{3\Delta}{h} - \theta_G \right) \qquad (2.32)$$

Applying slope-deflection equation of column BG and substituting for θ_B and θ_G from (2.8) and (2.30),

$$I_2 = \frac{(3n + 6{\cdot}5)\, Prh^3 I_3}{24\, E\Delta I_3 - 2(n + 1{\cdot}5)\, Ph^3} \qquad (2.33)$$

where I_3 is the column inertia of the storey above the bottom.

From (2.31) and (2.33)

$$I_1 = \frac{(n + 1)\, Prh^3 I_3}{12\, E\Delta I_3 - (n + 1{\cdot}5) Ph^3} \qquad (2.34)$$

Applying slope-deflection equation of column GJ and substituting for θ_G and θ_J from (2.30) and (2.32)

$$I_2 = \frac{(3n + 6{\cdot}5)\, Prh^3 I_4}{24 E\Delta I_4 - 8\, (n + 2{\cdot}5)\, Ph^3} \qquad (2.35)$$

where I_4 is the column inertia of the bottom storey.

From (2.33) and (2.35)

$$I_4 = \frac{4(n + 2{\cdot}5)}{(n + 1{\cdot}5)}\, I_3 \qquad (2.36)$$

Considering the external subassemblages, inertia of the external columns are again given as

$$I_3' = I_3 / 2 ; \quad I_4' = I_4 / 2 \qquad (2.37)$$

The cost of the bottom two storeys (figure 2.5c) is represented by

$$Z = \frac{mrh}{2} q_1 I_1 + mrhq_2 I_2 + (m-1) hq_3 I_3 + 2hq_4 I_3' + (m-1) hq_5 I_4 + 2hq_6 I_4' \qquad (2.38)$$

where q_5 and q_6 are the corresponding cost factors related to I_4 and I_4'.

Replacing I_1 , I_2 , I_4 , I_3' and I_4' in equation (2.38) by using (2.34) , (2.33), (2.36) and (2.37) and minimising,the optimum value of I_3 is given by

$$I_3 = \frac{Ph^3(n+1{\cdot}5)}{12E\Delta}\left[1 + r\sqrt{\frac{m\{q_1(n+1)+q_2(3n+6{\cdot}5)\}}{2(n+1{\cdot}5)\{(m-1)q_3+q_4\}+8(n+2.5)(m-1)q_5+q_6\}}}\right]$$

(2.39)

The pinned base frames require high values for I_2 and I_4 and relatively very low values for I_3 as the column BG and GJ have been allowed to deflect by the same amount, Δ. For typical values of n and r I_3 given by equation (2.39) will be less than the inertia required for the column above B, thus causing reverse taper. Also the value of I_1 given by equation (2.34) is found to be slightly different from that given for this beam by design of the storey above B.

It is therefore proposed that the design of the third storey be used to determine the values for I_1 , I_3 and I_3' in the bottom two storeys. The cost of the bottom two storeys can now be represented by

$$Z = mrhq_2 I_2 + (m-1)hq_5 I_4 + 2hq_6 I_4^1 + \text{constant terms} \qquad (2.40)$$

Substitution for I_2 and I_4' in (2.40) by using (2.35) and (2.37) and differentiation to minimise Z leads to

$$I_4 = \frac{Ph^3}{24E\Delta}\left[2(n+1{\cdot}5) + r\sqrt{\frac{2mq_2(n+2{\cdot}5)(3n+6{\cdot}5)}{(m-1)q_3+q_4}}\right] \qquad (2.41)$$

I_2 and I_4' are given by equation (2.40) and (2.35). Although equation (2.41) is for the bottom storey column, the value of n is the one appropriate for the storey next to the bottom.

2.6 EXPRESSIONS FOR THE BOTTOM TWO STOREYS OF FIXED BASE FRAME

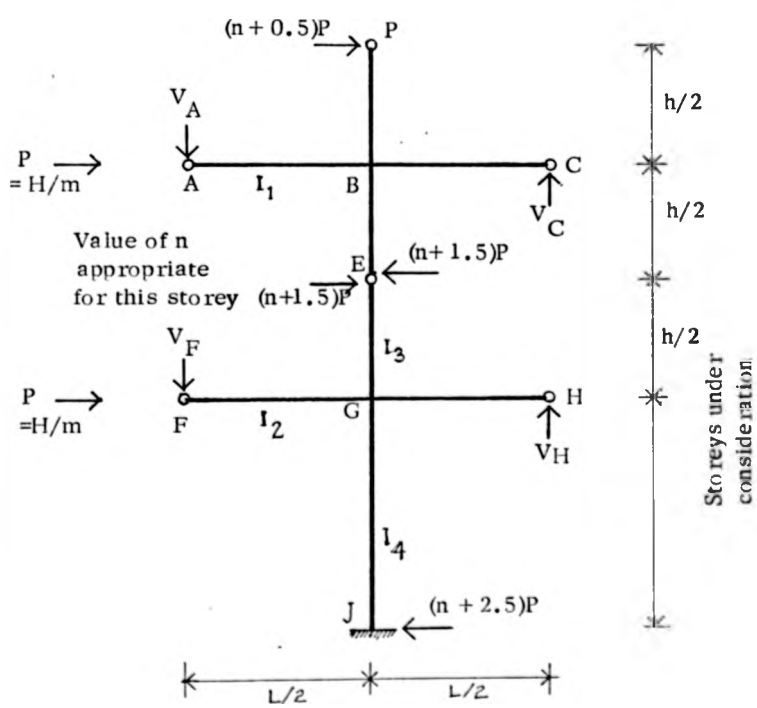

Figure 2.8

The design is based on the subassemblage shown in figure (2.8). Comparison with figure (2.3) shows that equation (2.8) can still be used for θ_B by taking the value of n appropriate for the storey next to the bottom.

The sway equation for GJ is given by

$$M_{GJ} + M_{JG} + (n + 2{\cdot}5)\,Ph = 0 \qquad (2.42)$$

and from slope deflection equations for GJ

$$M_{GJ} = \frac{EI_4}{h}\left(4\theta_G - \frac{6\Delta}{h}\right) \qquad (2.43)$$

$$M_{JG} = \frac{EI_4}{h}\left(2\theta_G - \frac{6\Delta}{h}\right) \qquad (2.44)$$

This leads to

$$\Delta = \frac{(n + 2{\cdot}5)\,Ph^3}{12EI_4} + \frac{h}{2}\theta_G \qquad (2.45)$$

Considering equilibrium of moments at joint G

$$M_{GF} + M_{GH} + M_{GJ} - (n + 1{\cdot}5)\,\frac{Ph}{2} = 0 \qquad (2.46)$$

By the slope deflection equations for FG and GH

$$M_{GF} = M_{GH} = \frac{6EI_2}{L}\,\theta_G$$

and M_{GJ} is given by (2.43).

Substituting in (2.46) and replacing Δ by using (2.45)

$$\theta_G = \frac{(n+2)\,Ph^2 L}{ELI_4 + 12\,EhI_2} \tag{2.47}$$

As in the case of pinned base frame , equations (2.10) - (2.12) and (2.14) also apply to the subassemblage of figure (2.7). The derivation of expressions for I_1 and I_2 therefore follows the same steps as the derivation of (2.13) and (2.15) with (2.47) replacing (2.9). The results are

$$I_1 = \frac{(n+1)(rI_4 + 12\,I_2)}{12\,(n+2)} \tag{2.48}$$

$$I_2 = \frac{12\,(n+2)\,Prh^3 I_3 + (n+1{\cdot}5)\,Prh^3 I_4 - 12\,E\Delta rI_3 I_4}{12[\,12\,E\Delta I_3 - (n+1{\cdot}5)\,Ph^3\,]} \tag{2.49}$$

The representation of cost is given by equation (2.38) in which I_3' and I_4' can be taken as half of I_3 and I_4 respectively.

Accurate analysis has shown that unless the frame is lower than four storeys or L is less than h , fixity of the column base will result in a higher value for I_3 than that for I_4 if the same amount of deflection, Δ , is allowed in both the storeys. To avoid reverse taper I_4 is therefore taken equal to I_3. Expressions for I_1 and I_2 change to

$$I_1 = \frac{(n+1)(r\,I_3 + 12\,I_2)}{12\,(n+2)} \tag{2.50}$$

$$I_2 = \frac{(13n + 25{\cdot}5)\,Prh^3 I_3 - 12\,E\Delta rI_3^{\,2}}{12[\,12E\,\Delta I_3 - (n+1{\cdot}5)\,Ph^3)\,]} \tag{2.51}$$

The cost expression is now given by

$$Z = \frac{mrh}{2} q_1 I_1 + mrhq_2 I_2 + 2(m-1)hq_3 I_3 + 4hq_4 I_3^* \qquad (2.52)$$

Using (2.50) and (2.51) I_1 and I_2 can be substituted in (2.52) and I_3^* taken as $I_3/2$. Differentiation of the expression for Z with respect to I_3 leads to the following expression if Z is to be a minimum ,

$$I_3 = \frac{Ph^3}{12E\Delta}\left[(n+1{\cdot}5) + r\sqrt{\frac{6m(n+1{\cdot}5)\{q_1(n+1)+2q_2(n+2)\}}{24\{(m-1)q_3+q_4\} - q_2 mr^2}}\right] \qquad (2.53)$$

I_2 and I_1 may now be calculated by using (2.50) and (2.51) while $I_4 = I_3$ and $I_4' = I_3^* = I_3/2$.

2.7 DESIGN OF A SIX-STOREY FOUR BAY FRAME

Use of the equations derived so far will be illustrated by designing the frame of figure (2.2) with H = 20 kN , h = 3·5 m, L = 7m , E = 210 kN/mm^2 and Δ = h/350. For the initial design the cost factors are taken as unity. As a result the design expressions are simplified as follows :

(i) Top storey

$$I_3 = \frac{Ph^3}{24E\Delta}\left(1 + r\sqrt{1{\cdot}5}\right) \qquad (2.54)$$

$$I_2 = \frac{I_3}{\sqrt{6}} \qquad (2.55)$$

I_1 is given by (2.24)

(ii) Intermediate storey

$$I_3 = \frac{Ph^3}{12E\Delta} (n + 1{\cdot}5)(1 + r) \qquad (2.56)$$

$$I_2 = \frac{n + 2}{n + 1{\cdot}5} I_3 \qquad (2.57)$$

I_1 is given by (2.13).

(iii) Bottom storeys (Pinned base)

$$I_4 = \frac{Ph^3}{12E\Delta} \left[4 (n + 2.5) + r\sqrt{(2n + 5)(3n + 6.5)} \right] \qquad (2.58)$$

Expressions for other members are the same as in Sec. (2.5).

(iv) Bottom storeys (Fixed base)

$$I_3 = \frac{Ph^3}{12E\Delta} \left[(n + 1{\cdot}5) + r\sqrt{\frac{6(n + 1{\cdot}5)(3n + 5)}{24 - r^2}} \right] \qquad (2.59)$$

Expressions for other members are the same as in Sec. (2.6).

The bottom two storeys of the frame have at first been designed considering the columns to be pinned at the base and then again as fixed base. The results are shown in table (2.3).

	Beams		Internal column		External columns	
	Member	Inertia cm^4	Member	Inertia cm^4	Member	Inertia cm^4
	AB	599	BD	1467	AC	734
	CD	2552	DF	3828	CE	1914
	EF	5104	FH	6380	EG	3190
	GH	7656	HK	8932	GJ	4466
pinned base	JK	10208	KM	8932	JL	4466
	LM	24292	MP	40934	LN	20467
fixed base	JK	10328	KM	11224	JL	5612
	LM	11040	MP	11224	LN	5612

Table 2.3

Although the beams EF and GH are designed twice, once as I_2 of the storey above the beam and then as I_1 of the storey below the beam, both the calculations will give identical values for a particular beam with cost factors as unity. Even when the exact weight-inertia ratios are taken as cost factors the differences do not exceed 6% of the larger value in frames having $L \geqslant h$. The beam CD has also been designed twice, as part of the top storey and part of an intermediate storey. The difference between the two inertias will not exceed 10% of the smaller value. In the fixed base case the beam JK has been designed twice and the higher value has been taken. Again, the difference between the two values will usually be very small.

To check the validity of the method, the pinned base design has been analysed by a computer program based on the matrix displacement method neglecting axial deformation of the members. Results showed the horizontal deflections, from top to bottom, as 9.73, 10·01, 9·99, 9·92, 10·30 and 10·06 mm. The overall sway was 60·02 mm. The low deflection of the top storey arose because the inertia adopted for the beam CD was that required to control the deflection over the storey height below CD. This was greater than the inertia given for CD by the top storey design equations. In the second storey up from the base, the points of contraflexure in the columns were 4% away from the midheight position assumed in deriving the expressions of Sec. (2.5). This resulted in the deflections for the bottom three storeys departing slightly from the permissible value. However, the results show that the proposed method is sufficiently accurate for the purpose of design.

The fixed base design has also been analysed by the computer, the corresponding deflections from top to bottom being 9·73, 10·01, 9·99, 9·96, 10·01 and 7·46 mm. The low value for the bottom storey is due to the column inertia for this level being governed by the need to avoid reverse taper.

The design equations, based on assumed points of contraflexure, give beam and column inertias which increase down the frame in proportion to the increasing horizontal shear. Intuitively this would seem to be the optimum arrangement. The success of the method in giving the optimum ratio between beam inertia and column inertia has also been examined.

As the q values have been taken as unity so far in the design of the six-storey four-bay frame, the cost, C, has been represented by

$$C = \Sigma IL \qquad (2.60)$$

the summation being over all the members of the frame.

To test optimality, the column inertias for the pinned base design were reduced by 5% and the beam inertias increased by 3·5% so as to maintain the same value of C as earlier. The frame was then analysed accurately. For a second alternative the column inertias of the original design were increased by 5% while the beams were reduced by 3·5%. The frame was analysed again.

In the first instance the deflection of the storeys, starting from the top, were 9·66 , 9·96, 9·94, 9·88, 10·32 and 10·12 mm, i.e. an overall deflection of 59·88 mm. When the columns were increased, the corresponding deflections were 9·84, 10·09, 10·07, 10·00, 10·31 and 10·05 mm, i.e. an overall deflection of 60·36 mm.

Comparison of these results with the deflections given by the design of table (2.3) show that by using slightly less stiff columns with stiffer beams a little more economy could be achieved for the same overall deflection. But this would lead to greater deflections in the bottom two storey violating the permissible limits.

Similar alternative analysis of the fixed base frame, however, showed that both the modified designs had greater overall deflections than those given by the proposed method. It is concluded that the method generates beam and column inertias which are sufficiently close to the optimum for practical design.

The initial design solution shown in table (2.3) is based on unit values of the cost factors. Once these inertias have been calculated and sections chosen, the values of the cost factors corresponding to the sections can be determined. The frame can then be redesigned using the actual 'q'-values. Iteration can be carried out with the latest 'q'-values until convergence onto one set of sections is obtained.

Table (2.4) shows the standard rolled sections selected from tables (2.1) and (2.2) for the members of the frame corresponding to the inertias given in table (2.3) for the fixed base frame.

Beams			Internal Columns			External Columns		
	UB sections	q $\times 10^{-4}$ kg/cm^5		UC sections	q		UC sections	q
AB	152 x 89(RSJ)	1.94	BD	152 x 152 x 30	1.72	AC	152 x 152 x 23	1.82
CD	254x102x 22	0.77	DF	203 x 203 x 46	1.01	CE	152 x 152 x 37	1.67
EF	305x102x 28	0.52	FH	203 x 203 x 71	0.93	EG	203 x 203 x46	1.01
GH	356x127x 33	0.40	HK	254 x 254 x 73	0.64	GJ	203 x 203 x46	1.01
JK	406x140x 39	0.31	KM	254 x 254 x 73	0.64	JL	203 x 203 x 60	0.99
LM	406x140z 39	0.31	MP	254 x 254 x 73	0.64	LN	203 x 203 x 60	0.99

Table 2.4

Beams		Internal Columns		External Columns	
Member	Inertia cm^4	Member	Inertia cm^4	Member	Inertia cm^4
AB	638	BD	1275	AC	637
CD	2779	DF	3290	CE	1645
EF	5748	FH	5213	EG	2606
GH	8661	HK	7250	GJ	3625
JK	12503	KM	8401	JL	4201
LM	14228	MP	8401	LN	4201

Table 2.5

Beams			Internal Columns			External Columns		
	UB sections	q $\times 10^{-4}$ kg/cm^5		UG sections	q		UC sections	q
AB	152 x 89(RSJ)	1.94	BD	152 x 152 x23	1.82	AC	152x152x23	1.82
CD	254 x102 x 22	0.77	DF	203 x 203 x46	1.01	CE	152x152x30	1.72
EF	356 x 127 x 33	0.40	FH	203 x 203 x52	0.99	EG	203x203x46	1.01
GH	406 x 140 x 39	0.31	HK	203 x 203 x71	0.93	GJ	203x 203x46	1.01
JK	406 x 140 x 39	0.31	KM	254 x 254 x73	0.64	JL	203x 203x46	1.01
LM	406 x 140 x 46	0.29	MP	254 x 254 x73	0.64	LN	203x 203x 46	1.01

Table 2.6

As discussed in Sec. (2.3) the cost factor consists of the terms 'a' and 'b' (equation 2.2). While the factor 'a' is the weight-inertia ratio of the rolled sections the factor 'b' was used to allow for

(i) different percentage increases on the weight of the members of a frame to include connections, stiffeners etc., and

(ii) different cost rates for different members.

It is common practice to assume that the same percentage increase and the same rate apply to all members. For a rigid-jointed frame a uniform increase of about 10% is generally made to allow for the connections, stiffeners etc. As 'b' is therefore constant the cost factor , q , may be assumed to depend solely upon the weight-inertia ratio of the sections selected which are shown in table (2.4). These values are now used in the equations to give revised inertias which are shown in table (2.5) and the corresponding rolled sections are shown in table (2.6). The relatively high q-values for the columns of the initial design have led to a redistribution of stiffness towards the beams to achieve optimality in the overall cost. When the procedure is repeated once more, using q-values of table (2.6) , changes in the inertias are not significant enough to cause any further change of sections.

Comparing the total weight of the members in tables (2.4) and (2.6) it is found that the final design is only 0·3% lighter than the initial design. This is due to the restricted range of available sections, showing that the use of equation (2.60) to represent the cost may be adequate. Design on the basis of equation (2.60) enables the use of simple expressions (equations 2.54 - 2.59) and avoids any iteration.

CHAPTER III

NON-UNIFORM MULTISTOREY FRAMES: OPTIMUM DESIGN TO DEFLECTION LIMITATIONS.

3.1 INTRODUCTION

Multistorey frames having unequal bay width and/or unequal storey heights are defined here as 'non-uniform' frames. 'Regular' frames with unequal horizontal loads acting at the joints shall also be considered to be in this category. Design equations for such frames will be complex compared to those for the 'regular' frames. Moreover, in frames with varying storey heights the design procedure for the bottom two storeys is not a straightforward one. Comparative design studies with different sets of equations satisfying the permissible deflections of each of the two storeys are necessary.

Figure (3.1) shows the intermediate storey subassemblage of a 'non-uniform' frame. According to the assumptions of the Portal method (Sec.1.1 of chapter I) the total horizontal shear at any level is divided between the bays in proportion to their relative widths.

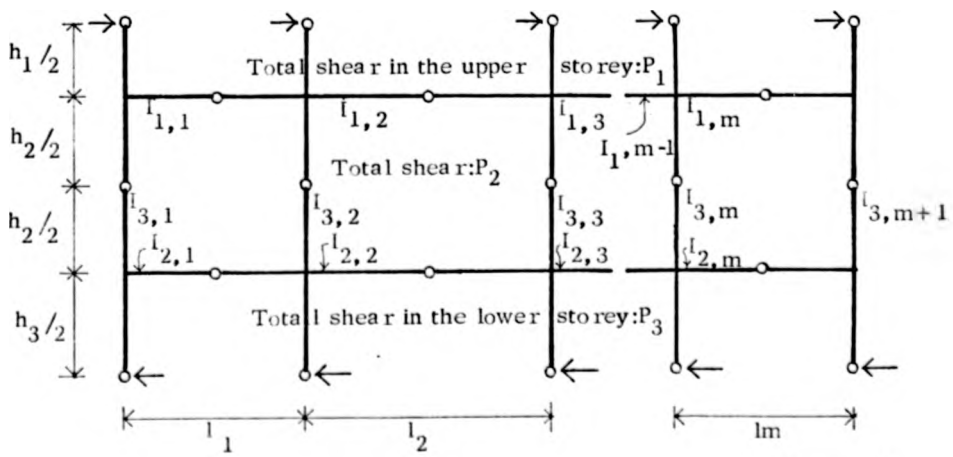

Figure 3.1

It can therefore be shown that for the columns ,

$$\frac{I_{3,1}}{l_1} = \frac{I_{3,2}}{l_1 + l_2} = \frac{I_{3,3}}{(l_2 + l_3)} = \ldots = \frac{I_{3,m+1}}{l_m} \qquad (3.1)$$

where $I_{3,1}$, $I_{3,2}$, $I_{3,3}$, ..., $I_{3,m+1}$ are the column inertias, m being the number of bays and

l_1, l_2, l_3, ..., l_m are the bay widths .

The beam stiffness will depend on the bay widths. Thus, for the lower beams of the storey,

$$\frac{I_{2,1}}{l_1^2} = \frac{I_{2,2}}{l_2^2} = \frac{I_{2,3}}{l_3^2} = \ldots = \frac{I_{2,m}}{l_m^2} \qquad (3.2)$$

and similarly for the upper beams of the storey ,

$$\frac{I_{1,1}}{l_1^2} = \frac{I_{1,2}}{l_2^2} = \frac{I_{1,3}}{l_3^2} = \ldots = \frac{I_{1,m}}{l_m^2} \qquad (3.3)$$

where $I_{2,1}$, $I_{2,2}$, $I_{2,3}$, ..., $I_{2,m}$ are the inertias of the lower beams ,

and $I_{1,1}$, $I_{1,2}$, $I_{1,3}$, ..., $I_{1,m}$ are the inertias of the upper beams.

It can therefore be shown that for the columns ,

$$\frac{I_{3,1}}{l_1} = \frac{I_{3,2}}{l_1 + l_2} = \frac{I_{3,3}}{(l_2 + l_3)} = \ldots\ldots = \frac{I_{3,m+1}}{l_m} \qquad (3.1)$$

where $I_{3,1}$, $I_{3,2}$, $I_{3,3}$, ..., $I_{3,m+1}$ are the column inertias, m being the number of bays and

l_1 , l_2 , l_3 ,....., l_m are the bay widths .

The beam stiffness will depend on the bay widths. Thus, for the lower beams of the storey,

$$\frac{I_{2,1}}{l_1^2} = \frac{I_{2,2}}{l_2^2} = \frac{I_{2,3}}{l_3^2} = \ldots. = \frac{I_{2,m}}{l_m^2} \qquad (3.2)$$

and similarly for the upper beams of the storey ,

$$\frac{I_{1,1}}{l_1^2} = \frac{I_{1,2}}{l_2^2} = \frac{I_{1,3}}{l_3^2} = \ldots.. = \frac{I_{1,m}}{l_m^2} \qquad (3.3)$$

where $I_{2,1}$, $I_{2,2}$, $I_{2,3}$, ... , $I_{2,m}$ are the inertias of the lower beams ,

and $I_{1,1}$, $I_{1,2}$, $I_{1,3}$, ... , $I_{1,m}$ are the inertias of the upper beams.

3.2 EXPRESSIONS FOR INTERMEDIATE STOREYS

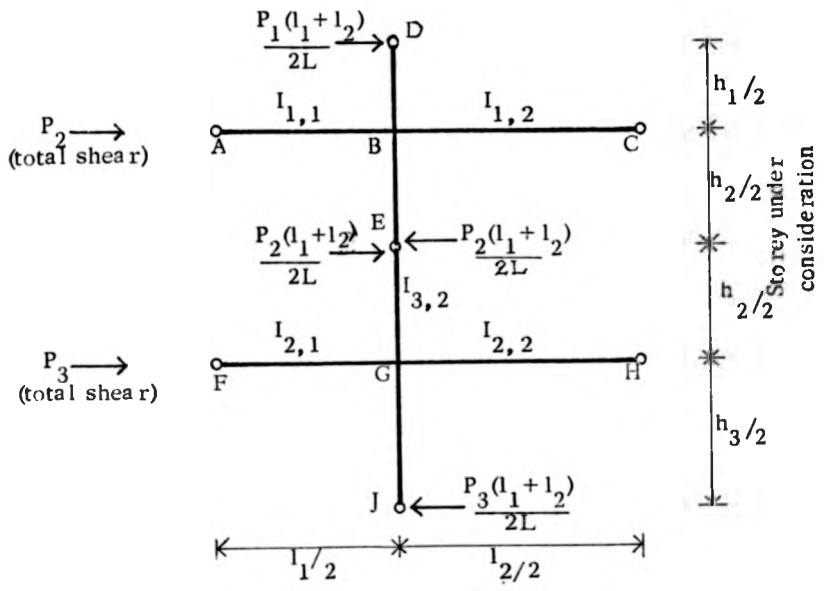

Figure 3.2.

Figure (3.2) shows the subassemblage consisting of the second column from the windward face, in between the first and second bay of a typical intermediate storey.

P_2 is the total horizontal shear in the columns of the storey under consideration while P_1 and P_3 are those in the storey above and below respectively. $L(= l_1 + l_2 + l_3 + \ldots + l_m)$ is the total width of the frame.

Proceeding as in Sec. (2.3),

$$\theta_B = \frac{(P_1 h_1 + P_2 h_2)\, l_2^2}{24\, E L\, I_{1,2}} \tag{3.4}$$

and $$\theta_G = \frac{(P_2 h_2 + P_3 h_3)\, l_2^2}{24\, E L\, I_{2,2}} \tag{3.5}$$

For $M_{BG} = M_{GB}$, $\theta_B = \theta_G$. From (3.4) and (3.5)

$$I_{1,2} = \frac{(P_1 h_1 + P_2 h_2)}{(P_2 h_2 + P_3 h_3)}\ I_{2,2} \tag{3.6}$$

Applying the slope deflection equations for column BG

$$M_{BG} = \frac{EI_{3,2}}{h_2}\ (4\theta_B + 2\theta_G - \frac{6\Delta}{h_2})$$

$$M_{GB} = \frac{EI_{3,2}}{h_2}\ (2\theta_B + 4\theta_G - \frac{6\Delta}{h_2}) \tag{3.7}$$

Δ being the horizontal deflection of the storey.

Again, taking moment about G, for GE

$$M_{GB} = -\frac{(l_1 + l_2)\, P_2 h_2}{4L} \tag{3.8}$$

Using (3.6), (3.7) and (3.8), $I_{2,2}$ is given as

$$I_{2,2} = \frac{(P_2 h_2 + P_3 h_3)\, h_2 l_2^2 I_{3,2}}{24\, E\Delta L\, I_{3,2} - (l_1 + l_2) P_2 h_2^3} \tag{3.9}$$

From (3.6) and (3.9)

$$I_{1,2} = \frac{(P_1 h_1 + P_2 h_2)\, h_2 l_2^2\, I_{3,2}}{24\, E \Delta L\, I_{3,2} - (l_1 + l_2)\, P_2 h_2^3} \qquad (3.10)$$

Applying the same principle as adopted for the regular frame (figure 2.4b) the cost function for an intermediate storey of 'non-uniform' frame may be expressed as

$$\begin{aligned} Z = {} & (I_{1,1} q_{1,1} l_1 + I_{1,2} q_{1,2} l_2 + \ldots\ldots + I_{1,m} q_{1,m} l_m)/2 + \\ & (I_{2,1} q_{2,1} l_2 + I_{2,2} q_{2,2} l_2 + \ldots\ldots + I_{2,m} q_{2,m} l_m)/2 + \\ & (I_{3,1} q_{3,1} + I_{3,2} q_{3,2} + \ldots\ldots + I_{3,m} q_{3,m} + I_{3,m} q_{3,m+1})\, h_2 \end{aligned} \qquad (3.11)$$

where

$q_{1,1}, q_{1,2} \ldots\ldots, q_{1,m}$ are the cost factor of the upper beams ,

$q_{2,1}, q_{2,2}, \ldots\ldots q_{2,m}$ are the cost factors of the lower beams ,

$q_{3,1}, q_{3,2} \ldots\ldots, q_{3,m+1}$ are the cost factors of the columns.

Using equations (3.1) , (3,2) and (3.3) in (3.11), Z can be expressed in terms of $I_{1,2}$, $I_{2,2}$ and $I_{3,2}$ as follows

$$Z = W_1 I_{1,2} + W_2 I_{2,2} + W_3 h_2 I_{3,2} \qquad (3.12)$$

where

$$W_1 = \frac{q_{1,1} l_1^3 + q_{1,2} l_2^3 + \ldots + q_{1,m} l_m^3}{2 l_2^2}$$

$$W_2 = \frac{q_{2,1} l_1^3 + q_{2,2} l_2^3 + \ldots\ldots + q_{2,m} l_m^3}{2 l_2^2}$$

$$W_3 = \frac{(q_{3,1}+q_{3,2})\,l_1 + (q_{3,2}+q_{3,3})\,l_2 + \ldots + (q_{3,m}+q_{3,m+1})\,l_m}{l_1 + l_2}$$

Equations (3.9) and (3.10) may now be used in (3.12) to express the cost functions in terms of $I_{3,2}$ alone. Differentiating Z with respect to $I_{3,2}$ and equating to zero, the optimum value of $I_{3,2}$ is given by

$$I_{3,2} = \frac{P_2 h_2^3 (l_1+l_2) + h_2 l_2 \sqrt{\frac{P_2 h_2 (l_1+l_2)}{W_3}\,[W_1(P_1h_1+P_2h_2) + W_2(P_2h_2+P_3h_3)]}}{24E\Delta L} \qquad (3.13)$$

During differentiation, q-terms were assumed to be constants. So, equations (3.13), (3.10) and (3.6) give the optimum inertias for column and beams of the second bay. Once these are found, the required inertias of the other members of the storey can be calculated by using (3.1), (3.2) and (3.3).

3.3. EXPRESSIONS FOR THE TOP STOREY

The cost function, Z, for the top storey of a non-uniform frame

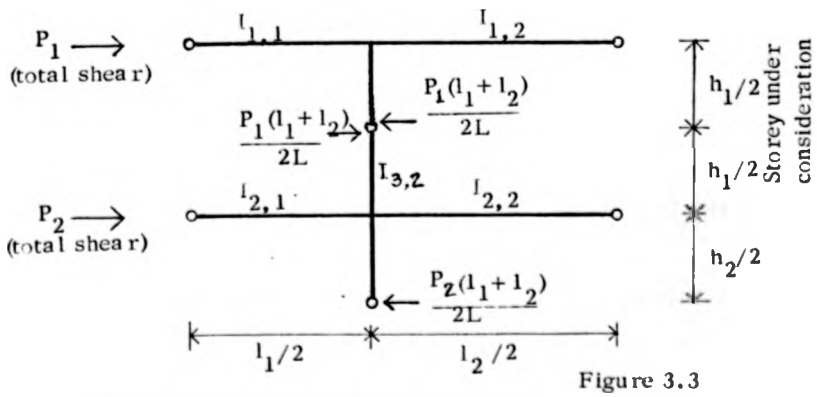

Figure 3.3

may be expressed in terms of the inertia of the members in its second bay (figure 3.3) as

$$Z = 2W_1 I_{1,2} + W_2 I_{2,2} + W_3 h_2 I_{3,2} \qquad (3.14)$$

where W_1, W_2 and W_3 are as defined previously.

Proceeding as in the previous cases, the optimum inertia of the members in the second bay are expressed by the following equations :

$$I_{3,2} = \frac{P_1 h_1^3 (l_1 + l_2) + h_1 l_2 \sqrt{\frac{P_1 h_1 (l_1 + l_2)}{W_3} [\, 2W_1 P_1 h_1 + W_2 (P_1 h_1 + P_2 h_2)\,]}}{24 E \Delta L} \qquad (3.15)$$

$$I_{2,2} = \frac{(P_1 h_1 + P_2 h_2) h_1 l_2^2 I_{3,2}}{24 E \Delta L l_{3,2} - P_1 h_1^3 (l_1 + l_2)} \qquad (3.16)$$

$$I_{1,2} = \frac{P_1 h_1}{P_1 h_1 + P_2 h_2} I_2 \qquad (3.17)$$

P_1, P_2, h_1, h_2, l_1 and l_2 are as shown in figure (3.3), Δ is the horizontal deflection of the top storey and L is the total width of the frame.

3.4 EXPRESSIONS FOR PINNED BASE BOTTOM STOREYS

Figure (3.4) shows the subassemblage consisting of the second column from the windward face of the pinned base bottom storeys of a non-uniform frame.

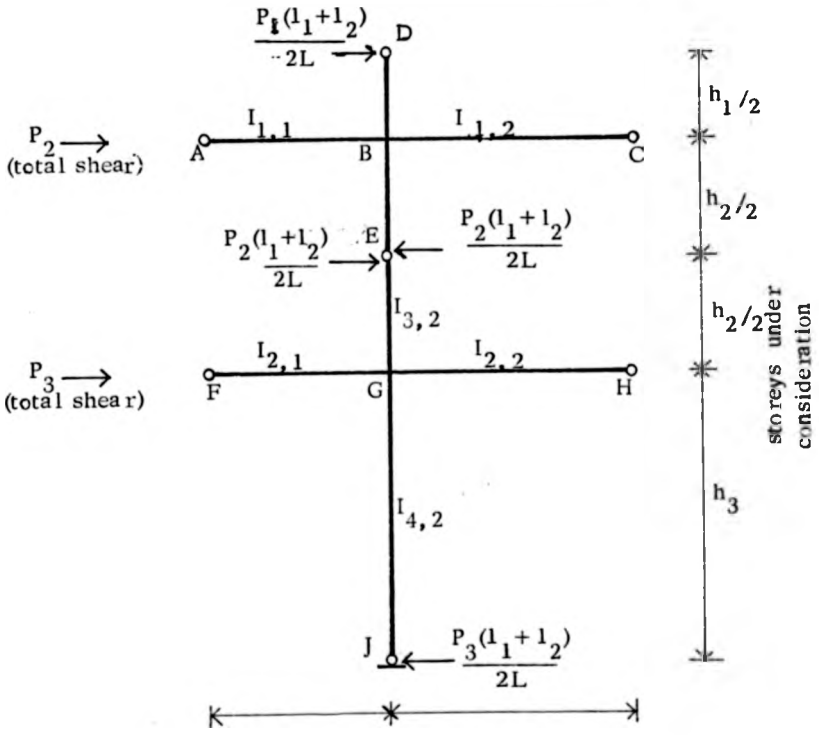

Figure 3.4

Unlike the case of 'regular' frame the bottom storeys of a 'non-uniform' frame may have different permissible values of deflection for the two

storeys (if $h_2 \neq h_3$) say, Δ_b for the bottom storey and Δ_t for the second storey from the bottom.

In a pinned-base frame, unless h_2 is significantly larger than h_3, the permissible deflection of the bottom storey, i.e. Δ_b, will govern the design and the required $I_{4,2}$ will be considerably larger than $I_{3,2}$. The beam $I_{2,2}$ will also be very large compared to $I_{1,2}$. Considering joint G and proceeding as earlier,

$$\theta_G = \frac{(P_2 h_2 + 2P_3 h_3) l_2^2}{24 E I_{2,2}} \qquad (3.18)$$

By using the slope-deflection of column GJ and the condition that $M_{JG} = 0$, rotation of the joint J is given as

$$\theta_J = \tfrac{1}{2} \left(\frac{3\Delta_b}{h_3} - \theta_G \right) \qquad (3.19)$$

and $$M_{GJ} = \frac{E I_{4,2}}{h_3} \left(4\theta_G + 2\theta_J - \frac{6\Delta_b}{h_3} \right) \qquad (3.20)$$

Again, $$M_{GJ} = - \frac{P_3 h_3}{2L} (l_1 + l_2) \qquad (3.21)$$

Using equations (3.18) - (3.21),

$$I_{2,2} = \frac{(P_2 h_2 + 2P_3 h_3) h_3 l_2^2 I_{4,2}}{24 E \Delta_b L I_{4,2} - 4 P_3 h_3^3 (l_1 + l_2)} \qquad (3.22)$$

storeys (if $h_2 \neq h_3$) say, Δ_b for the bottom storey and Δ_t for the second storey from the bottom.

In a pinned-base frame, unless h_2 is significantly larger than h_3, the permissible deflection of the bottom storey, i.e. Δ_b, will govern the design and the required $I_{4,2}$ will be considerably larger than $I_{3,2}$. The beam $I_{2,2}$ will also be very large compared to $I_{1,2}$.

Considering joint G and proceeding as earlier,

$$\theta_G = \frac{(P_2 h_2 + 2P_3 h_3) l_2^2}{24 E I_{2,2}} \qquad (3.18)$$

By using the slope-deflection of column GJ and the condition that $M_{JG} = 0$, rotation of the joint J is given as

$$\theta_J = \tfrac{1}{2} \left(\frac{3\Delta_b}{h_3} - \theta_G \right) \qquad (3.19)$$

and $$M_{GJ} = \frac{E I_{4,2}}{h_3} \left(4\theta_G + 2\theta_J - \frac{6\Delta_b}{h_3} \right) \qquad (3.20)$$

Again, $$M_{GJ} = - \frac{P_3 h_3}{2L} (l_1 + l_2) \qquad (3.21)$$

Using equations (3.18) - (3.21),

$$I_{2,2} = \frac{(P_2 h_2 + 2P_3 h_3) h_3 l_2^2 I_{4,2}}{24 E \Delta_b L l_{4,2} - 4 P_3 h_3^3 (l_1 + l_2)} \qquad (3.22)$$

From the discussion in Sec. (2.5) if $h_3 \geq h_2$, $I_{3,2}$ required to satisfy Δ_t will usually be smaller than the corresponding column inertia of the third storey from bottom, i.e. of column BD (figure 3.4). Also the required $I_{1,2}$ will be smaller than the inertia required for the same beam as part of the third storey. So, to avoid reverse taper in the column, the same section will be used in the second and third storeys.

The cost function for the bottom storeys can therefore be expressed, similar to equation (2.40), as

$$Z = 2W_2 I_{2,2} + W_4 h_3 I_{4,2} + \text{constant terms} \qquad (3.23)$$

where

$$W_4 = \frac{(q_{4,1} + q_{4,2})\, l_1 + (q_{4,2} + q_{4,3})\, l_2 + \ldots + (q_{4,m} + q_{4,m+1})\, l_m}{l_1 + l_2}$$

$q_{4,1}$, $q_{4,2}$, ... , $q_{4,\ m+1}$ being the cost factors of columns in the bottom storey.

Using (3.22) and (3.23) and differentiating, the optimum inertia of the bottom column is given as

$$I_{4,2} = \frac{P_3 h_3^3 (l_1 + l_2) + l_2 h_3 \sqrt{\frac{W2}{2W_4} (l_1 + l_2)(P_2 h_2 + 2P_3 h_3) P_3 h_3}}{6E \Delta_b L} \qquad (3.24)$$

The above arrangement will also be applicable to cases where h_2 is equal to or slightly larger than h_3 . However, to check whether the value of $I_{3,2}$ required to satisfy Δ_t is higher than the corresponding

column inertia of the third storey, which is possible if $h_2 > h_3$, an expression for $I_{3,2}$ in terms of Δ_t and $I_{2,2}$ is obtained in the following way.

Referring to figure (3.4), θ_B is given by equation (3.4) and θ_G has been expressed in (3.18). Slope-deflection equations and conditions of equilibrium give,

$$M_{GB} = \frac{EI_{3,2}}{h_2} \left(4\theta_G + 2\theta_B - \frac{6\Delta_t}{h_2}\right)$$

$$M_{GF} = \frac{6EI_{2,1}}{l_1} \theta_G = \frac{6EI_{2,2}l_1}{l_2^2} \theta_G$$

$$M_{GH} = \frac{6EI_{2,2}}{l_2} \theta G$$

M_{GJ} is given by (3.21)

Considering equilibrium of joint G,

$$M_{GF} + M_{GH} + M_{GB} + M_{GJ} = 0$$

which gives,

$$I_{3,2} = \frac{(l_1 + l_2) P_2 h_2^3 I_{2,2}}{24 E\Delta_t L I_{2,2} - (P_2 h_2 + 2P_3 h_3) h_2 l_2^2} \qquad (3.25)$$

$I_{3,2}$ given by (3.25) will be compared with the inertia of the corresponding column of the third storey and the higher value will be used for $I_{3,2}$.

In frames where h_2 is significantly larger than h_3 $I_{3,2}$ given by (3.25) may even be larger than $I_{4,2}$ given by (3.24) indicating that Δ_t will govern the design of both the storeys. In such a case, to avoid reverse taper, the bottom two storeys will have the same column sections, i.e., $I_{4,2}$ will be equal $I_{3,2}$, and the design criterion will be different from that considered above. The cost function will now be given by

$$Z = W_1 l_1 + 2W_2 l_2 + W_3 (h_2 + h_3) I_3 \qquad (3.26)$$

where W_3 corresponds to the second storey from the bottom.

By adopting the same procedure described above, expressions for the member inertias are given by

$$I_{3,2} = I_{4,2} = \frac{(l_1 + l_2) P_2 h_2^3 + l_2 h_2^2 \sqrt{\frac{[W_1(P_1 h_1 + P_2 h_2) + 2W_2(P_2 h_2 + 2P_3 h_3)](l_1 + l_2) P_2}{W_3(h_2 + h_3)}}}{24 E \Delta_t L} \qquad (3.27)$$

$$I_{2,2} = \frac{(P_2 h_2 + 2P_3 h_3) h_2 l_2^2 I_{3,2}}{24 E \Delta_t L I_{3,2} - (l_1 + l_2) P_2 h_2^3} \qquad (3.28)$$

$$I_{1,2} = \frac{(P_1 h_1 + P_2 h_2)}{P_2 h_2 + 2P_3 h_3} I_{2,2} \qquad (3.29)$$

The design procedure can be summarised as follows :

(i) Calculate $I_{4,2}$ and $I_{2,2}$ using (3.24) and (3.22).

(ii) Calculate $I_{3,2}$ using (3.25).

(iii) If $I_{3,2}$ is smaller than the inertia of the corresponding column in the third storey continue the same section down to the second storey. If not, use $I_{3,2}$ calculated in step (ii).

For $I_{1,2}$ use $I_{2,2}$ of the third storey obtained for the same beam.

If $I_{3,2}$ calculated in step (ii) is also larger than $I_{4,2}$ as calculated in step (i) redesign the members using the following steps.

(iv) Calculate $I_{3,2}$ ($= I_{4,2}$), $I_{2,2}$ and $I_{1,2}$ using (3.27) (3.28) and (3.29).

If $I_{1,2}$ calculated above is smaller than $I_{2,2}$ of the third storey use the larger value.

(v) Calculate inertia of the other members of the bottom two storeys using (3.1)(3.2) and (3.3).

3.5 EXPRESSIONS FOR FIXED BASE BOTTOM STOREYS

The fixed base subassemblage can be represented by figure (3.4) considering the joint J as fixed. All the other notations remain unchanged.

Due to restraint at the base of the columns, design of the bottom storey subassemblage will be governed by the deflection of second storey, i.e., Δ_t, unless h_3 is greater than h_2. To avoid reverse taper $I_{4,2}$ is made equal to $I_{3,2}$ and expressions are derived for the member inertias following a procedure similar to that in Sec. (3.4).

The sway equation for the column GJ and the condition of equilibrium at joint G can be used to find the rotation of joint G which is given as

$$\theta_G = \frac{h_3 l_2^2 (l_1 + l_2)(P_2 h_2 + P_3 h_3)}{24 E L h_3 (l_1 + l_2) I_{2,2} + l_2^2 I_{4,2}} \qquad (3.30)$$

θ_B is expressed by (3.4).

Using these expressions and the slope-deflection equations of column BG, the beam inertias can be found as

$$I_{2,2} = \frac{h_2 l_2^2 (P_2 h_2 + P_3 h_3) I_{3,2}}{24 E \Delta_t L I_{3,2} - P_2 h_2^3 (l_1 + l_2)} - \frac{l_2^2 I_{3,2}}{6 h_3 (l_1 + l_2)} \qquad (3.31)$$

$$I_{1,2} = \frac{h_2 l_2^2 (P_1 h_1 + P_2 h_2) I_{3,2}}{24 E \Delta_t L I_{3,2} - P_2 h_2^3 (l_1 + l_2)} \qquad (3.32)$$

The cost function is given by equation (3.26). Using (3.31) and (3.32) in the expression for cost function and differentiating, the column inertias are given as

$$I_{3,2} = I_{4,2} = \frac{h_2^2 (l_1 + l_2)(P_2 h_2 + l_2 Y)}{24 E \Delta_t L} \qquad (3.33)$$

where

$$Y = \sqrt{\frac{3P_2 h_3 [W_1 (P_1 h_1 + P_2 h_2) + 2W_2 (P_2 h_2 + P_3 h_3)]}{3W_3 h_3 (l_1 + l_2)(h_2 + h_3) - W_2 l_2^2}}$$

W_1, W_2 and W_3 are as defined earlier.

When $h_3 > h_2$ inertia of the bottom storey members calculated by using (3.31), (3.32) and (3.33) may cause the actual deflection of the bottom storey, δ_b, to be higher than the permissible value as these equations have been obtained by satisfying the deflection of the second storey from the bottom, Δ_t. This may be checked by calculating δ_b using the following expression which has been derived in terms $I_{4,2}$ and $I_{2,2}$, $I_{4,2}$ in this case being equal to $I_{3,2}$.

$$\delta_b = \frac{(h_3^2 l_2^2 (l_1 + l_2)(P_2 h_2 + P_3 h_3)}{8 EL [6h_3 (l_1 + l_2) I_{2,2} + l_2^2 I_{4,2}]} + \frac{P_3 h_3^3 (l_1 + l_2)}{24 E L I_{4,2}} \qquad (3.34)$$

If δ_b exceeds Δ_b, the permissible value, a satisfactory design can be obtained by using either of the two methods described below.

In the first method different sections are used for $I_{3,2}$ and $I_{4,2}$. While the values of $I_{3,2}$, $I_{2,2}$ and $I_{1,2}$ remain unaltered as calculated by (3.33), (3.21) and (3.22) respectively, a separate value for $I_{4,2}$ satisfying Δ_b is obtained by using the following quadratic equation which expresses the relationship between $I_{2,2}$ and $I_{4,2}$ in terms of Δ_b,

$$I_{4,2}^{2}[\,24E\Delta_b L\, l_2^{2}\,]$$

$$+\; I_{4,2}[\,144\,(l_1+l_2)\,h_3\,E\Delta_b LI_{2,2} - (l_1+l_2)(3P_2h_2+4P_3h_3)\,l_2^{2}h_3^{2}\,]$$

$$-\,6P_3h_3^{4}\,(l_1+l_2)^{2}\,I_{2,2} \;=\; 0 \qquad (3.35)$$

In the second method the same column section is used for $I_{3,2}$ and $I_{4,2}$ (i.e. $I_{4,2} = I_{3,2}$). The following expressions satisfying Δ_b have been obtained to calculate the inertias and also to calculate the actual deflection of the second storey, δ_t.

$$I_{4,2}^{2}[\,1152\,E^{2}\Delta_b^{2}L^{2}\,\{3W_3h_3(h_2+h_3)(l_1+l_2) - W_2l_2^{2}\}\,]$$

$$+\; I_{4,2}[\,96\,E\Delta_b LP_3h_3^{3}\,(l_1+l_2)\,\{W_2l_2^{2} - 3W_3h_3(h_2+h_3)(l_1+l_2)\}\,]$$

$$+\; P_3h_3^{5}(l_1+l_2)^{2}[\,6W_3P_3h_3^{2}(h_2+h_3)(l_1+l_2) - 2W_2l_2^{2}(3P_2h_2+4P_3h_3)$$

$$+\; 3W_1l_2^{2}\,(P_1h_1+P_2h_2)\,] \;=\; 0 \qquad (3.36)$$

$I_{4,2}$ ($= I_{3,2}$) can be obtained by using the above expression while equations for the other members are

$$I_{2,2} = \frac{[l_2^{2}h_3^{2}(l_1+l_2)(3P_2h_2+4P_3h_3)]\,I_{4,2} - 24E\Delta_b Ll_2^{2}I_{4,2}^{2}}{6h_3\,(l_1+l_2)[\,24E\Delta_b LI_{4,2} - P_3h_3^{3}(l_1+l_2)]} \qquad (3.37)$$

$$I_{1,2} = \frac{(P_1h_1+P_2h_2)\,l_2^{2}h_3\,I_{4,2}}{48E\Delta_b\,LI_{4,2} - 2P_3h_3^{3}(l_1+l_2)} \qquad (3.38)$$

$$\delta t \;=\; \frac{h_2h_3l_2^{2}\,(l_1+l_2)\,(P_2h_2+P_3h_3)}{4E\,L[\,6h_3(l_1+l_2)\,I_{2,2}+l_2^{2}I_{4,2}]} \;+\; \frac{P_2h_2^{3}(l_1+l_2)}{24E\,LI_{3,2}} \qquad (3.39)$$

On rare occasions δ_t may exceed Δ_t. In such a case a solution satisfying both Δ_b and Δ_t may be obtained by redesigning only the beam, $I_{2,2}$, using the expression given by (3.31) while other members remain unaltered.

Comparison of the weight of the members given by the two methods can be made before selecting the one producing minimum weight. If, however, it is desired to use the same column section in the two storeys for convenience of construction the first of the two methods can be avoided altogether and the second method used to calculate the inertias when members designed by (3.31), (3.32) and (3.33) have failed to satisfy Δ_b.

The design procedure can be summarized as follows :

(i) Assume $I_{4,2} = I_{3,2}$ and calculate $I_{3,2}$, $I_{2,2}$ and $I_{1,2}$ using (3.33), (3.31) and (3.32).

(ii) Calculate δ_b using (3.34)

If $\delta_b > \Delta_b$ revise the design using the following steps.

(iii) Calculate new values for $I_{4,2}$ using (3.35) while $I_{3,2}$, $I_{2,2}$ and $I_{1,2}$ remain as calculated in step (i).

(iv) Assume $I_{3,2} = I_{4,2}$ and calculate $I_{4,2}$, $I_{2,2}$ and $I_{1,2}$ using (3.36), (3.37) and (3.38).

Calculate δ_t using (3.39). If $\delta_t > \Delta_t$ revise $I_{2,2}$ using (3.31)

(v) Compare the total weight of members of the bottom two storeys given in steps (iii) and (iv).

Select the cheaper design .

(vi) Compare the value of $I_{1,2}$ with $I_{2,2}$ of the third storey and use the larger inertia.

(vii) Calculate inertia of other members of the bottom two storeys using (3.1), (3.2) and (3.3).

3.6 DESIGN OF A SIX-STOREY TWO-BAY FRAME

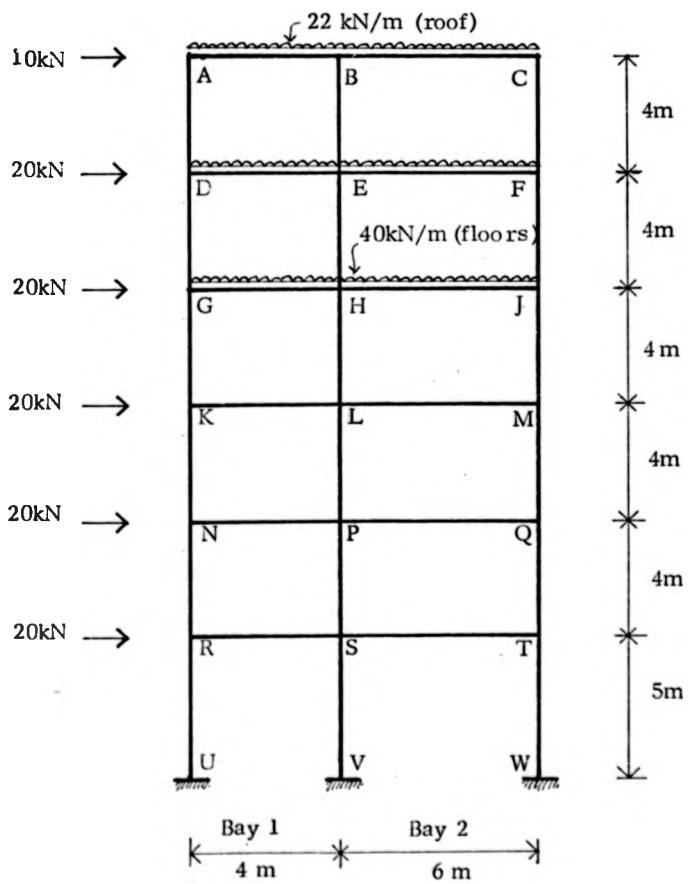

Figure 3.5

The 'non-uniform' frame shown in figure (3.5) will now be designed with the following constraints :

(i) Column and beam sections will only be changed every second storey to reduce fabrication cost.

(ii) No beam section shall have a nominal depth greater than 406 mm.

(iii) To satisfy strength requirements, members must resist the beam-mechanism collapse of plastic theory at a load factor of 1·5.

The permissible sway deflection is h/300, E is 210 kN/mm^2 and Fy = 240 N/mm^2.

To satisfy conditions (i) and (iii) sections required for the beam are 203 x 133 x 25 UB in bay (1) and 305 x 165 x 40 UB in bay (2). The required external columns are 152 x 152 x 30 UC. These constitute a lower-bound for the design.

In order to satisfy condition (i) it is convenient to start the design with the bottom two storeys. Using equations (3.31) - (3.34) it is found that the design will be governed by the permissible deflection of the lowest storey and the optimum inertias are therefore calculated using equations (3.36) - (3.38). From (3.39) it is found that Δ_t is satisfied. The optimum inertias are shown in table (3.1). The inertia required for beam ST is 30610 cm^4 which would necessitate a 457 mm deep UB, thus violating condition (ii). It is therefore decided to assign 406 x 178 x 74 UB to ST which has an inertia of 27280 cm^4. This value is now substituted into (3.37) and (3.38) to calculate feasible inertias of PSV and PQ. The values for RS, NP, NRU, QTW are then found using (3.1), (3.2) and (3.3). The feasible inertias and the respective rolled sections for the bottom two storeys

are shown in table (3.1). If the third storey is considered in isolation (3.13), (3.9) and (3.6) provide optimum inertias, those for beams PQ and NP being 24090 cm^4 and 10710 cm^4 respectively. However, due to the restrictions of condition (i) these two beams shall have the same sections as those of ST and RS which are 27280 cm^4 and 12410 cm^4 respectively. Provision of these excess inertias in the beams can be made use of by designing the columns and upper beams of this storey in relation to those inertias. In (3.9) the value of $I_{2,2}$ is taken as 27280 and $I_{3,2}$ is calculated, giving a feasible inertia for LP. (3.6) is then used to calculate the feasible inertia of LM. The values for the remaining members of the third storey are calculated using (3.1) - (3.3). Sections chosen for KL and LM are also assigned to GH and HJ to satisfy condition (i) and similarly the third storey column sections are continued up to the fourth storey. Design of the remaining two storeys follows in a similar manner using the sections already assigned to GH and HJ to calculate corresponding column and upper beam inertias. Resulting inertias and corresponding rolled sections for the intermediate and top storeys are shown in table (3.2). In this frame the initial lower-bound solution satisfying strength requirement has not governed the design of any of the members. This is because of the high wind load being distributed only in two bays causing permissible horizontal deflection to govern the design of all the storeys. This would not have been so if the frame had more bays or if the external wind forces were considerably smaller.

During the design procedure the cost factors, q, have been assigned unit values. If actual values of q are used,

Member	Optimum Inertia cm^4	Feasible Inertia cm^4	Feasible section
ST	30612	27279	406 x 178 x 74 UB
PQ	23215	20996	406 x 178 x 74 UB
RS	13605	12124	406 x 140 x 39 UB
NP	10318	9332	406 x 140 x 39 UB
PSV	23752	24853	305 x 305 x 118 UC
NRU	9501	9941	254 x 254 x 73 UC
QTW	14251	14912	254 x 254 x 89 UC

Table 3.1

Member	Feasible Inertia cm^4	Feasible Section
PQ	27279	406 x 178 x 74 UB
LM & HJ	20459	406 x 178 x 60 UB
KL &GH	9093	406 x 140 x 39 UB
LP & HL	13413	254 x 254 x 89 UC
KN & GK	5365	203 x 203 x 52 UC
MQ & JM	8048	254 x 254 x 73 UC
EF & BC	10760	406 x 140 x 39 UB
DE & AB	4782	254 x 146 x 31 UB
EH & BE	4195	203 x 203 x 46 UC
DG & AD	1678	152 x 152 x 30 UC
FJ & CF	2517	152 x 152 x 37 UC

Table 3.2

Member	Optimum Inertia cm^4	Feasible Inertia cm^4	Feasible section
ST	30612	27279	406 x 178 x 74 UB
PQ	23215	20996	406 x 178 x 74 UB
RS	13605	12124	406 x 140 x 39 UB
NP	10318	9332	406 x 140 x 39 UB
PSV	23752	24853	305 x 305 x 118 UC
NRU	9501	9941	254 x 254 x 73 UC
QTW	14251	14912	254 x 254 x 89 UC

Table 3.1

Member	Feasible Inertia cm^4	Feasible Section
PQ	27279	406 x 178 x 74 UB
LM & HJ	20459	406 x 178 x 60 UB
KL &GH	9093	406 x 140 x 39 UB
LP & HL	13413	254 x 254 x 89 UC
KN & GK	5365	203 x 203 x 52 UC
MQ & JM	8048	254 x 254 x 73 UC
EF & BC	10760	406 x 140 x 39 UB
DE & AB	4782	254 x 146 x 31 UB
EH & BE	4195	203 x 203 x 46 UC
DG & AD	1678	152 x 152 x 30 UC
FJ & CF	2517	152 x 152 x 37 UC

Table 3.2

the UB sections, having lower weight-inertia ratios than the UC sections, cause the inertia of beam members to increase with corresponding decrease of column inertias to satisfy optimisation requirements. In this particular frame, however, the design conditions (i) and (ii) would not permit any significant change on the design solution shown in tables (3.1) and (3.2) if iterations are carried out with actual q-values.

From the above exercise it is observed that the design expressions can also be used to find a feasible design solution satisfying restrictions on beam depth and on change of section; they also enable the designer to see the effect of these restrictions on section sizes. Even when there is no restriction on beam depth, use of standard rolled sections will usually necessitate the selection of some inertias higher than those given by the design solution. As the design equations for the beams and columns in a subassemblage are so expressed that the value of one is related to the value of the others, use of the higher inertia of rolled section selected for one member can be made to find the corresponding feasible inertia of the other members. This way the designer may be able to reduce some sections to offset others which are over-stiff.

Computer analysis of the six-storey two-bay frame of figure (3.5) with fixed bases shows that the sections given in tables (3.1) and (3.2) lead to acceptable sway deflections. This is expected as in general the inertias of the rolled sections provided are larger than those actually required.

To check the validity of the proposed method, each storey of the 'non-uniform' frame has also been designed without restriction

on beam depth and change of section. Actual inertias given by the equations were assigned to the members without particular sections being chosen. When this design was analysed by computer, the sway deflections showed excellent agreement with the permissible values. Deflections of the different storeys from top to bottom with permissible values in parentheses are shown below :

12·96 (13·33), 13·35 (13·33), 13·34 (13·33)
13·36 (13·33), 12·81 (13·33) and 16·65 (16·67)
all in mm.

The low deflections in the top storey and in the second storey from the bottom are due to similar reasons as mentioned in Sec.(2.7) of chapter II.

Optimality of the design has also been studied in the same way as described in Sec.(2.7). The results are similar to those for the regular frame with fixed bases. This indicates that the equations provide a distribution between beams and columns which, for practical purposes, can be regarded as the optimum.

3.7 EFFECT OF AXIAL FORCES

In the derivation of design expressions so far, the vertical load acting on the frame has been neglected under the assumption that such load has insignificant effect on the horizontal deflection of the frame.

But, as discussed in chapter I , axial load in the members causes deterioration of stiffness and renders the load-deflection relationship as non-linear (curve OD of figure (1.3)). Within the elastic limit of the 'allowable stress' method of design, however,

the effect of axial force is usually small.

The points of contraflexure assumed to exist in the mid-point of the members causes the internal columns of a 'regular' frame to have no axial force due to the applied horizontal load. In 'non - uniform' frames, proportioning the beam and column inertias according to the relationships shown in equations (3.1) - (3.3) also causes zero axial force in the internal columns. But in both the cases the external columns have axial forces caused by horizontal load and the vertical loading in the frame causes axial forces in all the columns.

To investigate the differences caused by considering the effects of axial forces, the design expressions for a 'regular' frame will be modified by using 'stability functions' s and c in the columns. The stability functions are given as,

$$s = \frac{(1 - 2\alpha\cot 2\alpha)\alpha}{\tan\alpha - \alpha} \tag{3.40}$$

$$c = \frac{2\alpha - \sin 2\alpha}{\sin 2\alpha - 2\alpha\cos 2\alpha} \tag{3.41}$$

where

$$\alpha = \frac{\pi\sqrt{p}}{2} \quad , \quad p = \frac{Vh^2}{\pi^2 EI_3}$$

V being the total axial force in the column of height h and inertia I_3.

Denoting the stability functions for the internal columns as s and c and and those for the external columns as s_1 and c_1 the expressions for the optimum inertias, derived following the same procedure as in Sec. (2.2)-(2.4), are as given below.

Top storey

$$I_3 = \frac{Ph^3}{4E\Delta s(1+c)}\left[1 + r\sqrt{\frac{mss_1(1+c)(1+c_1)(q_1+2q_2)}{12\,s_1(1+c_1)(m-1)q_3 + s(1+c)q_4}}\right] \tag{3.42}$$

$$I_3' = \frac{S(1+c)}{2s_1(1+c_1)}\, I_3 \tag{3.43}$$

$$I_2 = \frac{Prsh^3(1+c)\,I_3}{12E\Delta s\,(1+c)\,I_3 - 3Ph^3} \tag{3.44}$$

$$I_1 = I_2/4 \tag{3.45}$$

Intermediate storey

$$I_3 = \frac{Ph^3}{2E\Delta s(1+c)}\left[(n+1.5) + r\sqrt{\frac{mss_1(1+c)(1+c_1)(n+1.5)\{(n+1)q_1+(n+2)q_2\}}{12\{s_1(1+c_1)(m-1)q_3 + s(1+c)q_4\}}}\right] \tag{3.46}$$

$$I_2 = \frac{Prsh^3(1+c)(n+2)\,I_3}{12E\Delta s(1+c)I_3 - 6(n+1.5)\,Ph^3} \tag{3.47}$$

$$I_1 = \frac{n+1}{n+2}\, I_2 \tag{3.48}$$

I_3' is given by (3.43)

Top storey

$$I_3 = \frac{Ph^3}{4E\Delta s(1+c)}\left[1 + r\sqrt{\frac{mss_1(1+c)(1+c_1)(q_1+2q_2)}{12\,s_1(1+c_1)(m-1)\,q_3 + s(1+c)\,q_4}}\right] \qquad (3.42)$$

$$I_3' = \frac{S(1+c)}{2s_1(1+c_1)}\ I_3 \qquad (3.43)$$

$$I_2 = \frac{Prsh^3(1+c)\,I_3}{12E\Delta s\,(1+c)\,I_3 - 3Ph^3} \qquad (3.44)$$

$$I_1 = I_2/4 \qquad (3.45)$$

Intermediate storey

$$I_3 = \frac{Ph^3}{2E\Delta s(1+c)}\left[(n+1.5) + r\sqrt{\frac{mss_1(1+c)(1+c_1)(n+1.5)\{(n+1)q_1+(n+2)q_2\}}{12\{s_1(1+c_1)(m-1)q_3 + s(1+c)\,q_4\}}}\right] \qquad (3.46)$$

$$I_2 = \frac{Prsh^3(1+c)(n+2)\,I_3}{12E\Delta s(1+c)I_3 - 6(n+1.5)\,Ph^3} \qquad (3.47)$$

$$I_1 = \frac{n+1}{n+2}\ I_2 \qquad (3.48)$$

I_3' is given by (3.43)

Fixed base bottom storey

$I_3 = I_4$ is given by the quadratic equation

$$XI_3^2 + YI_3 + Z = 0 \qquad (3.49)$$

where

$$X = 4K_7 (K_7K_9K_{10} + K_7K_{10}K_{11}K_{12} - K_1K_2K_6K_8)$$

$$Y = 4K_4 (K_1K_2K_6K_8 - K_7K_9K_{10} - K_7K_{10}K_{11}K_{12})$$

$$Z = K_4 (K_4K_9K_{10} + K_4K_{10}K_{11}K_{12} - K_1K_2K_3K_5)$$

$$K_1 = 48 s_1 (1 + c_1)(n + 2)$$

$$K_2 = (n + 1) q_1 + 2 (n + 2) q_2$$

$$K_3 = 4 (1 + c)(n + 2) + (1 - c)(n + 1{\cdot}5)$$

$$K_4 = (n + 1{\cdot}5) Ph^3$$

$$K_5 = Pmsr^2h^4$$

$$K_6 = (1 + c)(1 - c)$$

$$K_7 = (1 + c) E\Delta s$$

$$K_8 = E\Delta mhr^2s^2$$

$$K_9 = mss_1hr^2 (1 + c_1)(1 - c) (n + 1) q_1$$

$$K_{10} = 48 (n + 2)$$

$$K_{11} = 96 (n + 2)$$

$$K_{12} = s_1 (1 + c_1)(m - 1) q_3 + s (1 + c) q_4$$

$$I_2 = \frac{Prsh^3\{ 2 (1 + c)(n + 2) + (1-c)(n + 1{\cdot}5)\} I_3 - 2(1 + c)(1-c) E\Delta rs^2 I_3^2}{48 (1 + c) E\Delta s I_3 - 24 (n + 1{\cdot}5) Ph^3} \qquad (3.50)$$

$$I_1 = \frac{(n + 1) \{24 I_2 + sr (1 - c) I_3\}}{24 (n + 2)} \qquad (3.51)$$

I_3' is given by (3.43)

In deriving the above expressions the stability functions were considered as constant terms while differentiating the cost function with respect to I_3.

Even if the q-values are taken as unity, use of these expressions requires iterative calculations initially assuming $s = s_1 = 4$ and $c = c_1 = 0{\cdot}5$ and then using the latest values of s, c, s_1 and c_1 corresponding to the set of sections chosen in the earlier operation. Iteration continues till successive operations result in the same set of sections.

A computer program suitable for desk-top computers has been written for design of 'regular' frames using the above expressions. Flow

diagram for design procedure has been shown in figure (3.6).

Similar programmes have also been written for the optimum design of 'regular' frames without considering the effect of axial forces using the expressions derived in chapter II and for the design of 'non-uniform' frames. These automatic design programmes use the discrete section properties (inertia and q-values) of the rolled sections shown in tables (2.1) and (2.2).

The regular 'frame' of figure (2.1) (Sec.2.7) has been designed by using these computer programmes (i) without considering the effects of axial load and then (ii) considering the effect of axial forces in the columns. In the latter case u.d. load of 35·9 kN/m has been taken in the roof and floors. Results showing the actual inertias required for the members by the two designs are shown in Table (3.3).

It is observed that the differences in the values of required insertias given by the two design solutions are small enough to be considered negligible for practical design purposes. The table also shows that the results shown in table (2.5) of chapter II for the same frame after a single iteration by hand calculation compare favourably with the final design given by the computer. While in the final design some of the beam inertias increase, there are corresponding reductions in the inertia of columns, thus keeping the total weight of the frame almost the same as given by hand calculation. In terms of rolled sections there is no difference between the results of table (2.5) (corresponding rolled sections shown in table 2.6) and those of table (3.3).

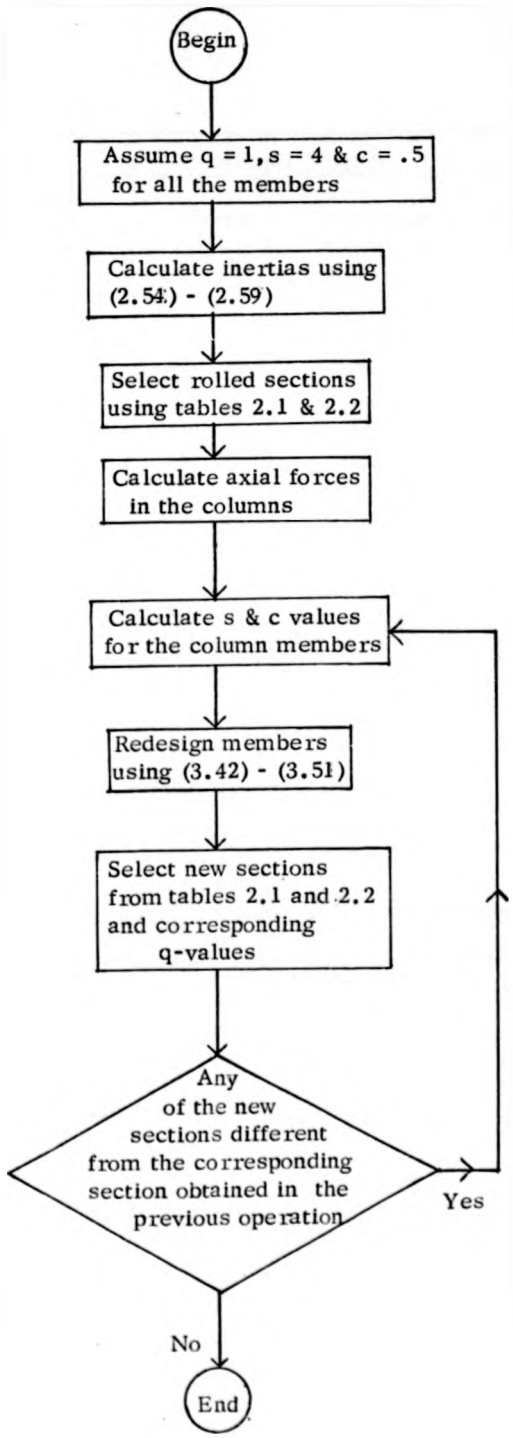
Begin
Assume q = 1, s = 4 & c = .5 for all the members
Calculate inertias using (2.54) - (2.59)
Select rolled sections using tables 2.1 & 2.2
Calculate axial forces in the columns
Calculate s & c values for the column members
Redesign members using (3.42) - (3.51)
Select new sections from tables 2.1 and 2.2 and corresponding q-values
Any of the new sections different from the corresponding section obtained in the previous operation
Yes
No
End

Figure 3.6

Beams			Internal Columns		External Columns	
Without axial force		With axial force	Without axial force	With axial force	Without axial force	With axial force
AB	639	640	BD 1274	1289	AC 637	640
CD	2914	2922	DF 3067	3093	CE 1534	1549
EF	5969	5987	FH 4946	5007	EG 2473	2484
GH	9401	9430	HK 6515	6588	GJ 3259	3282
JK	12687	12749	KM 8258	8336	JL 4133	4177
LM	14482	14651	MP 8258	8336	LN 4133	4177

Table 3.3

3.8 GRAPHICAL SOLUTION FOR INTERMEDIATE STOREYS OF REGULAR FRAMES

The expression for the optimum inertia of internal columns of the intermediate storeys of a regular frame is given by equation (2.23). The expression can be modified as

$$I_3 = C\left[\frac{Ph^3}{12E\Delta}\right] \tag{3.52}$$

where

$$C = (n+1{\cdot}5) + r\sqrt{\frac{m(n+1{\cdot}5)\{(n+1)q_1 + (n+2)q_2\}}{2(m-1)q_3 + 2q_4}}$$

A large number of 'regular' frames with different values for (i) load intensity, (ii) permissible sway deflection, (iii) bay width/ storey height ratio , (iv) number of bays and (v) number of storeys were designed by using the computer program discussed in Sec. (3.7). No vertical load was applied but the non-linear effect on exterior columns due to wind load was considered. Choice of sections was restricted to those shown in tables (2.1) and (2.2).

The final optimum inertia I_3 for the different intermediate storeys of the frames given by these designs corresponds to an approximate linear relationship between C and n for frames of the same width-height ratio (r) and number (m) of bays. Figure (3.7) shows this relationship for a two-bay frame. The five straight lines represent the C-n relationship for r-values of 1, 2, 3, 4 and 5. For any other value of r, between 1 and 5 , the corresponding value of C can be found by interpolation. Figures (3.8) - (3.11) show similar graphical solutions for 3-bay, 4-bay, 5-bay and 6-bay frames.

These graphs can be used to find the values of C for all the intermediate storeys of a frame corresponding to the n-value of each storey. The optimum inertia of the internal columns (I_3) of each storey is then obtained by using equation (3.51) of which $Ph^3/(12E\Delta)$ is constant for the frame. Once I_3 is known, I_2 , I_1 and I_3' can be calculated using (2.15) , (2.13) and (2.20) respectively.

Considering again the six-storey frame (Sec. 2.7), for which $m = 4$ and $r = 2.0$, figure (3.9) may be used to obtain the values of C for $n = 0$, 1 and 2 representing the three intermediate storeys. Table (3.4) shows these values and the required inertia of members given by the graphical approach.

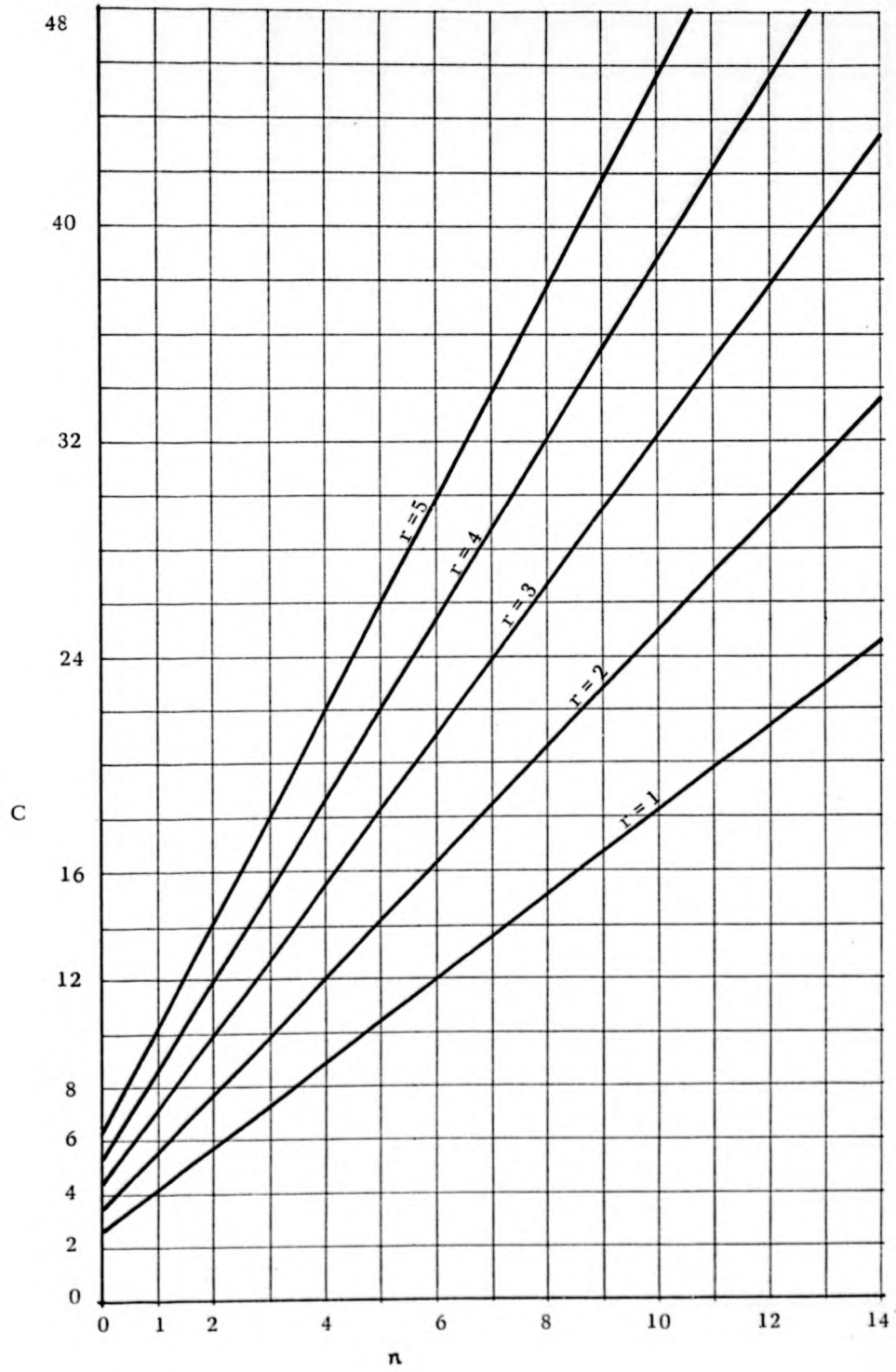

For 2-bay frame

Figure 3.7

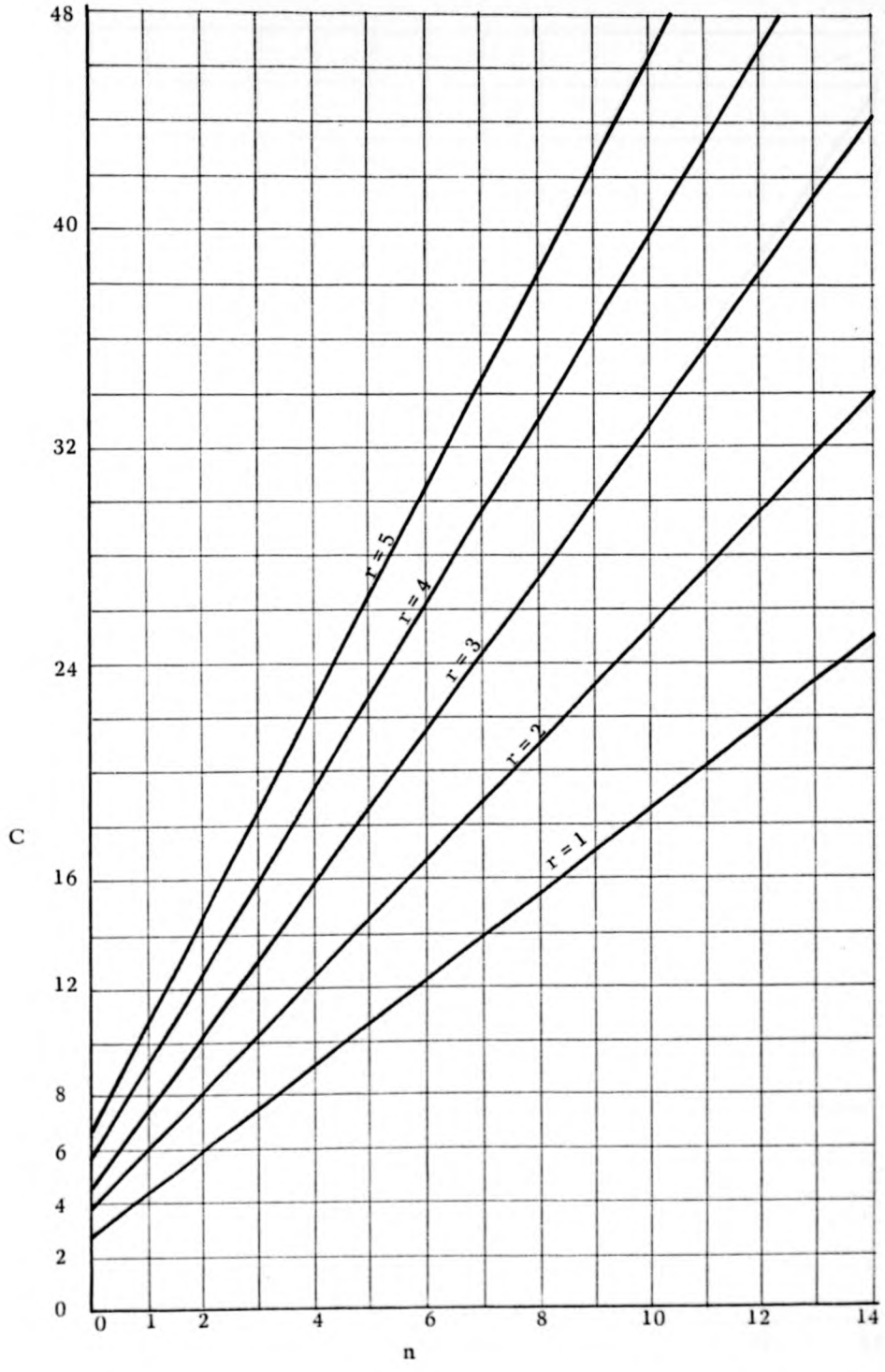

For 3-bay frame

Figure 3.8

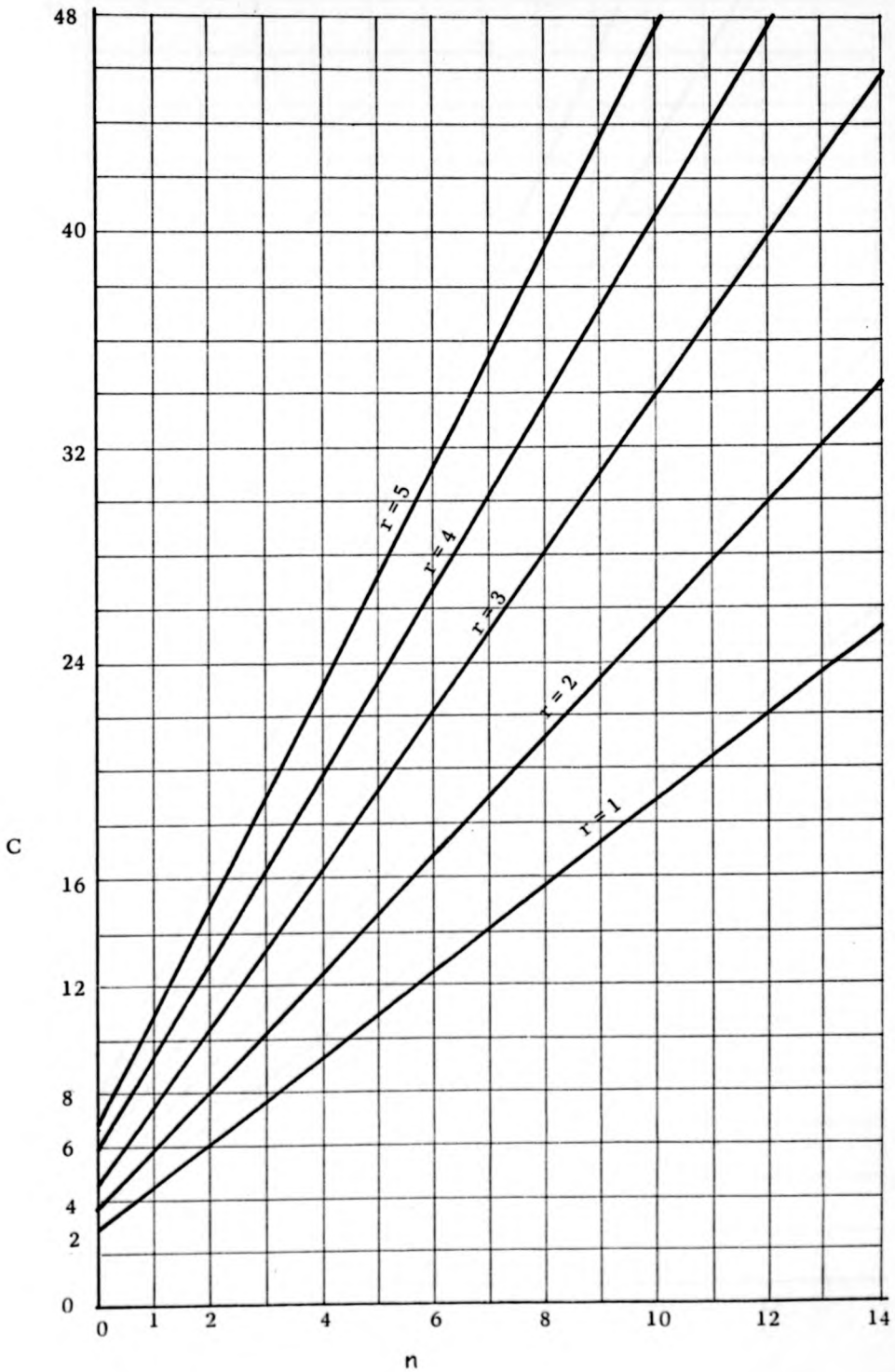

For 4-bay frame

Figure 3.9

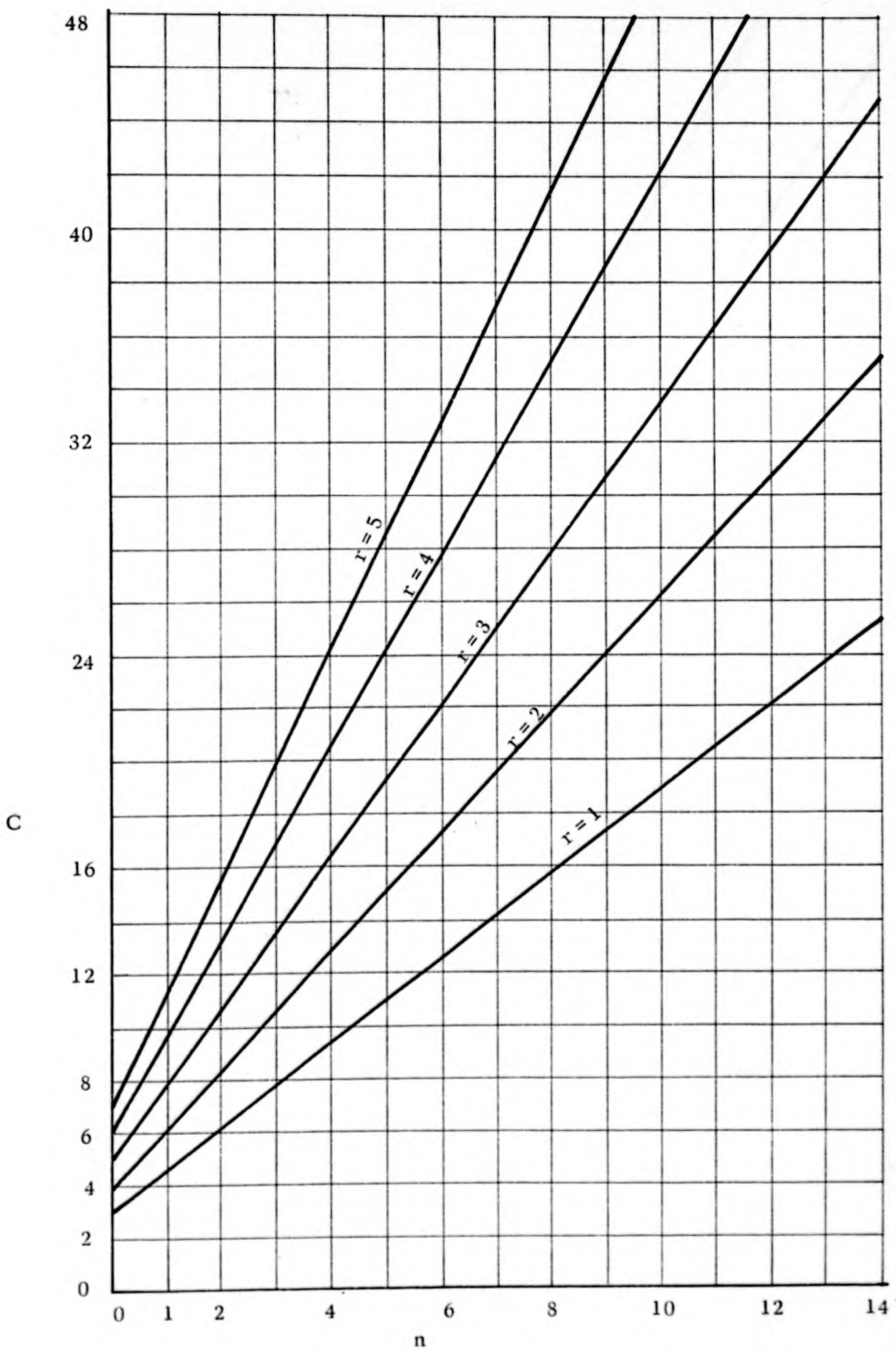

For 5-bay frame

Figure 3.10

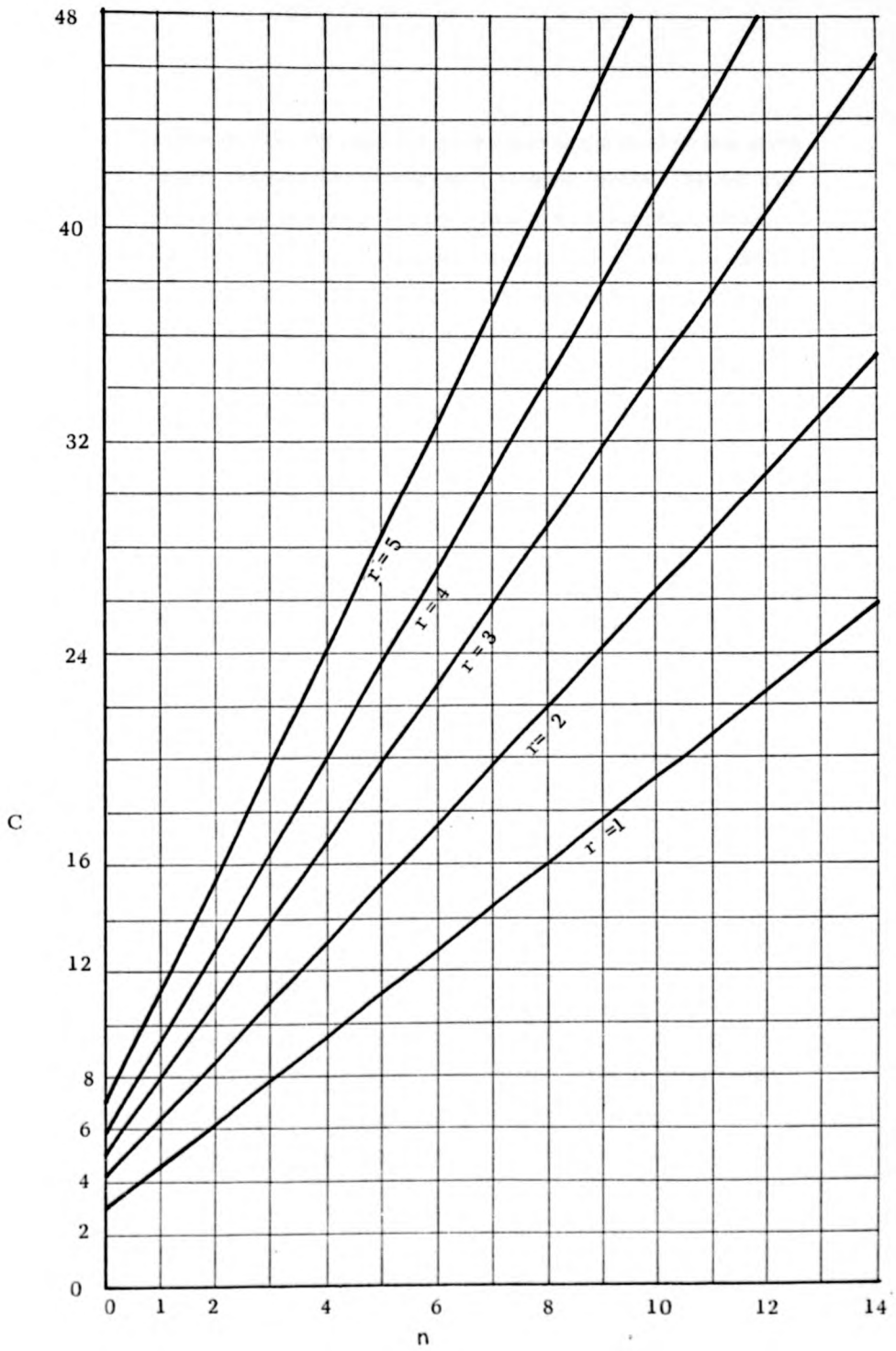

For 6-bay frame

Figure 3.11

It may be seen that the inertias are very close to the final values given by the iterative calculations by computer program (table 3·3) and are much improved than the initial values obtained by assuming q-values as unity (table 2·3). It has been found that for most of the 'regular' frames, if the initial design of intermediate storeys is carried out by using these graphs instead of using equations (2·54) and (2·55) in which'q'values have been taken as unity , one iteration is usually sufficient to reach the optimum solution and thus the designer can avoid the repetitive calculations required for convergence or the use of computer program.

n	C	Beams	Internal Columns	External Columns
0	3.7	CD 2811	DF 3233	CE 1616
1	5.95	EF 5869	FH 5062	EG 2531
2	8.05	GH 9030	HK 6849	GJ 3424
		JK 12687		

Table 3.4

3.9 CONCLUSIONS

Equations have been derived in the two chapters for the design of 'regular' and 'non-uniform' multistorey sway frames to permissible horizontal deflections. The equations have been validated for accuracy and optimality by comparing with accurate computer analysis.

In Chapter II , it has been shown that assumption of unit weight-inertia relationship of standard sections simplifies the expressions and renders the calculation of initial set of sections very simple. Subsequent iterations with actual weight-inertia ratios can be carried out by hand calculation.

In this chapter similar expressions for frames with unequal bay width and storey height have been derived. Beam and column inertias have been assumed to vary according to the relationship of equations (3.1) - (3.3) which eliminates axial forces in the interior columns and enables the derivation of simple design equations. For frames with large differences in bay widths this relationship may result in solutions slightly away from the optimum. Sometimes it may be found economical and convenient for construction to provide all beams at a particular level with the same inertia . But then, such arrangement would have non-zero axial forces in the columns and the derivation of design expressions would be very difficult.

It has also been found that the axial forces in the members due to vertical load do not have significant effect on the design of frames to limiting horizontal deflections.

The design expressions can be used for automatic optimum design of frames by desk-top computers by using the properties of rolled sections. When used for hand calculation of 'regular' or 'non-uniform' frames, one or two iterations give results reasonably close to the optimum. For 'regular' frames, however, a graphical method can be used to obtain the optimum solution considering the discrete weight-inertia relationship of rolled sections, but avoiding the large number of iterations.

For an unbraced multistorey frame subjected to high wind load, the design of which is expected to be governed by limitation on sway deflections, the proposed method can be used to obtain a practical minimum-cost design, taking account of restrictions on section sizes, limitations on the change of sections, and the lack of a continuous range of rolled sections.

For frames with low ratio of horizontal to vertical loading the proposed method may be used to satisfy strength and stability criteria.

It should be stated that no code insist that the sway in a column must be h/300 where h is the height. What the proposed code suggests is that the sway in a column must not be more than h/300. This means it is possible to produce a design of a frame in which the columns sway less than h/300. Now if the top column in a frame is allowed to sway by h/300 then the lower columns which are more stiff should, in the case of an optimum design, sway less than h/300. This is particularly the case with the fixed base ground floor columns. In this manner a cheaper frame can be obtained. For this reason, the design method proposed in chapters 2 and 3 are not optimum but may be economical.

CHAPTER IV

MULTISTOREY FRAMES :

HAND/DESK METHOD OF ELASTIC-PLASTIC ANALYSIS

4.1 INTRODUCTION

The overall stiffness of a multistorey sway frame is greatly reduced due to the non-linear effects of axial load, in-plane deflections causing P-Δ effects and the formation of plastic hinges in the members. Whereas the elastic approach of analysis gives no idea of the actual load-carrying capacity of a frame, the small-deflection theory associated with the plastic method causes instability problems in multistorey sway frames.

The non-linear elastic-plastic method , as explained in chapter I (Sec. 1.4) , is a more realistic approach for the analysis of sway frames as all the factors affecting the frame behaviour under loading may be taken into consideration in this approach. Following the simple methods proposed in chapters II and III for the design of sway frames to deflection limitations, a method of approximate elastic-plastic analysis of multistorey frames without recourse to full-size computers, will now be presented. The method produces the hinge formation pattern, joint and hinge rotations and the horizontal deflections at each storey level of a multistorey frame at the load factor at which it is analysed. The analysis procedure has been utilised to develop an optimum design method of multistorey sway frames to strength, deflection and stability requirements in the following chapter.

4.2 BASIC CRITERIA

Wood[5] suggested that the failure load of a frame can be estimated by computing the deteriorated elastic critical load with assumed plastic hinges located where the rigid plastic theory indicates their formation. In reference [11] he has shown how to use a substitute Grinter frame to calculate the deteriorated critical load for a given pattern of hinges in the beams. This would be the elastic-plastic failure load if the assumed pattern of hinges is the one that would actually exist at the point of collapse of the frame.

It has also been shown that the plastic hinges in columns should be the last to form. A column with two plastic hinges receives no rotational restraint from the beams and one plastic hinge in each of the columns of a storey causes the loss of all restraint at that level of the frame. For the beams, the tangential rotational stiffness of a member bending in symmetrical double curvature reduces from 3k to 0·75k if a hinge forms at one end of the beam, k being the nominal stiffness I/L of the beam. When the central hinge also appears the tangential rotational stiffness reduces to zero, thus eliminating the column restraint at that level and greatly reducing the overall frame stiffness. Both Wood[11] and Anderson[6] have shown that as soon as the central hinge starts to appear in beams already having one hinge the frame reaches the point of collapse quite suddenly. So, the assumption that a frame is close to collapse when the hinge pattern consists of extensive formation of one hinge per beam is a very realistic one.

The objective of the design may, therefore, be to force a desired plastic hinge pattern at a specific load factor by a suitable selection of sections for the members. This will involve analysis of the frame with trial sections to check the yield criterion and modify the design

till the desired pattern is obtained.

The proposed method of analysis will be described in this chapter. As use is made of the Grinter substitute frame this will first be described.

4.3 SUBSTITUTE FRAME ANALYSIS

Analysis of a multistorey frame is basically the calculation of joint displacements and hinge rotations. When these are known the member forces can be found easily. The joint displacements consist of rotation and the vertical and horizontal component of translation. In reference [11] Wood has shown how the substitute Grinter frame can also be used to calculate the horizontal deflection at any level of a multistorey frame.

The substitute frame analysis is based on the fact that for horizontal load acting on the real frame, the rotations of all joints at any level are approximately equal. Other assumptions necessary for the proposed method of analysis are (i) the relative vertical deflection of the joints at any level are negligible and (ii) the effect of axial forces on the stiffness of the beams is small.

As each beam restrains a column at both ends, its contribution to the rotational stiffness of the equivalent beam of the substitute frame at that level is given by (figure 4.1).

$$K_b = 1\tfrac{1}{2}\, k_b + 1\tfrac{1}{2}\, k_b = 3\, k_b = 3\left(\frac{M}{4E\theta}\right) \qquad (4.1)$$

where $k_b = I/L = M/(4E\theta)$ is the nominal stiffness of of the beam at each end, M and θ being the moments and joint rotation at the ends, and E the Young's modulus of elasticity .

till the desired pattern is obtained.

The proposed method of analysis will be described in this chapter. As use is made of the Grinter substitute frame this will first be described.

4.3 SUBSTITUTE FRAME ANALYSIS

Analysis of a multistorey frame is basically the calculation of joint displacements and hinge rotations. When these are known the member forces can be found easily. The joint displacements consist of rotation and the vertical and horizontal component of translation. In reference [11] Wood has shown how the substitute Grinter frame can also be used to calculate the horizontal deflection at any level of a multistorey frame.

The substitute frame analysis is based on the fact that for horizontal load acting on the real frame, the rotations of all joints at any level are approximately equal. Other assumptions necessary for the proposed method of analysis are (i) the relative vertical deflection of the joints at any level are negligible and (ii) the effect of axial forces on the stiffness of the beams is small.

As each beam restrains a column at both ends, its contribution to the rotational stiffness of the equivalent beam of the substitute frame at that level is given by (figure 4.1).

$$K_b = 1\tfrac{1}{2}\, k_b + 1\tfrac{1}{2}\, k_b = 3\, k_b = 3\left(\frac{M}{4E\theta}\right) \qquad (4.1)$$

where $k_b = I/L = M/(4E\theta)$ is the nominal stiffness of of the beam at each end, M and θ being the moments and joint rotation at the ends, and E the Young's modulus of elasticity .

So, the equivalent beam stiffness of the substitute frame at any level is $\Sigma(3k_b)$, whereas the equivalent column stiffness at any level taking due consideration of the effects of axial forces in the real frame, is $\Sigma(k_c \frac{n}{4})$ where k_c and n are respectively the nominal rotational stiffness and no-shear stability function of the columns at that level.

The sidesway due to horizontal load at any level is calculated in two stages. In the first stage all the beams of the substitute frame are considered to be infinitely stiff and therefore cause fixed-end moments in the columns. Ignoring the effects of axial load in this stage, these moments are given by -Fh/2 where F is the total shear in the frame above the level and h is the storey height.

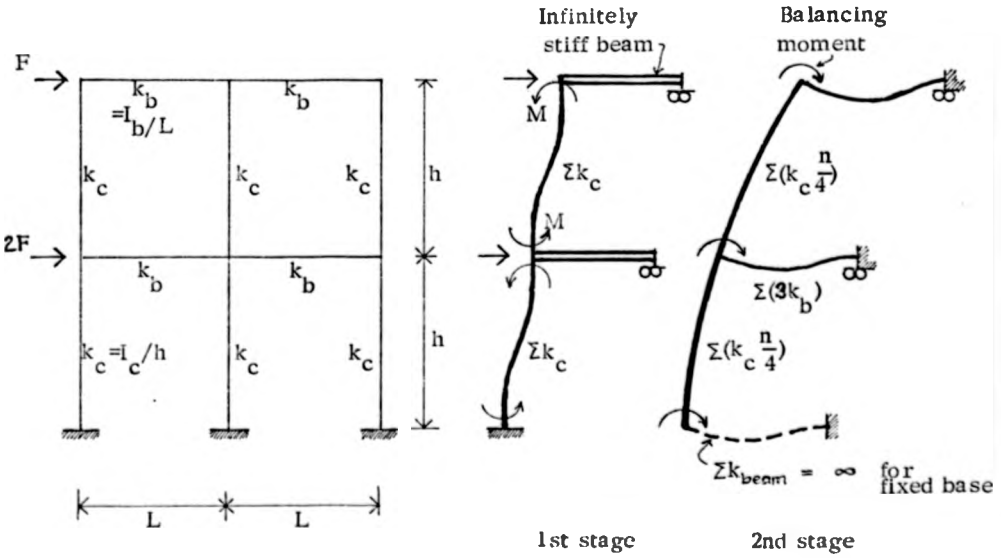

Figure 4.1

In the second stage these moments are released and the stiffness is distributed once from the top of the frame to the bottom and then from the bottom to the top. Stiffness distribution is carried out by successively evaluating the column stiffness from

$$K'' = K_c \frac{n}{4} \left[1 - \left(\frac{o}{n}\right)^2 \left(\frac{K_c \frac{n}{4}}{K_c \frac{n}{4} + \Sigma k'_b} \right) \right] \qquad (4.2)$$

where $K_c = \Sigma k_c$ is the stiffness of a column in the substitute frame

$\Sigma K'_b$ is $K'' + \Sigma (3k_b)$ of the preceding joint,

$\Sigma(3k_b)$ being the stiffness of a beam in the substitute frame, and o is the other no-shear stability function.

The total stiffness at a joint, ΣK_j, is given by the summation of stiffnesses, i.e. K'' from top + K'' from bottom + K_b, at every joint. The direct moment distribution follows the stiffness distribution in the same manner, downwards and upwards independently. If the sum, at any joint, of the increased fixed-end moment from all the frame above plus that from all the frame below is designated as Σ (FEM)', then the joint rotation is given by

$$\theta = - \Sigma(FEM)'/(4E\Sigma K_j) \qquad (4.3)$$

The horizontal sway, Δ, of a storey is calculated from the sway-angle ϕ of the storey, which is the summation of the sway angles at the two stages of the frame.

The first-stage sway-angle is given by

$$\phi_1 = Fh/(E\Sigma k_c ss'') \qquad (4.4)$$

where $s'' = s(1 - c^2)$ is the Merchant function [45], s and c being the stability functions. F is the total shear.

The second-stage sway-angle is given by

$$\phi_2 = (\theta_t + \theta_b) / (s\,(1-c)) \qquad (4.5)$$

where θ_t & θ_b are the rotations at the top and bottom joints of the storey given by the equation (4.3)

The total sway-angle of the storey is

$$\phi = \phi_1 + \phi_2 \qquad (4.6)$$

and the sway-deflection of the storey is

$$\Delta = \phi h \qquad (4.7)$$

The procedure described above is a direct method, proposed by Wood [11] for finding the sway-deflections in the elastic range. The stiffness distribution method has also been used [11] to find the deteriorated elastic critical load of a frame after the formation of hinges in the beams by reducing the beam stiffnesses in the following manner.

As a fully plastic hinge is treated like a real hinge, except that it rotates at constant moment M_p, the total tangential rotational stiffness of a beam having plastic hinge at one end is given by

$$K'_b = 3/4\, k_b + 0 = 3/4\, k_b = 3/4\, (M/(4E\theta)) \qquad (4.8)$$

Thus, comparing with equation (4.1), the stiffness of a beam reduces by 75% after the formation of a hinge. After the formation of a second hinge the beam loses all its stiffness for further increase of load, i.e.

$$K'_b = 0 \qquad (4.9)$$

Although the non-linear effects due to axial forces are neglected the moment-rotation relationship of a beam is non-linear due to the formation of hinges. K'_b should be defined as tangential rotational stiffness and expressed as

$$K'_b = \frac{1}{4E} \frac{dM}{d\theta}$$

as it is the tangential stiffness at a particular loading level which determines the deteriorated elastic critical load at that level.

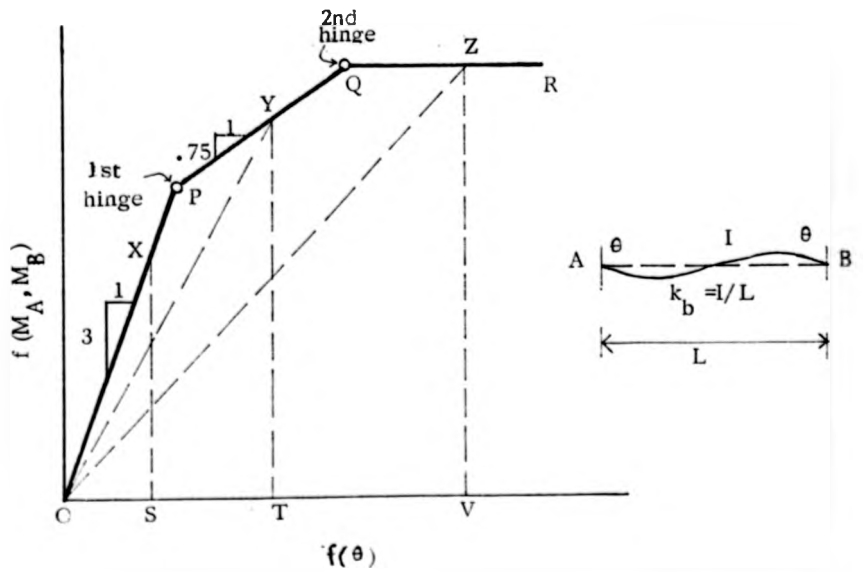

Figure 4.2

Figure (4.2) shows an idealised moment-rotation relationship in terms of the rotational stiffness of a beam with incremental loading. The line OPQR represents the rotational stiffness in the form K'_b/k_b at various stages of loading before and after the formation of plastic hinges. Before the formation of any hinge the tangential rotational stiffness of the beam is represented by the slope of the line OP which is $3\,k_b$. After the formation of the first hinge at the point P the tangential stiffness reduces to the slope of the line PQ ($= \cdot 75\,k_b$) and when the second hinge forms at Q the slope indicates zero tangential stiffness (equations 4.1 , 4.8 and 4.9).

For the calculation of sidesway at a particular load level, it is the resultant stiffness of the beam up to that level and not the tangential stiffness that has to be used. This resultant stiffness is termed the 'secant' stiffness, K_b. The value of K_b will be different from the value of K'_b, the tangential stiffness, at every stage of loading after the formation of the first hinge. Referring to fig.4.2, at some point X in the elastic range, the secant $K_b/k_b = SX/OS$ which is the slope of the line OP, i.e. the same as the tangential K'_b/K_b at the point X. But at the point Y, i.e. after the formation of the first hinge the secant stiffness is indicated by TY/OT which is much larger than the slope of PQ. Even after the tangential stiffness has vanished, e.g. at the point Z, the secant K_b / k_b given by VZ/OV has a substantial positive value. Fig. (4.3) shows a case of comparative values of tangential stiffness and secant stiffness of a typical beam under increasing total loading.

Once the hinge pattern in a frame at a particular load level is assumed, the tangential stiffnesses of its member at that load level is known (equations 4.1, 4.8 and 4.9). But, as shown in figures (4.2 and 4.3), the secant stiffnesses of the members, other than those

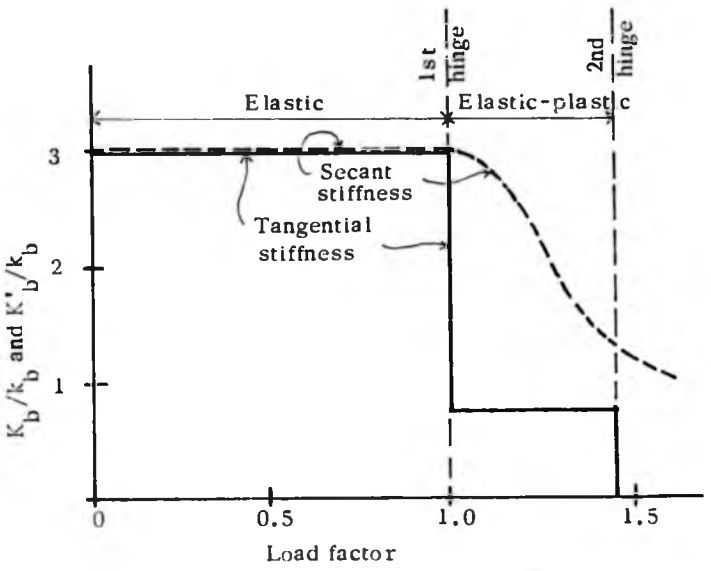

Figure 4.3

which are assumed to remain elastic, are unknown and can only be calculated when the joint and hinge rotations and the end moments of the members have been found. The relationship between the secant stiffness of a beam and its end rotations and moments will now be derived.

4.4 MOMENT ROTATION CHARACTERISTICS OF A BEAM WITH PLASTIC HINGE

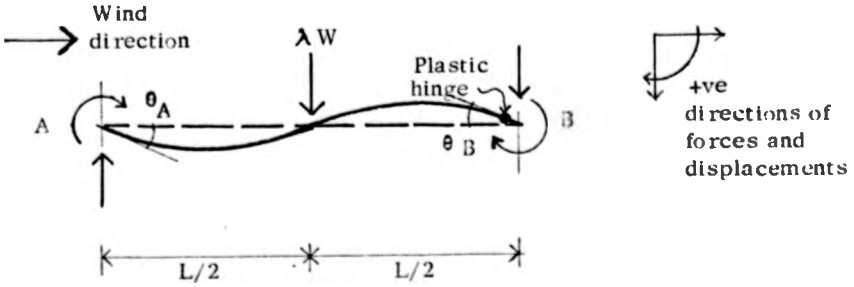

Figure 4.4

Figure (4.4) shows a beam in a multistorey frame subject to combined loading with predominating effects of horizontal loading. Considering the leeward end B of beam AB has a hinge at a load factor λ, the end-moments are given by (figure 4.4)

$$M_{AB} = \frac{EI}{L} [4\theta_A + 2(\theta_B + \theta_H)] - \frac{\lambda WL}{8} \qquad (4.10)$$

$$M_{BA} = \frac{EI}{L} [2\theta_A + 4 (\theta_B + \theta_H)] + \frac{\lambda WL}{8} \qquad (4.11)$$

Assuming $\theta_A = \theta_B = \theta$, the 'secant' stiffness of the beam can be expressed as

$$K_b = \frac{M_{AB}}{4E\theta} + \frac{M_{BA}}{4E\theta}$$

Using equations (4.10) and (4.11) and solving

$$K_b = \frac{I}{L} (3 + 1{\cdot}5 \frac{\theta_H}{\theta})$$

$$= 3k_b + 1{\cdot}5\, k_b \frac{\theta_H}{\theta} \qquad (4.12)$$

Equation (4.12) implies that, as due to the effect of combined loading θ_H will be a negative rotation, the value of K_b will be less than $3k_b$. Furthermore, to maintain constant moment M_p at this end of the beam, negative rotation of the hinge will increase with incremental loading, thus reducing K_b further. On the other hand, when θ_H is zero, i.e. before the formation of a hinge, K_b is given as $3k_b$ which is the expected value. A similar phenomenon has been observed in figures

(4.2 and 4.3).

Proceeding further, as the moment at the end B is M_p, the plastic moment of the beam AB, then equation (4.11) can be written as :

$$M_{BA} = M_p = \frac{EI}{L}(6\theta + 4\theta_H) + \frac{\lambda WL}{8} \qquad (4.13)$$

Solving for θ_H,

$$\theta_H = \frac{8M_p - \lambda WL}{32 Ek_b} - 1.5\theta \qquad (4.14)$$

From equations (4.11 and 4.12)

$$K_b = .75 k_b + \frac{24M_p - 3\lambda WL}{64 E \theta} \qquad (4.15)$$

Equation (4.15) expresses the secant stiffness of a beam with a plastic hinge in terms of its span length, section properties, vertical load and the joint rotations. It also implies that when the joint rotations are very large, i.e. $\theta \gg 0$, K_b is equal to $.75 k_b$ which is the tangential stiffness.

By assuming initial values of K_b for the beam-members of a frame in which a hinge pattern has been assumed to occur, the substitute frame analysis of Sec. (4.3) can be used to find the joint rotations of the frame (equation 4.3). Then these θ-values can be used in equation (4.15) to modify the secant stiffnesses and the substitute frame analysis can be performed again. Iterations may continue up to a reasonable degree of convergence. Final values of the joint rotations will give the hinge rotations (equation 4.14). A positive value of hinge rotation at the end of a beam where the joint rotation is also positive would indicate that no hinge has actually formed. This is because the value of a hinge

rotation given by the analysis is that required to satisfy the yield condition assumed initially, i.e. to cause a resultant moment equal to M_p, at the end where a plastic hinge has been assumed to occur (equation 4.13). Such a beam will be treated as having no plastic hinge and its secant stiffness taken as $3k_b$ for the next iteration. Final values of the joint and hinge displacements given by the analysis will enable the member forces to be calculated at the specified load factor.

Intuitive assumptions may be made for the initial values of the secant stiffnesses of the beams. Anderson[6], in his elastic-plastic computer analysis of several frames, has found that if the second hinge in a beam forms soon after $\lambda = 1{\cdot}4$, the first hinge of that beam would have formed at about $\lambda = 1{\cdot}1$. So, if the analysis of a frame is to be carried out at a load factor of $1{\cdot}4$, assuming a pattern of one hinge per beam at this load factor, it is likely that the beam in which the very first hinge has formed would have a secant stiffness of less than $1{\cdot}5\, k_b$ at $\lambda = 1{\cdot}4$. The beam in which the last hinge has formed will have a secant stiffness close to its elastic value, i.e. about $3k_b$. All the other beams, except those which have been assumed to remain elastic, will have K_b values in between the two.

Some or all of these assumptions may be wrong because before analysing the frame it is not known what the actual hinge pattern and the sequence of hinge formation is, or whether at the load factor $1{\cdot}4$ any hinge forms at all.

However, if the frame that is being analysed was originally designed to carry combined vertical and wind load and the selected member sections were not far off from the design requirements, then the sequence of hinge formation can be roughly estimated.

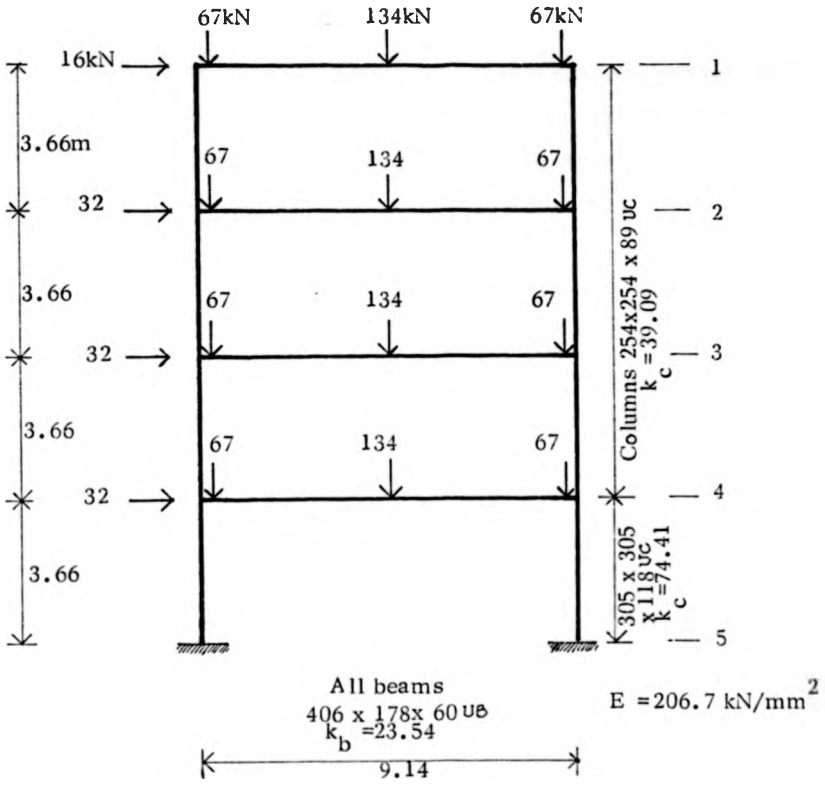

Figure 4.4

In a four-storey one-bay frame like the one shown in figure (4.4), it may be assumed that the first hinge will form in the beam at level 4, followed by hinges at levels 3, 2 and 1 respectively. Alternatively, if the base is fixed, the first hinge may form in level 3 followed by 4, 2 and 1. Also, due to the low value of wind shear compared to the vertical load in the roof beam, no hinge may form there even at collapse under combined loading. However, the sequence of hinge formation and their location will also depend

on the relative additional strength provided in the members over that required by design because of having to select the nearest available standard section and also because of the consideration of safety against local mechanisms.

So, one way of starting the analysis process is by assuming the initial secant stiffness values of $3k_b$ for all the beams of the frame irrespective of the hinge pattern. In such a case the number of iterations required for convergence may be larger than that which would have been necessary if accurate values could be chosen intuitively.

4.5 FOUR-STOREY ONE-BAY FRAME

The four-storey one-bay frame shown in figure (4.4) has been analysed by assuming the proposed method as described in Sec.(4.3 and 4.4).

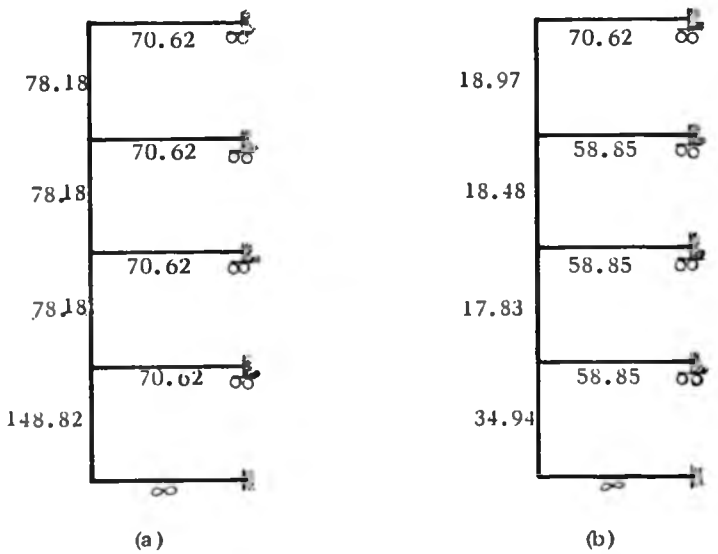

Figure 4.5

Figure (4.5a) shows the equivalent substitute frame considering all the members as elastic and no axial load on the columns. To facilitate comparison of the results of analysis by the proposed method with that of elastic-plastic computer analysis, a load factor of 1.39 is selected and it is assumed that all the four beams develop a hinge at their right-hand ends at this load factor. Initial secant stiffness of the beam at level 1 was assumed to be $3k_b$ and those of all the others were assumed as $2{\cdot}5\ k_b$.

Figure (4.5b) shows the equivalent substitute frame with assumed initial secant stiffnesses for the beams and actual stiffnesses of the colums considering the effects of axial forces ($\Sigma k_c \frac{n}{4}$). Table (4.1) shows the results of the initial analysis and Table (4.2) those of the fourth iteration. The $^{\Delta}$-values given by the fourth

Level	ϕ	$\overset{\Delta}{mm}$	θ	θ_H	K_b/k_b
1	0·00298	10.90	0.00138	+0.00218	3.000
2	0.00641	23.44	0.00370	- 0.00131	2.470
3	0.00876	32.05	0.00641	- 0.00538	1.742
4	0.00487	17.91	0.00654	- 0.00557	1.723

Table 4.1

Level	ϕ	$\overset{\Delta}{mm}$	θ	θ_H	K_b/k_b
1	0.00384	14.05	0.00169	0.0	3.000
2	0.00894	32.72	0.00510	- 0.00340	1.998
3	0.01198	43.82	0.01002	- 0.01079	1.385
4	0.00642	22.83	0.00924	- 0.00963	1.438

Table 4.2.

Figure (4.5a) shows the equivalent substitute frame considering all the members as elastic and no axial load on the columns. To facilitate comparison of the results of analysis by the proposed method with that of elastic-plastic computer analysis, a load factor of 1.39 is selected and it is assumed that all the four beams develop a hinge at their right-hand ends at this load factor. Initial secant stiffness of the beam at level 1 was assumed to be $3k_b$ and those of all the others were assumed as $2{\cdot}5\ k_b$.

Figure (4.5b) shows the equivalent substitute frame with assumed initial secant stiffnesses for the beams and actual stiffnesses of the colums considering the effects of axial forces ($\Sigma k_c \frac{n}{4}$). Table (4.1) shows the results of the initial analysis and Table (4.2) those of the fourth iteration. The $^{\Delta}$-values given by the fourth

Level	ϕ	Δ_{mm}	θ	θ_H	K_b/k_b
1	0·00298	10.90	0.00138	+0.00218	3.000
2	0.00641	23.44	0.00370	- 0.00131	2.470
3	0.00876	32.05	0.00641	- 0.00538	1.742
4	0.00487	17.91	0.00654	- 0.00557	1.723

Table 4.1

Level	ϕ	Δ_{mm}	θ	θ_H	K_b/k_b
1	0.00384	14.05	0.00169	0.0	3.000
2	0.00894	32.72	0.00510	- 0.00340	1.998
3	0.01198	43.82	0.01002	- 0.01079	1.385
4	0.00642	22.83	0.00924	- 0.00963	1.438

Table 4.2.

iteration and those of the third iteration are found to differ by 2.24%, 3.3%, 1.75% and 0.9% in beam levels 1, 2, 3 and 4 respectively. As this indicated a reasonable degree of convergence no further iteration was carried out.

Results obtained by non-linear elastic-plastic analysis using computer are shown in figure (4.6) and table (4.3). The figure shows the sequence of hinge formation and the respective load factors, while the table shows the joint and hinge rotations and the average sway in each storey. Comparing the two results it is observed that the hinge pattern, magnitude of hinge rotations and the sway deflections given by the proposed iterative substitute frame analysis have satisfactory agreement with those given by the computer. The joint rotations, however, vary considerably.

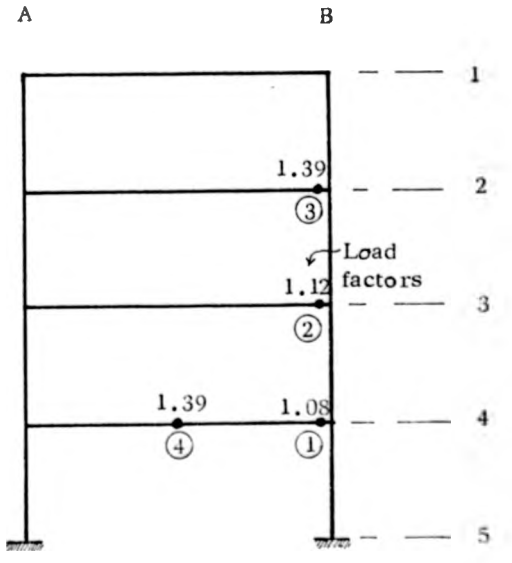

Figure 4.6

Level	θ_A	θ_B	θ_H	Δ mm
1	0.00650	-0.00289	0	14.48
2	0.00666	0.00411	-0.00384	33.81
3	0.01180	0.00869	-0.01104	44.55
4	0.01073	0.00802	-0.00986	23.01

Table 4.3

Though the effects of vertical load are considered in reducing the column stiffness and also in causing plasticity and thus reducing the beam stiffness, the basis of substitute frame analysis is the assumption of equal rotations for all the joints at any level of the frame which is approximately true under the effects of horizontal load only. In the substitute frame vertical load is not used directly and the assumption of symmetrical double-curvature bending of the beams is maintained.

Actual rotations of the different joints at any level under the action of combined loading are usually different, except for those of the internal joints of a 'regular' frame. In the upper beams of a multi-storey frame, where the effect of vertical load is more prominent than that of horizontal load, these differences will be significant. In many cases the roof beams and even some beams in the floor/floors below may bend in single curvature. These differences in the rotation of joints at a frame level reduce gradually towards the bottom and in high-rise multibay frames rotation of the internal joints at the lower levels are very nearly equal in each level.

The single-value joint rotation at any level of the frame given by the substitute frame analysis is very nearly the average of actual joint rotations at that level and they produce sway deflection values which are very close to the actual deflections. This shows that the vertical load has very little influence on the relative sway deflections of the different storeys of a frame or on the overall sway deflection of the frame itself.

However, as the actual rotation of the joints in a level of the frame generally are significantly different, rather than equal, use of the joint rotations given by the analysis in the calculation of member end-moments and secant stiffnesses of beams may lead to erroneous results.

As the sway deflections given by the analysis are found to be acceptable, use of these deflection values can be made in calculating the approximate joint and hinge rotations by considering a limited frame similar to the no-sway limited substitute frame of the JCR2 method [29]. This will be presented in the following Section.

4.6 LIMITED FRAME ANALYSIS FOR JOINT ROTATIONS

An iterative method has been developed to find the joint rotations of a frame by using a limited part of the frame for each joint. Assumptions (i) and (ii) of the substitute frame analysis (Sec. 4.3) regarding vertical deflections and the effects of axial forces in beams are also made in this analysis.

Expressions for the rotation of joints have been derived by using the slope-deflection relationship and for various cases of yield conditions of the adjoining beams.

Case 1 All the beams (LA, AB and BR) are elastic.

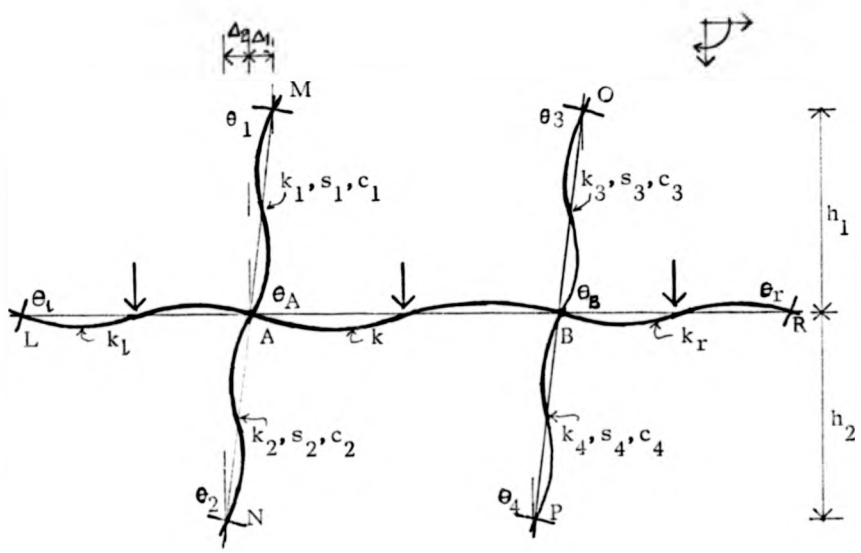

Figure 4.7

A typical interior joint A and the members of the limited part of the frame that effects its rotation are shown in the figure . k , k_l, k_r, k_1, k_2, k_3 and k_4 are the nominal rotational stiffnesses (I/L) of the members, s_1 , s_2 , s_3 , s_4 and c_1 , c_2 , c_3 , c_4 are the stability functions for the four columns and θ_l , θ_A , θ_B , θ_r , θ_1, θ_2 , θ_3 and θ_4 are the joint rotations at L, A, B, R, M, N, O, and P respectively. h_1 and h_2 and Δ_1 and Δ_2 are respectively the heights and sway deflections of the two storeys. FM_{AL} , FM_{AB} , FM_{BA} and FM_{BR} are the fixed end moments due to vertical load.

At joint A slope-deflection equations give the member end moments as

$$M_{AB} = Ek\,(4\theta_A + 2\theta_B) + FM_{AB}$$

$$M_{AL} = Ek_L\,(4\theta_A + 2\theta_L) + FM_{AL}$$

$$M_{AM} = Ek_1\left[s_1\theta_A + s_1 c_1 \theta_1 - \frac{s_1(1+c_1)\Delta_1}{h_1}\right]$$

$$M_{AN} = Ek_2\left[s_2\theta_A + s_2 c_2 \theta_2 - \frac{s_2(1+c_2)\Delta_2}{h_2}\right]$$

Similarly, at joint B

$$M_{BA} = Ek\,(2\theta A + 4\theta_B) + FM_{BA}$$

$$M_{BR} = Ek_r\,(4\theta_B + 2\theta_r) + FM_{BR}$$

$$M_{BO} = Ek_3\left[s_3\theta_B + s_3 c_3 \theta_3 - \frac{s_3(1+c_3)\Delta_1}{h_1}\right]$$

$$M_{BP} = Ek_4\left[s_4\theta_B + s_4 c_4 \theta_4 - \frac{s_4(1+c_4)\Delta_1}{h_2}\right]$$

For $\Sigma M_A = 0$, i.e., $M_{AB} + M_{AL} + M_{AM} + M_{AN} = 0$ and

$\Sigma M_B = 0$, i.e., $M_{BA} + M_{BR} + M_{BO} + M_{BP} = 0$ and equating

$$\theta_A = \frac{2k\,(Y_2 - Z_2) - X_2\,(Y_1 - Z_1)}{X_1 X_2 - 4k^2} \qquad (4.16)$$

where ,

$$X_1 = 4k + 4k_l + s_1k_1 + s_2k_2$$

$$Y_1 = (FM_{AB} + FM_{AL})/E$$

$$Z_1 = \frac{s_1(1+c_1)k_1}{h_1}\Delta_1 + \frac{s_2(1+c_2)k_2}{h_2}\Delta 2 - s_1c_1k_1\theta_1 - s_2c_2k_2\theta_2 - 2k_l\theta_l$$

$$X_2 = 4k + 4k_r + s_3k_3 + s_4k_4$$

$$Y_2 = (FM_{BA} + FM_{BR})/E$$

$$Z_3 = \frac{s_3(1+c_3)k_3}{h_1}\Delta_1 + \frac{s_4(1+c_4)k_4}{h_2}\Delta_2 - s_3c_3k_3\theta_3 - s_4c_4k_4\theta_4 - 2k_r\theta_r$$

Case 2 - Plastic hinge in beam AB

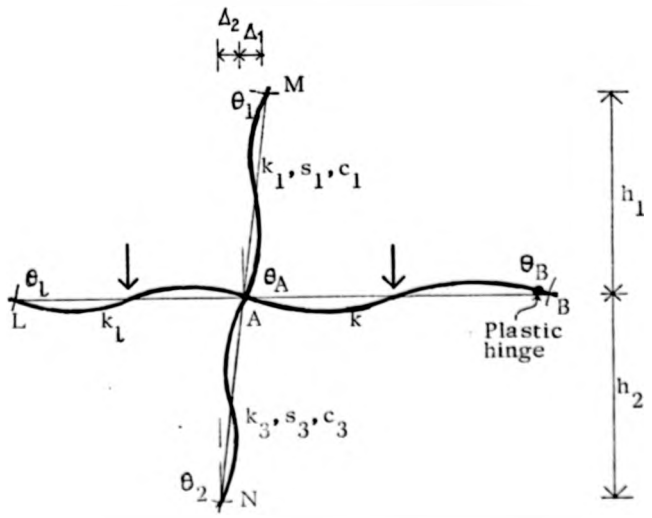

Figure 4.8

Figure (4.8) shows the limited frame with a plastic hinge at the right-hand end of beam AB. As the moment at B is now known, columns BO and BP and beam BR have been excluded from the subassemblage. The notations are as defined in Case 1 and have the same definitions in the subsequent cases, only the values of X_1, X_2, Y_1, Y_2, Z_1 and Z_2 are different in different cases.

Proceeding as in Case 1, at joint A

$$M_{AB} = Ek[\,4\theta_A + 2(\theta_B + \theta_H)\,] + FM_{AB}, \quad \theta_H \text{ being the hinge rotation}$$

$$M_{AL} = Ek_1(4\theta_A + 2\theta_1) + FM_{AL}$$

$$M_{AM} = Ek_1\left[s_1\theta_A + s_1c_1\theta_1 - \frac{s_1(1+c_1)\Delta_1}{h_1}\right]$$

$$M_{AN} = Ek_2\left[s_2\theta_A + s_2c_2\theta_2 - \frac{s_2(1+c_2)\Delta_2}{h_2}\right]$$

At joint B,

$$M_{BA} = Ek[\,2\theta_A + 4(\theta_B + \theta_H)\,] + FM_{BA}$$

$$= M_p, \text{ plastic moment of beam AB}$$

Equating for θ_H,

$$\theta_H = \frac{M_p - FM_{BA}}{4Ek} - \frac{\theta_A}{2} - \theta_B \qquad (4.17)$$

Using equation (4.17) in the expression for M_{AB} and equating for $\Sigma M_A = 0$,

$$\theta_A = \frac{Z_1 - Y_1}{X_1} \qquad (4.18)$$

where ,

$$X_1 = 3k + 4k_L + s_1k_1 + s_2k_2$$

$$Y_1 = \frac{2FM_{AB} + 2FM_{AL} - FM_{BA} + M_p}{2E}$$

$$Z_1 = \frac{s_1(1 + c_1)k_1}{h_1}\,\Delta_1 + \frac{s_2(1 + c_2)k_2}{h_2}\,\Delta_2 - 2k_L\theta_L - s_1c_1k_1\theta_1 - s_2c_2k_2\theta_2$$

Case 3 Plastic hinge in beam LA

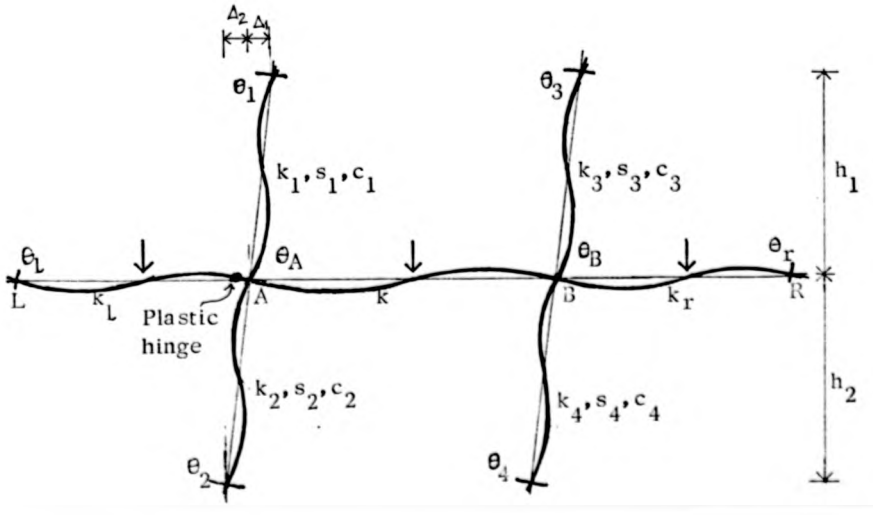

Figure 4.9

Figure (4.9) shows the limited frame with a plastic hinge at the right-hand end of beam LA.

At joint A ,

$$M_{AB} = Ek\,(4\theta_A + 2\theta_B) + FM_{AB}$$

$M_{AL} = M_{pl}$, plastic moment of beam LA

$$M_{AM} = Ek_1\left[\, s_1\theta_A + s_1c_1\theta_1 - \frac{s_1\,(1+c_1)}{h_1}\,\Delta_1 \,\right]$$

$$M_{AN} = Ek_2\left[\, s_2\theta_A + s_2c_2\theta_2 - \frac{s_2\,(1+c_2)}{h_2}\,\Delta_2 \,\right]$$

At joint B the member end moments are the same as in Case 1. For $\Sigma M_A = 0$ and $\Sigma M_B = 0$ and equating, θ_A is given by the same expression as in equation (4.16) with

$$X_1 = 4k + s_1k_1 + s_2k_2$$

$$Y_1 = (FM_{AB} + M_{pl})/E$$

$$Z_1 = \frac{s_1\,(1+c_1)\,k_1}{h_1}\,\Delta_1 + \frac{s_2(1+c_2)\,k_2}{h_2}\,\Delta_2 - s_1c_1k_1\theta_1 - s_2c_2k_2\theta_2$$

$$X_2 = 4k + 4k_r + s_sk_3 + s_4k_4$$

$$Y_2 = (FM_{BA} + FM_{BR})/E$$

$$Z_2 = \frac{s_3(1+c_3)\,k_3}{h_1}\,\Delta_1 + \frac{s_4(1+c_4)\,k_4}{h_2}\,\Delta_2 - s_3c_3k_3\theta_3 - s_4c_4k_4\theta_4 - 2k_r\theta_r$$

Case 4 - Plastic hinge in beam BR

Referring to figure (4.10) the plastic hinge is in beam BR while

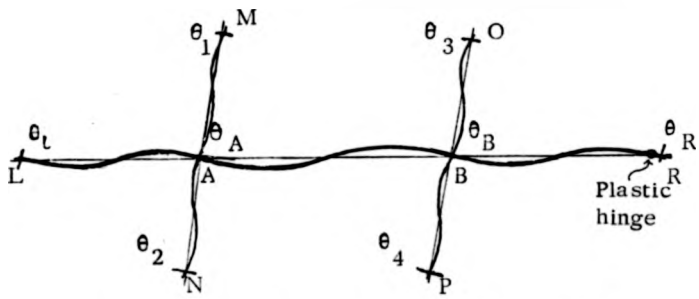

All other notations same as in figure (4.7)

Figure 4.11

both LA and AB are elastic. Proceeding as in the preceding cases θ_A can again be expressed by equation (4.16) with

$$X_1 = 4k + 4k_1 + s_1k_1 + s_2k_2$$

$$Y_1 = (FM_{AB} + FM_{AL}) / E$$

$$Z_1 = \frac{s_1(1+c_1)k_1}{h_1}\Delta_1 + \frac{s_2(1+c_2)k_2}{h_2}\Delta_2 - 2k_1\theta_1 - s_1c_1k_1\theta_1 - s_2c_2k_2\theta_2$$

$$X_2 = 4k + 3k_r + s_3k_3 + s_4k_4$$

$$Y_2 = \frac{2FM_{BA} + 2FM_{BR} + M_{pr} - FM_{RB}}{2E}$$, M_{pr} being the plastic moment of beam BR

$$Z_2 = \frac{s_3(1+c_3)k_3}{h_1}\Delta_1 + \frac{s_4(1+c_4)k_4}{h_2}\Delta_2 - s_3c_3\theta_3 - s_4c_4\theta_4$$

Case 5 - Plastic hinges in beams LA and AB

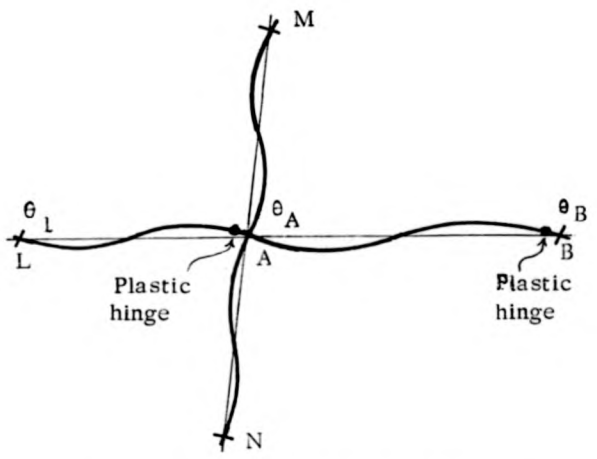

All other notations same as in figure (4.8)

Figure 4.11

Figure (4.11) shows the limited frame with plastic hinges in the beams LA and AB. Expression for θ_A is given by the equation (4.18) with

$$X_1 = 3k + s_1 (1 + c_1) k_1 + s_2 k_2$$

$$Y_1 = \frac{2FM_{AB} - FM_{BA} + M_p + 2M_{Pl}}{2E}$$

$$Z_1 = \frac{s_1 (1 + c_1) k_1}{h_1} \Delta_1 + \frac{s_2 (1 + c_2) k_2}{h_2} \Delta_2$$

Case 6 - Plastic hinges in beams LA and BR

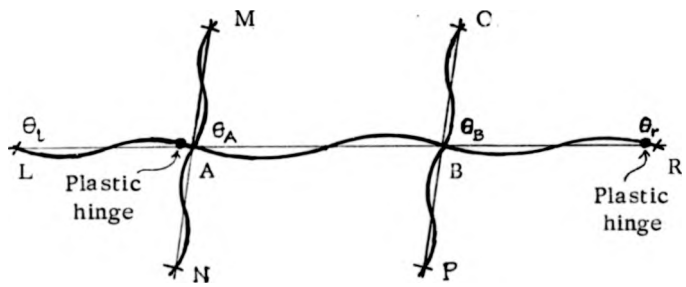

All other notations same as figure(4.7)

Figure 4.12

Figure (4.12) shows the limited frame with plastic hinges in the beams LA and BR while AB is elastic.

Expression for θ_A is the same as given by equation (4.16) with

$$X_1 = 4k + s_1k_1 + s_2k_2$$

$$Y_1 = (FM_{AB} + M_{Pl})/E$$

$$Z_1 = \frac{s_1(1+c_1)k_1}{h_1}\Delta_1 + \frac{s_2(1+c_2)k_2}{h_2}\Delta_2 - s_1c_1k_1\theta_1 - s_2c_2k_2\theta_2$$

$$X_2 = 4k + 3k_r + s_3 k_3 + s_4 k_4$$

$$Y_2 = \frac{2FM_{BA} + 2FM_{BR} - FM_{RB} + M_{Pr}}{2E}$$

$$Z_2 = \frac{s_3 (1+c_3) k_3}{h_1} \Delta_1 + \frac{s_4 (1+c_4) k_4}{h_2} \Delta_2 - s_3 c_3 k_3 \theta_3 - s_4 c_4 k_4 \theta_4$$

The six cases considered above represent all the possible plastic hinge patterns in the beams that will affect the rotation of joint A.

Separate expressions have been derived for the joints at the extreme right-hand (leeward) column which are as follows.

Case 7 End joint; Beams elastic (figure 4.13)

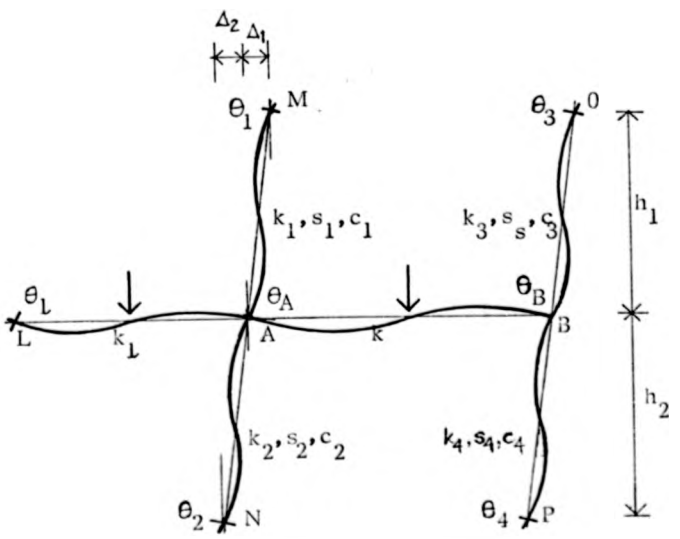

Figure 4.13

$$\theta_B = \frac{2k\,(Y_1 - Z_1) - X_1\,(Y_2 - Z_2)}{X_1 X_2 - 4k^2} \qquad (4.19)$$

where

$$X_1 = 4k + 4k_L + s_1 k_1 + s_2 k_2$$

$$Y_1 = (FM_{AB} + FM_{AL})/E$$

$$Z_1 = \frac{s_1(1+c_1)k_1}{h_1}\,\Delta_1 + \frac{s_2(1+c_2)k_2}{h_2}\,\Delta_2 - s_1 c_1 k_1 \theta_1 - s_2 c_2 k_2 \theta_2 - 2k_L\theta_L$$

$$X_2 = 4k + s\,k_3 + s_4 k_4$$

$$Y_2 = FM_{BA}/E$$

$$Z_2 = \frac{s_3(1+c_3)}{h_1}\,\Delta_1 + \frac{s_4(1+c_4)k_4}{h_2}\,\Delta_2 - s_3 c_3 k_3 \theta_3 - s_4 c_4 k_4 \theta_4$$

Case 8 End Joint :plastic hinge in beam LA (figure 4. 14)

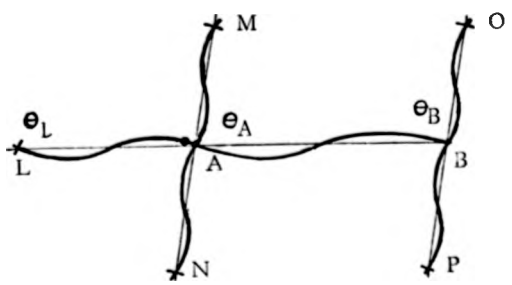

Other notations same as in figure (4.13)

Figure 4.14

Expression for θ_B is the same as given by equation (4.19) with

$$X_1 = 4k + s_1k_1 + s_2k_2$$

$$Y_1 = (FM_{AB} + M_{pl})/E$$

$$Z_1 = \frac{s_1(1+c_1)k_1}{h_1}\Delta_1 + \frac{s_2(1+c_3)k_2}{h_2}\Delta_2 - s_1c_1k_1\theta_1 - s_2c_2k_2\theta_2$$

$$X_2 = 4k + s_3k_3 + s_4k_4$$

$$Y_2 = FM_{BA}/E$$

$$Z_2 = \frac{s_3(1+c_3)k_3}{h_1}\Delta_1 + \frac{s_4(1+c_4)k_4}{h_2}\Delta_2 - s_3c_3k_3\theta_3 - s_4c_4k_4\theta_4$$

Case 9 End joint: plastic hinge in beam AB (figure 4.15).

Expression for θ_B is given by

$$\theta_B = \frac{Z_2 - Y_2}{X_2} \qquad (4.20)$$

where

$$x_2 = s_3k_3 + s_4k_4$$

$$Y_2 = M_{P/E}$$

$$Z_2 = \frac{s_3(1+c_3)k_3}{h_1}\Delta_1 + \frac{s_4(1+c_4)k_4}{h_2}\Delta_2\ s_3c_3k_3\theta_3 - s_4k_4\theta_4$$

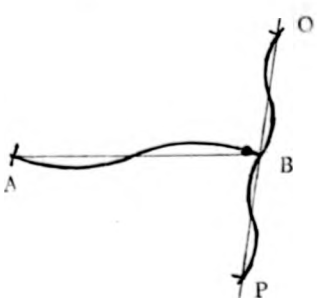

Figure 4.15

4.7 FRAME ANALYSIS PROCEDURE

As discussed in Sec. (4.5), the iterative substitute frame analysis described in Sec. (4.4) gives fairly accurate values of the sway deflections of a frame at the load factor at which the analysis is done. Although the plastic hinge pattern given by the analysis may not be very accurate, it gives some idea about possible location of hinges.

The frame analysis procedure is proposed to start with such an iterative analysis at the load factor at which the frame behaviour is desired to be studied. Results of this analysis give the initial values of Δ_1 and Δ_2 in a typical expression for θ_A and also enable to make an initial assumption for the hinge formation case (Sec. 4.6) for the subassemblage.

As the expressions for θ_A involve a number of other unknown rotations (θ_i , θ_Z, θ_L, ... etc) of the surrounding joints, modification of these expressions are necessary to be able to use them for finding the initial values of θ_A . The suggested modifications are explained below.

Calculation of joint rotations in a multi-bay multi storey frame

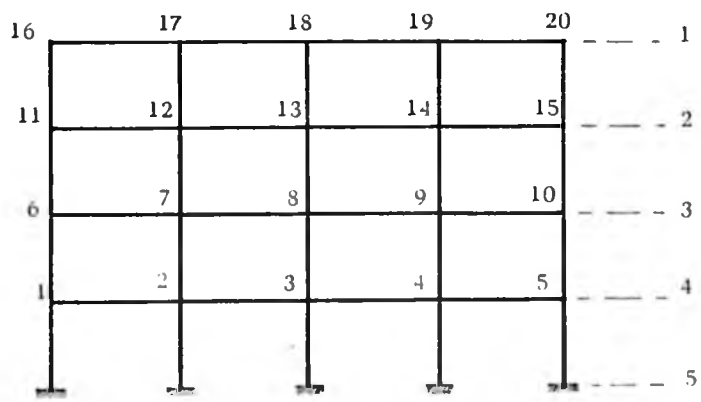

Figure 4.16

starts at the windward joint of the lowest beam level, i.e. at joint (1) of level 4 in figure (4.16). According to the plastic hinge pattern of the subassemblage surrounding joint (1) appropriate expression for θ_A (figure 4.17), representing rotation of joint 1, is chosen. Δ_1 and Δ_2 are known. For a fixed base frame $\theta_2 = \theta_4 = 0$.

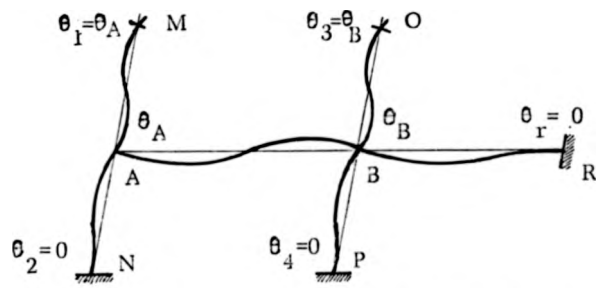

All other notations same as in figure (4.7)

Figure 4.17

Referring to the figures of the preceding sections, beam LA on the left side of joint A is absent, θ_1 and θ_3 are assumed as equal to θ_A and θ_B respectively and the joint R is considered to be fixed, i.e. $\theta_r = 0$. The last condition is assumed irrespective of the yield condition of beam BR given by the substitute frame analysis.

For no hinge in beam AB, the joint rotation at A is now given by

$$\theta_A = \frac{2k\,(Y_2 - Z_2) - X_2\,(Y_1 - Z_1)}{X_1 X_2 - 4k^2} \qquad (4.21)$$

where,

$$X_1 = 4k + s_1 (1 + c_1) k_1 + s_2 k_2$$

$$Y_1 = FM_{AB} / E$$

$$Z_1 = \frac{s_1 (1 + c_1) k_1}{h_1} \Delta_1 + \frac{s_2 (1 + c_2) k_2}{h_2} \Delta_2$$

$$X_2 = 4k + 4k_r + s_3 (1 + c_3) k_3 + s_4 k_4$$

$$Y_2 = (FM_{BA} + FM_{BR}) / E$$

$$Z_2 = \frac{s_3 (1 + c_3) k_3}{h_1} \Delta_1 + \frac{s_4 (1 + c_4) k_4}{h_2} \Delta_2$$

For a hinge in beam AB, the joint rotation is given by

$$\theta_A = \frac{Z_1 - Y_1}{X_1} \qquad (4.22)$$

where ,

$$X_1 = 3k + s_1 k_1 (1 + c_1) + s_2 k_2$$

$$Y_1 = \frac{2FM_{AB} - FM_{BA} + M_P}{2E}$$

$$Z_1 = \frac{s_1 (1 + c_1) k_1}{h_1} \Delta_1 \quad \frac{s_2 (1 + c_2) k_2}{h_2} \Delta_2$$

Equations (4.21) and (4.22) are the same as equations (4.16) and (4.18) respectively but all the terms of the two equations are now known.

After the rotation of joint A has been obtained the internal joints 2, 3, 4 and the external joint 5 are calculated in that order. As in the preceding case (referring to figure 4.7), $\theta_2 = \theta_4 = \theta_r = 0$, $\theta_1 = \theta_A$ and and $\theta_2 = \theta_B$ (Figure 4.18). For joint 2, θ_L is the rotation of joint 1 which has just been calculated and is a known quantity. Depending on the

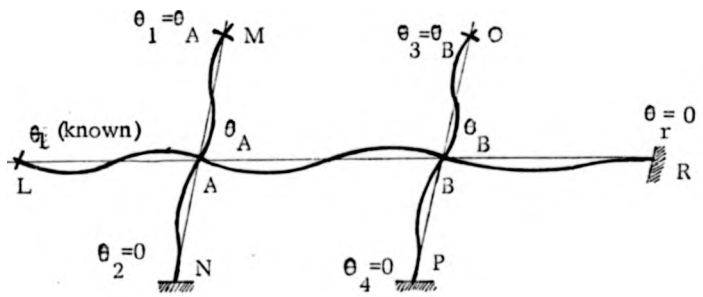

Figure 4.18

hinge formation criterion of beams LA and AB the appropriate equation for θ_A is chosen from Sec. (4.6) and modified for these conditions. If there is a hinge in beam AB, then the assumption of $\theta_r = 0$ is irrelevant and if there is a hinge in beam LA then the value of θ_L given by the immediately preceding calculation is not required.

Having calculated the rotations of all the joints in this floor, joints of the floor immediately above are calculated starting from the windward side, i.e., joint 6 of level 3 in figure (4.16). Referring to figure (4.7), θ_2 and θ_4 are now known from the calculation of rotations of the floor level below this level. θ_1 and θ_3 are again assumed as

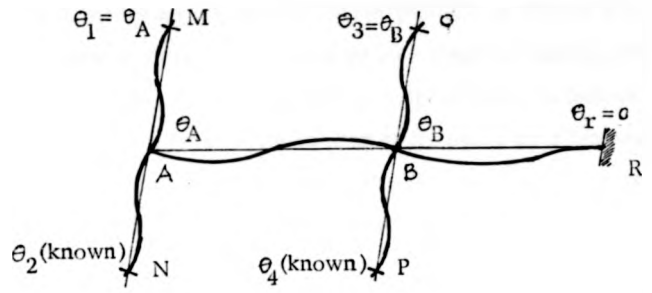

Figure 4.19

equal to θ_A and θ_B and the joint R as fixed, i.e. $\theta_r = 0$ (figure 4.19). For the internal joints 7, 8, 9 and the external joint 10, θ_L is given by the calculation of immediately preceding joint, while θ_2 and θ_4 are given by the calculation of the preceding floor (figure 4.20).

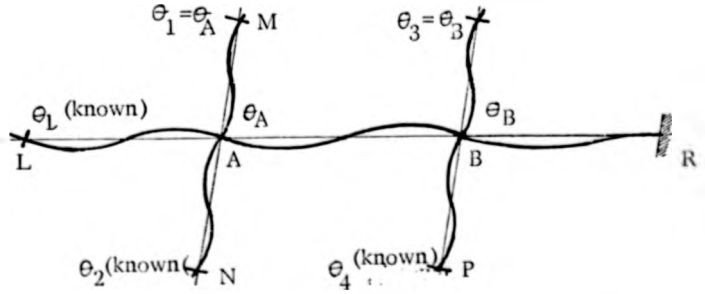

Figure 4.20

For the joint rotations at the roof level (level 1 of figure 4.16) a similar procedure is to be followed by choosing the appropriate expressions for the given plastic hinge criterion of the beams. Modification of the expressions is then to be made by eliminating all the terms related to columns AM and BO , i.e., s_1 , c_1 , k_1 , θ_1 and s_3 , c_3 , k_3 , θ_3 and the deflection Δ_i .

Now that a set of values for all the joint rotations has been obtained, the exact equations (4.16 - 4.20) may be used to calculate modified values of the rotations . θ_1 , θ_2 , θ_l, ...etc. may now be taken from these initial values and used in equations for θ_A .

The modifications are carried out exactly in the same sequence as the procedure adopted to calculate their initial values. For a typical internal joint (ref. figure 4.7) rotations at L, M, N, O, P and R are now known from their earlier calculations as specified below.

(i) θ_1 , θ_3 and θ_r are the values for the joints M, O & R given by the previous iteration.

(ii) θ_2 and θ_4 are given by the calculation of joint rotations for the preceding floor of the same iteration.

(iii) θ_l is the rotation of the immediately preceding joint of the same level calculated in the same iteration.

In this way use is made of the most recently modified rotation values of the surrounding joints.

This process of modification may be repeated till the θ-values given by successive calculations are very close. However, before proceeding

any further with the joint rotations the pattern of hinges given by the modified θ-values are evaluated in the following manner. At first the hinge rotations, θ_H, are calculated for all the beams, irrespective of their initial yield conditions by using equation (4.17). As explained earlier a positive value of this rotation where the corresponding joint rotation is also positive indicates that no hinge has formed in the beam. As the value of M_p has been taken as positive in equation (4.17) assuming a clockwise moment causing plasticity in beams, negative values of θ_H always indicate the formation of plastic hinges irrespective of the sense of the corresponding joint rotation. Thus, the directionsof the hinge rotations enable us to revise the hinge formation pattern initially given by the substitute frame analysis and the next modification process of joint rotatioms are carried out according to this revised hinge pattern.

Just one such iteration on the value of rotations is sufficient for reasonable convergence and the given values of rotations compare well with computer results. Exceptions arise in the cases of frames where, in the final analysis, θ_1 is expected to be of opposite sign to that of θ_A indicating single-curvature bending of the column AM (figure 4.7). The reason for the discrepancy in such cases may be attributed to the assumption of $\theta_1 = \theta_A$ for the initial calculations. Although this assumption is found to be reasonable in the lower storeys of the frame, for some joints in the upper storeys, where the column AM is expected to bend in single curvature, a better approach for the initial calculation of joint rotations could possibly be to assume fixed joints at M and O (figure 4.7), i.e. $\theta_1 = \theta_3 = 0$. But it is difficult to predict

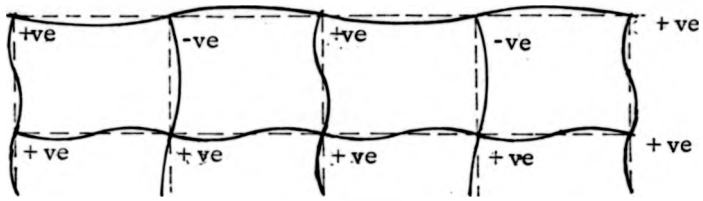

(a)

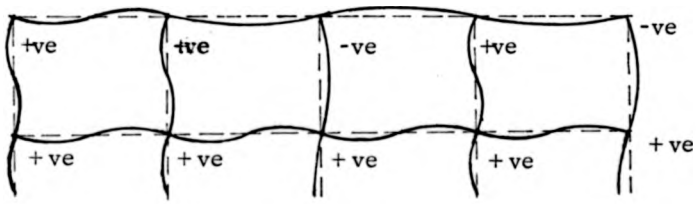

(b)

Figure 4.21

the bending pattern of the upper floors where the selection of member sections is not usually guided by the combined load criterion. Various combinations of bending pattern , especially in non-uniform frames are possible and figure (4.21) shows two of them. As the majority of the joints in a multistorey frame subjected to combined loading rotate in the same direction (clockwise for positive direction of wind forces) and differences of their values in successive levels of a column reduce gradually towards the bottom, a general assumption of $\theta_1 = \theta_A$ and $\theta_3 = \theta_B$ in the initial calculations is more realistic than $\theta_1 = \theta_3 = 0$.

Even in non-uniform frames, two iterations of limited frame calculations, however, modify the θ-values appreciably and it has been found that after the second, or sometimes the third, iteration, there is no significant change in the θ-values in subsequent iterations. The 'limited frame' iterations can be summarised as shown in the

flow diagram of figure (4.22).

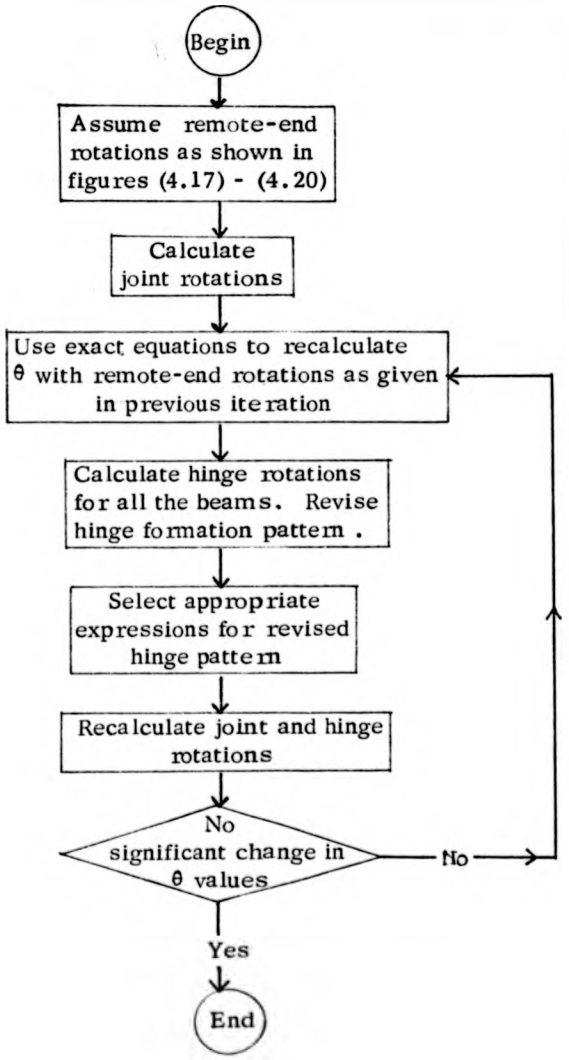

Figure 4.22

The 'limited frame' iterations which give the final value of the joint rotations are based on the sway-deflections obtained by the substitute frame analysis done in the beginning. As discussed in Sec. (4.5) the secant stiffness of elastic-plastic beams calculated and used in this iterative analysis may not have been very accurate because of the assumption of equal rotations for all the joints at any level. As such, in a frame with extensive formation of plastic hinges, the sway deflections given by the analysis can be significantly different from the actual values.

As more realistic values of the joint rotations have now been obtained by the 'limited frame' calculations the secant stiffnesses of the elastic-plastic beams may be calculated by using these values and their respective hinge rotations. The secant stiffness is given by

$$K_b = \frac{M_{rA}}{4E\theta_A} + \frac{M_{rB}}{4E\theta_B} \qquad (4.23)$$

where M_{rA} and M_{rB} are the moments at the ends A and B of a beam due to the joint and hinge rotations and θ_A and θ_B are rotations at A and B respectively. Secant stiffnesses of elastic beams are taken as 3k and the substitute frame analysis is carried out again.

It has been discussed in Sec. (4.5) that the vertical load has very little effect on the horizontal deflection of sway frames. Equivalent Grinter-type substitute frames subject to horizontal load only have been used [11] to calculate the sway deflections of actual frames carrying combined loading in the elastic range after necessary modification of column stiffnesses due to the effects of axial forces. The same principle is now being used to find the sway deflections

at a certain load factor for a frame in which plastic hinges form in some of the beams at that load factor. For the columns, where no plastic hinges are assumed to occur, stability functions are used to calculate the reduced stiffnesses caused by the action of axial forces. The stiffness of an elastic-plastic beam deteriorates due to the formation of plastic hinge and continues to do so as the loading increases further. To simulate a similar condition in the substitute frame its secant stiffness, representing the deteriorated stiffness at the particular load factor, has to be calculated in advance and used in the substitute frame. As the effect of axial forces in the beams has been assumed to be negligible no such modification of stiffness is required for the elastic beams.

Because of using these anticipated secant stiffnesses the substitute-frame analysis this time is not an iterative one, and only a single analysis is performed to calculate modified sway deflections. If the deflections given by this analysis differ significantly from those found earlier the whole process of limited-frame calculation for the joint rotations, as shown in the flow diagram of figure (4.22), is carried out again using the new values of deflections. The final joint displacements and hinge rotations given by the analysis are then used to calculate moments at the end and middle of beams and the end of columns throughout the frame.

The whole process of frame analysis can be summarised as follows:

Step 1

(i) Assume a probable/desired hinge pattern and secant stiffness values for the beams.

(ii) Perform iterative substitute frame analysis to find sway deflections and initial hinge pattern.

Step 2

(i) Perform iterative limited-frame calculations to find the joint and hinge rotations and the modified hinge pattern.

(ii) Calculate secant stiffnesses of elastic-plastic beams.

Step 3

(i) Find new values of sway deflections by single analysis of substitute frame and compare with values given in Step 1 (ii).

Step 4

Repeat step 2 if differences in the two sets of sway deflections are significant.

If in step 3 the deflections are found to differ by large proportions, then another round of calculations involving steps 3 and 4 produce improved results.

Step 5

Calculate moments and check yield criterion for all the members of the frame.

4.8 SIX-STOREY ONE-BAY FRAME

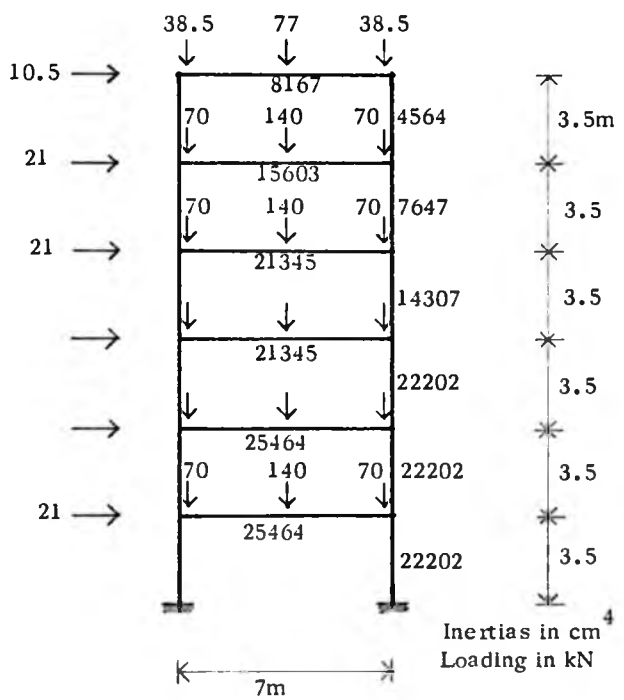

Figure 4.23.

Different aspects of the frame analysis procedure proposed in Sec.(4.7) are now demonstrated by analysing the six-storey one-bay frame which is shown in figure (4.23). The frame is at first analysed at a load factor of 1.54 to facilitate comparison with results given by non-linear elastic-plastic computer analysis.

Figure(4.24) shows the initial assumptions of hinge pattern and the secant stiffnesses of beams.

Figure (4.25) shows the results of substitute frame analysis after three iterations.

The initial values of joint rotations have been calculated by using the sway deflections shown in figure (4.25) and the modified limited frame expressions. These are shown in figure (4.26). Three

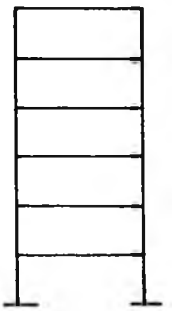

Figure 4.24

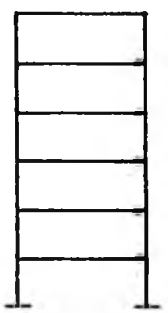

K_b/k_b	Δ in mm ×10	θ	θ_H
3.0	1.509	.00166	0
1.337	2.863	.00513	-.00569
1.431	3.850	.00779	-.00815
1.230	4.444	.01105	-.01303
1.347	4.348	.01144	-.01261
1.455	2.442	.00968	-.00997

Figure 4.25

θ_A	A	B	θ_B
.00715			- . 00342
.00782			. 00051
.00912			. 00558
.01137			. 00968
.01179			. 01077
.01071			. 00919

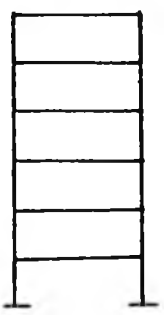

Figure 4.26

iterations have been performed with the actual limited frame expressions. The resulting hinge formation pattern, joint and hinge rotations and the secant stiffnesses of the beams are shown in figure (4.27).

θ_A		θ_B	θ_H	K_b/k_b
	A B			
.00718		- .00358	+ . 00342	3.0
.00789		.00109	- . 00303	2.718
.00919		.00616	- . 00723	1.516
.01171		.01030	- . 01262	1.244
.01186		.01101	- . 01239	1.355
.01047		.00873	- . 00942	1.488

Figure 4.27

Single analysis of the substitute frame with secant stiffness values of (4.27) gives the following deflections (figure 4.28).

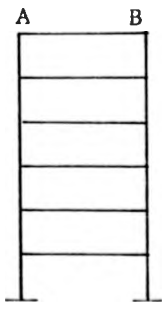

Δ in mm

10.63
23.64
36.97
43.81
43.04
24.20

Figure 4.28

Differences between these values and those given by the first analysis (figure 4.25) are quite significant. So, two rounds of limited-frame calculations have been done using the substitute frame analysis in between

to modify the deflections. Final results are shown in figure (4.29).

θ_A		θ_B	θ_H	Δ in mm
	A B			
.00651		- .00402	+ . 00419	.10.06
.00651		- .00093	- . 00031	22.49
.00828		.00504	- . 00564	36.02
.01133		.00989	- . 01203	43.35
.01165		.01076	- . 01204	42.78
.01133		.00857	- . 00919	24.10

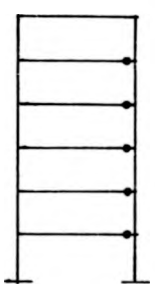

Figure . 4.29

Member moments are shown in figure (4.30)

Column moments	Beam moments			Column moments
5956	-5956	12944	9607	-9607
5957				-7934
1863	-7820	22471	22601	-14667
3455				-9308
-5054	1589	24532	27897	-18587
86				-10395
-7543	7458	27462	27897	-17509
-6714				-15252
-8091	14807	28714	32742	-17487
-11525				-23182
-273	11788	27204	32742	-9533
-27075				-31779

Moments in kNcm

Figure 4.30

to modify the deflections. Final results are shown in figure (4.29).

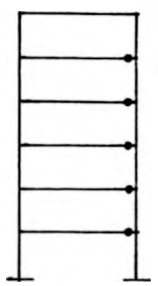

θ_A	θ_B	θ_H	Δ in mm
.00651	- .00402	+ . 00419	.10.06
.00651	- .00093	- . 00031	22.49
.00828	.00504	- . 00564	36.02
.01133	.00989	- . 01203	43.35
.01165	.01076	- . 01204	42.78
.01133	.00857	- . 00919	24.10

Figure . 4.29

Member moments are shown in figure (4.30)

Column moments	Beam moments			Column moments
5956	-5956	12944	9607	-9607
5957				-7934
1863	-7820	22471	22601	-14667
3455				-9308
-5054	1589	24532	27897	-18587
86				-10395
-7543	7458	27462	27897	-17509
-6714				-15252
-8091	14807	28714	32742	-17487
-11525				-23182
-273	11788	27204	32742	-9533
-27075				-31779

Moments in kNcm

Figure 4.30

As mentioned earlier, the frame has been analysed at $\lambda = 1.54$ so that the results given by the proposed analysis can be compared with those of computer analysis. However, the frame has also been analysed at load factors of 1.0 , 1.1 , 1.2, 1.3, 1.4, 1.5 and 1.6 to find out the sequence of hinge formation and also to predict the collapse load factor by studying the load-deflection behaviour. The number of hinges formed and the sway deflections at these load factors are shown in figure (4.31). The load-deflection curve is shown in figure(4.32.) The curve becomes asymptotic at a load factor of 1.62. So the collapse load factor can be taken as 1.62. It may be observed that at $\lambda = 1.6$ two of the beams have two plastic hinges each. The calculated deflections and rotations at this load factor are therefore not accurate, because the basis of calculation of secant stiffnesses for the substitute frame (equation 4.23) and of the limited frame expressions (Sec. 4.6) are not valid for beams with two plastic hinges.

Non-linear elastic-plastic computer analysis shows very close agreement with all these results. The sequence and load factor of hinge formation are shown in figure (4.33). The first hinge forms at a load factor of 1.23. The failure load is given as 1.61. Figure (4.34) shows the joint and hinge rotations and sway deflections of the different storeys at the load factor of 1.54. This load factor has been chosen to compare the two analyses as the last hinge (hinge no.5) before the appearance of the second beam-hinge forms at this load factor. Resulting moments in the members are shown in figure (4.35).

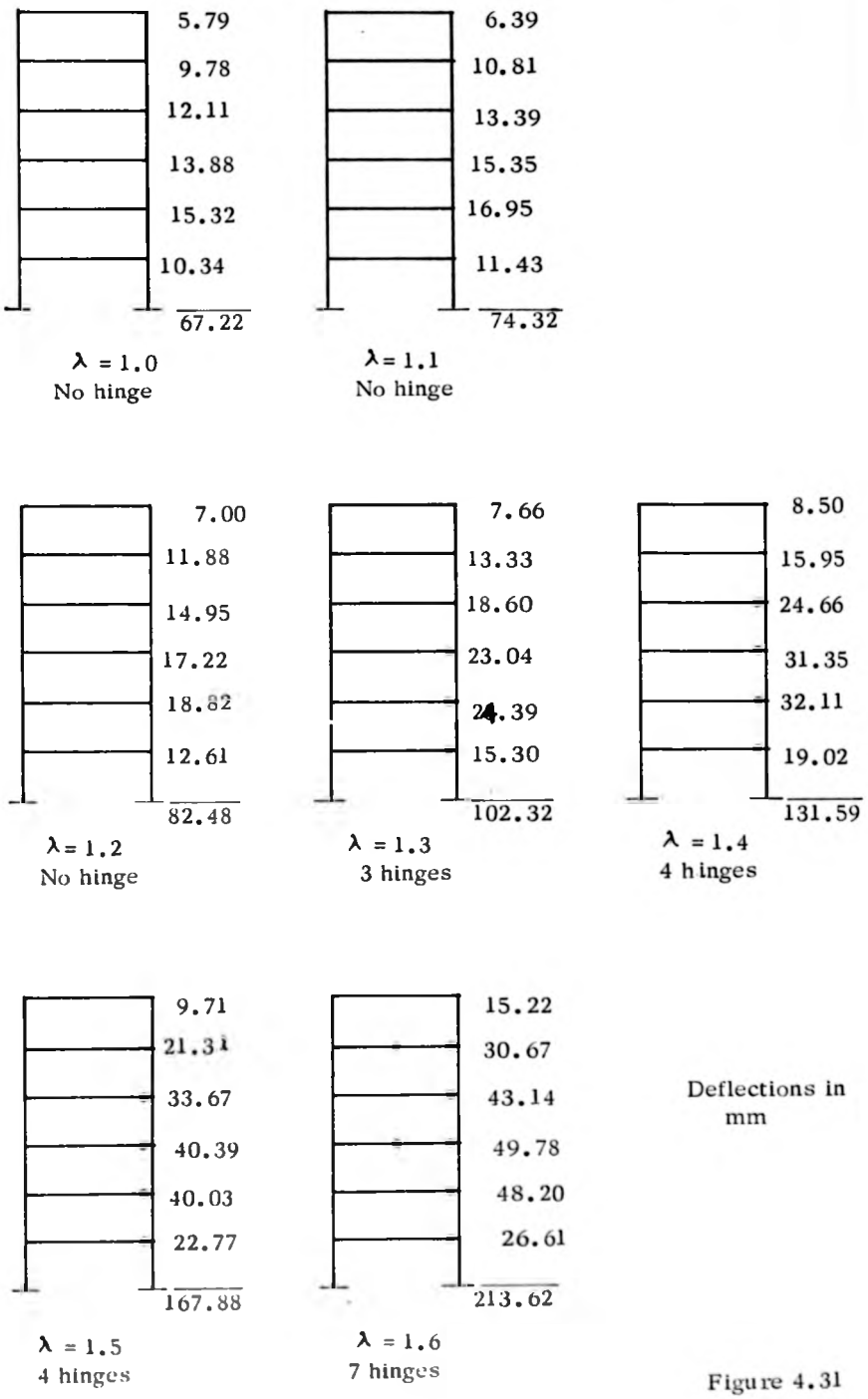
5.79
9.78
12.11
13.88
15.32
10.34
67.22
λ = 1.0
No hinge
6.39
10.81
13.39
15.35
16.95
11.43
74.32
λ = 1.1
No hinge
7.00
11.88
14.95
17.22
18.82
12.61
82.48
λ = 1.2
No hinge
7.66
13.33
18.60
23.04
24.39
15.30
102.32
λ = 1.3
3 hinges
8.50
15.95
24.66
31.35
32.11
19.02
131.59
λ = 1.4
4 hinges
9.71
21.31
33.67
40.39
40.03
22.77
167.88
λ = 1.5
4 hinges
15.22
30.67
43.14
49.78
48.20
26.61
213.62
λ = 1.6
7 hinges
Deflections in mm

Figure 4.31

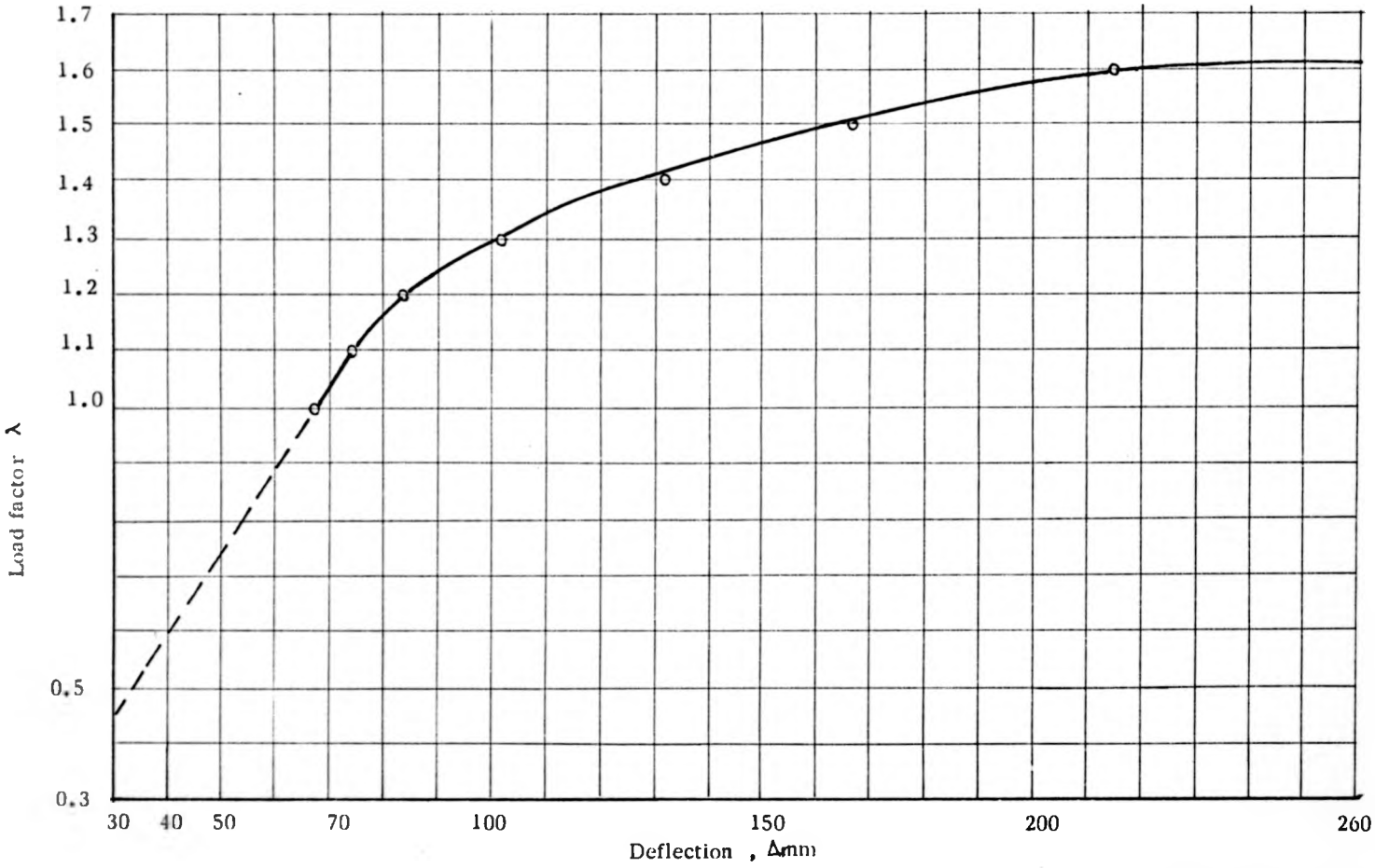
1.7
1.6
1.5
1.4
1.3
1.2
1.1
1.0
0.5
0.3
Load factor λ
30
40
50
70
100
150
200
260
Deflection , Δmm

Figure 4.32

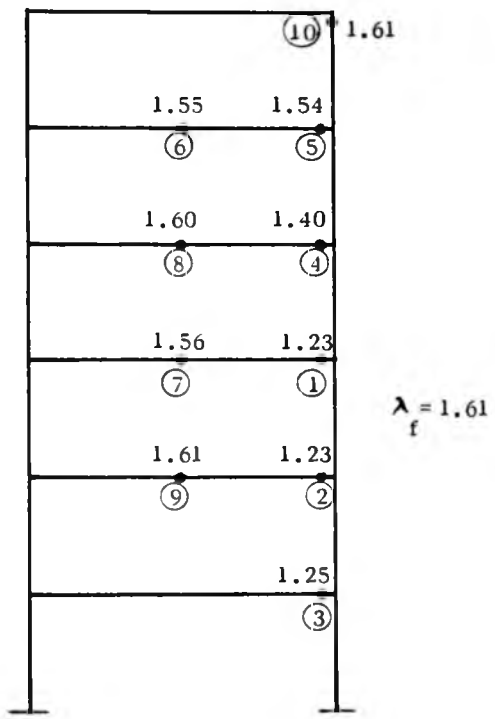

Figure 4.33

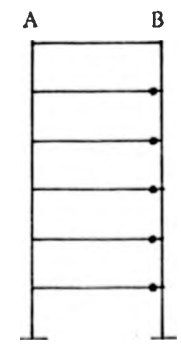

θ_A	θ_B	θ_H	Δ mm
.00655	- .00402	+.00419	9.86
.00635	- .00117	0(just formed)	21.08
.00780	.00440	- .00477	33.62
.01075	.00924	- .01108	41.25
.01118	.01022	- .01126	41.16
.01003	.00821	- .00867	23.42

Figure 4.34

Column moments	Beam moments			Column moments
5934	-5934	12962	9603	-9603
5828				-8046
2219	-8048	22368	22601	-14555
3525				-9558
-4194	669	24079	27897	-18339
773				-10205
-7094	6321	26905	27897	-17692
-5953				-15151
-7768	13721	28184	32742	-17591
-10784				-22810
- 298	11081	26863	32742	- 9932
-26455				-31104

Moments in kNcm

Figure 4.35

4.9 ALTERNATIVE APPROACH

Analysis of some frames may be found to be simpler by adopting an alternative approach but using the same basic principles. The procedure is as follows :

Step 1

(i) Assume the frame to be elastic at the specified load factor. So, K_b/k_b for all the beams are 3.0.

(ii) Perform single analysis of the substitute frame to find sway deflections.

Step 2

(i) Use deflection values of Step 1 in the appropriate limited-frame expressions (i.e. for all beams elastic) and find joint rotations. Calculate hinge rotations.

If no hinges are formed, analysis is complete and no further calculation is necessary.

(ii) If hinges form, repeat limited-frame calculations according to the hinge pattern. Calculate hinge rotations and find the new hinge pattern. Repeat the calculations till the hinge pattern is constant.

Step 3

Perform substitute frame analysis (no iteration) with secant stiffnesses of Step 2 to find new values of deflections.

Step 4

Repeat Step 2 with new deflections.

Step 5

Repeat Step 3 and Step 4 till the hinge pattern is constant.

Step 6

Calculate moments and check yield criterion for all the members of the frame.

As the iterative analysis of the substitute frame has been avoided, this approach is very convenient when analysing the frame at lower load factors when very few or no hinges are expected to form. If no hinges are found in Step 2(i) the analysis can be stopped there without any further calculation as has been the case in the six-storey one-bay frame (Sec. 4.8) at the load factors of 1.0, 1.1 and 1.2. In the earlier approach of analysis also calculations up to Step 2 (i) (Sec.4.7)

were sufficient at these load factors but involved an iterative analysis with the substitute frame.

At higher load factors, however, when an extensive hinge formation pattern is expected , the alternative approach will be disadvantageous as it involves iterations in Step 2 as well as the possibility of several repetitions in Step 5.

4.10 SIX-STOREY THREE-BAY FRAME

The six-storey three-bay frame shown in figure (4.36) was analysed at a load factor of 1.44 using the proposed method.

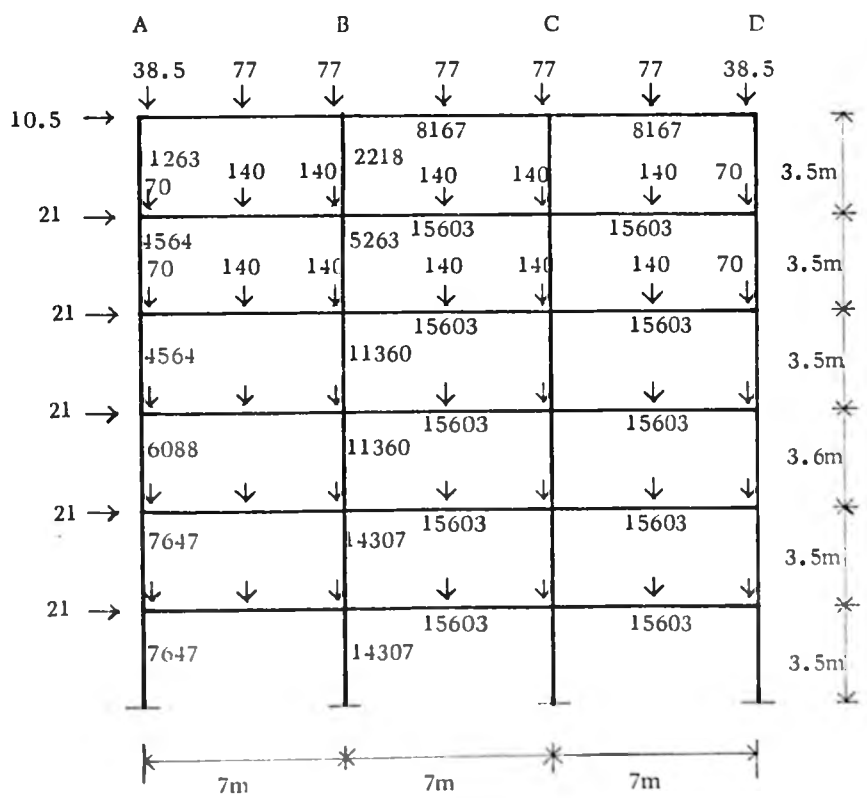

Figure 4.36

Figure (4.37) shows the hinge formation pattern and the sway deflections (upper values) given by the proposed analysis method, while figure (4.38) shows the hinge pattern and sequence of their formation as given by the computer analysis. The lower values of figure (4.37) show the deflections given by the computer analysis. Figure (4.39) shows the joint rotations, upper figures are those given by the proposed analysis and the lower figures are those of computer analysis. Similarly, the hinge rotations and the member moments are shown in figures (4.40 and 4.41).

It may be observed that the proposed method of analysis did not produce the hinges no.(10) and (11) (figure 4.38) given by the computer. However, the comparative differences in the rotations are very small. The moments given by the proposed analysis are very near to the plastic moment of the section (figure 4.41) and yielding at these points may be considered to have occurred.

Figure (4.37) shows the hinge formation pattern and the sway deflections (upper values) given by the proposed analysis method, while figure (4.38) shows the hinge pattern and sequence of their formation as given by the computer analysis. The lower values of figure (4.37) show the deflections given by the computer analysis. Figure (4.39) shows the joint rotations, upper figures are those given by the proposed analysis and the lower figures are those of computer analysis. Similarly, the hinge rotations and the member moments are shown in figures (4.40 and 4.41).

It may be observed that the proposed method of analysis did not produce the hinges no.(10) and (11) (figure 4.38) given by the computer. However, the comparative differences in the rotations are very small. The moments given by the proposed analysis are very near to the plastic moment of the section (figure 4.41) and yielding at these points may be considered to have occurred.

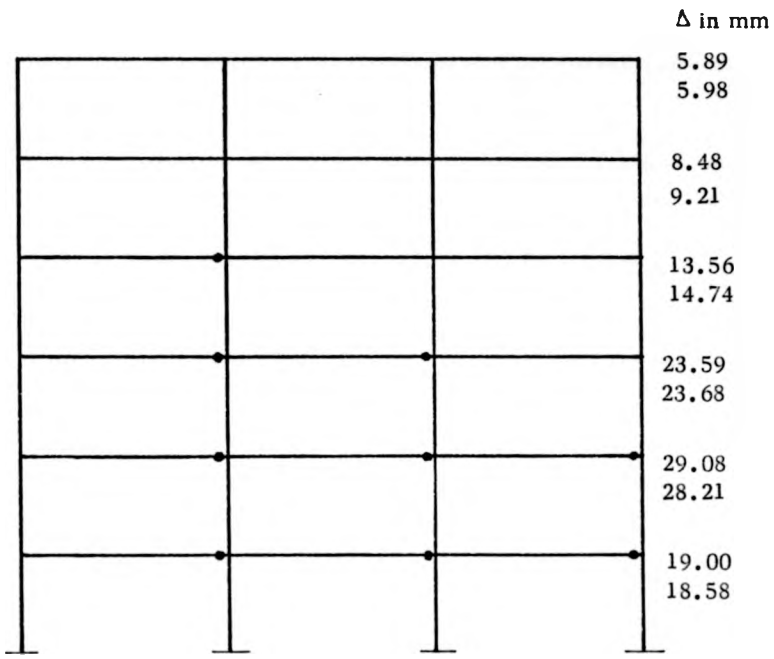

Figure 4.37

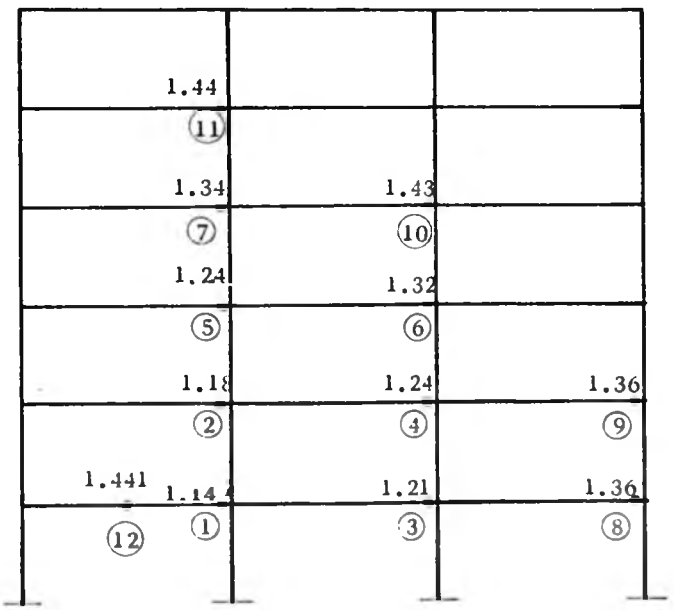

Figure 4.38

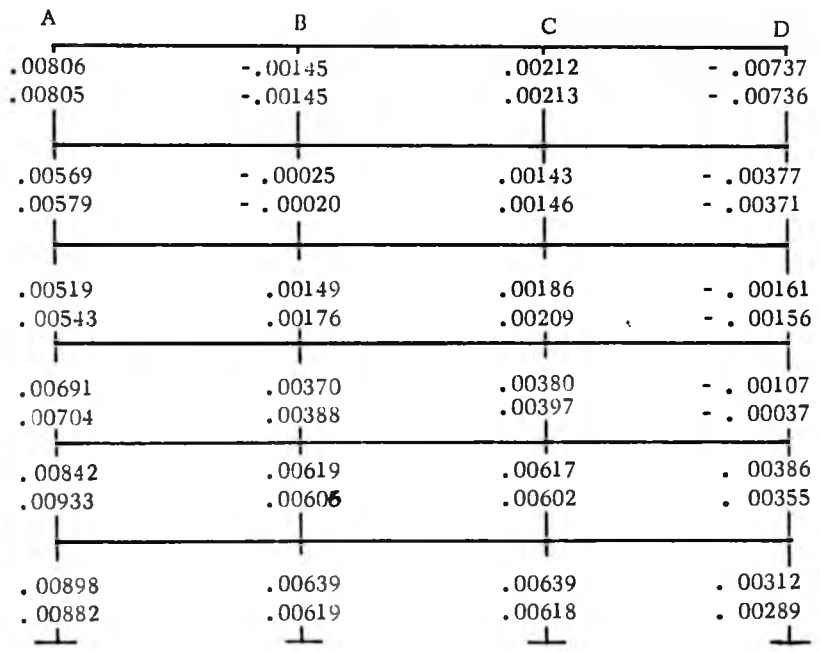

Figure 4.39

A	B	C	D
	+ .00150 0	+.00269 0	+ .01039 0
	+ .00005 - .00007	+ .00133 0	+ .00570 0
	-.00144 -.00184	+ .00004 -.00033	+ .00332 0
	-.00451 -.00477	-.00301 - .00327	+ .00181 0
	- . 00775 - . 00759	- .00662 -. 00641	-.00430 -.00391
	- . 00823 - . 00795	- .00694 - .00663	- .00368 -. 00334

Figure 4.40

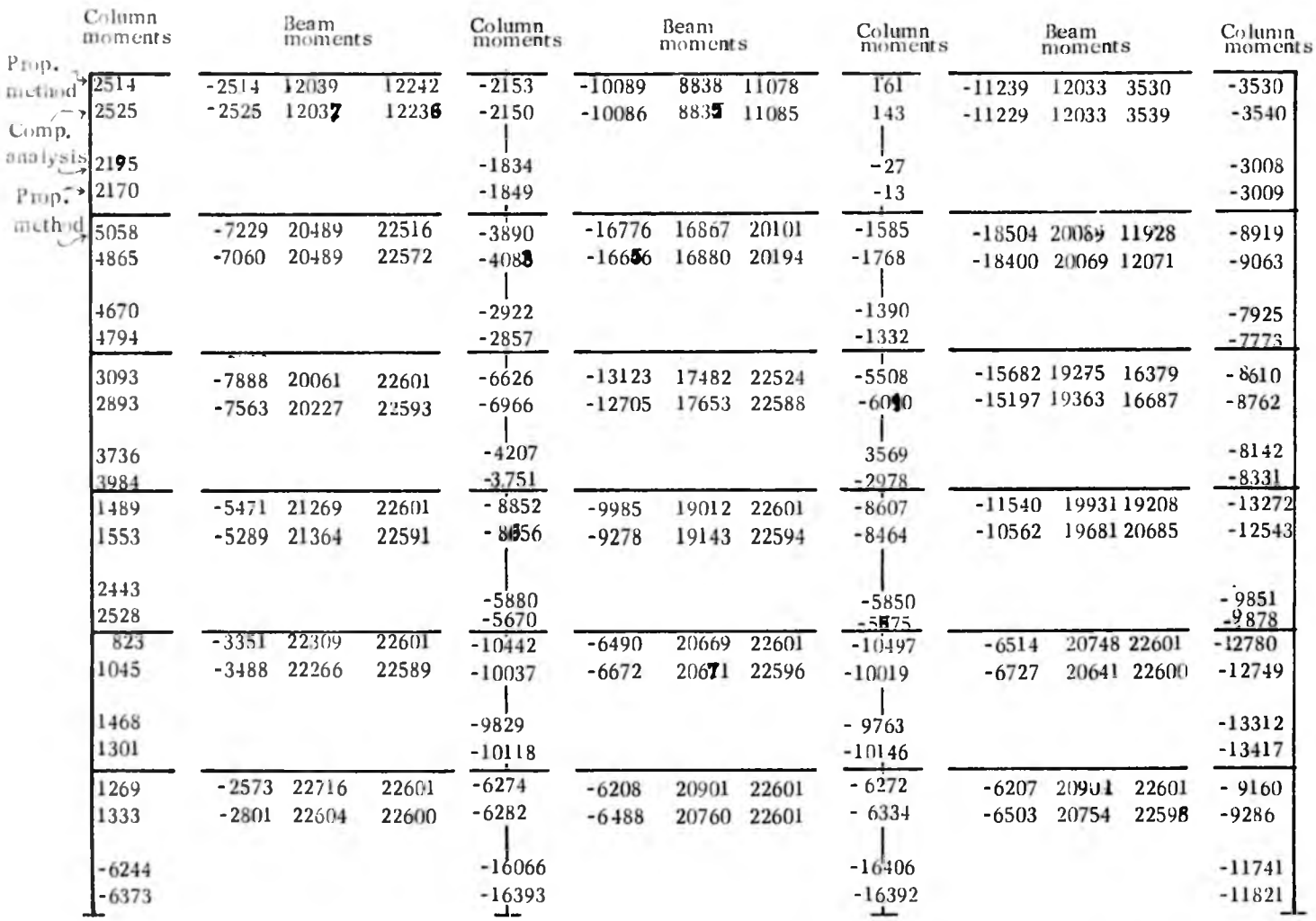

Moments in kNcm

Figure 4.41

CHAPTER V

MULTISTOREY FRAMES : OPTIMUM DESIGN TO STRENGTH, DEFLECTION AND STABILITY REQUIREMENTS

5.1 INTRODUCTION

In multistorey sway frames, the effect of combined vertical and horizontal loading causes plastic hinges to form at the leeward end of beams. As discussed in the preceding chapter, stability of a frame deteriorates suddenly, indicating imminent collapse when the second hinge appears in a beam or hinge forms in a column. It has also been observed [6] that a frame remains stable even if all the beams have a hinge formed at their leeward ends, although in such a case collapse follows immediately on the formation of the next hinge, either in the middle of a beam or at the end of a column.

So, for a frame specified not to fail before a certain load factor, the aim of design is to select, by some procedure, member sizes so that under the action of factored loading there is no more than one plastic hinge per beam and there are no hinges in the columns . The optimum solution is the one where there are as many single-hinged beams in the frame at the desired load factor as is possible without causing the possibility of local beam-mechanisms. In other words, the overall objective is to force a desired hinge pattern in the frame at a specific load factor by suitable choice of sections for the members.

If, by quick and simple techniques a lower-bound design solution containing undesirable plastic hinges, and thus not satisfying the design constraints, can be obtained then the problem of minimum-

weight design develops into a process of reaching the desired hinge pattern by increasing the member sizes in such a way that the increase in overall weight of the frame has been kept to the minimum.

Basically there are three main constraints in the ultimate load design of a multistorey sway frame. These are,

(i) strength requirement for the individual members to resist failure due to local collapse mechanism,

(ii) stiffness requirement for the frame as a whole against overall instability ,

(iii) deflection limitations to prevent loss of efficiency of the structure.

For the present study, the local member instability (lateral-torsional and local buckling) is not considered as a design constraint.

While the maintenance of a desirable hinge pattern will satisfy constraints (i) and (ii), satisfaction of the third constraint is not guaranteed by it.

In this chapter a method of design satisfying all the three constraints will be developed by using the frame analysis procedure proposed in the previous chapter.

5.2 THE LOWER-BOUND SOLUTION

If the constraint on deflection is not considered for the moment, one way of finding the lower-bound solution for a multi-storey sway frame would be to select the member sizes to resist local mechanisms.

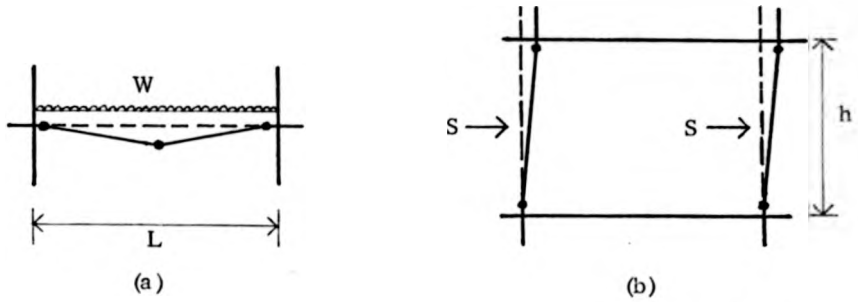

Figure 5.1

Referring to figure (5.1a) the required plastic moment for a beam Mp_b is given by the beam mechanism as

$$Mp_b = \frac{\lambda_1 WL}{16} \qquad (5.1)$$

where λ_1 is the design load factor and W is the total vertical load in the beam of span L.

Similarly, a lower-bound section for the column can be obtained by using the sway mechanism (figure 5.1b), the required plastic moment for a column , Mp_c being given by

$$Mp_c = \frac{\lambda_2 Sh}{2} \qquad (5.2)$$

where λ_2 is the design load factor and S is the total horizontal shear in the column of height h.

To satisfy the beam mechanism criterion of the adjoining beam, the minimum Mp_c of an external column shall be half of the Mp_b of the corresponding beam and that of the topmost external column shall be equal to the Mp_b of the corresponding roof beam.

For most of the examples presented in this chapter, values of λ_1 and λ_2 have been taken as 1.75 and 1.4 although lower values are in common use in current practice. The B/20 Draft Specification also recommends a lower value for λ_1.

It is very unlikely that the lower-bound solution obtained by the above procedure will satisfy the design constraints set up in the preceding section.

5.3 DESIGN TO SATISFY STRENGTH AND STABILITY CONSTRAINT

Having obtained the lower-bound solution, the next step is to set up the desired hinge pattern and analyse the frame at the specified load factor by the method described in chapter IV. If the yield condition has not been violated anywhere on the frame, i.e. the hinge pattern has either remained unaltered or some hinges have disappeared, the lower-bound solution will give the optimum design.

If, however, there are additional hinges in the beams, or if any of the columns have developed plasticity, then the initial design will have to be modified by increasing the sizes of the members. It may not be necessary to increase the sizes of all the members where undesirable hinges have appeared because of the redistribution of moment that takes place after a member is increased to the next higher standard section.

As discussed in the previous chapter the analysis procedure cannot be considered as accurate when dealing with frames having hinges in the columns or having beams with two hinges. So the analysis result of the lower-bound frame may not produce the actual hinge pattern. For the accuracy of the substitute frame analysis hinges in columns are more undesirable than the second hinge in the beams. Referring to figure (4.2) of Chapter IV when the second hinge appears in a beam, though the tangential stiffness becomes zero the secant stiffness does not have a sudden reduction. But when there is a hinge in the column the underlying principles of the substitute frame in calculating deflections are not applicable.

In modifying the lower-bound design, therefore, the columns shall be made free of hinges first and then the second hinges from the beams removed. However, analysis with several alternative arrangements of beam and column sizes may be necessary to ensure that the final solution is the optimum.

Finally, as it has been accepted that in an unbraced multistorey frame plasticity should not be allowed to develop at the service load [40] the final design solution shall be analysed at $\lambda = 1.0$. If any hinge appears further modification has to be carried out to satisfy this condition.

5.4 SIX-STOREY ONE-BAY FRAME

The six-storey one-bay frame of Sec. (4.8) will now be designed for the external loading and specifications shown in figure (5.2). Only the economical sections shown in tables (2.1 and 2.2) will be considered for the members.

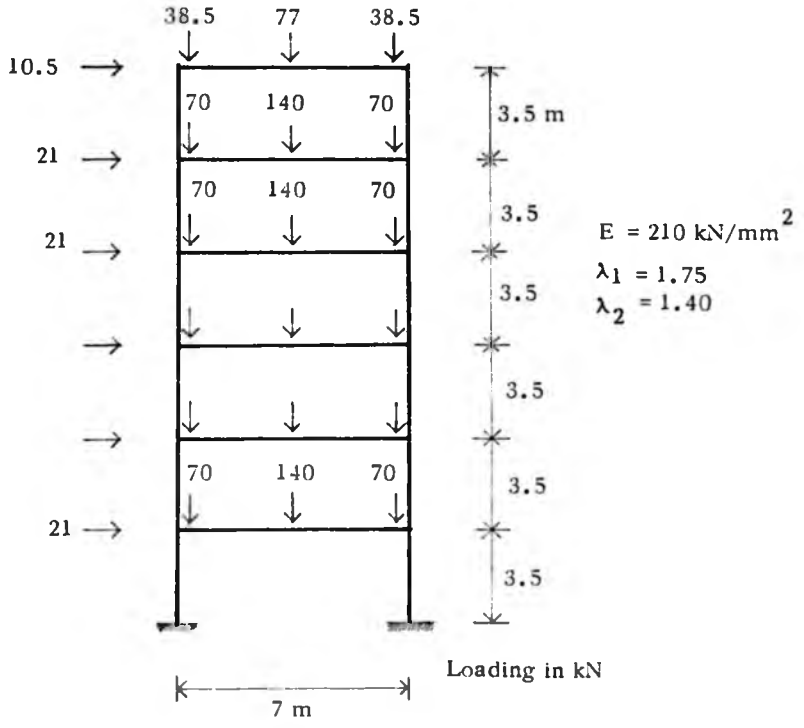

Figure 5.2

The aim of the design procedure is to find the optimum solution which will produce the most extensive formation of one hinge per beam at a load factor of 1.4 without causing any beam mechanism at $\lambda = 1.75$.

The lower-bound solution is given by the equations of Sec. (5.2). Figure (5.3a) shows the inertias of the different members in the lower bound design and (5.3b) shows the hinge pattern at $\lambda = 1.4$ after analysis by the method described in the previous chapter.

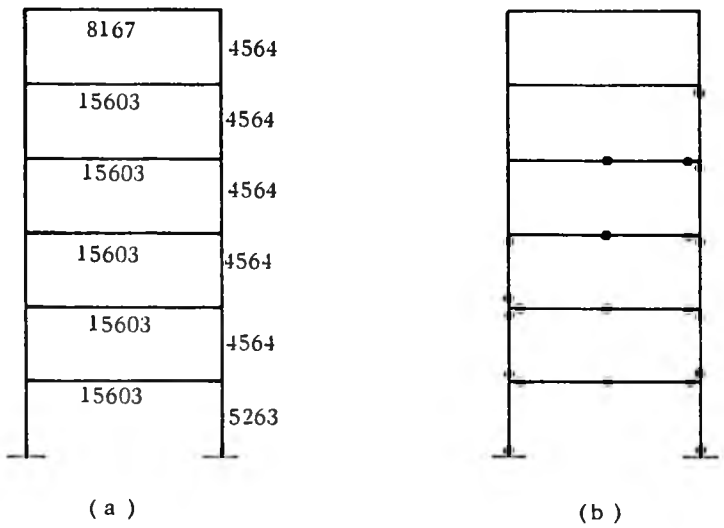

Figure 5.3

The hinge pattern shows that the design is a lower-bound solution and the frame would collapse at a load factor much lower than 1.4. Reasons for some of the members remaining elastic are

(i) design of beams was governed by the local mechanism criterion at $\lambda = 1.75$,

(ii) minimum column sizes were governed by the M_{Pb} of the adjoining beam, and

(iii) non-availability of a continuous range of standard section results in different proportion of surplus strength for different members.

Iterations are now carried out to reach at the desired solution, i.e. no hinge in the column and a maximum of one hinge per beam, each time increasing the size of one beam or those of one pair of columns to the immediately larger available section. Guided by the amount of

excessive moment in the members given by the analysis it may be possible to increase the sizes of more than one member at a time. After checking for optimality by analysing some alternative arrangements, the final design inertias are as shown in figure (5.4a) along with the hinge pattern at $\lambda = 1.4$.

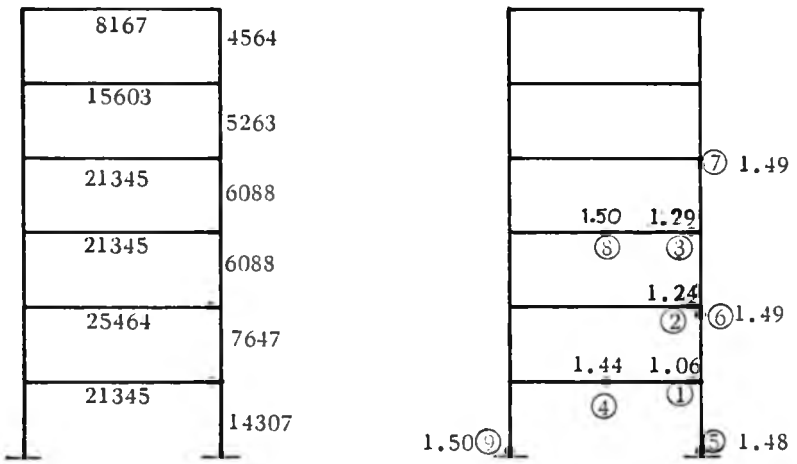

Figure 5.4

Figure (5.4b) shows the sequence of hinge formation and the load factors at which they form as given by the non-linear elastic-plastic analysis by computer. It confirms that three hinges in identical locations, hinge numbers 1, 2 and 3, form within load factor of 1.4 while the fourth hinge forms at $\lambda = 1.44$

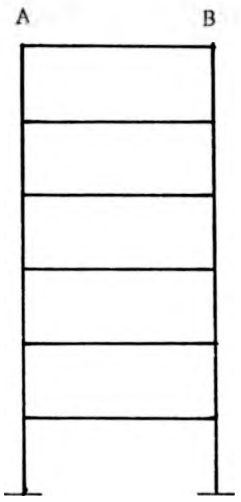

	θ_A	θ_B	θ_H	Δ in mm
	.00572	.00357	0	8.22
	(.00593)	(.00371)	(0)	(8.47)
	.00581	.00183	0	16.98
	(.00600)	(.00189)	(0)	(17.41)
	.00668	.00008	0	32.67
	(.00679)	(.00002)	(0)	(32.33)
	.01049	.00609	-.00714	51.73
	(.01053)	(.00593)	(-.00720)	(51.39)
	.01212	.00937	-.01033	(58.20)
	(.01229)	(.00944)	(-.01066)	(59.09)
	.01298	.01062	-.01292	31.72
	(.01332)	(.01095)	(-.01361)	(32.46)
				199.52
				(201.15)

(a)

Column moments	Beam moments		Column moments
5575 (5725)	-5575	11708	(-8981)-8740
5624 (5766)	(-5725)	(12079)	(-7998)-7798
2359 (2431)	-7982	20724	(-11738)-11372
2895 (2911)	(-8197)	(21364)	(-10592)-10204
-2960 (-2596)	65	21380	(-15706)-15701
- 289 (35)	(-314)	(22024)	(-11559)-11487
-8088 (-7706)	8379	24541	(-16338)-16412
-6963 (-6478)	(7670)	(25217)	(-13942)-14146
-11467 (-11566)	18430	27144	(-18799)-18587
-10728 (-10673)	(18044)	(27982)	(-17515)-17503
-2431 (-2357)	13156	26930	(-10380)-10405
-23883 (-24529)	(13029)	(27897)	(-28302)-27961

(b)

Figure 5.5

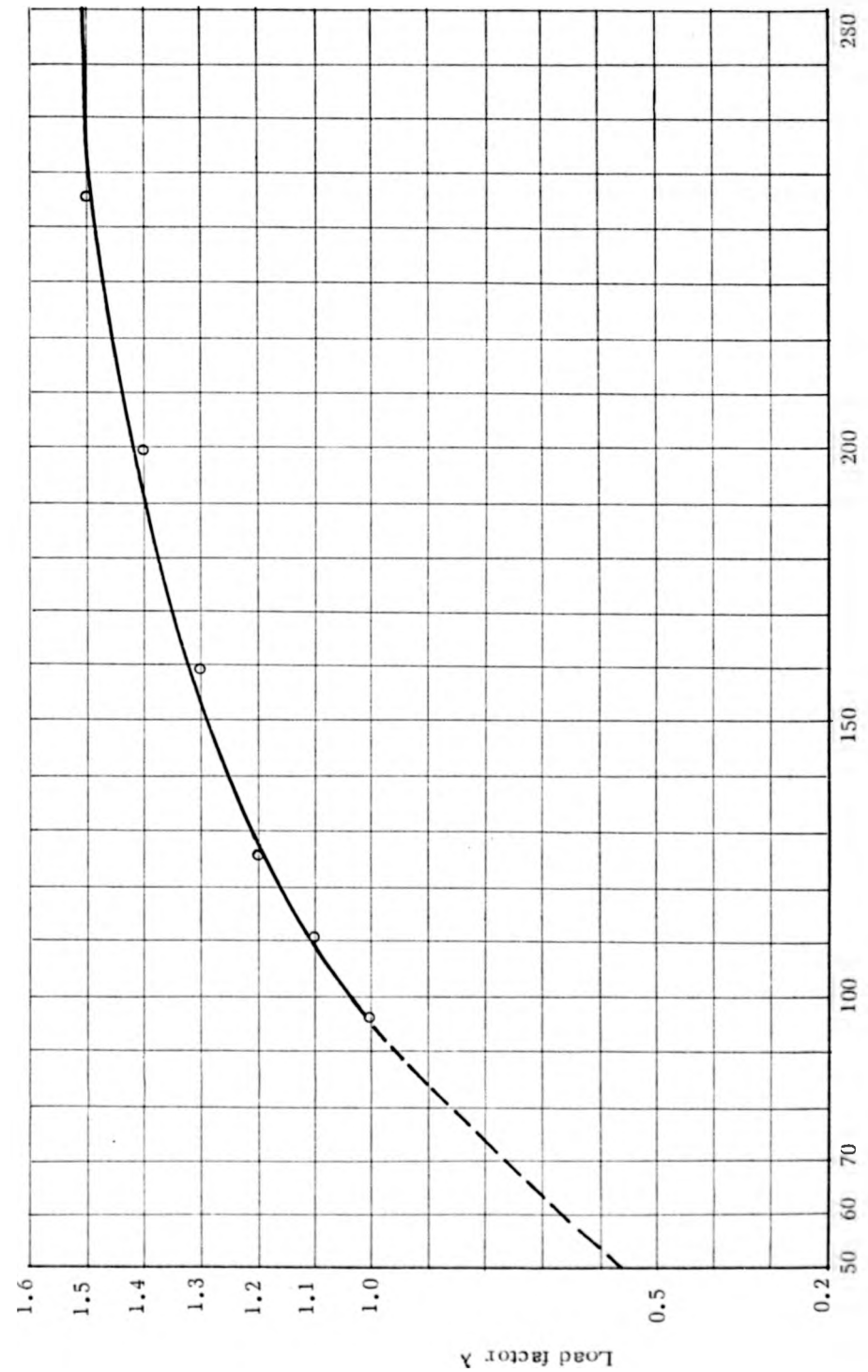
Load factor λ
1.6
1.5
1.4
1.3
1.2
1.1
1.0
0.5
0.2
50
60
70
100
150
200
280
Deflection Δ in mm

Figure 5.6

Figure 5.5a shows the joint and hinge rotations and horizontal deflections of each storey. Figures in parenthesis show the results of computer analysis at $\lambda = 1.44$. The two results have very satisfactory agreement. Figure (5.5b) shows the corresponding moments in the members and these also have similar agreements .

To determine the approximate failure load factor by using the load deflection curve, the frame is analysed to calculate the sway deflections at different values of λ , i.e. at $\lambda = 1.0$, 1.1, 1.2, 1.3 and 1.4. These are then plotted (figure 5.6) and the curve becomes assymptotic at about $\lambda = 1.5$, indicating infinite deflection, i.e. failure of the frame. So the approximate failure load factor , λ_f , can be taken as 1.5. The computer analysis has also given $\lambda_f = 1.50$ (figure 5.4) .

To check the yield criterion at service load the frame is analysed at $\lambda = 1.0$. No hinges form at this load factor. Computer analysis also showed that the first hinge forms at $\lambda = 1.06$ (figure 5.4b). Horizontal deflections at the various storey levels at $\lambda = 1.0$ along with those given by computer analysis are shown in figure (5.7).

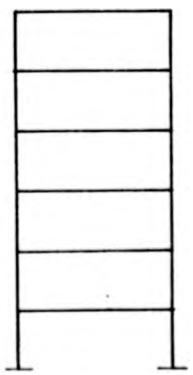

Deflections in mm	
Proposed method	Computer analysis
5.74	5.84
11.35	11.35
16.80	16.81
22.78	22.78
25.18	25.09
14.67	14.59
96.52	96.46

At $\lambda = 1$: no plastic hinge

Figure 5.7

The optimum design solution shown in figure (5.4a) has been arrived at after a number of iterations. The initial lower-bound solution produced too many undesirable hinges at the design load factor necessitating the modification of sizes for nearly all the members of the frame. As a result, compared to the size of the frame, the variables of the optimisation problem were too many. For a large multibay multistorey frame the process of optimum design by using such a lower-bound solution is likely to be a lengthy one.

It has been discussed in the previous chapter that the proposed method of analysis is inaccurate when dealing with frames in which plastic hinges are expected in the columns. So, in the design procedure described in Sec.(5.3), this type of hinge had to be removed first. Therefore a more convenient lower-bound solution would be one in which there is no hinge in the columns at the design load factor but at the same time their sizes are not large enough to hinder the optimality of the final solution.

If the third constraint as discussed in Sec.(5.1), i.e. the constraint on deflection, is also brought within the scope of the design criterion it may be possible to find a realistic lower-bound solution which is closer to the final optimum design satisfying all the three constraints.

5.5 DESIGN TO SATISFY STRENGTH, STABILITY AND DEFLECTION LIMITATIONS

As the horizontal deflection is quite significant in multistorey sway frames it has been realised and accepted that its limitation to a reasonable proportion is necessary to ensure serviceability of the structure. Recommendations of BS 449 and the B/20 Draft

Specification in respect of maximum permissible horizontal deflections have been stated in chapter II (Sec. 2.1).

In chapters II and III simple expressions have been derived for the design of multistorey sway frames satisfying deflection limitations at working load. It has also been shown that member inertias given by these expressions result in the optimum design of a frame for deflection constraints only.

Use of these expressions may be made to design the columns of a frame to obtain a realistic lower-bound solution assuming that the sizes of columns required for the optimality against deflection constraint will be the same or smaller than those required for the optimum design satisfying all the three constraints.

Modified lower-bound solution

The following procedure is adopted to find the modified lower-bound design solution.

(i) Calculate the inertias required for the columns using the appropriate expressions given in chapters II and III (for unit q-values) and select standard sections from table (2.2).

(ii) Select beam sizes required to satisfy the beam mechanism criterion using equation (5.1) and table (2.1).

(iii) Modify the sizes of external columns to satisfy the beam mechanism criterion of the adjoining beam by using the following expressions :

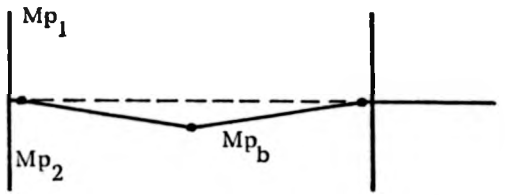

(a)

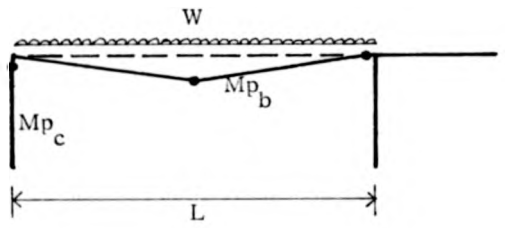

(b)

Figure 5.8

For the intermediate floor (figure 5.8a)

$$Mp_1 + Mp_2 \geq Mp_b \qquad (5.3)$$

For the top floor (figure 5.8b)

$$M_{pc} \geq \frac{\lambda_1 WL}{4} - 3Mp_b \qquad (5.4)$$

The six-storey one-bay frame of Sec.(5.4) will now be designed again with a modified lower-bound solution. All the dimensions and specifications remain the same as shown in figure (5.2). The value of Δ, the permissible deflection, for each floor is taken as h/300,

which is 11.67 mm. Member inertias provided in the initial lower-bound solution are shown in figure (5.9a), the figures in brackets being the corresponding plastic moment capacity, Mp_b, of the beam members. Figure (5.9b) shows the result of analysis of the lower-bound frame at $\lambda = 1.4$. There are no hinges in the columns and there are four undesirable hinges at the midpoint of beams. Corresponding moments at these points are shown in the figure.

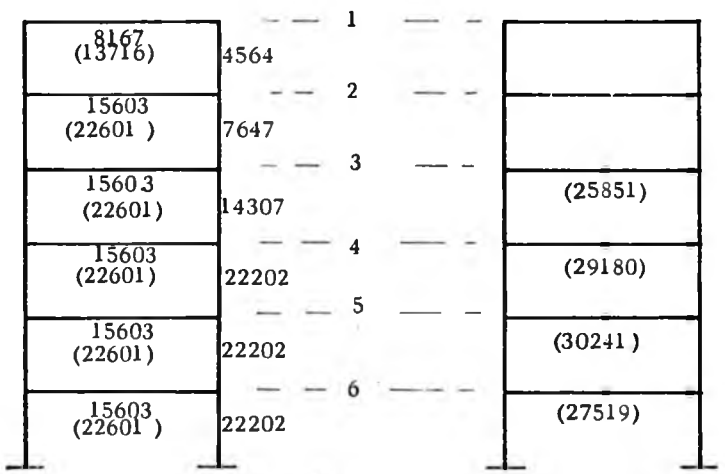

Inertias in cm^4, Moments in kNcm.

(a) (b)

Figure 5.9

In the first iteration beams at levels 5 and 6 are increased to the next larger size (figure 5.10a) and the modified frame is analysed again. Results are shown in figure (5.10b).

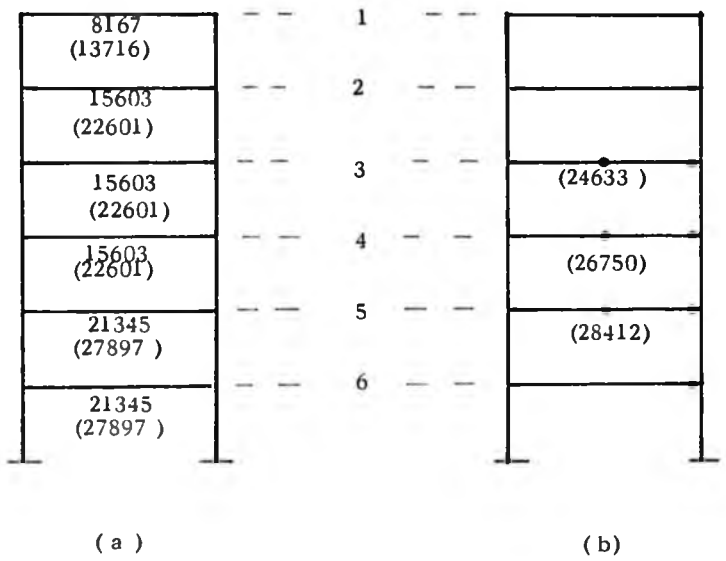

Figure 5.10

The hinge at level 5 has not disappeared in spite of the increase of beam section at this level. Hinges at levels 3 and 4 remain as earlier. Instead of increasing the beam size at level 5 any further, only the beam at level 4 is increased for the next iteration. Figure (5.11a) shows the modified frame and (5.11b) shows the analysis results.

The midspan hinge at level 4 as well as that at level 5 have now disappeared, leaving only the one at level 3. So the beam at this level is also increased to the next higher size and the frame analysed again.

Figure (5.12) shows the results which satisfy the desired constraints for strength and stability , i.e. maximum of one hinge per beam and no hinges in columns at the specified load factor.

To check whether the design solution also satisfies the third constraints, i.e. the deflection limitations, analysis at $\lambda = 1.0$ has to be done. This analysis is also necessary to find out whether the frame is free of plastic hinges at working load. Results of the analysis are shown in figure (5.13). There is no hinge in the frame but the deflections at levels 3, 4 and 5 are in excess of the permissible value of 11.67 mm.

Further increase in the member sizes is necessary to reduce the deflections to their permissible value. Iterative analyses with alternative arrangements of beam and column sizes have been made to reach the optimum solution. The final design is shown in figure (5.14).

It may be observed that in the final optimum design, sizes of columns have remained unaltered from those selected for the initial lower-bound solution. The frame has been analysed by the proposed method at $\lambda = 1.4$ and no hinge formed at this load factor. The computer analysis showed the formation of first hinge at $\lambda = 1.48$, whereas the failure load factor was given as $\lambda_f = 1.72$.

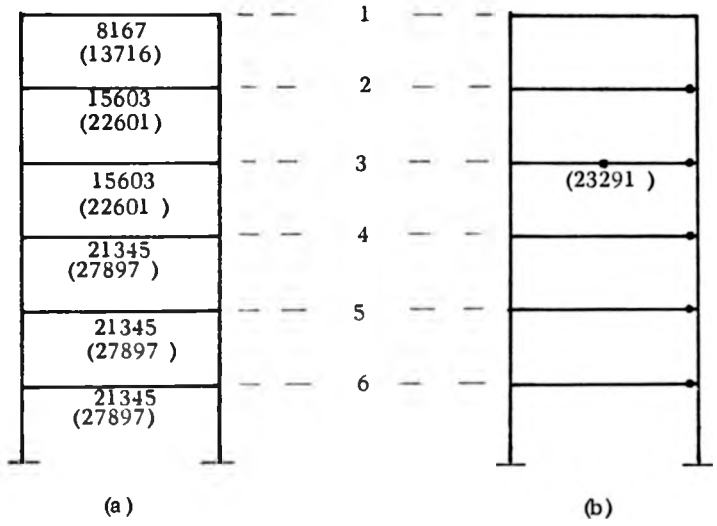

Figure 5.11

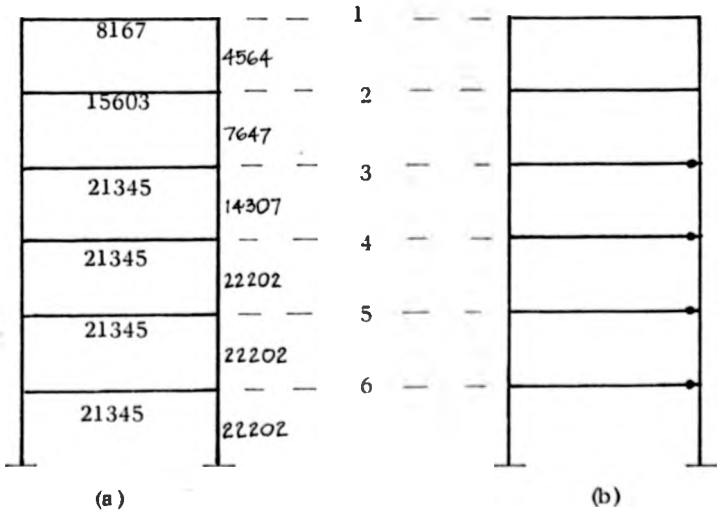

Figure 5.12

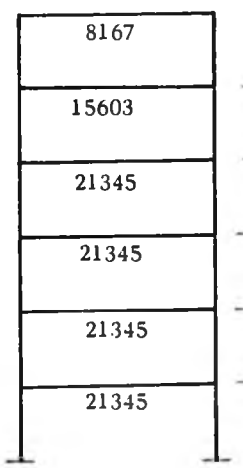

	Deflections in mm	
	Proposed method	Computer analysis
1	5.80	5.80
2	9.83	9.82
3	12.36	12.37
4	15.01	15.00
5	17.11	17.12
6	11.22	11.22
	71.33	71.33.

At $\lambda = 1$: no plastic hinge

Figure 5.13

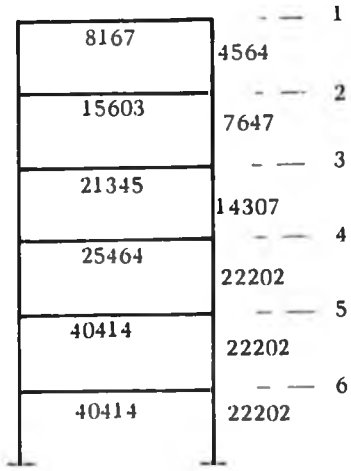

1	5.77
2	9.58
3	10.92
4	10.87
5	11.44
6	8.46
	57.04

Figure 5.14

Optimum design to deflection limitations only

The six storey one bay frame will now be designed for deflection limitations using the expressions derived for a regular frame and unit q values given in Chaper II. Again, the economic standard sections given in tables (2.1 and 2.2) will only be considered.

The calculated inertias required for the different members of the frame are shown in figure (5.15a) and using the corresponding Universal sections the optimum design solution is shown in figure (5.15b).

In calculating the inertias, columns were designed first, corresponding rolled sections selected, and the beam inertias were then found by using the actual column inertias already selected.

It is interesting to note that the optimum design solution for strength, stability and deflection constraints under the effects of combined

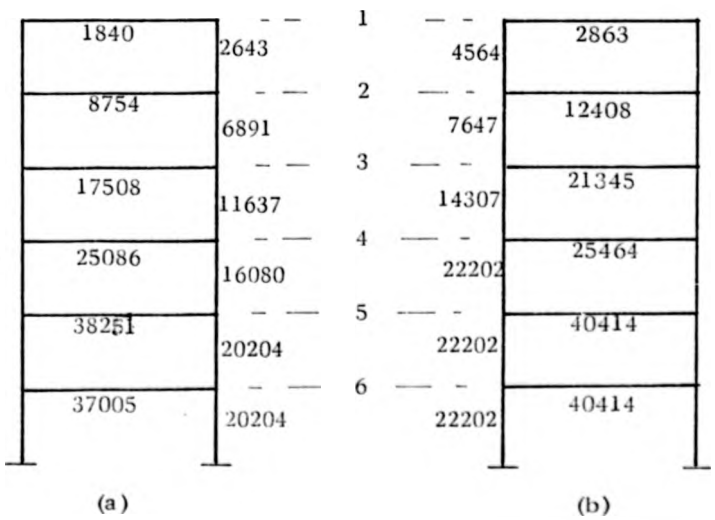

Figure 5.15

vertical and wind loading (figure 5.14) is the same as that required to satisfy deflection constraints of the frame subjected to wind load only except for the sizes of beams at levels 1 and 2. If the local rigid-plastic beam mechanism is taken into consideration in the latter case, as has been suggested in the design procedure of chapter II, then these two beams will also have identical sizes in the two design solutions.

5.6 EIGHT-STOREY TWO-BAY FRAME

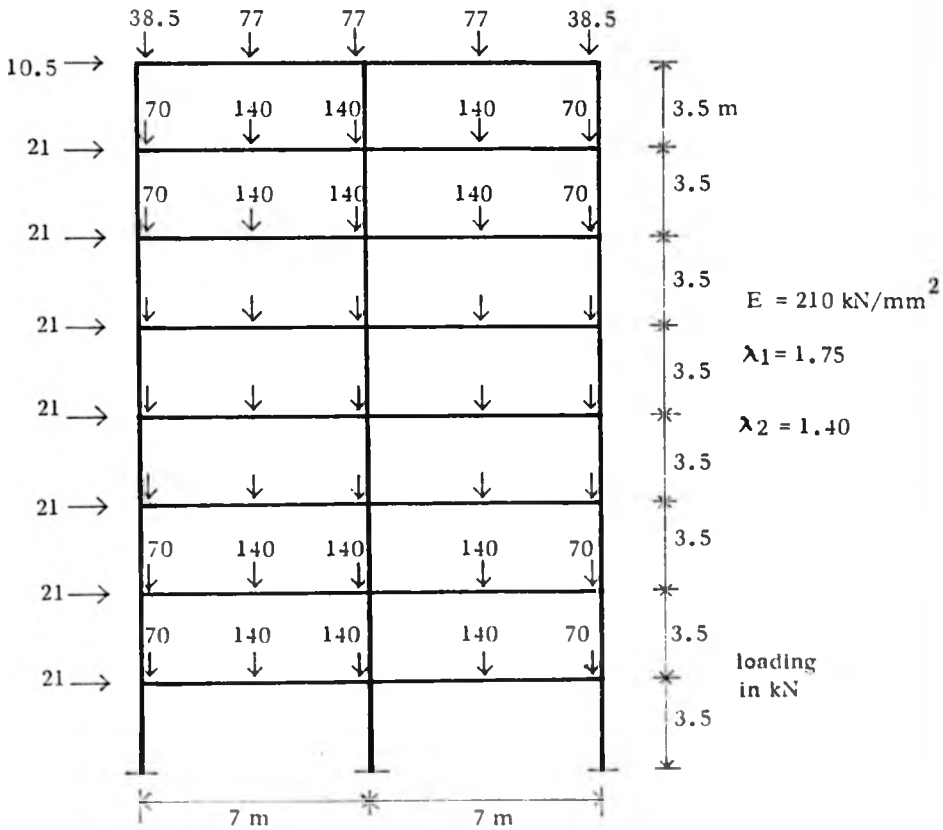

Figure 5.16

The eight-storey two-bay frame is shown in figure (5.16). Design objective is the same as that of the previous example, i.e. to have one plastic hinge per beam at a load factor of 1.4 with no hinges in columns and to limiting sway deflection of h/300 in each storey.

In the previous example (Sec. 5.4) the frame was subjected to a high intensity of wind pressure, i.e. 1.5 kN per square metre of the surface area which is equivalent to a wind velocity of 51 metres per second for this frame. In this example the frame is subjected to the same intensities of wind pressure and vertical load. Thus the ratio of horizontal to vertical load in a bay of the frame is reduced to half of that of the previous example.

The initial lower-bound solution is obtained by proceeding as in Sec. (5.5) and the corresponding standard sections chosen from table (2.1 and 2.2) are shown in figure (5.17).

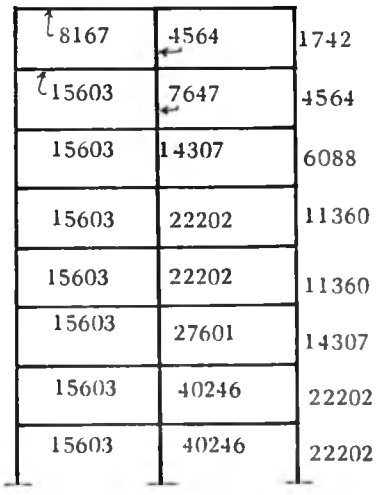

Figure 5.17

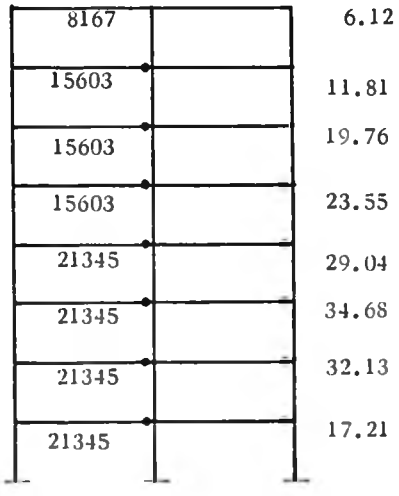

Column inertias same as in figure (5.17)
$\lambda = 1.4$ 12 hinges

Figure 5.18

The eight-storey two-bay frame is shown in figure (5.16). Design objective is the same as that of the previous example, i.e. to have one plastic hinge per beam at a load factor of 1.4 with no hinges in columns and to limiting sway deflection of h/300 in each storey.

In the previous example (Sec. 5.4) the frame was subjected to a high intensity of wind pressure, i.e. 1.5 kN per square metre of the surface area which is equivalent to a wind velocity of 51 metres per second for this frame. In this example the frame is subjected to the same intensities of wind pressure and vertical load. Thus the ratio of horizontal to vertical load in a bay of the frame is reduced to half of that of the previous example.

The initial lower-bound solution is obtained by proceeding as in Sec. (5.5) and the corresponding standard sections chosen from table (2.1 and 2.2) are shown in figure (5.17).

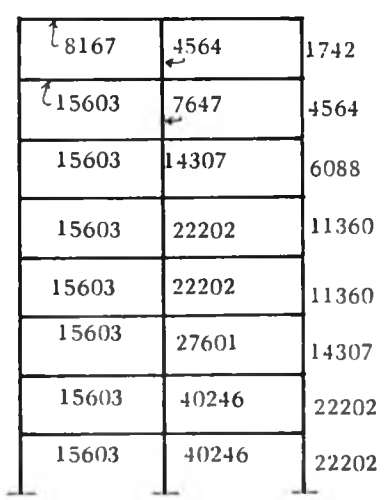

Figure 5.17

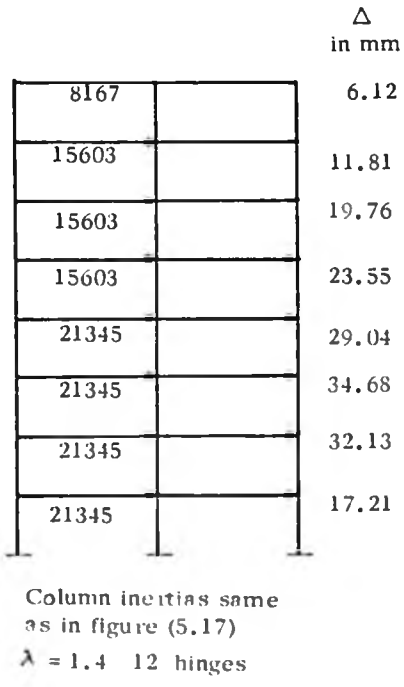

Figure 5.18

The solution satisfying strength and stability constraints at $\lambda = 1.4$ is shown in figure (5.18) along with location of hinges and sway deflections at the storey levels. Figure (5.19) shows the joint and hinge rotations and the bending moment in the members are shown in figure (5.20).

The frame has been analysed by computer using accurate elastic-plastic method. Figure (5.21) shows the sequence of hinge formation with corresponding load factors and the sway deflections at load factors 1.37 (upper figures) and 1.45 (lower figures). Corresponding joint and hinge rotations are shown in figure (5.22) and the bending moments in figure (5.23). All these results have excellent agreement with those given by the proposed method.

Analysis by the proposed method at load factors of 1.0, 1.1, 1.2 and 1.3 are shown in figure (5.24). The sequence of hinge formation agrees with the computer analysis. The deflections at working load (figure 5.24a) show that permissible value is exceeded at floor levels 5, 6 and 7. Subsequent iterations to satisfy the deflection constaints give the optimum solution as shown in figure (5.25). Figures in parenthesis show the deflections given by non-linear elastic analysis by computer at $\lambda = 1$. Figure (5.26) shows the required inertias of the members when the frame is designed to satisfy the deflection constraints only, using the equations given in chapter II. Figure (5.26a) shows the required column inertias and figure (5.26b) shows the required beam inertias on the basis of actual column sections chosen from table (2.2). Corresponding beam sections after providing for safety against beam mechanism at $\lambda_1 = 1.75$ are the same as those in figure (5.25)

In spite of the reduced effects of wind load, compared to the previous example, the optimum design solution of the frame for strength, stability and

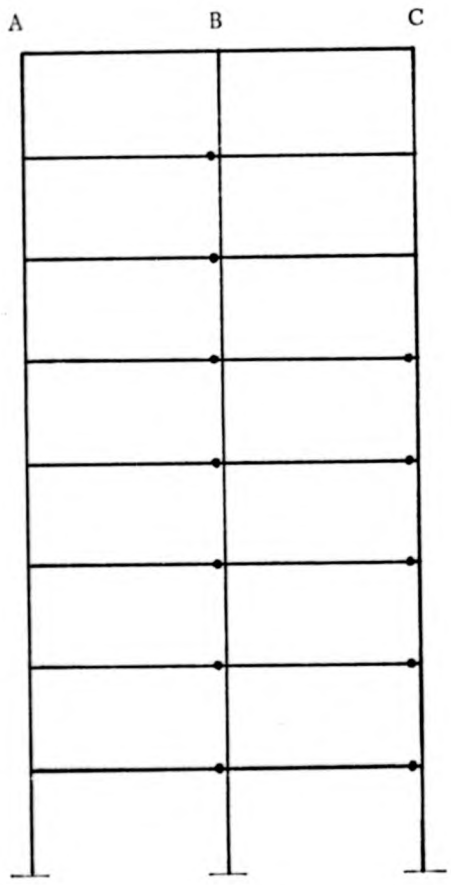

θ_A	θ_B	θ_C	$\theta_{H(AB)}$	$\theta_{H(BC)}$
.00650	.00058	- .00567	0	0
.00563	.00127	- .00348	- .00118	0
.00606	.00323	-.00132	-.00335	0
.00723	.00535	.00309	-.00606	- .00286
.00696	.00550	.00380	- .00479	- .00236
.00881	.00759	.00615	- .00780	- .00575
.00936	.00862	.00800	- .00910	- .00811
.00793	.00691	.00596	- .00668	-.00521

Figure 5.19

Column moments	Beam moments			Column moments	Beam moments			Column moments
2779	-2779	10885	13182	-1536	-11645	10962	4162	-4162
2602				-1164				-3719
3918	-6520	19740	22601	-3936	-18028	19375	11823	-9997
4147				-2211				-8851
1767	-5914	20043	22601	-8696	-12341	19277	17705	-11890
2589				-5170				-8797
1675	-4266	20867	22601	-10524	-6906	19547	22601	-13803
1308				-10141				-12864
-2897	1588	21146	27897	-16558	-1207	19748	27897	-15011
-470				-11213				-11934
-4677	5144	22924	27897	-19438	2805	21754	27897	-16021
-3769				-16174				-12974
-2419	6199	23451	27897	-16434	4774	22739	27897	-14882
-6117				-24425				-20159
2652	3455	21579	27897	-4974	1492	21098	27897	-7721
-17783				-37131				-23073

Moments in kNcm

Figure 5.20

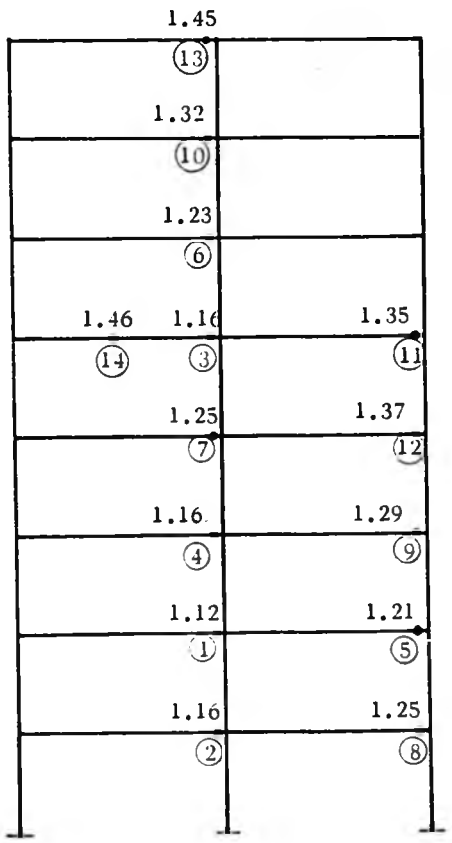

	Δ in mm	
	At $\lambda = 1.37$	At $\lambda = 1.45$
	6.40	7.51
	11.86	14.36
	17.29	22.65
	18.86	26.43
	23.57	32.24
	29.40	38.10
	28.03	35.09
	15.46	18.58

Figure 5.21

deflection requirements is the same as that required for deflection constraints only and the simple equations of chapters II and III are adequate for the design purpose. In the next example, the effect of wind load has been reduced further to investigate the applicability of the design methods proposed in chapters II and III in such frames by comparing with the design solution for strength, stability and deflection requirements.

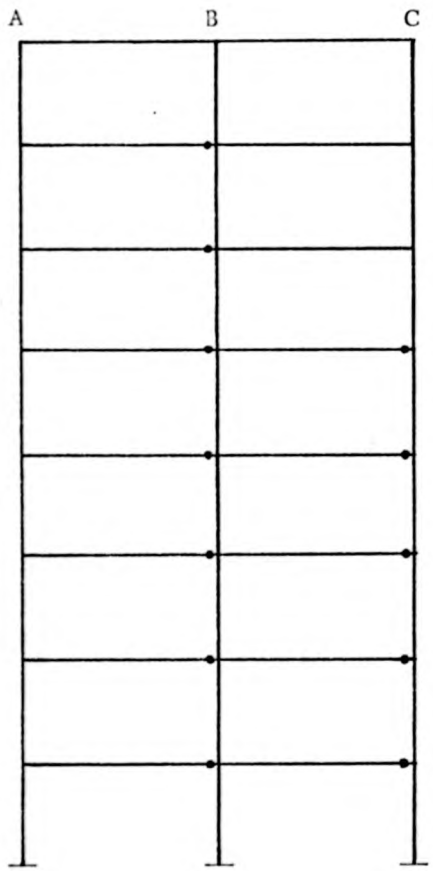

θ_A	θ_B	θ_C	$\theta_{H(AB)}$	$\theta_{H(BC)}$
.00638	.00062	- .00558	0	0
.00677	.00067	-.00582	0	0
.00554	.00128	- .00291	-.00094	0
.00627	.00182	-.00297	-.00235	0
.00574	.002940	-.00066	-.00269	0
.00680	.00389	-.00042	-.00468	0
.00620	.00426	. 00171	-.00424	-.00073
.00804	.00618	.00389	-.00760	-.00437
.00570	.00412	. 00229	-.00262	0
.00774	.00630	.00463	-.00620	-.00381
.00744	.00614	.00460	-.00552	-.00332
.00966	.00850	.00716	-.00936	-.00744
.00814	.00732	.00660	-.00705	-.00591
.01025	.00952	.00892	-.01067	-.00970
.00710	.00603	.00503	-.00523	-.00369
.00862	.00758	. 00663	-.00792	-.00645

Upper figures at $\lambda = 1.37$, lower figures at $\lambda = 1.45$

Figure 5.22

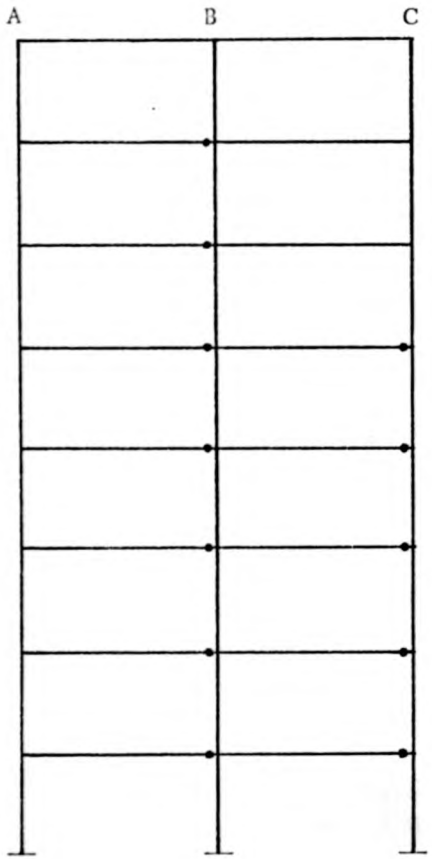

θ_A	θ_B	θ_C	$\theta_{H(AB)}$	$\theta_{H(BC)}$
.00638	.00062	- .00558	0	0
.00677	.00067	-.00582	0	0
.00554	.00128	- .00291	-.00094	0
.00627	.00182	-.00297	-.00235	0
.00574	.002940	-.00066	-.00269	0
.00680	.00389	-.00042	-.00468	0
.00620	.00426	. 00171	-.00424	-.00073
.00804	.00618	.00389	-.00760	-.00437
.00570	.00412	. 00229	-.00262	0
.00774	.00630	.00463	-.00620	-.00381
.00744	.00614	.00460	-.00552	-.00332
.00966	.00850	.00716	-.00936	-.00744
.00814	.00732	.00660	-.00705	-.00591
.01025	.00952	.00892	-.01067	-.00970
.00710	.00603	.00503	-.00523	-.00369
.00862	.00758	. 00663	-.00792	-.00645

Upper figures at $\lambda = 1.37$, lower figures at $\lambda = 1.45$

Figure 5.22

2658	-2658	10630	12955	1612	-11343	10737	4055	- 4055
2776	-2776	11236	13717	- 1779	-11937	11332	4365	- 4365
2486				- 1263				- 3512
2674				- 1169				- 3885
3587	-6073	19193	22583	- 4223	-17097	18720	12504	- 8992
3794	-6468	20899	22580	- 4321	-17090	19951	13852	- 10068
3692				- 2760				- 7796
4075				- 2505				- 8715
2098	-5790	19328	22594	- 7962	-11872	18445	18279	- 10484
1644	-5719	21266	22594	- 9260	-10829	19726	20566	- 11850
2427				- 5784				- 8817
2515				- 5461				- 8835
2713	-5139	19657	22587	- 8937	-7867	18290	22601	- 13778
1468	-3983	22137	22590	-10545	-6584	20832	22598	- 13763
2043				- 9296				- 13017
1069				-10241				- 12779
-1792	-250	19448	27895	- 15314	-3284	17930	27897	- 14880
-3315	2246	22599	27896	-17142	- 516	21219	27897	- 15118
513				-10142				- 11853
- 779				-11527				- 11817
-3619	3105	21127	27893	-18353	602	19873	27897	- 16044
-5165	5944	24449	27893	-20082	3716	23332	27897	- 16080
-2456				-14593				- 12750
-4199				-16853				- 13193
-1988	4444	21799	27887	-16165	2870	21009	27894	- 15144
-2857	7057	25008	27886	-16701	5668	24309	27894	- 14701
-4713				-22211				- 19205
-7092				-25742				- 20588
2275	2438	20791	27897	- 6074	388	19766	27896	- 8691
3159	3933	23441	27896	- 4104	1850	22449	27897	- 7309
-16134				-34131				- 21607
-19163				-39331				- 24307

Moments in kNcm

Figure 5.23

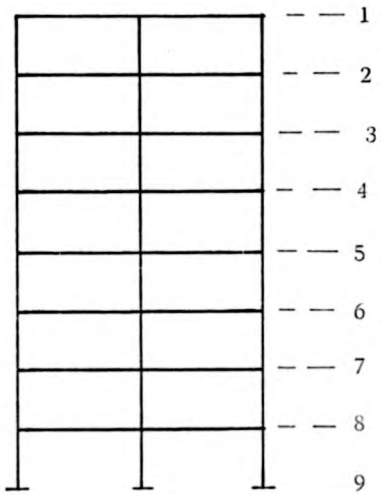

Δ in mm

4.21

7.17

9.73

10.37

12.30

13.76

13.19

8.27

λ=1.0; no hinge

(a)

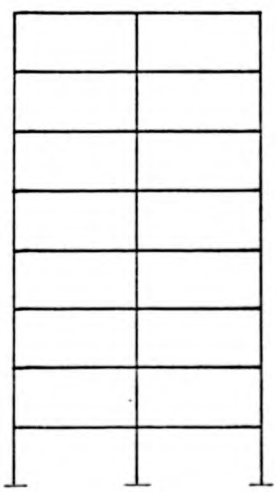

λ =1.1 : no hinge

(b)

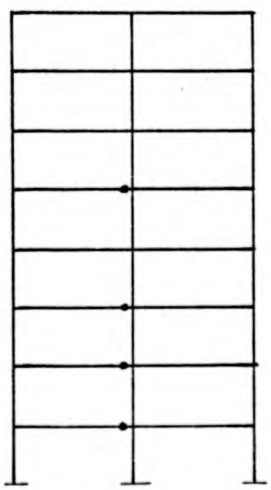

λ = 1.2; 4 hinges

(c)

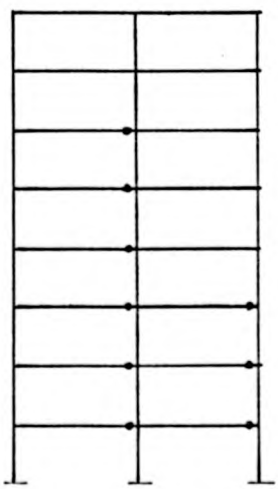

λ = 1.3 : 9 hinges

(d)

Figure 5.24

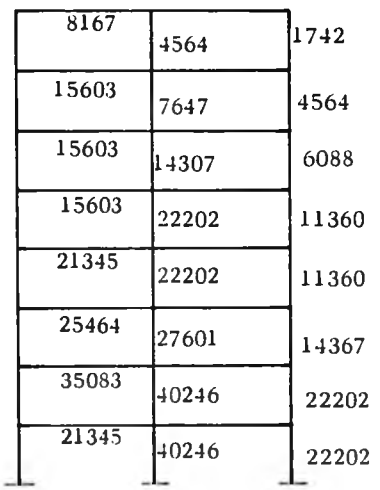

	Δ in mm at λ = 1	
	Proposed method	Computer analysis
1742	4.21	(4.21)
4564	7.16	(7.17)
6088	9.70	(9.71)
11360	10.22	(10.22)
11360	11.30	(11.30)
14367	11.10	(11.11)
22202	11.03	(11.04)
22202	7.88	(7.89)

Figure 5.25

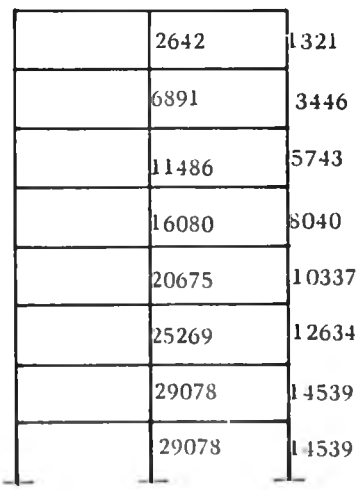

(a)

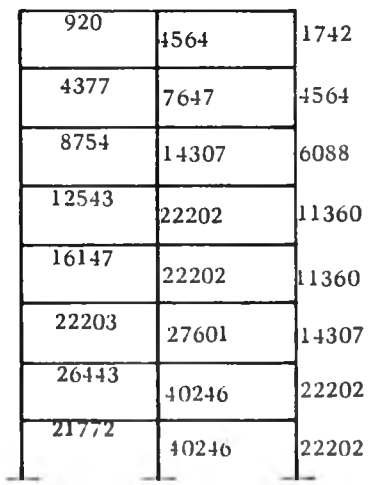

(b)

Figure 5.26

5.7 FIVE-STOREY FOUR-BAY FRAME

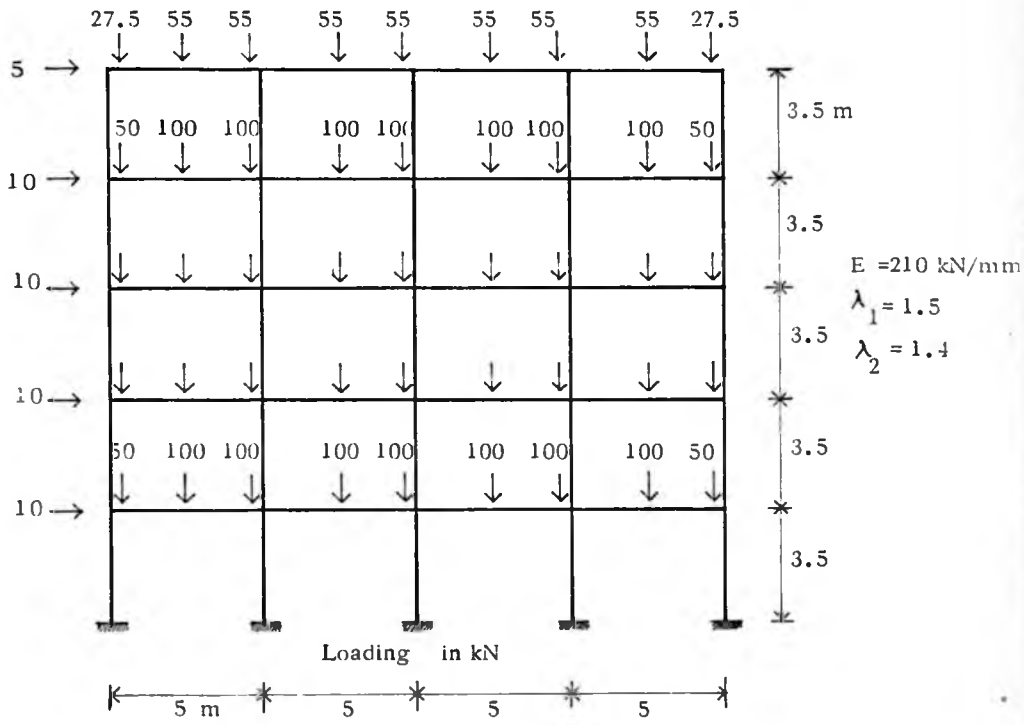

Figure 5.27

The multibay frame is shown in figure (5.27). Vertical unit load is the same as that of the previous examples, but the bay width is now 5 m (compared to 7 m of the previous examples). Intensity of wind pressure has been reduced to a very low value of 0.735 kN/m^2 equivalent to a wind velocity of 38 metres per second. The total wind force is distributed amongst four bays. So this example represents a case where the effects of wind load in a frame are very small.

The lower-bound solution is shown in figure (5.28a). The design solution satisfying strength and stability constraints is shown in figure (5.28b) while the hinge formation in the members is shown in figure (5.29a). Analysis at working load by the proposed method shows no hinge in the members and the sway deflections are within permissible limits (figure 5.29b). Figure (5.30) shows the sequence of hinge formation within $\lambda = 1.4$ when analysed by elastic-plastic computer program, the failure load factor being given as 1.59 .

Design of the frame by using the expressions of chapter II, i.e.,for deflection constraints only, gives the required member inertias as shown in figure (5.31a). After modifying these inertias to satisfy local mechanisms and selecting the corresponding rolled sections, the design solution is the same as that shown in figure (5.28a). Although elastic-plastic analysis of the frame by computer gives a failure load of $\lambda = 1.56$, there are three double-hinged beams in the frame at $\lambda = 1.4$ (given both by the computer analysis and the analysis by proposed method) as shown in figure (5.31b).

Thus this example illustrates that, for the frames where the effect of wind load is very small, design to deflection constraints by the method proposed in chapters II and III may be inadequate in satisfying the strength and stability requirements. However, the expressions developed in those two chapters can be used in finding the lower-bound solution of a multistorey frame with any intensity of wind loading and then designed by the method proposed in this chapter.

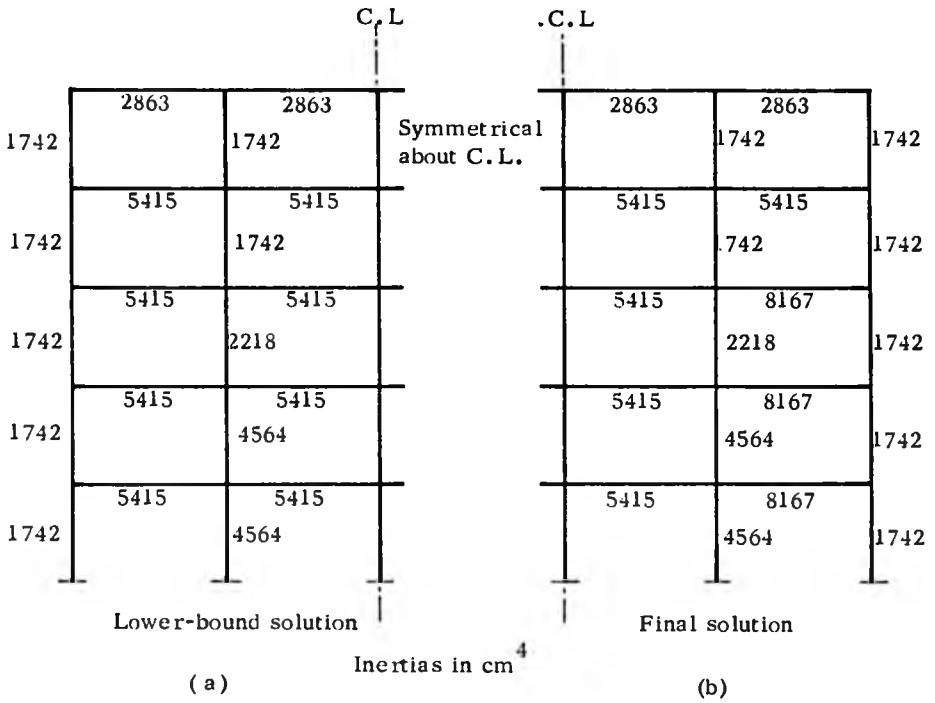

Figure 5.28

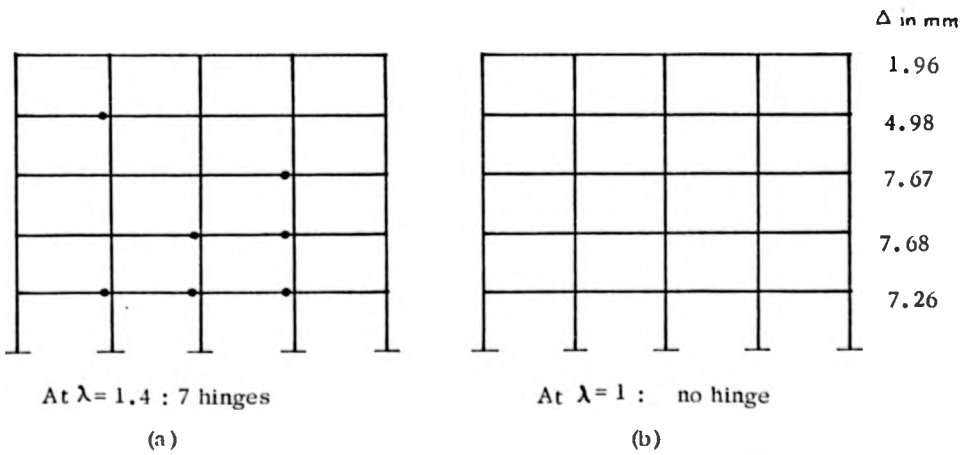

Figure 5.29

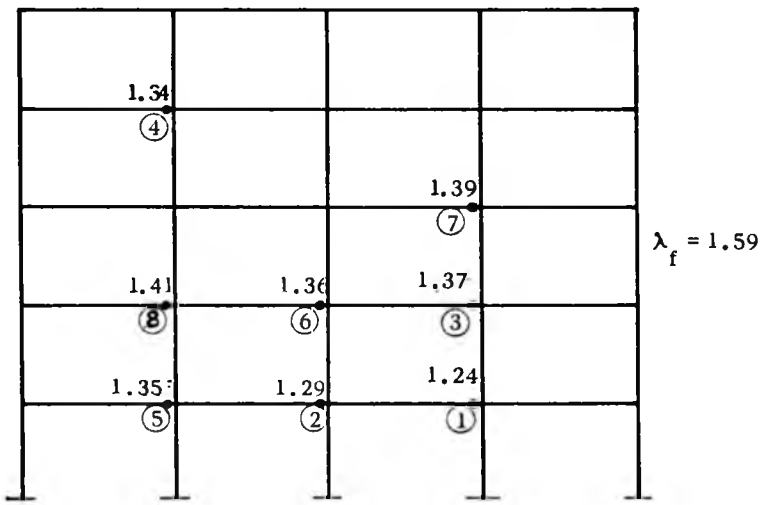

Figure 5.30

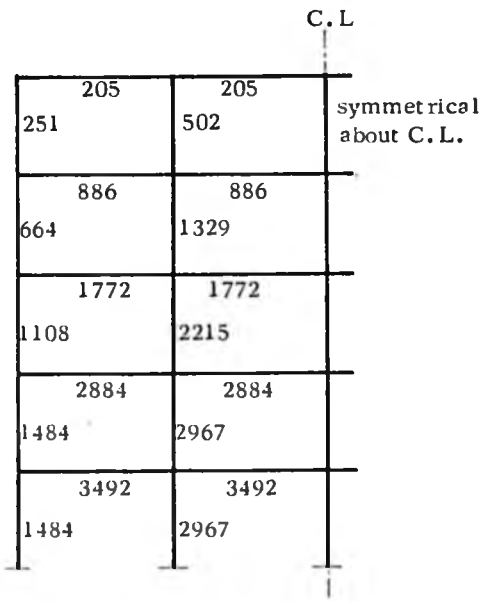

(a)

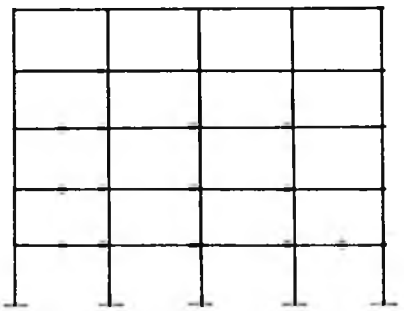

At $\lambda = 1.4$

(b)

Figure 5.31

Design with the same beam section at a particular level

The satisfactory design solution shown in figure (5.28b) has been obtained by gradually eliminating the undesirable plastic hinges in the lower-bound frame (figure 5.28a and 5.31b). Considering the possibility of reversible wind direction, symmetry has been maintained while modifying the beam inertias. It has, however, not been attempted to use the same inertia for all the beams in a particular floor level. Such an arrangement will enable corresponding reduction in the column inertias and may result in slightly cheaper overall design solution in some cases.

Figure (5.32) shows the beam inertias using the same rolled section throughout a particular floor level and the corresponding column sections required to satisfy the deflection constraint at working load. The result of the analysis at $\lambda = 1.4$ is shown in figure (5.33a). There is only one hinge, at point 1 , although the bending moment at point 2 , 136.93 kNm, is very close to the plastic moment of the beam, 137.16 kNm. The result of analysis by computer is shown in figure (5.33b). The failure load factor is given as 1.66. The weight of the frame given by the first solution (figure 5.28b) is 5865 kg , whereas the frame with uniform floor beams (figure 5.32) weighs 5801 kg, thus providing a more economical solution with a saving of 1.1% by weight .

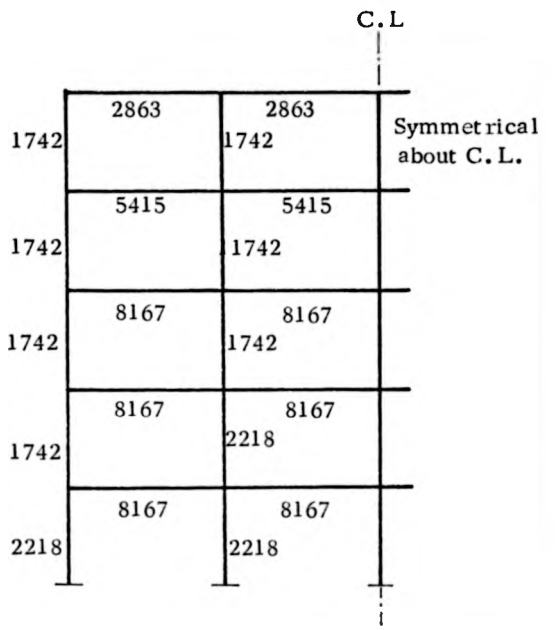

Figure 5.32

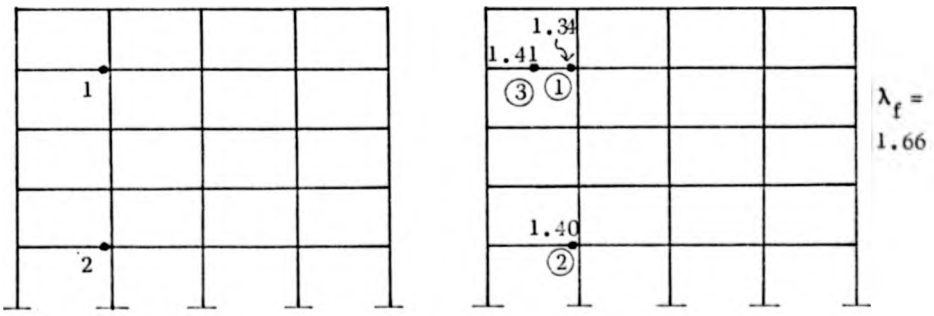

By proposed method
At $\lambda = 1.4$
(a)

By computer analysis
(b)

Figure 5.33

5.8 DESIGN OF NON-UNIFORM FRAME

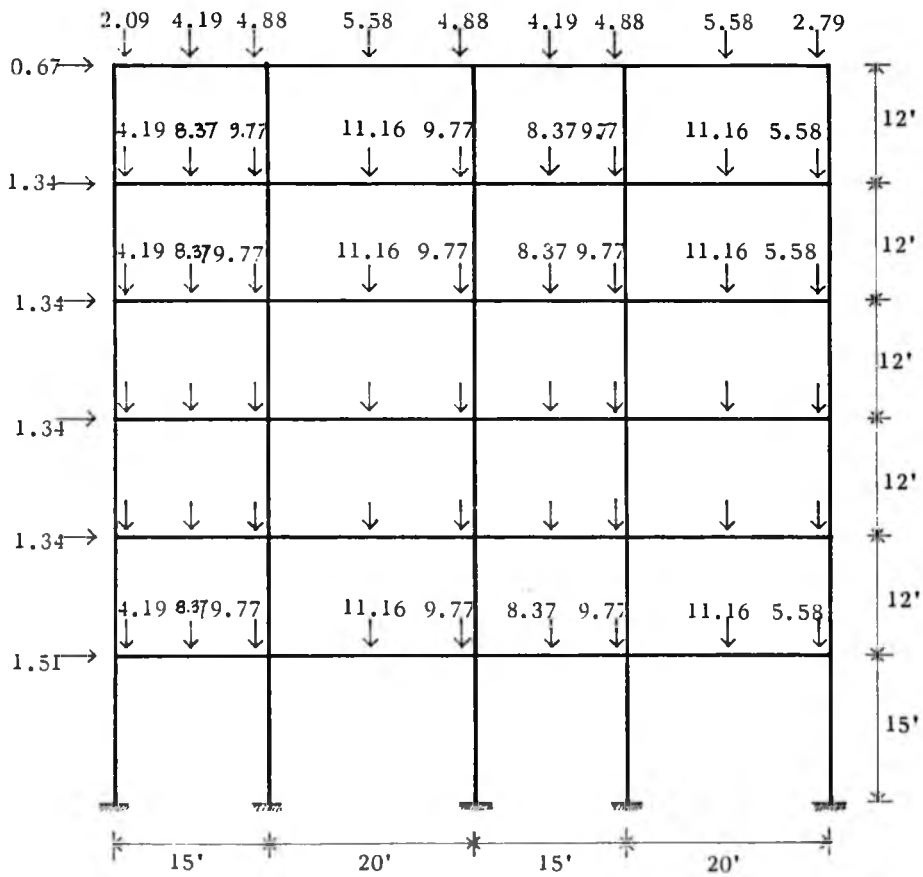

Loading in ton

Figure 5.34

To illustrate the use of the proposed method in non-uniform frames, the six-storey four-bay frame shown in figure (5.34) has been chosen. It is the one used by Heyman [17] and later on Holmes and Gandhi

used it to illustrate the design method proposed in reference [18]. Figure (5.35) shows the design solution obtained by the latter. For the convenience of comparison with the earlier work, imperial units will be used in this example.

The frame of figure (5.35) has been analysed by the proposed method. The analysis at $\lambda = 1.4$ shows no hinge formation in the members and the analysis at $\lambda = 1$ gives sway deflections as shown in figure (5.35). Elastic-plastic analysis by computer shows the formation of first hinge at $\lambda = 1.59$ and the failure at $\lambda = 1.96$.

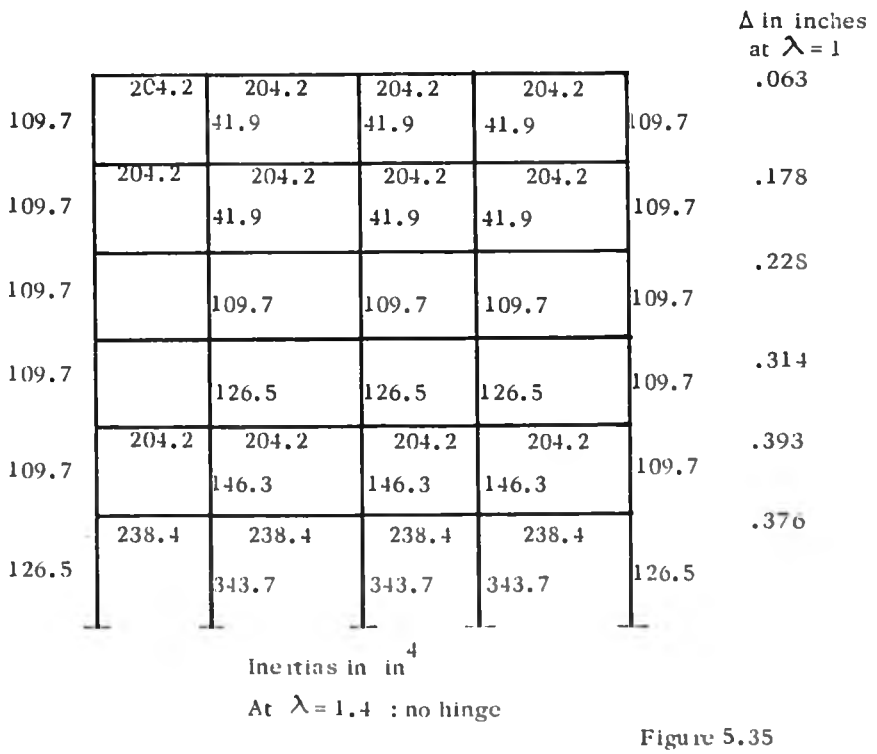

Figure 5.35

The frame will now be designed using the proposed method with the following specifications :

Fy = 16 tons/sq in , E = 13400 tons/sq in
Permissible sidesway at h/300 are
0.6 inches for the bottom storey and 0.48 inches
for the other storeys.
$\lambda_1 = 1.75$

The initial solution is shown in figure (5.36). Analysis of the frame at $\lambda = 1.4$ shows that there is no undesirable hinge in the members and so the initial lower-bound solution satisfies the strength and stability requirements. Analysis at $\lambda = 1$ shows that the sway deflections are within permissible limits. Location of hinges and the deflections are also shown in figure (5.36). The result of elastic-plastic analysis by computer is shown in figure (5.37) which is very close to that obtained by the proposed method, the failure load factor being 1.53. The total weight of the frame given by the proposed method is 9.11 tons compared to 10.87 tons of the frame of figure (5.35) which is a reduction of 16.2%.

The frame has been designed again with the following additional specifications :

(i) Same beam sections to be used in a particular floor level.

(ii) Maximum depth of beams to be restricted to 12 ".

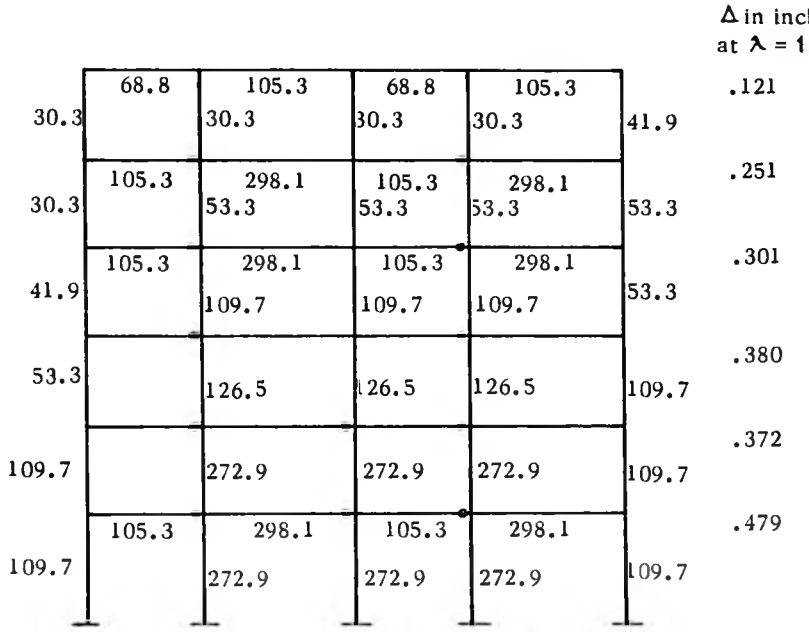

Hinge formation at $\lambda = 1.4$

Figure 5.36

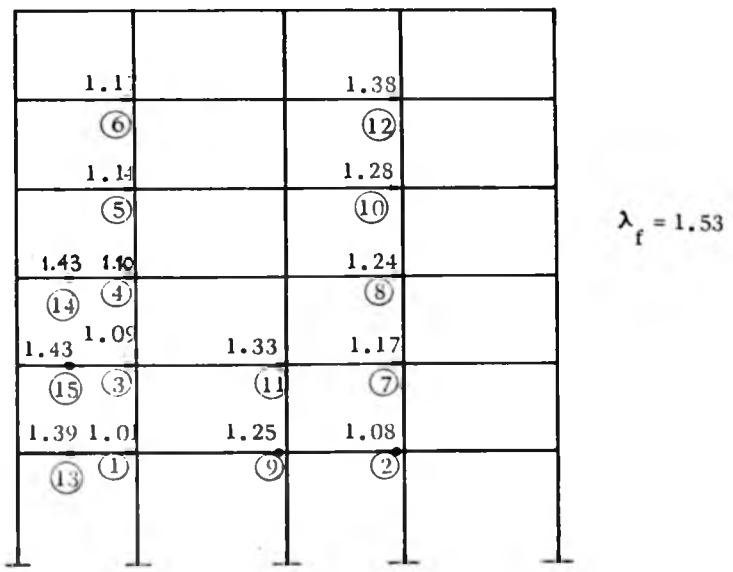

$\lambda_f = 1.53$

Figure 5.37

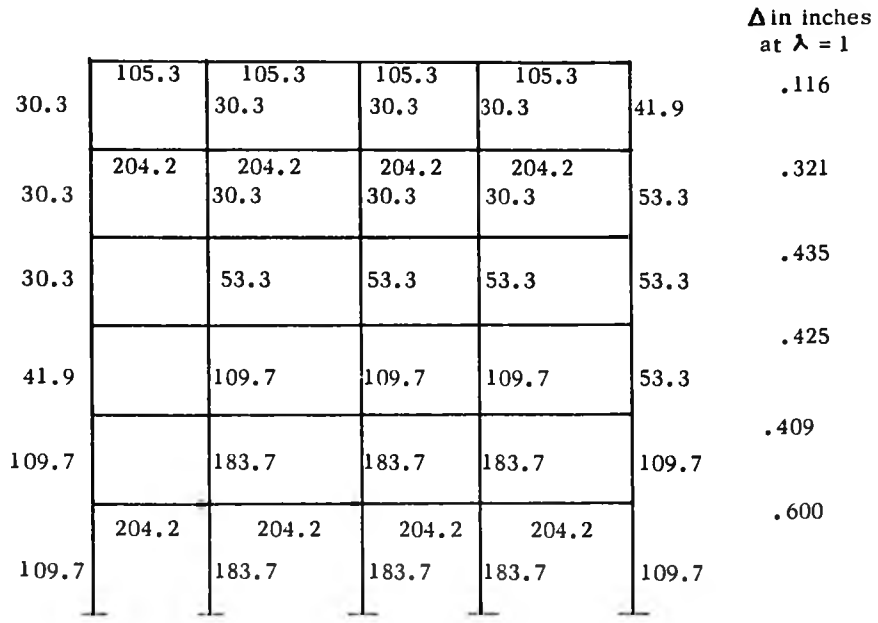

Hinge formation at $\lambda = 1.4$

Figure 5.38

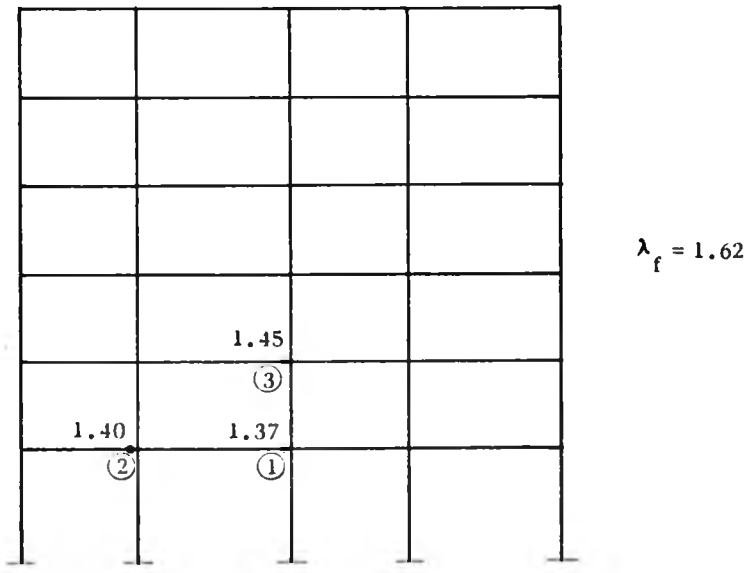

$\lambda_f = 1.62$

Figure 5.39

Figure (5.38) shows the initial frame with the hinge formation pattern at $\lambda = 1.4$ and the sway deflections at $\lambda = 1$. It satisfies the strength, stability and deflection requirements. Figure (5.39) shows the result of elastic-plastic analysis by computer which has complete agreement with the design by the proposed method. The total weight of this frame is 9.49 tons, which is still 12.7% lower than the design given by the method of reference [18].

5.9 CONCLUSION

The analysis and design method developed in the preceding and current chapters takes into consideration nearly all the different factors causing frame instability that have been included in the non-linear elastic-plastic method [6, 7, 8]. Although the deteriorating effect of axial forces in the beams has not been included in the proposed method, it has been found by comparative study that the overall effect of such forces on the failure load and hinge formation pattern at failure is negligible. Like the elastic-plastic computer method, the advantageous effects of strain-hardening and composite action of cladding have also been excluded from the proposed method.

A single analysis of a frame at a given load factor gives the hinge formation pattern, joint displacements and hinge rotations at that load level. A few additional analyses below the given load factor enable the actual behaviour of the frame to be traced from the formation of first hinge up to the given load factor. The load-deflection relationship given by these analyses also enables the approximate failure load for the frame to be assessed.

The analysis method is simple in the sense that the calculations, although repetitive and sometimes lengthy, are not complicated,

and do not require any matrix inversion. For small frames, e.g. the four-storey one-bay frame of Sec. (4.5), the analysis can be carried out by hand calculation. However, computer programmes written for the 'substitute-frame' calculation of sway deflections and the computation of joint and hinge rotations by using the 'limited frame' are within the range of desk-top computers commonly used by design offices. With the Burroughs B6700 computer the iterative 'substitute frame' analysis, even for a very large frame, requires less than one second of CPU time , while that for the 'limited frame' analysis is within two seconds. Of course, with desk-top computers the process times will be longer, but the size of the problem is always expected to be within the capacity of such computers. Thus the services of a large-capacity computer, as required by the non-linear elastic-plastic analysis, has been avoided.

The analysis and design methods presented in the two chapters have been proposed as approximate elastic-plastic methods. The discrepancies between the values of rotations and displacements given by the proposed analysis method and those given by accurate elastic-plastic computer analysis are very small and insignificant from the viewpoint of structural design. It may have been noticed that, in all the examples presented so far, the differences were so small that the hinge formation pattern at a particular load factor given by the two methods has always been identical or very nearly so.

The proposed design method provides a better alternative to indirect design by the modified Merchant-Rankine formula. Wood [11] has mentioned the possibility of a variable stiffness approach similar to his work on columns [46] . This would require a stiffness-load relationship curve to be found for the whole frame, something similar to figure (4.3) of chapter IV , where a particular case of a single

beam has been shown. The proposed method takes into consideration the reduced stiffness of individual members at different stages of loading, although no direct relationship between the overall stiffness of the frame and the load factor has been found.

As for the optimality aspect of the design method, it has been shown that for frames controlled by limiting deflections (sec.5.5 and 5.6) an iterative approach of analyses with alternative arrangement of member sizes produces the optimum solution. As these analyses are only the calculation of sway deflections using the substitute frame at $\lambda = 1$, hand calculations can be used conveniently. However, the final solution of the six-storey one-bay frame (sec.5.5), using the computer programmes for all the calculations, required only 16 seconds of CPU time in the Burroughs B6700 computer.

For the frames controlled by strength and stability requirements the design solution given by the proposed method should usually be the optimum one as the feasible solution is obtained from the lower-bound design by increasing the inertia of one beam at a time to that of the next rolled section. Moreover, it is also possible to reduce the size of one member, which has been increased earlier, to make alternative studies.

It has also been shown that the design of a multistorey sway frame is usually governed by the limitations on horizontal deflections unless the effect of wind load is very small. Therefore,the design procedure may always start with the use of the simple method proposed in chapters II and III to obtain the optimum solution for limiting deflections. The solution may then be checked and modified, if necessary, for strength and stability requirements by the method proposed in chapters IV and V.

CHAPTER VI

ANALYSIS OF PORTAL FRAMES WITH VARYING CROSS-SECTIONS

6.1 INTRODUCTION

The pitched-roof portal frame is one of the most extensively used structural forms adopted for present-day industrial buildings. When rolled sections are used in the design of such buildings it is common practice to provide haunches in the rafters to obtain an economic design solution. Further economy can be achieved by using fabricated plate girders for both the rafter and the stanchion with linearly varying web depth. The thickness and width of flange plate and the thickness of web may also be changed at desired intervals along the length of the frame. When the strength requirements control the design, cross-sectional dimensions of non-uniform girders may be proportioned according to the bending moment envelope of the frame. The number of cross-sectional parameters to be varied is, however, dependent on the relative economy in terms of the material cost due to such variation and the additional expenditure involved in fabrication.

The simplest approach to the analysis of such frames is to divide each rafter and stanchion into a number of smaller members and to consider these members as of uniform section with average cross-sectional dimensions. The frame is then analysed by the matrix displacement method. This approach to analysis is an approximate one, but leads to convergence as the number of divisions increases. However, a large amount of computer time and storage is then required.

In this chapter a method has been developed for the elastic analysis of frames with tapered members which is quicker both in data preparation and computer time, as it does not require any subdivision of the members. Slope-deflection equations have been derived for a tapered member which have then been used to produce a member stiffness matrix. In this chapter the stiffness matrix has been used to analyse frames with tapered members by displacement method. In the following chapter this analysis procedure has been used in the optimum design of single-bay pitched-roof portal frame to strength and deflection constraints.

6.2 STOPE-DEFLECTION EQUATIONS FOR A TAPERED MEMBER

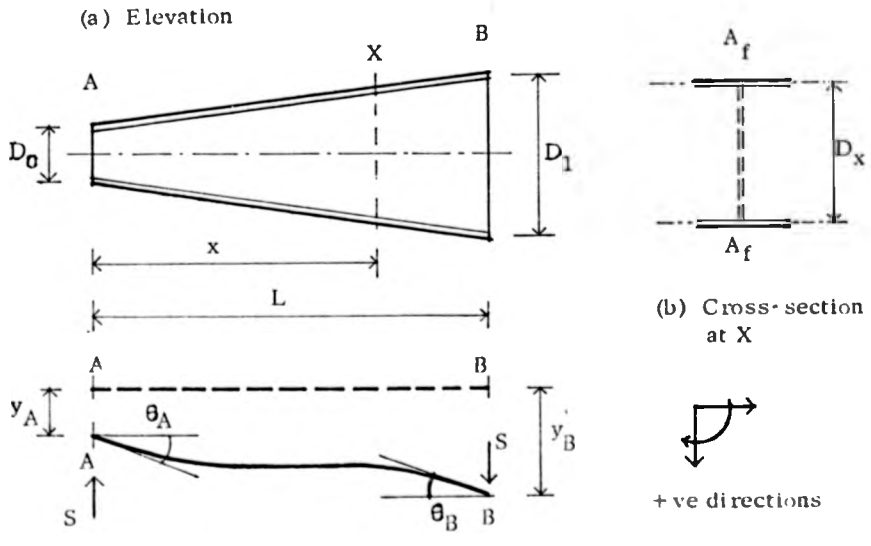

Figure 6.1

Figure (6.1) shows a tapered member of linearly varying web depth and constant flange width, flange thickness and web thickness. Let L be the length of the member, A_f the cross-sectional area of each flange, D_o and D_1 the depths between the centre line of flanges at A and B respectively. It is assumed that the member is not subjected to any load at intermediate points between A and B. Let θ_A and θ_B be the rotation of ends of the deformed member while y_A and y_B are the transverse displacements. Longitudinal displacements are not considered for the moment.

If the area of web is neglected and the thickness of flange is assumed to be small in comparison with the overall dimension of the section, the moment of inertia of the member at a point X, at a distance x from A, is given by

$$I_x = A_f \frac{Dx^2}{2} \qquad (6.1)$$

where Dx is the depth at X and is given by

$$Dx = D_o + (D_1 - D_o) \frac{x}{L}$$

Therefore, letting $\gamma = \frac{D_1 - D_o}{L}$ and $G = D_o / \gamma$

$$I_x = \frac{A_f \gamma^2}{2} (x + G)^2 \qquad (6.2)$$

If M_A and M_B are the moments at A and B and S the shear force, for equilibrium

$$SL + M_A + M_B = 0 \qquad (6.3)$$

Assuming hogging bending moment at X ,

$$EI_x \frac{d^2y}{dx^2} = - M_A - Sx \qquad (6.4)$$

Using (6.2) for I_x and letting $A' = -\frac{EA_f\gamma^2}{2}$,

$$A' \frac{d^2y}{dx^2} = \frac{M_A + Sx}{(x+G)^2} \qquad (6.5)$$

$$\therefore \quad A' \frac{dy}{dx} = \int \frac{M_A + Sx}{(x+G)^2}$$

$$= S \ln (x+G) + \frac{GS - M_A}{x+G} + U \qquad (6.6)$$

and

$$A'y = \int \left[S \ln (x+G) + \frac{GS - M_A}{x+G} + U \right]$$

$$= \ln (x+G)(Sx + 2GS - M_A) - Sx + Ux + V \qquad (6.7)$$

where U and V are constants.

Boundary condition of the frame gives ,

(i) at $x = 0$, $y = y_A$ and $\frac{dy}{dx} = \theta_A$ and

(ii) at $x = L$, $y = y_B$ and $\frac{dy}{dx} = \theta_B$

Using boundary condition (i) in equations (6.6) and (6.7),

$$U = A'\theta_A - S(\ln G + 1) + M_A/G \tag{6.8}$$

and $$V = A'y_A + (M_A - 2GS)\ln G \tag{6.9}$$

The following expressions for the member-forces can be derived by using the boundary condition (ii) and the values of U and V (equations 6.8 and 6.9) in equations (6.6) and (6.7)

$$M_A = \frac{A'}{(GH^2L + G^2H^2 - L^2)}\left[(GL^2 + 2G^2L - 2GHL^2 - 2G^3H)\theta_A \right.$$

$$\left. + GHL^2 + 3G^2HL + 2G^3H - 2GL^2 - 2G^2L)\theta_B + (GL - G^2H - GHL)\Delta \right] \tag{6.10}$$

$$M_B = \frac{A'}{(GH^2L + G^2H^2 - L^2)}\left[(3G^2HL + GHL^2 + 2G^3H - 2GL^2 - 2G^2L)\theta_A \right.$$

$$\left. + (L^3 + 2G^2L + 3GL^2 - 4G^2HL - 2GHL^2 - 2G^3H)\theta_B + (L + G)(GH - L)\Delta \right] \tag{6.11}$$

$$S = \frac{A'}{(GH^2L + G^2H^2 - L^2)}\left[(GL - GHL - G^2H)\theta_A + (GHL + G^2H - GL - L^2)\theta_A + L\Delta \right] \tag{6.12}$$

where $H = \ln\left(1 + \frac{L}{G}\right)$ and

$\Delta = y_B - y_A$, i.e., the relative transverse deflection of the member ends.

With $D_1 = D_o$, equations (6.10 - 6.12) give the normal slope-deflection equations for uniform members.

6.3 OVERALL STIFFNESS MATRIX OF A FRAME WITH TAPERED MEMBERS

Equations (6.10)- (6.12) can be written in matrix form as :

$$\begin{bmatrix} S \\ M_A \\ M_B \end{bmatrix} = C' \begin{bmatrix} L & (GL-GHL-G^2H) & (GHL+G^2H-GL-L^2) \\ (GL-G^2H-GHL) & (GL^2+2G^2L-2G^2HL-2G^3H) & (GHL^2+3G^2HL+2G^3H \\ & & -2GL^2-2G^2L) \\ (G+L)(GH-L) & (3G^2HL+GHL^2+2G^3H-2G^2L) & (L^3+2G^2L+3GL^2 \\ & & -4G^2HL-2GHL^2-2G^3H) \end{bmatrix} \begin{bmatrix} \Delta \\ \theta_A \\ \theta_B \end{bmatrix} \tag{6.13}$$

where

$$C' = \frac{A'}{(GH^2L+G^2H^2-L^2)}$$

In abbreviated form equation (6.13) can be expressed as

$$\underline{P} = \underline{k}.\underline{Z} \tag{6.14}$$

where

$\underline{P}$ is the vector for member forces, $\underline{Z}$ is the joint displacement vector , and $\underline{k}$ is the stiffness matrix.

The vector $\underline{Z}$ expresses the joint displacements in terms of the member. These can be converted into the overall coordinate system of the frame (figure 6.1) by using the relationship stated below.

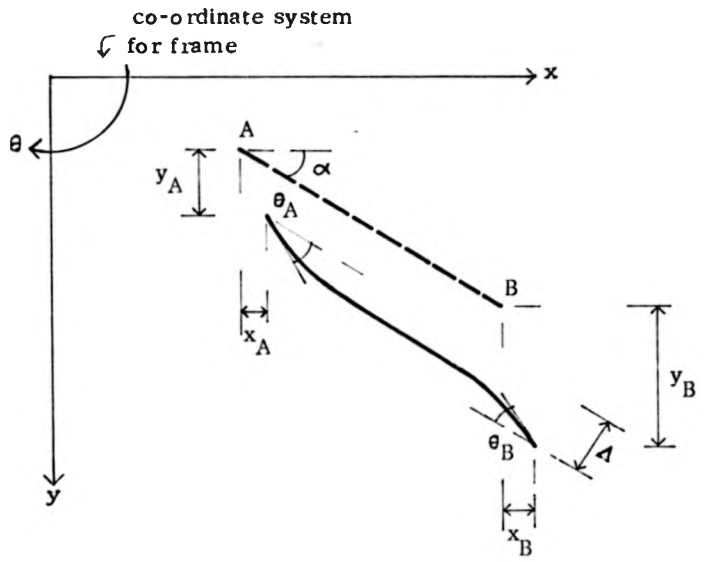

Figure 6.2

Referring to figure (6.2) the displacement vector $\underline{Z}$ can be expressed as

$$\begin{bmatrix} \Delta \\ \theta_A \\ \theta_B \end{bmatrix} = \begin{bmatrix} \sin\alpha & -\cos\alpha & 0 & -\sin\alpha & \cos\alpha & 0 \\ 0 & 0 & 1 & 0 & 0 & 0 \\ 0 & 0 & 0 & 0 & 0 & 1 \end{bmatrix} \begin{bmatrix} x_A \\ y_A \\ \theta_A \\ x_B \\ y_B \\ \theta_B \end{bmatrix} \qquad (6.15)$$

where α is the inclination of the member with respect to x -coordinate of the overall system. x_A, y_A, θ_A and x_B, y_B, θ_B are the displacements of the joints A and B in the x, y and θ directions of the overall system.

Equation (6.15) can be abbreviated as

$$\underline{Z} = \underline{A} \cdot \underline{X} \tag{6.16}$$

where $\underline{X}$ is the joint displacement vector in the overall system and $\underline{A}$ is known as the displacement transformation matrix.

By equating work done on the member to the strain energy stored, it can be shown that [8]

$$\underline{L} = \underline{A}' \cdot \underline{P} \tag{6.17}$$

where $\underline{L}$ is the applied load vector, corresponding term for term to $\underline{X}$, and $\underline{A}'$ is the transpose of matrix $\underline{A}$.

From (6.14), (6.16) and (6.17),

$$\underline{L} = \underline{A}' \underline{k} \cdot \underline{A} \cdot \underline{X}$$

or simply

$$L = \underline{K}\ \underline{X} \tag{6.18}$$

where $\underline{K}$ ($= \underline{A}' \cdot \underline{k} \cdot \underline{A}$) is the overall stiffness matrix of the member.

Using the values of $\underline{k}$ (equation 6.13) and $\underline{A}$ (equation 6.15) the overall stiffness matrix for a tapered member, $\underline{K}$, is given by

$$\underline{K} = \begin{bmatrix} a & & & & & \\ -b & d & & \text{symmetrical} & & \\ -c & e & f & & & \\ -a & b & c & a & & \\ b & -d & -e & -b & d & \\ g & -h & r & -g & h & q \end{bmatrix} \tag{6.19}$$

where

$$a = C'L \sin \alpha^2$$

$$b = C'L \sin \alpha \cos \alpha$$

$$c = C'G (GH + HL - L) \sin \alpha$$

$$d = C'L \cos \alpha^2$$

$$e = C'G (GH + HL - L) \cos \alpha$$

$$f = C'G (L^2 + 2GL - 2GHL - 2G^2H)$$

$$g = C'(G + L)(GH - L) \sin \alpha$$

$$h = C'(G + L)(GH - L) \cos \alpha$$

$$q = C'(G + L)(L^2 + 2GL - 2GHL - 2G^2H)$$

$$r = C'G(G + L)(2GH + HL - 2L)$$

The overall stiffness matrix of the frame may now be constructed by assembling the stiffness matrices of the members. Considering equation (6.18) as the load-displacement relationship for the whole f rame, displacements of the frame are given by

$$\underline{X} = \underline{K}^{-1} \cdot \underline{L} \qquad (6.20)$$

In this case $\underline{X}$ will represent the displacement vector for all the joints in the frame, $\underline{K}$ the overall stiffness matrix and $\underline{L}$ the external load vector of the frame.

6.4 ANALYSIS PROGRAM

The analysis of a frame with tapered members by the matrix displacement method is based on the equation (6.20). Once the terms of the stiffness matrices of individual members (equation 6.19) are calculated and assembled to form the overall stiffness matrix of the frame, i.e. $\underline{K}$ of equations (6.20), the joint displacements can be calculated by using the same equation, the external load vector, $\underline{L}$, being a known quantity.

The joint displacements enable the value of Δ to be determined for each member and the member end moments can then be calculated by using equations (6.10) and (6.11). The 'compact elimination 'technique developed by Jennings [23] is used to solve the stiffness equation (6.20) after the stiffness matrix has been stored by the economical method proposed by the same author, as discussed in chapter I (Sec.1.4). The compact technique is based on the Gaussian elimination method for the direct solution of linear simultaneous equations.

In deriving equations (6.10) - (6.12) the inertias have been calculated neglecting the cross-sectional area of the web. This may cause significant error in the analysis of a frame. To avoid this error an 'equivalent effective depth' of the members has been used which is explained below .

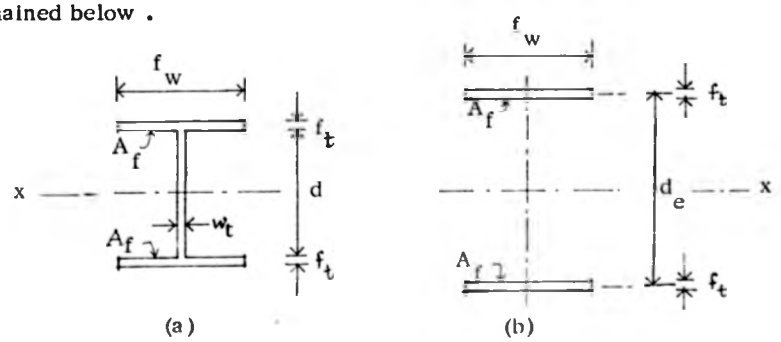

Figure 6.3

6.4 ANALYSIS PROGRAM

The analysis of a frame with tapered members by the matrix displacement method is based on the equation (6.20). Once the terms of the stiffness matrices of individual members (equation 6.19) are calculated and assembled to form the overall stiffness matrix of the frame, i.e. $\underline{K}$ of equations (6.20), the joint displacements can be calculated by using the same equation, the external load vector , $\underline{L}$, being a known quantity.

The joint displacements enable the value of Δ to be determined for each member and the member end moments can then be calculated by using equations (6.10) and (6.11). The 'compact elimination 'technique developed by Jennings [23] is used to solve the stiffness equation (6.20) after the stiffness matrix has been stored by the economical method proposed by the same author, as discussed in chapter I (Sec.1.4). The compact technique is based on the Gaussian elimination method for the direct solution of linear simultaneous equations.

In deriving equations (6.10) - (6.12) the inertias have been calculated neglecting the cross-sectional area of the web. This may cause significant error in the analysis of a frame. To avoid this error an 'equivalent effective depth' of the members has been used which is explained below .

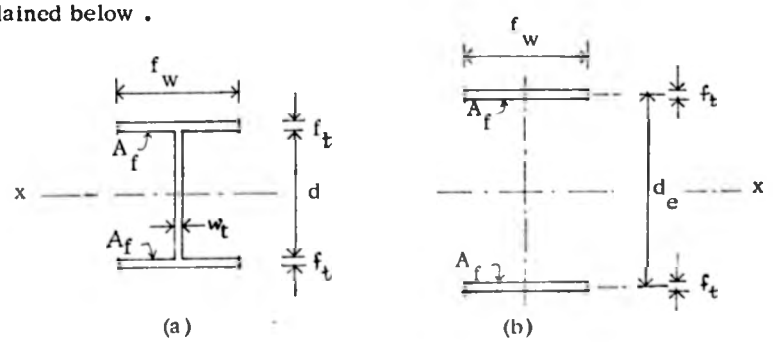

Figure 6.3

The cross-sectional dimensions of an I-section are shown in figure (6.3a). The moment of inertia of the section about the major axis (x - x) is given by

$$I_1 = w_t \frac{d^3}{12} + \frac{A_f}{2} (d + ft)^2 + f_w \frac{f_t^3}{6} \qquad (6.21)$$

Let the section shown in Figure (6.3b), composed of two flange plates only, have the same inertia about x - x axis as that of the I-section. If the dimensions of flange plates in both the sections are the same, the inertia of the section of figure (6.36b) is given by

$$I_2 = A_f \frac{d_e^2}{2} + f_w \frac{f_t^3}{6} \qquad (6.22)$$

Equating (6.21) and (6.22) the 'equivalent effective depth' d_e is given as

$$d_e = \sqrt{\frac{w_t d^3}{6A_f} + (d + f_t)^2} \qquad (6.23)$$

In calculating the terms of the stiffness matrices (6.19) the values of D_o and D_1 may now be modified by using (6.23) before calculating the terms of the stiffness matrix. The amount of error involved in the results of the analysis by using d_e is very small. In terms of inertia the maximum average error will not exceed 2% for members with $D_1/D_o = 2$. The error reduces as the taper gets shallower.

The analysis procedure can be summarised as follows :

(i) Calculate the equivalent depths at the ends of each member (equation 6.23).

(ii) Calculate the terms of the member stiffness matrix (equation 6.19).

(iii) Construct the overall stiffness matrix of the frame, $\underline{K}$, by assembling the member stiffness matrices.

(iv) Construct the external load vector, $\underline{L}$, from the given loading data.

(v) Solve the stiffness equation (6.20) to find the displacement vector $\underline{X}$.

(vi) Calculate the values of Δ for all the members

(vii) Calculate the member forces (Equations 6.10 - 6.12)

6.5 MODIFICATION FOR AXIAL DISPLACEMENT

The axial displacement of the member was neglected in deriving the slope-deflection equations (6.10) - (6.12). The analysis method, therefore, needs to be modified to include the effect of axial displacement and to calculate the axial forces in the member.

Referring to figure (6.1), if the cross-sectional area of the member is assumed to be the average of the area at the two ends of the member the slope-deflection equations can be modified as

$$
\begin{array}{l}
P \\ S \\ M_A \\ M_B
\end{array}
= C'
\left[\begin{array}{cccc}
\frac{1}{C'}\,\frac{EA}{L} & 0 & 0 & 0 \\
0 & L & (GL-GHL-G^2H) & (GHL+G^2H-GL-L^2) \\
0 & (GL-G^2H-GHL) & (GL^2+2G^2L-2G^2HL & (GHL^2+3G^2HL+2G^3H \\
 & & -2G^3H) & -2GL^2-2G^2L) \\
0 & (G+L)(GH-L) & (3G^2HL+GHL^2+2G^3H & (L^3+2G^2L+3GL^2-4G^2HL \\
 & & -2GL^2-2G^2L) & -2GHL^2-2G^3H)
\end{array}\right]
\left[\begin{array}{c} u \\ \Delta \\ \theta_A \\ \theta_B \end{array}\right]
$$

(6.24)

where P is the axial force inthe member

A is the average cross-sectional area and

u is the axial deformation of the member

Equation (6.24) replaces equation (6.13) and $\underline{k}$ is now a 4 x 4 matrix. The displacement transformation matrix, $\underline{A}$,takes the form

$$\begin{bmatrix} -\cos\alpha & -\sin\alpha & 0 & \cos\alpha & \sin\alpha & 0 \\ \sin\alpha & -\cos\alpha & 0 & -\sin\alpha & \cos\alpha & 0 \\ 0 & 0 & 1 & 0 & 0 & 0 \\ 0 & 0 & 0 & 0 & 0 & 1 \end{bmatrix} \qquad (6.25)$$

By using the modified expressions for the matrices $\underline{k}$ and $\underline{A}$ the overall member stiffness matrix can be found. This can still be represented by the equation (6.19) with the terms a, b and d modified as follows :

$$a = C'L \sin\alpha^2 + \cos\alpha^2 \frac{EA}{L}$$

$$b = C'L \sin\alpha \cos\alpha - \sin\alpha \cos\alpha \frac{EA}{L}$$

$$d = C'L \cos\alpha^2 + \sin\alpha^2 \frac{EA}{L}$$

Thc axial force in a member is given by

$$P = u \frac{EA}{L}$$

where $u = -\cos\alpha (x_A - x_B) - \sin\alpha (y_A - y_B)$

6.6 EXAMPLES

A computer program has been written in Burroughs Algol following the steps shown in Sec.(6.4) with modifications made in Sec.(6.5). To check the validity of the method in analysing frames with tapered members the simple portal frame shown in figure (6.4) is taken as the first example.

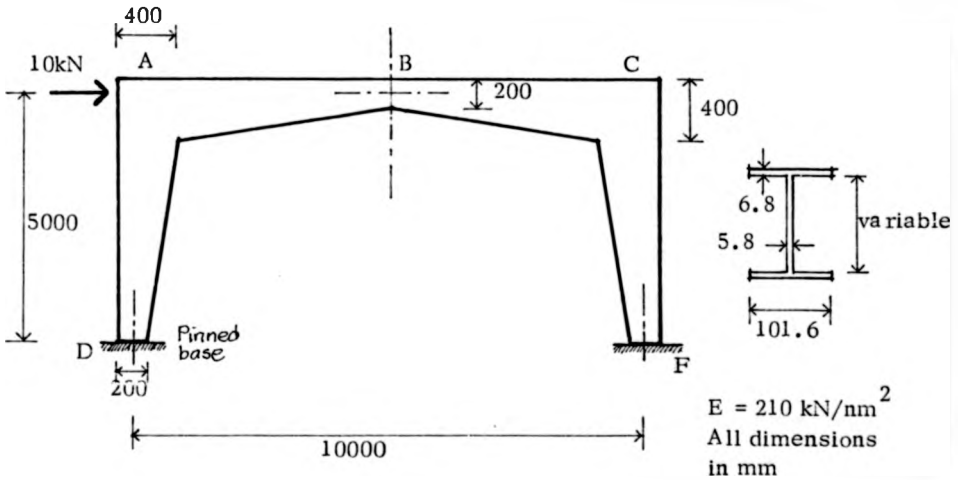

Figure 6.4

Table (6.1) shows the results of the analyses. The upper row shows the deflections and moments given by the proposed method, while the lower row shows the results given by analysing a 'stepped' frame obtained by dividing each of the members AD, AB, BC and CF into sixteen smaller members of average uniform depth. A standard computer program for analysis by the matrix displacement method has been used for the latter analysis. The results show excellent agreement.

	Horizontal deflection at A mm	Vertical deflection at B mm	Bending moment at A kNm	Bending moment at B kNm	Bending moment at C kNm
Proposed method	40.987 to right	4.382 up	31.316	4.472	18.676
'Stepped' analysis	40.151 to right	4.315 up	31.324	4.459	18.676

Table 6.1

As the next example, the frame used by Just [36] to illustrate his method using finite element technique, will be analysed by the proposed method. The frame is shown in figure (6.5). Analyses were carried out for (i) a vertical load of 100 kN at B, and then for (ii) a horizontal load of 100 kN acting at A. The results are shown in table (6.2). While the moments given by the two methods are nearly the same, the differences in the value of the deflections are also negligible.

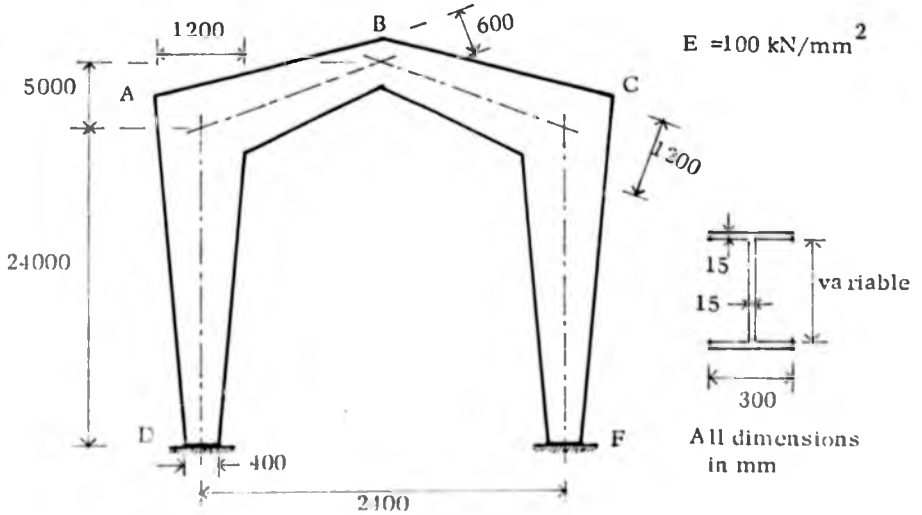

Figure 6.5

	For vertical load		For horizontal load	
	Proposed method	Just's method	Proposed method	Just's method
Horizontal deflection at A mm	24.17 to left	24.79 to left	495.49 to right	510.1 to right
Deflection at B mm	59.08 down	60.61 down	485.64 to right	500.0 to right
Horizontal deflection at C mm	24.17 to right	24.79 to right	474.83 to right	488.9 to right
Moment at D kNm	77.48	78.1	446.01	445.6
Moment at A kNm	264.31	263.4	896.70	897.0
Moment at B kNm	264.48	265.4	109.99	110.4
Moment at C kNm	264.31	263.4	676.15	677.2
Moment at F kNm	77.48	78.1	381.14	380. 2

Table 6.2

The above examples show that the proposed method gives reasonably accurate analysis results for frames with tapered members. The C.P.U. time required in Burroughs 6700 computer to analyse a single-bay portal frame is always a fraction of a second.

CHAPTER VII

PITCHED-ROOF PORTAL FRAMES:
OPTIMUM DESIGN TO STRENGTH AND DEFLECTION REQUIREMENTS

7.1 INTRODUCTION

As discussed in chapter I, one of the main problems associated with the design of portal frames is to satisfy the deflection limitations. Design of such frames by the plastic theory, which ignores the deflections altogether, is a comparatively simple exercise. But the calculation of deflections at working load, required to satisfy the limitations specified by the code, is often the difficult part of the design. To arrive at a satisfactory solution, several analyses of trial designs may be necessary and the eventual design solution may not be the most economic one.

This has led to the adoption of elastic design at working load using fabricated plate girders with varying cross-sections. A tapered portal frame designed to be stressed right up to the permissible elastic value throughout its length is an alternative to plastically designed frame using uniform rolled sections. As the tapered members are built up from plates, it is possible to use thin, deep web plates leading to higher inertia/weight ratio than is possible with rolled sections. The additional advantage of using such deep sections is the reduction in in-plane deflections of the frame.

However, due to the requirement to satisfy the permissible stresses as well as deflections at different combination of loading, including the reversibility of wind direction, it is not usually possible to maintain sections stressed up to the permissible value at a particular load case. In spite of this, considerable economy may be achieved

by using tapered members if the variation in the cross-sectional dimension of the frame can be optimised to satisfy the design requirements.

The analysis method developed in the preceding chapter can be used to design a frame by a process of iteration. If such a design operation starts with a lower-bound solution and subsequent increments in the cross-sectional dimensions are obtained by a mathematical programming technique for minimisation of the weight function, then the optimum design solution for the frame may be found.

Basically, mathematical programming techniques are procedures for determining the values of a set of variables that either maximise or minimise a numerical function of the variables subject to satisfying some other relationships also expressed as numerical function of the variables. The function to be minimised or maximised is called the 'objective function' and the equations expressing the relationship of the variables to be satisfied are known as the 'constraint equations'. The objective function is usually expressed as :

Minimise or maximise

$$f(v_1, v_2, v_3, \ldots\ldots, v_m) \qquad (7.1)$$

where $v_1, v_2, \ldots\ldots, v_m$ are the m number of variables.

The constraint functions may either be equalities or inequalities. The former expresses an exact relationship between the variables, e.g.,

$$g_1(v_1, v_2, v_3, \ldots\ldots, v_m) = c_1 \qquad (7.2)$$

The inequality constraints represent the relationships for some limitations, e.g.,

$$g_2(v_1, v_2, v_3, \ldots\ldots, v_m) \leq c_2 \qquad (7.3)$$

or

$$g_3(v_1, v_2, v_3, \ldots\ldots, v_m) \geq c_3 \qquad (7.4)$$

c_1, c_2 and c_3 are constant terms.

The space bounded by the constraint equations is known as the 'feasible region' and the values of the variables in the final solution must lie within this region.

When the objective function and all the constraint equations of an optimisation problem are linear the problem is classified as one of 'linear programming'. When this is not true the problem is one of non-linear programming. Although comparatively simple techniques, e.g. simplex method, are available for dealing with linear programming [32], solution techniques for non-linear programming problems are still relatively complex in nature.

In a structural design problem the variables for a frame of fixed geometry are usually the numerical values of cross-sectional dimensions at different locations of the frame and the constraints are of the form shown in equation (7.3) with the term c_2 representing the specific value of stress or deflection which must not be exceeded. The objective function is either a cost function or a weight function. The relationship between the weight and cost of a multistorey framed structure using rolled sections has been discussed in chapter II (Sec. 2.2). In a fabricated portal frame with welded tapered members the minimum-weight design is likely to be very close to the most economic solution if the practical constraints regarding the available and convenient dimensions of plate are taken into consideration and the number of changes in the

cross-sectional dimensions of the frame is related to the additional cost of welding etc. required for such changes.

A method has been developed for the absolute minimum-weight design of single-bay pitched roof portal frames to strength requirements and limiting deflections. Subsequently the same basic principles have been used to produce a second approach for design considering the practical constraints of fabrication and realistic dimensions for plates.

7.2 BASIC PRINCIPLES OF DESIGN

A general linear minimisation problem which could be solved by the simplex method can be expressed as :

Minimise

$$Z = k_1 v_1 + k_2 v_2 + \ldots\ldots + k_j v_j + \ldots + k_m v_m \qquad (7.5)$$

Subject to the constraints

$$\sum_{j=1}^{m} a_{ij} v_j \leq \text{or} = \geqslant c_i \qquad (7.6)$$

$$v_j \geqslant 0 \qquad (7.7)$$

for $i = 1, 2, 3 \ldots\ldots\ldots, n$

where

a_{ij}, c_i and k_j are constants

m is the number of variables

and n is the number of constraints.

cross-sectional dimensions of the frame is related to the additional cost of welding etc. required for such changes.

A method has been developed for the absolute minimum-weight design of single-bay pitched roof portal frames to strength requirements and limiting deflections. Subsequently the same basic principles have been used to produce a second approach for design considering the practical constraints of fabrication and realistic dimensions for plates.

7.2 BASIC PRINCIPLES OF DESIGN

A general linear minimisation problem which could be solved by the simplex method can be expressed as :

Minimise

$$Z = k_1 v_1 + k_2 v_2 + \ldots\ldots + k_j v_j + \ldots + k_m v_m \qquad (7.5)$$

Subject to the constraints

$$\sum_{j=1}^{m} a_{ij} v_j \leq \text{or} = \geqslant c_i \qquad (7.6)$$

$$v_j \geqslant 0 \qquad (7.7)$$

for $i = 1, 2, 3 \ldots\ldots\ldots, n$

where

a_{ij}, c_i and k_j are constants

m is the number of variables

and n is the number of constraints.

In the following paragraphs the procedure adopted to express the optimum design problem of a single-bay pitched-roof portal frame in the above form (equations 7.5 - 7.7) has been explained.

Figure (7.1) shows the line-diagram of a pitched roof portal frame. The design constraints for such a frame relating to the permissible stresses will usually be the maximum stresses at A, B , C , ..., L

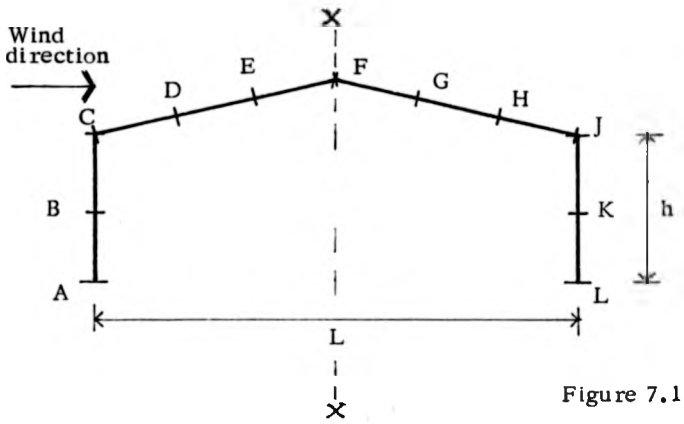

Figure 7.1

assuming that all the external loads act at these points. These are the locations where the angle of taper and plate thickness of the members AC, CF, FJ and JK will be allowed to change, with linear variations in depth between A and B, B and C, C and D etc. The other constraints may be the vertical deflection at F and the horizontal deflection at J.

Starting with an initial lower-bound solution, the variables for the problem will be the increases of girder depths at A, B, C , ...,L , thickness and width of flanges and thickness of web for the lengths AB, BC, CD, ... , KL. If the cross-sectional dimensions of

the initial frame are selected on the basis of (i) minimum available plate thickness, (ii) code specifications on minimum requirements to prevent local buckling, and (iii) minimum sizes specified by the architect, equation (7.7) will be satisfied as the variables will have non-negative values. Such an initial design for the frame will be an infeasible one and it is likely that most of the design constraints (equations 7.6) will remain unsatisfied. The simplex operation will then produce values of the variables required to satisfy the constraint equations with minimum increase in the value of the objective function (equation 7.5) . The number and location of the points where a change of plate size and a change of slope in the girder profile occur, i.e. the points B, D, E, G, H and K , may be chosen by the designer on the basis of fabrication constraints and the relative economy between reduction in volume and increase of fabrication cost. As the frame shall have to be symmetrical about its vertical axis (X - X of figure 7.1), to be able to satisfy the reversibility of horizontal loading and the architectural requirements, the number of variables may be reduced to those in one half of the frame, with identical dimensions in the other half.

As stated in chapter II (sec.2.1) , the permissible horizontal deflection at J due to the combination of dead and windload, according to BS 449, will be h/325 and according to the B/20 Draft Specification, h/300. For vertical deflection at C due to imposed load, the corresponding values are L/360 and L/200 respectively. Permissible stresses at the points A, B, C , ... , L will vary depending on the sectional properties of the members at these points as well as the effective length of the compression flanges. Formulae and tables to calculate these values are given in BS 449.

On analysing the initial frame, let f_1 be the value of the 'stress index' given by the interaction formula (clause 14a of BS 449) at a point, say B, of the frame of figure (7.1), i.e.

$$f_1 = \frac{f_c}{p_c} + \frac{f_{bc}}{p_{bc}} \qquad (7.8)$$

where

f_c = the calculated average axial stress at B,

p_c = the permissible axial stress at B,

f_{bc} = the calculated maximum bending stress at B,

and p_{bc} = the permissible bending stress at B.

In a feasible solution f_1 should be less than 1, but as the initial design is not feasible, the value of f_1 is likely to be greater than 1.

The frame may now be analysed, after increasing, by unit value, the dimension corresponding to one of the variables, say, the stanchion depth at C, keeping all the other dimensions unaltered. A new set of values for stresses and deflections for the different points in the frame is given by the analysis. If the total stanchion depth at C and the stress constraint at B are designated at v_1 and c_1 respectively, the rate of change of the constraint c_1 with respect to that of v_1 is given as

$$\frac{\partial c_1}{\partial v_1} = f_1' - f_1 \qquad (7.9)$$

where f_1' is the new stress index at B.

Similarly the rate of change of all the other constraints for unit change of depth at C can be calculated by subtracting the respective values of the stress indexes and deflections given by the initial analysis from those of the latter analysis. The general relationship can be expressed as

$$\frac{\partial c_i}{\partial v_1} = f_i' - f_i$$

$i = 1, 2, 3, \ldots\ldots\ldots n$

where n is the total number of constraints.

Proceeding in a similar way, i.e. by increasing the dimensions corresponding to the other variables by unit values, one at a time, and analysing the frame, all the values for these 'sensitivity coefficients'[42] can be calculated. The general expression for the sensitivity coefficient may be given as

$$\frac{\partial c_i}{\partial v_j} \quad , \; i = 1, 2, 3, \ldots\ldots, n \text{ and}$$
$$j = 1, 2, 3, \ldots\ldots, m$$

where m is the total number of design variables.

If the unknown changes to be made in the variables are designated as Δv_j, the constraint equations can be expressed as

$$f_1 + \frac{\partial c_1}{\partial v_1}\Delta v_1 + \frac{\partial c_1}{\partial v_2}\Delta v_2 + \ldots\ldots + \frac{\partial c_1}{\partial v_j}\Delta v_j + \ldots\ldots + \frac{\partial c_1}{\partial v_m}\Delta v_m \leq cp_1$$

$$f_2 + \frac{\partial c_2}{\partial v_1}\Delta v_1 + \frac{\partial c_2}{\partial v_2}\Delta v_2 + \ldots\ldots + \frac{\partial c_2}{\partial v_j}\Delta v_j + \ldots\ldots + \frac{\partial c_2}{\partial v_m}\Delta v_m \leq cp_2$$

$$\ldots\ldots \qquad \ldots\ldots \qquad \ldots\ldots \qquad \ldots\ldots$$

$$f_i + \frac{\partial c_i}{\partial v_1}\Delta v_1 + \frac{\partial c_i}{\partial v_2}\Delta v_2 \ldots + \frac{\partial c_i}{\partial v_j}\Delta v_j + \ldots + \frac{\partial c_i}{\partial v_m}\Delta v_m \leq cp_i$$

$$\ldots\ldots \qquad \ldots\ldots \qquad \ldots\ldots \qquad \ldots\ldots$$

$$f_n + \frac{\partial c_n}{\partial v_1}\Delta v_1 + \frac{\partial c_n}{\partial v_2}\Delta v_2 + \ldots\ldots + \frac{\partial c_n}{\partial v_j}\Delta v_j + \ldots + \frac{\partial c_n}{\partial v_m}\Delta v_m \leq cp_n$$

(7.10)

where $cp_1, cp_2, \ldots\ldots, cp_n$ and $f_1, f_2, \ldots\ldots, f_n$ are respectively the permissible and the initial values for stresses and deflections.

In a general form the above constraint equations (7.10) can be expressed as

$$f_i + \frac{\partial c_i}{\partial v_j} \Delta v_j \leq cp_i \qquad (7.11)$$

If the objective function for the problem can now be found in linear expression of the variables, the simplex method of linear programming may be used to calculate the values of Δv_1, Δv_2 ..... , Δv_m required to satisfy the constraints.

However, although the constraint equations (7.10) have been expressed in a linear form, the sensitivity coefficients $\frac{\partial c_i}{\partial v_j}$ are not actually linear, i.e. the rates of change of the stresses and deflections with respect to those of the variable dimensions are not linear. A typical representation of these relationships is shown in figure (7.2). The curve A_1A_5 shows the non-linear reduction in the value of a constraint, say c_i, from D_1 to D as the cross-sectional dimension, v_j, increases from F_1 to F. If the permissible value of the constraint is represented by the vertical line DE which intersects the curve at the point A_5 and the initial value is given by the point D_1 corresponding to the point A_1 in the curve, increase of v_j from F_1 to F is necessary to satisfy the constraint. Or, in other words, the required value of $\Delta v_j = F_1F$.

The sensitivity coefficient, $\frac{\partial c_i}{\partial v_j}$, of the lower-bound solution is given by the tangent line A_1B_1 intersecting the line DE at B_1. The optimum design process using the simplex method will follow this tangent line and give the value of the variable $\Delta v_j = F_1F_2$ as the requirement to reduce the constraint from D_1 to D. However, if the frame is

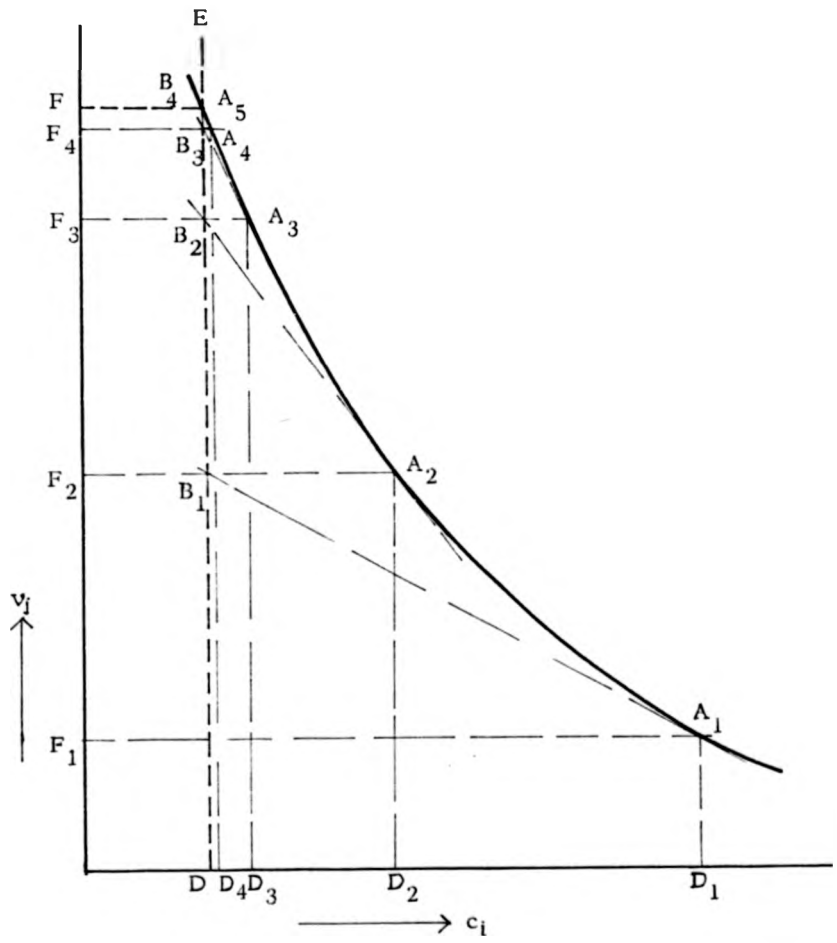

Figure 7.2

analysed after increasing the value of vj by the amount Δvj ($= F_1F_2$) it will be found that the constraint has actually reduced upto the point D_2 corresponding to A_2 of the curve. So, the constraint (7.10) will have to be reformulated and the optimisation problem resolved. By

incrementing the revised value of v_j, corresponding to F_2, and reanalysing, the 'sensitivity coefficient $\frac{\partial c_i}{\partial v_j}$ will now be represented by the tangent line A_2B_2. A second simplex operation at this stage will give the value of $\Delta v_j = F_2F_3$ as the requirement to satisfy the constraint. As shown in figure (7.2) the constraint will actually be reduced upto D_3 corresponding to the point A_3 in the curve. By further iteration the point A_5 in the curve corresponding to the permissible constraint line DE can be closely reached, following the path $A_1B_1A_2B_2A_3B_3A_4B_4$.

In the procedure described above only one variable and one constraint has been considered. In a problem with more than one variable and constraint each of the variables has its effect on all the constraints and similarly each of the constraints is effected by all the variables. Equation (7.10) shows this relationship. It is unlikely that the optimum solution of such problems will be given by the above procedure. The reasons for this and the modifications necessary to use the same basic principles in solving such problems are explained below.

In figure (7.3), let AB and CD represent the variation of the constraint c_i

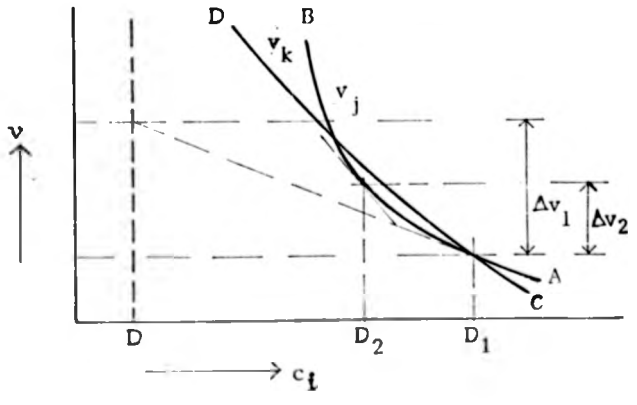

Figure 7.3

with respect to variables v_j and v_k. Let the value of c_i in the initial frame and the permissible value of the same constraint be given by the points D_1 and D respectively. It may be seen that corresponding to the point D_1 the sensitivity coefficient of AB, i.e. $\frac{\partial c_i}{\partial v_j}$ is of higher magnitude than that of CD, i.e. $\frac{\partial c_i}{\partial v_k}$. The linear programming operation at this stage may therefore produce an increase in the value of v_j by the amount Δv_1 without increasing v_k at all, provided their respective influence in the objective function are not very much different. If, instead of increasing v_j by the amount Δv_1, it is increased by a smaller amount Δv_2, the corresponding reduction in the constraint value would be upto the point D_2. A fresh analysis at this point may show a higher value for $\frac{\partial c_i}{\partial v_k}$ than that of $\frac{\partial c_i}{\partial v_j}$. This will cause subsequent increment of v_k only and in the final design the value of v_j may not have increased by more than Δv_2. As there are a number of variables representing a family of curves having various slopes with respect to the constraints it is essential that the increments of the variables dimensions, after each iteration, are restricted to a limited proportion of the corresponding original dimensions. This will also enable the optimisation procedure to deal with cases where one or more of the variable-constraint relationship curves are convex in nature. As the variables are only permitted to increase (equation 7.7) the problem of oscillation during the process of iteration has been avoided.

As stated earlier, use of the simplex method is possible if the objective function is a linear equation in terms of the variables. The objective function for this problem will be the total increase in the volume of the frame due to the increments in the cross-sectional dimensions. The changes of depth in a member length, say Δv_1 and Δv_2 at A and B of the member AB, cause linear variation in depth

between A and B. Hence, if the thickness of web in AB is kept constant, the increase of the volume of web remains a linear function of the variables Δv_1 and Δv_2. Similarly, if the flange area is considered as a variable, i.e. its uniform increase within the lengths, AB, BC, CD ,.. , etc., are each considered as a separate variable, the rise in the volume of flange will also be a linear function of these variables. To avoid terms containing the product of two variables it is not possible to consider the thickness and width of the flange as two different variables. For similar reasons the thickness of web cannot be treated as a variable. This, however, has very little influence on optimality as the code specification (Clause 27f of BS 449) on the requirement of depth/thickness ratio of unstiffened webs will govern the thickness of web plates in portal frames as the shear stress will always be low.

So, referring to the constraint equations (7.10), the objective function for the simplex program can be expressed as

Minimise

$$Z = k_1\Delta v_1 + k_2\Delta v_2 + \ldots\ldots + k_j\Delta v_j + \ldots + k_m\Delta v_m \ldots \quad (7.12)$$

where k_1 , k_2 ,.... , k_m are constants.

7.3 FORMULATION OF THE OPTIMISATION PROBLEM

Figure (7.4) shows the profile of a pitched-roof portal frame. The stanchion of the frame has been divided into n_1 divisions and the rafter is divided into n_2 members.

The total number of members in the frame is then $2(n_1 + n_2)$ and the number of joints, besides the two support joints, will be $2(n_1+n_2) - 1$.

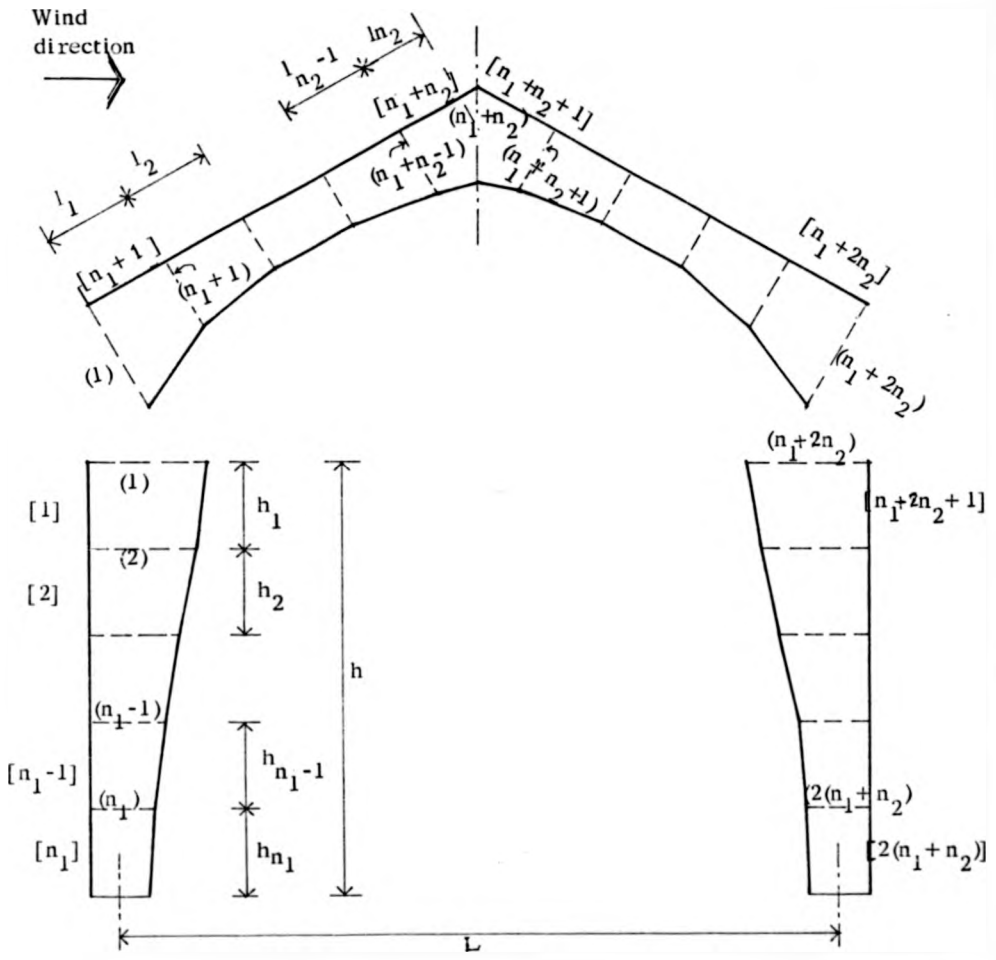

(n_1) indicates joint number

$[n_1]$ indicates member number

Figure 7.4

Since all the external loads will be converted into equivalent concentrated loads at the joints, constraints for satisfying the strength requirements of the frame will be the stresses at these joints. At the two eaves, i.e. at joint numbers 1 and $n_1 + 2n_2$ the stanchion and the rafter will be allowed to have different girder depths. Hence, the number of stress constraints

for the frame will be $2(n_1 + n_2) + 3$. Considering two constraints for the deflections – (i) the vertical deflection at the ridge, i.e .at joint number $n_1 + n_2$, and (ii) the horizontal deflection at the leeward eave, i.e. at joint number $n_1 + 2n_2$, the total number of constraints is $2(n_1 + n_2) + 5$. The constraints have been numbered as follows :

Constraint No.1	:	stress index at the first end of member [1]
" " 2	:	" " at the joint (2)
" " 3	:	" " at the joint (3)
...		... ...
Constraint No. n_1	:	" " at the joint(n_1)
" " $n_1 + 1$	:	" " at the first end of member[$n_1 + 1$]
" " $n_1 + 2$	:	" " at the joint ($n_1 + 1$)
" " $n_1 + 3$	:	" " at the joint ($n_1 + 2$)
...		... ...
Constraint No. $n_1 + 2n_2$	:	" " at the joint($n_1 + 2n_2 - 1$)
" " $n_1 + 2n_2 + 1$	:	" " at the second end of member[$n_1 + 2n_2$]
" " $n_1 + 2n_2 + 2$	:	" at the first end of member[$n_1 + 2n_2 + 1$]
" " $n_1 + 2n_2 + 3$	:	" " at the joint($n_1 + 2n_2 + 1$)
...		...
Constraint No. $2(n_1 + n_2) + 1$	:	" " at the joint($2(n_1 + n_2)$)
" " $2(n_1 + n_2) + 2$	:	" " at the second end of member[n_1]
" " $2(n_1 + n_2) + 3$	:	" " at the second end of member[$2(n_1 + n_2)$]
" " $2(n_1 + n_2) + 4$	:	" " at vertical deflection of joint ($n_1 + n_2$)
" " $2(n_1 + n_2) + 5$	:	" " horizontal deflection at joint($n_1 + 2n_2$)

All the above stress constraints, except constraint nos.1, $n_1 + 1$, $n_1 + 2n_2 + 1$, $n_1 + 2n_2 + 2$, $2(n_1 + n_2) + 2$ and $2(n_1 + n_2) + 3$, have been defined as stress indices at joints . A joint consists of the end of two adjoining members each having, at that point, the same internal forces and the same overall girder depth. The other cross-sectional dimensions of the two members may, however, be different and this may lead to two different stress indices at every joint. So, for accurate design, two different stress constraints should be considered at a joint which will increase the total number of stress constraints from $2(n_1 + n_2) + 3$ to $4(n_1 + n_2)$. To avoid large computer storage and time it has been decided to consider one stress constraint for each joint taking that stress index which is violated by the greater amount.

To get the optimum design solution for the frame, provision should be made to vary the depth and thickness of the web, as well as the flange area. As the dimensions have to be symmetrical about the vertical axis of the frame, the number of depth variables in the frame (figure 7.4) is $n_1 + n_2 + 2$. Assuming uniform flange area and web thickness in each subdivided member and keeping the flange width constant for the frame, the number of variables for flange thickness is $n_1 + n_2$. To satisfy clause 27b of BS 449 on maximum outstand of flanges, the lower-bound dimensions will be chosen accordingly. As the subsequent increase will only be in the thickness of flange, this clause will not be violated during the design process. As explained earlier, the thickness of web of a subdivided member will not be treated as a variable parameter for optimisation. To satisfy Clause 27f of BS 449, however, the web thickness of each of the member lengths will be increased corresponding to the increase in the depth after every simplex operation. So the total number of variables

for the problems remains at $2(n_1 + n_2) + 2$. The variables have been numbered as follows,

Variable No.1	:	depth of stanchion at joint 1
" " 2	:	" " " at joint 2
...		... ...
Variable No. n_1	:	depth of stanchion at joint n_1
" " $n_1 + 1$	:	" " rafter at joint 1
" " $n_1 + 2$	:	" " " at " $n_1 + 1$
" " $n_1 + 3$	:	" " " at joint $n_2 + 2$
...		... ...
Variable No. $n_1 + n_2 + 1$	:	depth of rafter at joint $n_1 + n_2$
" " $n_1 + n_2 + 2$	:	" " stanchion at left support
" " $n_1 + n_2 + 3$	:	flange thickness of member 1
" " $n_1 + n_2 + 4$	:	" " " " 2
...		... ...
Variable No. $2n_1 + n_2 + 2$	:	flange thickness of member n_1
" " $2n_1 + n_2 + 3$	:	" " " " $n_1 + 1$
...		... ...
Variable No. $2(n_1 + n_2) + 2$	:	flange thickness of member $n_1 + n_2$

As stated earlier (Sec.7.2), initial lower-bound cross-sectional dimensions of the frame will not reduce any further during the process of design. So the variables for the problem will actually be the increases of depths at the $n_1 + n_2 + 2$ locations and the increases of flange thickness for the $n_1 + n_2$ members. Figure (7.5) shows the location and numbering of the variables

indicated as Δv_1 , Δv_2 , ... , $\Delta v_{2(n_1 + n_2)+2}$

To calculate the stress indices at the different locations using the interaction formula (equation 7.8) it is necessary to find the permissible stresses on the basis of the latest cross-sectional dimensions at these locations. The permissible compressive axial stress, p_c is calculated using the strut formula given in Appendix B of BS 449 and the permissible compressive bending stress, p_{bc} , is determined by Clause 20 of the code. Effective lengths for the members to calculate the permissible stresses are to be determined according to the lateral restraint of the compression flanges. For the rafter members the effective length is generally taken to be the spacing of purlins assuming the top flange to be always under compression. Near the eaves, however, a considerable part of the rafter may have its bottom flange in compression and this should be taken into consideration when determining the effective length for the rafter members. For the members in the stanchion, the effective lengths will depend on the spacing of effective horizontal bracing in the stanchion.

The right-hand side of the constraint equations (7.10 and 7.11) consist of the permissible values, cp_i . For the stress constraints these are 1 and for the last two equations, the permissible values of vertical and horizontal deflections.

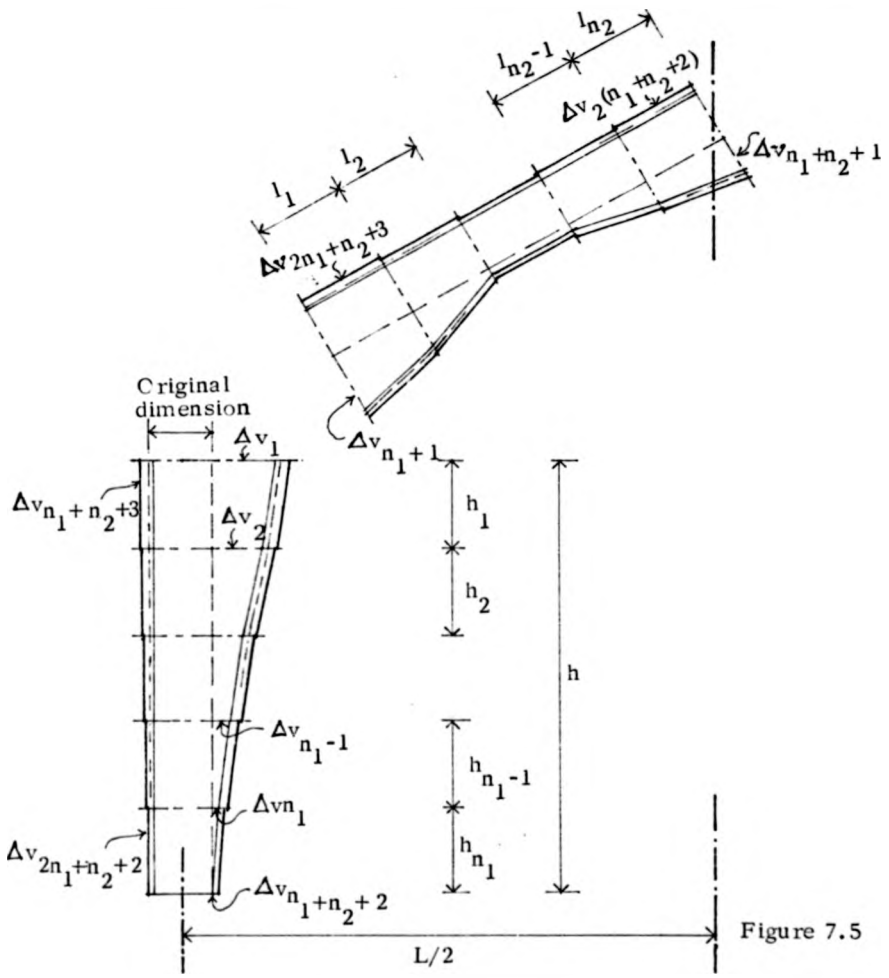

Figure 7.5

The objective function to be minimised will consist of the increase in the volume of half the frame due to increases in the dimensions required to satisfy the constraints. In other words, it is a linear numerical function of the variables Δv_1 , Δv_2 , ... , $\Delta v_{2(n_1+n_2)+2}$. Figure (7.5) shows the frame with original dimensions indicated by the dotted lines and the variables numbered according to the sequence described earlier .

The objective function can be expressed as,

$$Z = \Delta v_1 \frac{h_1}{2} wt_1 + \Delta v_2 \frac{(h_1+h_2)}{2}(wt_1 + wt_2) + \ldots + \Delta v_{n_1} \frac{(h_{n_1-1} + h_{n_1})}{2}(wt_{n_1-1} + wt_{n_1})$$

$$+ \Delta v_{n_1+1} \frac{l_1}{2} wt_{n_1+1} + \Delta v_{n_1+2} \frac{(l_1+l_2)}{2}(wt_{n_1+1} + wt_{n_1+2}) + \cdots$$

$$\cdots + \Delta v_{n_1+n_2} \frac{l_{n_2}}{2}(wt_{n_1+n_2-1} + wt_{n_1+n_2})$$

$$+ \Delta v_{n_1+n_2+1} \frac{l_{n_2}}{2} wt_{n_1+n_2} + \Delta v_{n_1+n_2+2} \frac{h_{n_1}}{2} wt_{n_1}$$

$$+ 2\Delta v_{n_1+n_2+3} h_1 fw_1 + 2\Delta v_{n_1+n_2+4} h_2 fw_2 + \ldots\ldots + 2\Delta v_{2n_1+n_2} h_{n_1} fw_{n_1}$$

$$+ 2\Delta v_{2n_1+n_2+3} l_1 fw_{n_1+1} + 2\Delta v_{2n_1+n_2+4} l_2 fw_{n_1+2} + \ldots + 2\Delta v_{2(n_1+n_2)+2} l_{n_2} fw_{n_1+n_2} \quad (7.13)$$

where $h_1, h_2, h_3, \ldots, h_{n_1}$ are the lengths of the stanchion members,

$l_1, l_2, l_3, \ldots\ldots, l_{n_2}$ are the lengths of the rafter members

$wt_1, wt_2, wt_3, \ldots\ldots, wt_{n_1+n_2}$ are the thicknesses of web

and $fw_1, fw_2, fw_3 \ldots\ldots, fw_{n_1+n_2}$ are the width of flanges.

The objective function can be expressed as,

$$Z = \Delta v_1 \frac{h_1}{2} wt_1 + \Delta v_2 \frac{(h_1+h_2)}{2}(wt_1+wt_2) + \ldots + \Delta v_{n_1} \frac{(h_{n_1-1}+h_{n_1})}{2}(wt_{n_1-1}+wt_{n_1})$$

$$+ \Delta v_{n_1+1} \frac{l_1}{2} wt_{n_1+1} + \Delta v_{n_1+2} \frac{(l_1+l_2)}{2}(wt_{n_1+1}+wt_{n_1+2}) + \cdots$$

$$\cdots + \Delta v_{n_1+n_2} \frac{l_{n_2}}{2}(wt_{n_1+n_2-1}+wt_{n_1+n_2})$$

$$+ \Delta v_{n_1+n_2+1} \frac{l_{n_2}}{2} wt_{n_1+n_2} + \Delta v_{n_1+n_2+2} \frac{h_{n_1}}{2} wt_{n_1}$$

$$+ 2\Delta v_{n_1+n_2+3} h_1 fw_1 + 2\Delta v_{n_1+n_2+4} h_2 fw_2 + \ldots\ldots + 2\Delta v_{2n_1+n_2} h_{n_1} fw_{n_1}$$

$$+ 2\Delta v_{2n_1+n_2+3} l_1 fw_{n_1+1} + 2\Delta v_{2n_1+n_2+4} l_2 fw_{n_1+2} + \ldots + 2\Delta v_{2(n_1+n_2)+2} l_{n_2} fw_{n_1+n_2}$$

(7.13)

where $h_1, h_2, h_3, \ldots, h_{n_1}$ are the lengths of the stanchion members,

$l_1, l_2, l_3, \ldots\ldots, l_{n_2}$ are the lengths of the rafter members

$wt_1, wt_2, wt_3, \ldots\ldots, wt_{n_1+n_2}$ are the thicknesses of web

and $fw_1, fw_2, fw_3 \ldots\ldots, fw_{n_1+n_2}$ are the width of flanges.

As the width of flange will be the same throughout the length of the frame fw_1 , fw_2 ,.... etc. will have the same value in this case.

7.4 DESIGN PROCEDURE

The design of a pitched roof portal frame will start with a decision concerning initial data for the frame . Firstly, the stanchion and the rafter have to be divided into smaller member lengths. The number of divisions, i.e. the values of n_1 and n_2 , will depend on how many changes in the slope of the girder profile and changes in the flange thickness are desired in the frame. The values will usually be chosen after a comparative study of the cost of welding and the cost of material and examination of other fabrication constraints. Once these values are selected, the number of variables, m, and the number of constraints (considering two deflection constraints) , n, are given by

$$m = 2(n_1 + n_2) + 2$$
$$n = 2(n_1 + n_2) + 5 \qquad (7.14)$$

A lower-bound solution for the frame will then be specified which will provide the cross-sectional dimensions of the initial design. Minimum thickness of available steel plates and the minimum depth and flange width of the girders required for convenience of fabrication and to satisfy clauses 27b and 27f of B.S.449 will usually be the guiding factors in deciding about the lower-bound dimensions of the frame.

The external loading is converted into equivalent loads at the joints created by the division of the frame into smaller members. The frame will then be analysed by using the procedure developed in

chapter VI and the stress factors and deflections are stored. By repeated analysis of the frame 'sensitivity coefficients' for the simplex tableau is calculated by following the procedure described in Sec. (7.2). The right-hand side parameters of the constraint equations and the coefficients of the objective function (equation 7.13) are then calculated and the first simplex operation carried out.

Values of the variables Δv_1 , Δv_2 ... etc given by the simplex operation are inspected and the corresponding cross-sectional dimensions are increased by these amounts subject to a maximum increase specified as a certain percentage of the original dimensions. In most of the examples presented in this chapter, this 'increment factor' has been taken as 10%. The thickness of web is then examined in view of the increases in the depth of the girders and are modified to satisfy clause 27f of BS 449.

As the profile of the girder changes with unequal increase of girder depth, the longitudinal axis of the subdivided members rotates from their original axis and the inclinations of the member axes in relation to the overall axis take new values (figure 7.6 a). The length

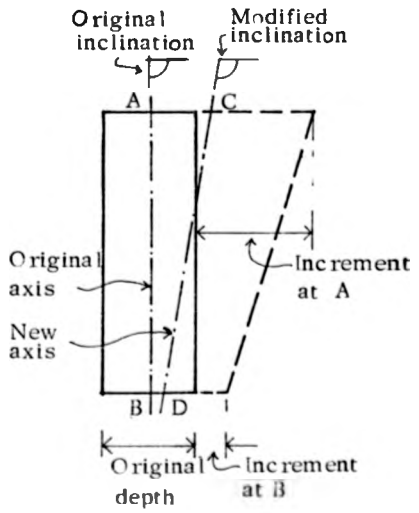

Figure 7.6a

of the member also changes from AB to CD. These changes are now incorporated and the frame geometry is revised accordingly.

The frame is analysed again and the stresses and deflections are examined. If all of these are within a specified tolerance of the permissible values, the optimum solution has been obtained. Otherwise, if any of the constraints have not yet been satisfied, the modified frame with its new cross-sectional dimensions is considered as a new lower-bound frame. Sensitivity coefficients are calculated again by repeated analysis, coefficients for the objective functions calculated and another simplex operation performed to find the values of further increases in cross-sectional dimensions necessary to satisfy the constraints. Iteration is carried out until all the constraints are satisfied.

A computer program in Burroughs Algol has been written for the automatic optimum design of single-bay pitched-roof portal frames based on the above procedure. The flow diagram shown in figure (7.6b) summarises the design procedure. A number of frames have been designed and comparative studies made by using alternative dimensions for the lower-bound frame and by using different increment factors for the variables of optimisation. The effect of using different number of divisions, i.e. the values of n_1 and n_2, on the optimality of the final design solution has also been studied. All these topics are presented and discussed in the following examples.

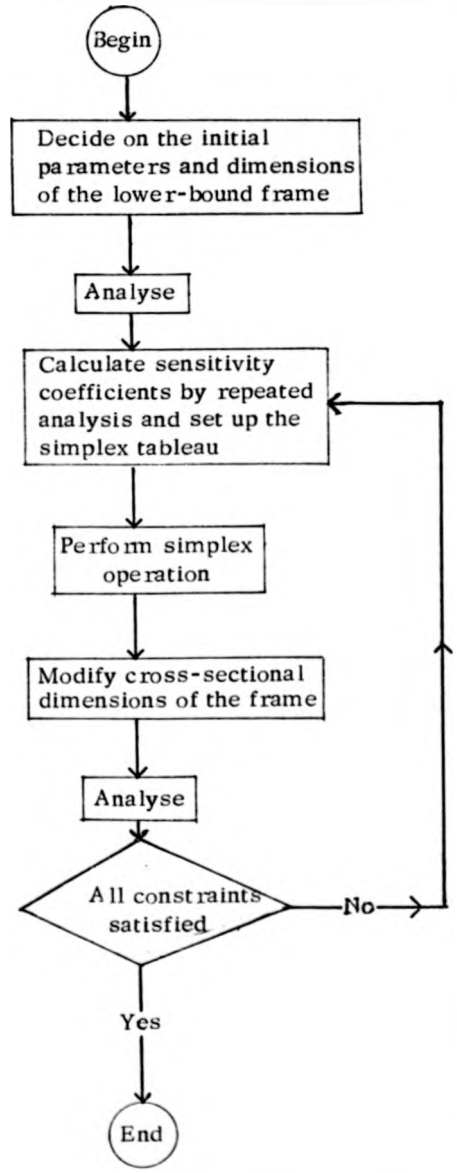
Begin
Decide on the initial parameters and dimensions of the lower-bound frame
Analyse
Calculate sensitivity coefficients by repeated analysis and set up the simplex tableau
Perform simplex operation
Modify cross-sectional dimensions of the frame
Analyse
All constraints satisfied
No
Yes
End

Figure 7.6b

7.5 EXAMPLE 1

To illustrate the application of the proposed design method the pitched-roof portal frame shown in figure (7.7) is taken as the first example. The frame has been designed to satisfy strength and

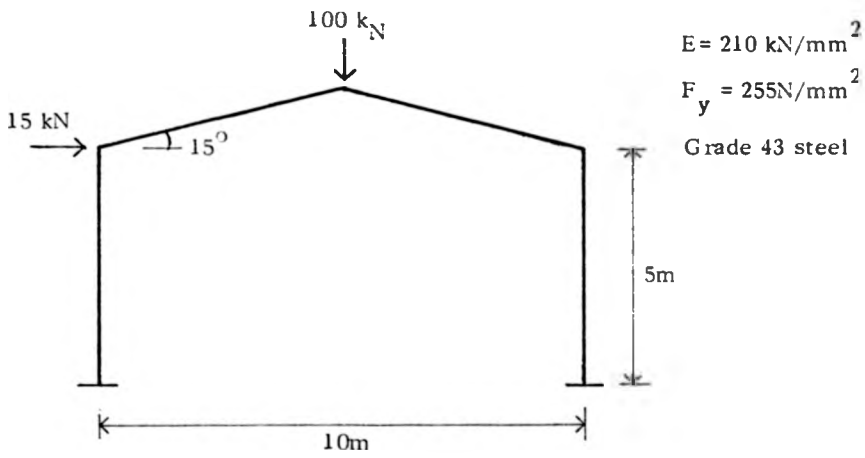

Figure 7.7

deflection requirements under the effect of combined vertical and horizontal loading without allowing the 25% increase in the permissible stresses (Clause 13 of BS 449). Permissible vertical and horizontal deflections have been taken as L/360 and h/325 and a tolerance of 5% on the permissible values of stresses and deflections have been allowed. The increment factor has been taken as 10% of the original dimensions after each linear programming operation.

The following initial dimensions have been used for the lower-bound frame throughout its length :

Flange thickness	6 mm
Web thickness	4 mm
Girder depth	150 mm
Flange width	150 mm, to remain unchanged.

Both the stanchion and the rafter (half-span) have been divided into five equal-length members. Effective length for calculating the permissible compressive stresses of the stanchion members has been taken as 2000 mm and that for the rafter members as 1500 mm.

The frame has at first been designed as having fixed supports and then as a pinned-base frame. In both the cases the optimum design to satisfy the strength requirements, i.e. to satisfy stress constraints only, as well as the design to stress and deflection constraints have been carried out. The results are shown in figures (7.8) - (7.11). Other information on the design process and the weight of the designed frames is given in table (7.1)

	Fixed base		Pinned base	
	stress constraints only	stress and deflection constraints	stress constraints only	stress and deflection constraints
Number of iterations required	16	16	18	45
CPU time in seconds	382	372	400	887
Weight of frame in kg	576.56	582.85	650.18	848.62

Table 7.1

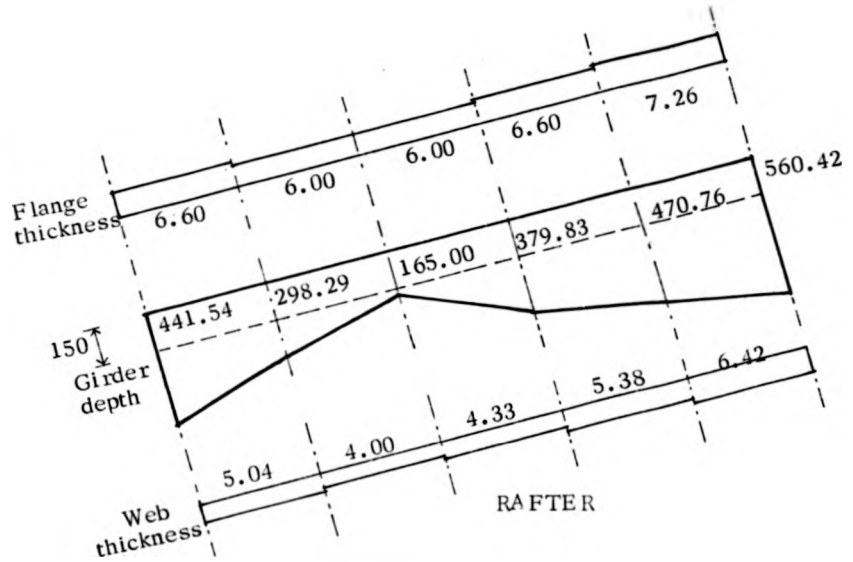

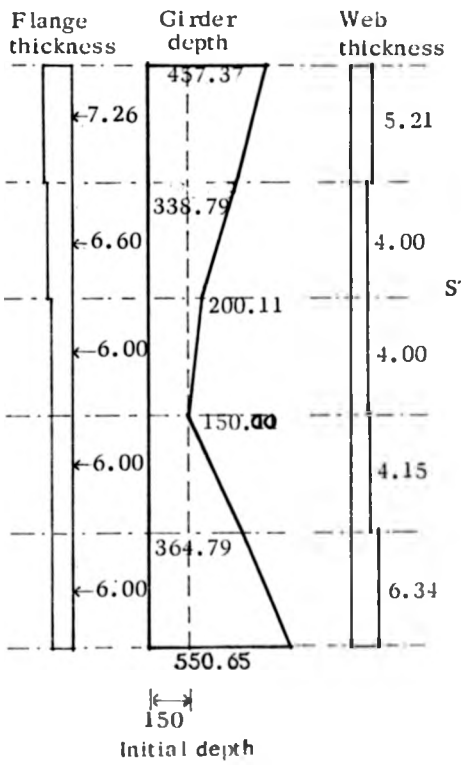

STANCHION

Fixed base

Stress constraints only

All dimensions in mm

Figure 7.8

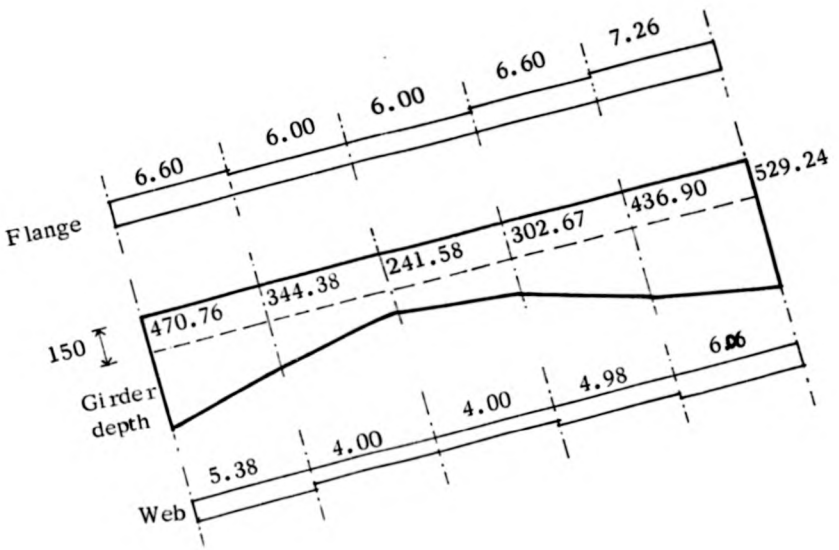

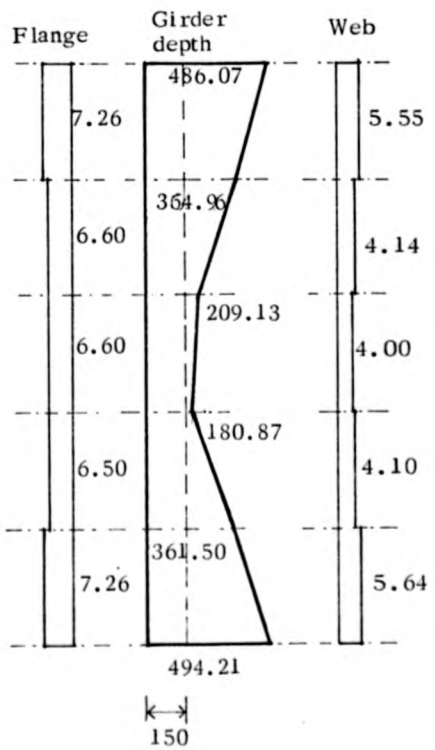

Fixed base

Stress and deflection constraints

All dimensions in mm

Figure 7.9

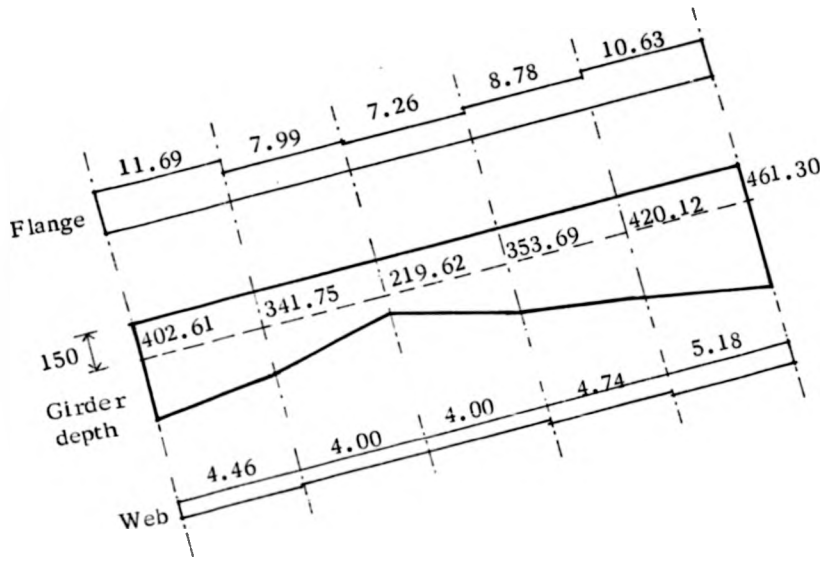

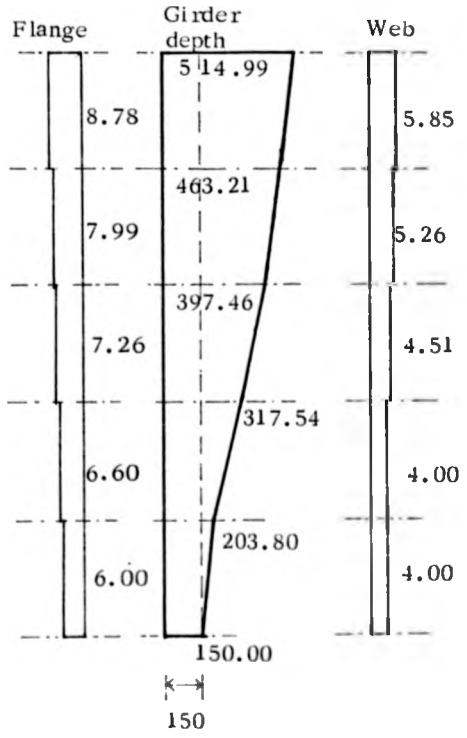

Pinned base

Stress constraints only

All dimensions in mm

Figure 7.10

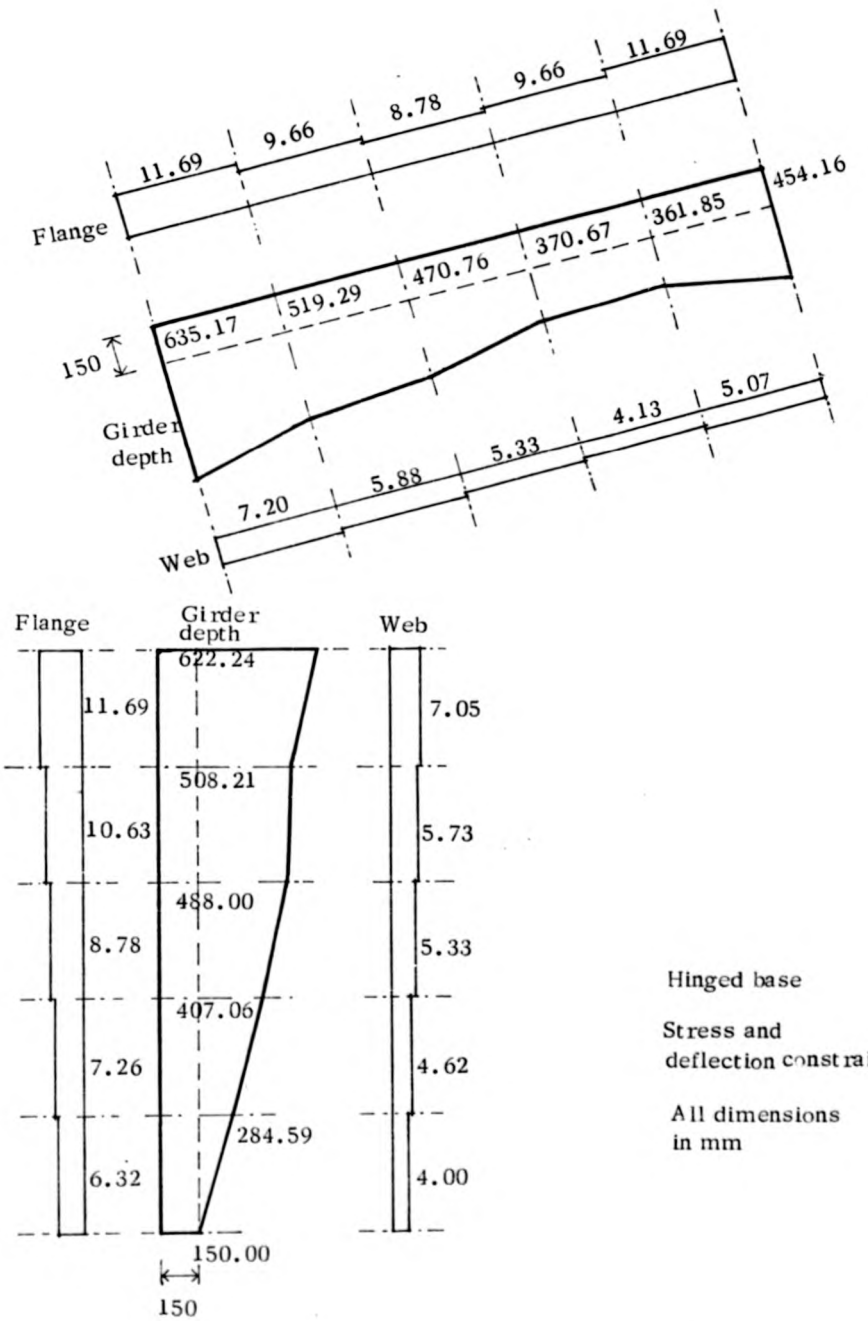

Hinged base

Stress and deflection constraints

All dimensions in mm

Figure 7.11

The fixed-base frame has then been designed with different lower-bound dimensions for the depth of girder. Instead of 150 mm uniform depth all-through, the initial depths were taken as varying from 190 mm to 150 mm as shown in figure (7.12). There are differences in the final dimensions

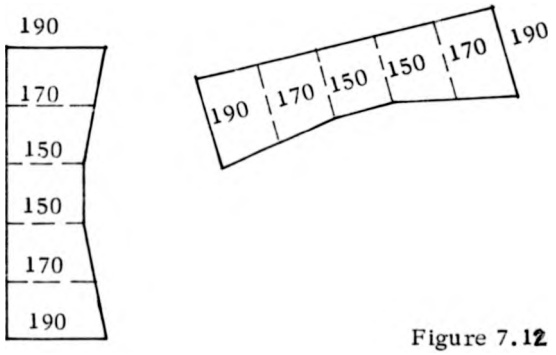

Figure 7.12

given by this design and the earlier one, which are mainly because of the fact that the calculation of sensitivity coefficients has always been based upon different frame dimensions in the two cases. To explain this, let us consider the stanchion depth at the eaves which has increased to 486.07 mm (figure 7.9 — for stress and deflection constraints) in the earlier design and to 476.83 mm in the latter design. During successive calculation of the sensitivity coefficients, the values of this depth in the first design were 150, 165, 181.5, 199.65, 219.62, 241.58, 265.73, 292.31 ..etc., each time increasing by 10% , whereas in the second design the values were 190, 209, 229.9, 252.89, 278.18, 306.00..etc. There is, however, very little difference in the weight of the two frames in the final solution. Compared to 582.85 kg given by the first design, the second design solution has a weight of 584.58 kg. When

the same frame was designed for stress constraints only, with these increased lower-bound dimensions, the weight of the final design was given as 578.36 kg compared to 576.56 kg of the earlier design.

The frame (for stress constraints only) has also been designed with alternative values for the increase of variable dimensions after each iteration. Instead of 10% the increment factor was changed to 5%, $7\frac{1}{2}$%, $12\frac{1}{2}$% and 15%. There is practically no difference in the total weight of the frames given by these designs, the maximum difference between the two extreme values being less than 0.5%, although the design process in the first case (i.e. with 5%) took 659 seconds of CPU time compared to 382 seconds in the earlier design (i.e. with 10%). The last design (i.e. with 15%) required 261 seconds. However, when the frame was designed once again without restricting the increment of the variable dimensions (i.e. with infinite increment factor), the weight of the designed frame was 602.88 kg, i.e. an increase of about 5% although the design process has been completed in 95 seconds with only 4 iterations.

To test the optimality of the designed solutions some of the frames were analysed by keeping the total volume the same, but slightly redistributing the material, e.g. reducing the web depth while increasing the flange thickness and vice versa. For example, the girder depths at the eaves of the frame of figure (7.11) was reduced by 10% with corresponding decrease of web thickness. Flange thickness was increased to maintain the same volume. On analysing, the horizontal deflection constraint was found to be violated by .23 mm, i.e. about 1.4%. Similar results were obtained when the girder depths were increased with corresponding decrease of flange thickness.

only one load case at a time, optimum design solution will be obtained for load case 1 (figure 7.13a) and the given solution will be used as the initial lower-bound frame for the subsequent design for load case 2 (figure 7.13b).

The rafter has been divided into three equal parts while the stanchion is being considered as a single member. The modulus of elasticity, yield stress, steel grade and the effective length for the members have been kept the same as those for example 1. The optimum solution is shown in figure (7.14a). The resulting frame has been analysed for load case 2 and found to satisfy the stress and deflection constraints. So no further design is necessary.

To examine the effect of the variation in the number of divisions the frame has been designed again with three equal divisions of the stanchion and five equal divisions of the rafter. All other parameters remain unaltered. The solution is shown in figure (7.14b). The total weight of the frame has reduced by more than 10%. The second design, though economical in respect of the cost of material, will involve additional expenses in fabrication. Thus, comparative study of total costs with alternative set of divisions may be made before selecting the most economical design.

The proposed design method works satisfactorily in deriving the optimum solutions for pitched-roof portal frames subject to the following limitations:

(i) The optimum plate thicknesses given in fractional figures, like 7.26 mm, shall have to be rounded off to the next available size, i.e. 8 mm. This may cause departure from optimality.

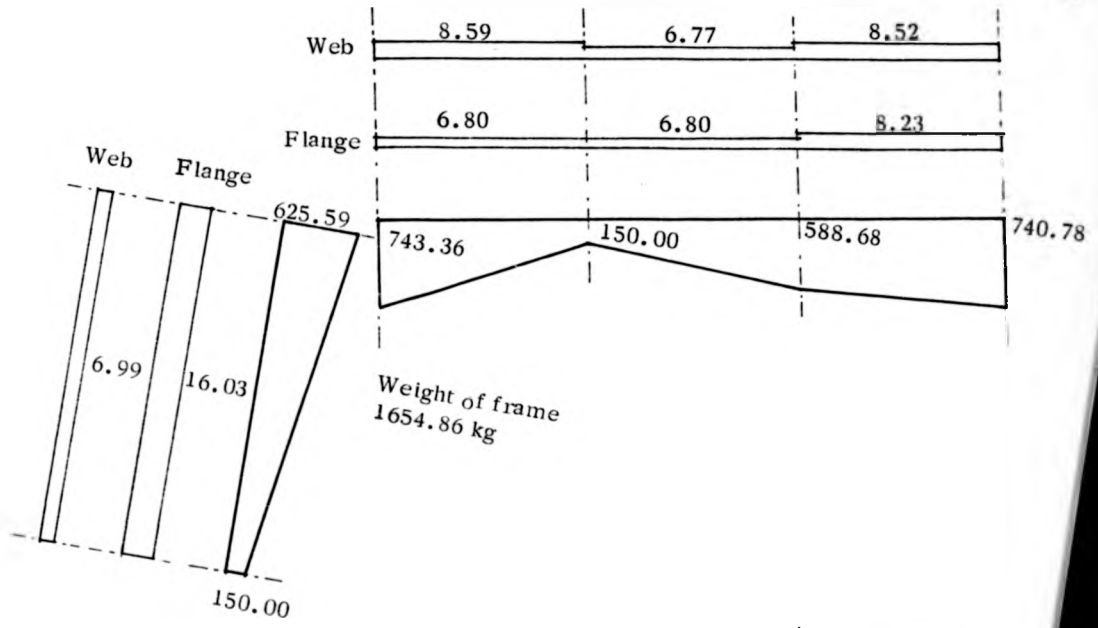

(a)

All dimensions in mm

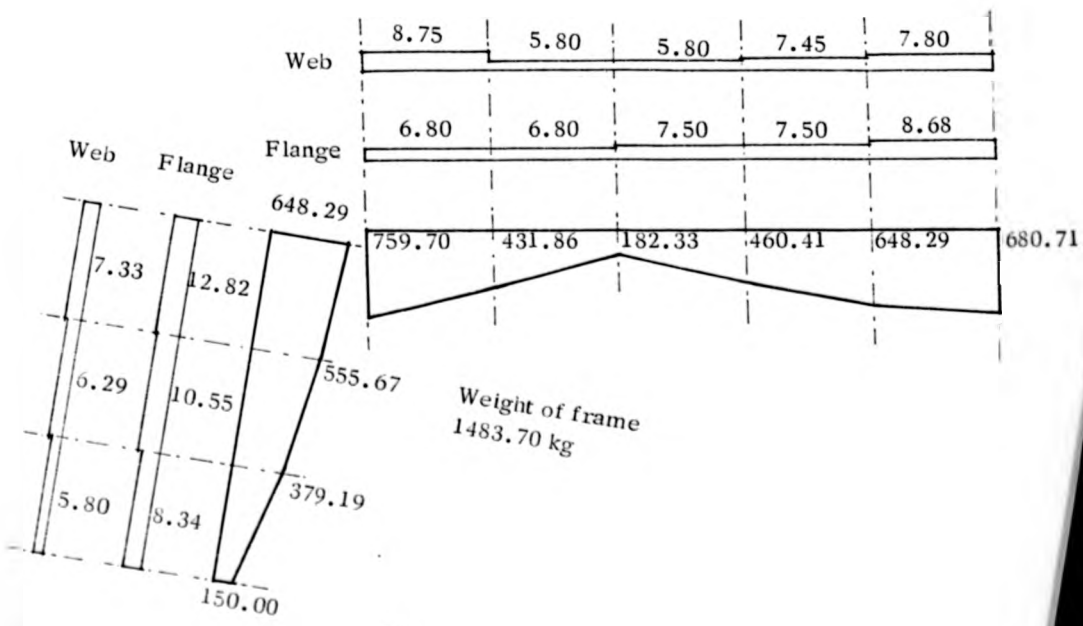

(b)

Figure 7.14

(ii) As the width of flange has been kept constant throughout the frame allowing only the thickness to increase from member to member, the advantage that would have been obtained by increasing the outstand of flanges in terms of minor-axis inertia which controls the permissible compressive stresses has not been utilised. Although, in the proposed method, the width of flange can be made variable by maintaining constant thickness, there will be no control on the length of outstand in such a case and Clause 27b may be violated.

(iii) In the proposed method changes in the thickness of flange and web occur at the same points which cause these points to have splicing all over the cross-section. A more desirable arrangement would be to separate the flange and web splicings by locating them at different cross-sections of the member.

The first of the above-mentioned limitations can be dealt with by choosing the thickness of flange plates by intuitive judgement instead of always selecting the next higher standard thickness. Referring to the second design solution of example 2 (figure 7.14b) and assuming the available plate thickness to be 4, 5, 6, 8, 10, 12, 14 , ... mm , the chosen dimensions can be as shown below .

Flange thickness

Required	12.82	10.55	8.34	6.80	6.80	7.50	7.45	8.68
Selected	12	10	8	8	6	8	8	8

satisfy all the constraints and its total weight is 4.66% higher. If, after choosing the plate thicknesses in this manner, the frame is found not to satisfy all the constraints, one or two alterations will be sufficient to produce a feasible design.

7.7 DESIGN METHOD CONSIDERING THE PRACTICAL CONSTRAINTS

To avoid all the three limitations mentioned earlier, a modified design procedure has been developed using the same basic principles of the previous method. The following changes have been incorporated in the revised method :

(i) The thickness and/or width of the flange plate may change at any desired point in the frame independent of the location of changes in other cross-sectional dimensions. Starting from the lower-bound dimensions the width of a flange is increased first and the thickness increases as soon as no further increment of the width is possible without violating the specification on maximum permissible outstand.

(ii) Similarly, the thickness of web also changes at any desired point without having any relation to the number and location of changes in slope.

(iii) The plate thicknesses increase from one standard size to the next higher size.

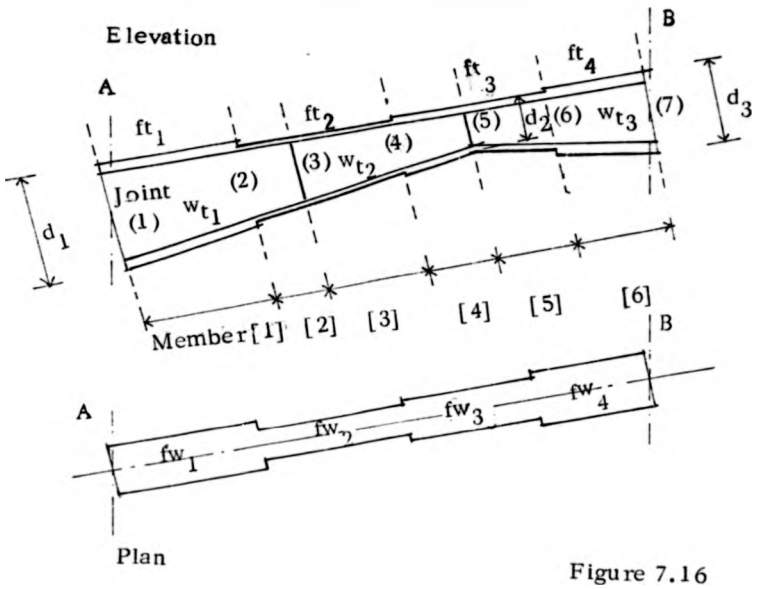

Figure 7.16

Figure (7.16) shows a possible arrangement of variation of plate thickness, width of flange and depth of girder for a rafter AB. Such an arrangement enables the frame to be composed of flange and web plates having lengths which are convenient for fabrication. When these lengths are fixed, corresponding thickness and width/depth are given by the optimum design solution.

In the analysis process a joint is assumed at every point where there is a change of slope, width or plate thickness and the portion of the frame between two successive joints is considered as a member.

A new program has been written incorporating all the modifications mentioned above and a number of frames have been designed. In general, the design of frames by this program requires lesser number of iterations and computer time compared to the previous program. This is mainly because of (i) the increments being of

larger proportions than 10% (due to the movement from one discrete dimension to another) and (ii) the number of divisions being usually less than the earlier case due to the use of convenient length of plates. The particular example given below has been chosen to be able to compare the results given by the proposed method with those obtained by using a trial and error method adopted by Butler Buildings (U.K.) Ltd., a tapered frame manufacturer.

7.8 EXAMPLE 3

The frame and the two loading combinations are shown in figure (7.17a and 7.17b). The limiting deflections have been taken as L/250 (vertical) and h/325 (horizontal). The maximum increment of depth at each iteration has been restricted to 10% while the flanges are allowed to increase in the following steps :

150 mm (width) x 6mm (thickness) , 170 x 6, 192 x 6,
192 x 8 , 212 x 8, 234 x 8, 256 x 8 , 256 x 10 , 276 x 10,298 x 10,
320 x 10, 320 x 12, 340 x 12, 362 x 12, 384 x 12, 384 x 14,
404 x 14 , 484 x 14 ...

Permissible web thicknesses are

4, 5, 6, 8, 10, 12, 14 , ... If the simplex operation gives the value of the increase of flange area as more than half of the difference between the area of two consecutive plates, the next higher plate is chosen. Otherwise the plate dimensions remain unaltered. As for the web plate, the change is from one of the above permissible thicknesses to the next higher one. As soon as the thickness violates

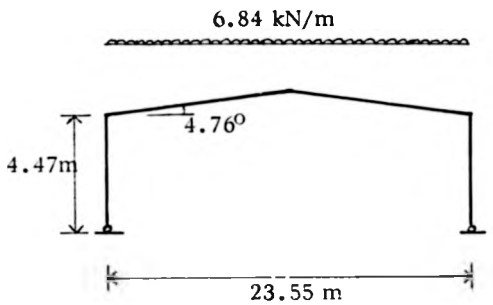

(a) Load case 1

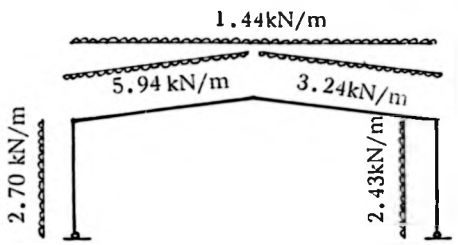

(b) Load case 2

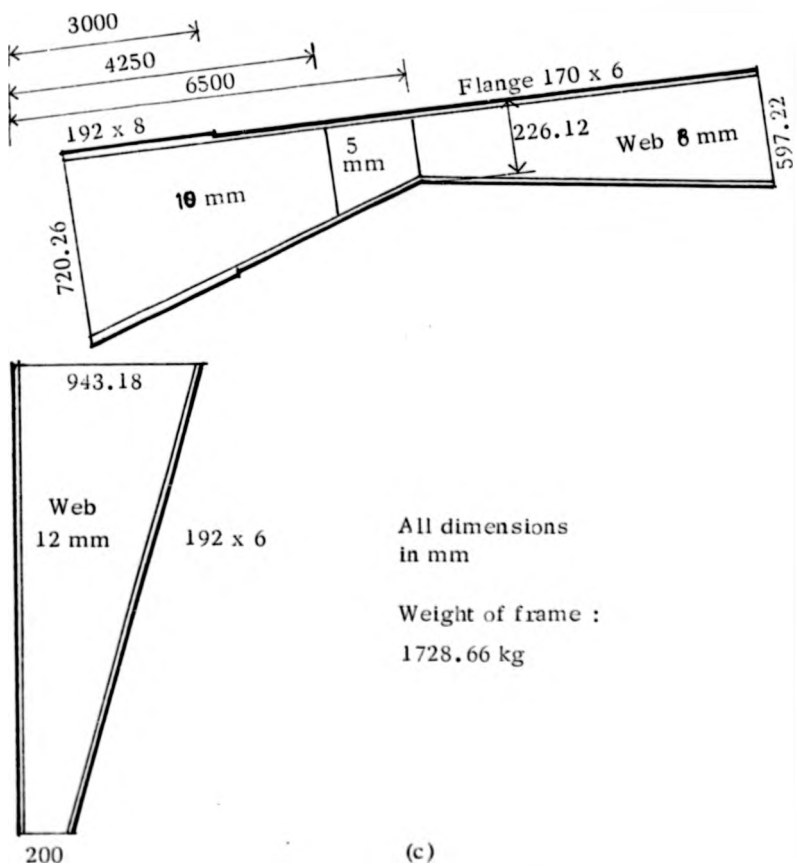

All dimensions in mm

Weight of frame : 1728.66 kg

(c)

Figure 7.17

were required. The two results are in close agreement, the direct design obtained by the proposed method being 4.84% heavier. The main reasons for this discrepancy are as follows : (i) While in the proposed method the effective lengths for calculating the permissible compressive stresses have been taken as 2250 mm for the stanchion members and 1500 mm for the rafter members, in the trial-and-error method smaller effective lengths were used for some of the members. (ii) To make the proposed method an automatic direct design procedure, selection of flanges had to be restricted to a number of discrete sizes which effects the optimality of the solution. (iii) In formulating the objective function for the problem (equation 7.13) indirect effect of any increase of depth, i.e. the related increase of web thickness to satisfy Clause 27f of the code, has not been taken into consideration. As a result of this, the simplex operation finds the increment of depth as more beneficial than actually it is. It may be observed that the depths of girder are higher in the design solution given by the proposed method than those obtained by the trial-and-error method.

7.9 CONCLUSION

An automatic optimum design procedure for pitched-roof portal frames has been developed using the matrix displacement method and simplex method of linear programming. Design solutions can be obtained to satisfy both stress and deflection constraints under one loading case.

The non-linear constraint functions usually associated with such optimisation problem have been avoided by using repeated analysis of the frame and following an assumed multi-linear path to reach the

optimum solution. The assumed constraint-variable relationship curves shown in figure (7.3) are not likely to be as smooth as shown in the figure. With changes in the cross-sectional dimensions of the members the slope of these curves may vary considerably and some of the curves may even be convex in nature. By adopting restricted increment of the variables at each iteration these problems have been solved to a satisfactory degree.

The objective function has been linearised by excluding the thickness of web from the variables for optimisation and considering the area of flange, as a whole, as the variable.

In the design examples presented the final solution of some of the frames show the web thickness to be higher than the flange thickness at certain cross-sections. This has occurred as the thickness of web could not be considered as a variable due to the restrictions imposed by clause 27f of BS 449.

CHAPTER VIII

SUGGESTIONS FOR FURTHER WORK

In the direct design method for multistorey frames to deflection limitations presented in chapters II and III members can be chosen from all the available standard rolled sections when using hand calculation. The design charts presented for quick solutions and the computer method for automatic design are, however, based on a set of 'economical' sections. As discussed earlier, it may not always be convenient or lead to overall economy of the structure if the selection of the members is restricted to such a set of sections. Moreover, use of UB sections for some column members may sometimes be found economical. Design charts and computer programmes may be developed taking all these points into consideration.

Furthermore, design charts may also be prepared for the topmost storey and the bottom two storeys of fixed-base and pinned-base frames. The automatic design procedure for a multistorey frame may also include the design of beam members for the local collapse mechanism which is now done by separate calculations.

The approximate elastic-plastic analysis method presented in chapter IV uses a substitute Grinter frame for the calculation of sway deflections in the post-elastic range. As realistic values for the secant stiffness of beams are used the given deflections compare very favourably with accurate results obtained by elaborate computer analysis. Calculation of joint rotations, however, depends on initial assumptions for the remote-end rotations of members connected to the joint. The principle used for these assumptions and the possibility of error in the upper storeys have been discussed in Sec. (4.7).

problem can be formulated more accurately, including the effect of indirect increase of web thickness when the depth of girder is increased.

REFERENCES

1. 'British standard 449 : Part 2 : 1969. Specification for the use of structural steel in building .' British Standard Institution.

2. Allwood, B.O., et al. 'Steel frames for multistorey buildings: Some design examples to conform with the requirements of BS 449 : 1959' B.C.S.A.Publication No.16, 1961.

3. Allwood, B.O., et al. 'Steel designers manual.' Crossby-Lockwood, London, 1966.

4. Steel Structures Research Committee. 'Final report.' H.M.S.O., 1936.

5. Wood, R.H. 'The stability of tall buildings.' Proc.I.C.E., Vol. 11 , September 1958.

6. Anderson, D. 'Investigation into the design of plane structural frames.' Ph.D. thesis, University of Mahchester, 1969.

7. Majid, K.I. and Anderson, D. 'The computer analysis of large multistorey framed structures.' The Structural Engineer, Vol. 46, November 1968.

8. Majid, K.I. 'Non-linear Structures.' London Butterworths, 1972.

9. Rankine, W.J.M. 'Useful rules and tables.' London, 1866.

10. Merchant, W. 'The failure load of rigid jointed frameworks as influenced by stability.' The Structural Engineer, Vol.32, July 1954.

11. Wood, R.H. 'Effective lengths of columns in multi-storey buildings.' The Structural Engineer, Vol. 52, July-September 1974.

12. Horne, M.R. 'An approximate method for calculating the elastic critical loads of multi-storey plane frames.' The Structural Engineer, Vol. 53, June 1975.

13. Bolton, A. 'A simple understanding of elastic critical load.' The structural Engineer, Vol. 54, June 1976.

14. Williams, F.W. 'Simple design procedures for unbraced multi-storey plane frames.' Proc.I.C.E., Vol.63, June 1977.

15. Neal, B.G. and Symonds, P.S. 'The rapid calculation of plastic collapse loads for a framed structure.' Proc. I.C.E., Vol.1, April 1952.

16. Horne, M.R. 'A moment distribution method for the analysis and design of structures by the plastic theory.' Proc.I.C.E., Vol. 3, April 1954.

17. Heyman, J. 'An approach to the design of tall steel buildings.' Proc.I.C.E., Vol. 17, December 1960.

18. Holmes, M. and Gandhi, S.N. 'Ultimate load design of tall steel building frames allowing for instability.' Proc. I.C.E., Vol.30, January 1965.

19. Holmes, M. and Sinclair-Jones, H.W. 'Plastic design of multi-storey sway frames.' Proc.I.C.E., Vol.47, September 1970.

20. Driscoll, G.C. , et al. 'Plastic design of multistorey frames.' Dept. of Civil Engineering, Lehigh University, Bethlehem, 1965.

21. Livesley, R.K. 'The application of an electronic digital computer to some problems of structural analysis.' The Structural Engineer, Vol.34, January 1956.

30. Horne, M.R. 'Plastic theory of structures.' Thomas Nelson, 1971.

31. Toakley, A.R. 'Optimum design using available sections.' Proc. A.S.C.E., Vol. 94, No ST5, May 1968.

32. Majid, K.I. 'Optimum design of structures.' London Newnes-Butterworths, 1974.

33. Horne, M.R. and Chin, M.W. 'Plastic design of portal frames in steel to BS 968' B.C.S.A. Publication No. 29, 1966.

34. Horne, M.R. 'The plastic design of columns' B.C.S.A. Publication No. 23, 1964.

35. Lee, G.C., et al. 'Design of tapered members.' Welding Research Council Bulletin No. 173, June 1972.

36. Just, D.J. 'Plane frameworks of tapering box and I-section.' Proc. A.S.C.E., Vol 103 , No.ST1, January 1977.

37. Stevens, L.K. 'Direct design by limiting deformations.' Proc. I.C.E., Vol. 16, July 1960.

38. Stevens, L.K. 'Control of stability by limiting deformations.' Proc.I.C.E., Vol. 28, July 1964.

39. Majid, K.I. and Elliott, D.W.C. 'Optimum design of frames with deflection constraints by non-linear programming.' The Structural Engineer, Vol. 49, April 1971.

40. Moy, F.C. 'Control of deflections in unbraced steel frames.' Proc.I.C.E., Vol. 57, December 1974.

41 Moy, F.C. 'Multistorey frame design using storey stiffness concept.' Proc.A.S.C.E., Vol.102,No ST6,June 1976.

42. Anderson, D. and Salter, J. 'Design of structural frames to deflection limitations.' The Structural Engineer, Vol.53, August 1975.

43. Horne, M.R. and Morris, L.J. 'Optimum design of multistorey rigid frames.' Optimum structural design: Theory and applications, Ed.Gallagher, R.H. and Zienkiewiez, O.C. , Wiley , 1973.

44. Wood, R.H. and Roberts, E.G. 'A graphical method of predicting sidesway in the design of multistorey buildings.' Proc.I.C.E., Vol.59, June 1975.

45. Livesley, R.K. and Chandler, D.B. 'Stability functions for structural frameworks.' Manchester University Press, 1956.

46. Wood, R.H. 'A new approach to column design.' Building Research Establishment, HMSO, 1974.